Design and development of pharmaceutical dosage forms for gene and siRNA delivery

Ghonaim, Hassan

Award date:
2008

Awarding institution:
University of Bath

Design and Development of Pharmaceutical Dosage Forms for Gene and siRNA Delivery

Hassan M. Ghonaim

A thesis submitted for the degree of Doctor of Philosophy

University of Bath

Department of Pharmacy and Pharmacology

September 2008

Signed:……..

Contents

Title i

Contents ii

Acknowledgements vi

Abstract vii

Abbreviations viii

Chapter 1 Introduction and Literature Review 1

1.1. Introduction 2

1.2. Gene Therapy Clinical Trials Update in March 2008 4

1.3. Gene Delivery – an Introduction 6

1.3.1. Mechanisms in NVGT 9

1.3.2. Naked Plasmid DNA Transfection 12

1.3.3. Complexed Plasmid DNA Transfection 13

1.3.4. Basic Principles of Cationic Lipid-Mediated Gene Transfection 16

1.3.5. Basic Structural Features of Cationic Lipids 18

1.4. siRNA Delivery – an Introduction 21

1.4.1. Mechanisms in RNAi 22

1.4.2. Methods of Delivery 23

1.4.3. Chemically Modified siRNA Molecules 24

1.4.4. Liposomes and Nanoparticles 24

1.4.5. Cationic Lipids 25

1.4.6. siRNA Delivery Steps 26

1.4.7. In Vitro Use of siRNA 27

1.4.8. Delivering siRNA In Vivo Using Non-viral Carriers 30

1.4.9. Delivering siRNA In Vivo Using Local Administration 30

1.4.10. siRNA Delivery In Vivo Using Systemic Administration 31

1.5. Aims 32

Chapter 2 Materials and Methods 33

2.1. Chemicals **34**

2.2. Buffers and Media **35**

2.3. Suppliers **36**

2.4. Methods **37**

2.4.1. Amplification and Purification of Plasmid DNA **37**

2.4.2. DNA Condensation Studies **41**

2.4.3. DNase I Sensitivity Assay **46**

2.4.4. RiboGreen Intercalation Assay **46**

2.4.5. Tissue Culture and Transfection Experiments **47**

2.4.6. Fluorescence Activated Cell Sorting Experiment **51**

2.4.7. siRNA Transfection Experiments in the Presence of Serum for FEK4 and HtTA Cells **52**

2.4.8. Preparation of Cell Samples for FACS Analysis for both DNA and siRNA **53**

2.4.9. Cytotoxicity (MTT) Assay of the Formed DNA-Lipoplexes on Transfected Cell Lines **54**

2.4.10. Cytotoxicity (MTT) Assay of the Formed siRNA-Lipoplexes **55**

2.4.11. Characterization of the Formed Nanoparticles **56**

2.4.12. Confocal Microscopy Studies **59**

Chapter 3 Design and Development of Pharmaceutical Dosage Forms for Gene Delivery 61

3.1. Introduction **62**

3.1.1. Methods for Cationic Liposome Formulation **64**

3.1.2. DNA Condensation **67**

3.1.3. Ethidium Bromide Fluorescence Quenching Assay **67**

3.1.4. Light Scattering Assay **72**

3.1.5. Agarose Gel Electrophoresis **73**

3.1.6. Cell Culture and Transfection Experiments **74**

3.1.7. In Vitro Cytotoxicity **76**

3.1.8. Characterization of the Lipoplex Formulations **77**

3.2. N^1,N^{12}-Diacyl Spermines: SAR Studies on Non-Viral Lipopolyamine Vectors for pDNA Formulation **80**
3.2.1. DNA Condensation **80**
3.2.2. Lipoplex Particle Size and ζ-Potential **81**
3.2.3. pEGFP Transfection and In Vitro Cytotoxicity **82**
3.3. Varying The Chain Length in N^4,N^9-Diacyl Spermines: Non-Viral Lipopolyamine Vectors for Efficient pDNA Formulation **86**
3.3.1. DNA Condensation **88**
3.3.2. Lipoplex Particle Size and Zeta-Potential Measurements **89**
3.3.3. DNase I Protection **90**
3.3.4. Transfection Experiments and In Vitro Cytotoxicity **91**
3.3.5. Confocal Microscopy Visualization **97**
3.4. Very Long Chain N^4,N^9-Diacyl Spermines: Non-Viral Lipopolyamine Vectors for Efficient pDNA Delivery **100**
3.4.1. DNA Condensation **101**
3.4.2. Lipoplex Particle Size and Zeta-Potential Measurements **102**
3.4.3. pEGFP Transfection Experiments and In Vitro Cytotoxicity **103**
3.4.4. Confocal Microscopy Visualization **106**
3.5. Unsymmetrical N^4,N^9-Diacyl Spermines: Non-Viral Lipopolyamine Vectors for Efficient pDNA Delivery **107**
3.5.1. DNA Condensation **109**
3.5.2. Lipoplex Particle Size and Zeta-Potential Measurements **110**
3.5.3. pEGFP Transfection Experiments and In Vitro Cytotoxicity **111**
3.5.4. Confocal Microscopy Visualization **115**
3.6. Varying The Heterocyclic Endgroups in N^4,N^9-Diacyl Spermines for Efficient pDNA Formulation **118**
3.6.1. pEGFP Transfection Experiments and In Vitro Cytotoxicity **119**
3.6.2. Confocal Microscopy Visualization **124**

Chapter 4 Design and Development of Pharmaceutical Dosage Forms for siRNA Delivery 125
4.1. Introduction **126**

4.2. N^1,N^{12}-Diacyl Spermines: SAR Studies of Non-Viral Lipopolyamine Vectors for siRNA Formulation **131**
4.2.1. RNA Binding (RiboGreen Intercalation Assay) **131**
4.2.2. Lipoplex Particle Size and ζ-Potential **132**
4.2.3. siRNA Delivery and In Vitro Cytotoxicity in the Presence of Serum **133**
4.3. N^4,N^9-Diacyl Spermines: SAR Studies of Non-Viral Lipopolyamine Vector siFection Efficiency versus Toxicity **137**
4.3.1. RNA Binding (RiboGreen Intercalation Assay) **137**
4.3.2. Lipoplex Particle Size Measurements **137**
4.3.3. siRNA Delivery and In Vitro Cytotoxicity **138**
4.3.4. Confocal Microscopy Visualization **142**
4.4. Very Long Chain N^4,N^9-Diacyl Spermines: Non-Viral Lipopolyamine Vectors for Efficient siRNA Delivery **144**
4.4.1. Lipoplex Particle Size and Zeta-Potential Measurements **144**
4.4.2. siRNA Delivery and In Vitro Cytotoxicity **144**
4.4.3. RNA Binding (RiboGreen Intercalation Assay) **146**
4.4.4. Confocal Microscopy Visualization **148**
4.5. Unsymmetrical N^4,N^9-Diacyl Spermines: Non-Viral Lipopolyamine Vectors for Efficient siRNA Delivery **149**
4.5.1. Lipoplex Particle Size and Zeta-Potential Measurements **149**
4.5.2. RNA Binding (RiboGreen Intercalation Assay) **149**
4.5.3. siRNA Delivery and In Vitro Cytotoxicity **150**
4.6. Heterocyclic N^4,N^9-Diacyl Spermines: Non-Viral Lipopolyamine Vectors for Efficient siRNA Delivery **155**
4.6.1. Zeta-Potential Measurements **155**
4.6.2. siRNA Delivery and In Vitro Cytotoxicity **156**

Chapter 5 **Conclusions** **161**

References **170**

Appendix Publications and Presentations Arising from this Work **188**

Publications **189**

Presentations **190**

Acknowledgments

I would like to thank Dr Ian S. Blagbrough for his continuous guidance and support without which this work would not have been possible.

I would also like to thank Dr. Charareh Pourzand for her advice and support in the biological evaluation studies.

I am grateful to Prof R. M. Tyrrell (University of Bath) for the FEK4 and HtTA cell lines.

I am grateful to my colleagues in Dr Blagbrough's research group: Dr Osama A. Ahmed, Dr Moustafa K. Soltan and Shi Li for synthesising the lipospermines.

I thank the research and technical staff in the Department of Pharmacy and Pharmacology: Kevin Smith, Jo Carter, Don Perry and Adrian Rogers.

I also gratefully acknowledge the financial support of this work from the Egyptian Government.

Finally, I would like to thank my colleagues in the Department, my family, especially my parents and my wife for their continuing support.

Abstract

These investigations are focused on the design and formulation of novel non-viral lipopolyamine vectors capable of efficiently and safely delivering DNA to the nucleus, and siRNA to the cytoplasm, in two tissue cultured (primary and cancer) cell lines. The thesis starts with a focussed literature review on the non-viral gene therapy (NVGT) vectors currently used in the formulation of DNA and siRNA.

The first experimental part tests the ability of our novel lipospermines in NVGT, this includes structure-activity relationship (SAR) studies changing the: position, length, saturation or symmetry of the fatty chains of N^4,N^9-diacyl, N^1,N^{12}-diacyl and N^4,N^9-dialkyl spermines. The ability of these lipospermines in DNA condensation is investigated using ethidium bromide fluorescence-quenching, and gel electrophoresis (including gel shift and DNase protection) assays followed by nanoparticle characterization techniques (particle size and zeta potential). Transfection efficiency of pEGFP (using FACS) and cytotoxicity (using MTT) were studied in both cancer and primary cell lines and compared with Lipogen™ (N^4,N^9-dioleoyl spermine). Some of these novel lipospermines are shown to be as good as, but not better than N^4,N^9-dioleoyl spermine as efficient DNA transfecting agents. N^4,N^9-Dioleoyl spermine is the best transfecting agent from the all tested novel lipospermines displaying the lowest N/P ratio, highest transfection efficiency and the lowest cytotoxicity on both tested cell lines.

We extended this SAR study to examine the same lipospermines in siRNA delivery. The ability of these compounds to bind siRNA was studied using the RiboGreen intercalation assay followed by similar nanoparticle characterization techniques. Transfection efficiency for delivery of Label IT® RNAi Delivery Control (using FACS) and cytotoxicity (MTT) were also studied in both cancer and primary cell lines, and compared with a market leader siRNA transfecting agent Trans-IT™ Twelve of these non-viral vectors, led by N^4,N^9-dieicosenoyl spermine and N^4,N^9-dierucoyl spermine, showed both transfection efficiency and cell viability over 75%.

Abbreviations

bp	base pair
DEPC	diethylpyrocarbonate
DMSO	dimethylsulfoxide
DNA	deoxyribonucleic acid
DOGS	dioctadecylamidoglycylspermine
DOPE	dioleoylphosphatidyl ethanolamine
DOSPA	2,3-dioleyloxy-*N*-[2(spermine-carboxamido)ethyl]-*N,N*-dimethyl-1-propanaminium trifluoroacetate
DOTMA	*N*-[1-(2,3-dioleyloxy)propyl]-*N*,*N*,*N*-trimethylammonium chloride
EDTA	ethylenediamine tetra-acetic acid
EGFP	enhanced green fluorescent protein
EMEM	Earle's minimal essential medium
EthBr	ethidium bromide
FACS	fluorescence activated cell sorting
FCS	foetal calf serum
HEPES	*N*-(2-hydroxyethyl)piperazine-*N*'-2-ethanesulfonic acid
LB	Luria Bertani
MTT	(3-(4,5-dimethylthiazol-2-yl)-2,5-diphenyltetrazolium bromide
NLS	nuclear localization signal
N/P	ammonium/phosphate
NPC	nuclear pore complex
NVGT	non-viral gene therapy
PBS	phosphate-buffered saline
RNA	ribonucleic acid
SAR	structure-activity relationships
siRNA	small interfering RNA
TE	tris-EDTA
TAE	tris-acetate-EDTA
UV	ultra-violet

CHAPTER 1

Introduction and Literature Review

1.1. INTRODUCTION

Polynucleic acid delivery has many potential applications in medicine. One of the main applications is DNA delivery for gene therapy or siRNA delivery. Gene therapy, an approach to the treatment or prevention of diseases associated with defective gene expression, involves the insertion of a therapeutic gene into cells, followed by expression and production of the required protein(s). This approach enables the introduction of new genes, replacement of damaged genes, or inhibition of the expression of undesired genes. Gene delivery for therapeutic applications currently involves two strategies: corrective and cytotoxic gene therapy. The former includes correction of genetic defects in target cells. This strategy is exploited for the treatment of diseases with single gene disorders (e.g., severe combined immuno-deficiency syndromes SCID, cystic fibrosis, hemophilia, sickle cell anemia, β-thalassemia, muscular dystrophy) and malignant tumours including ovarian carcinoma. The latter strategy includes the destruction of target cells using a cytotoxic pathway. This strategy is used for treatment of uterine leiomyomata and of malignant tumours, including ovarian, breast, and endometrial carcinoma (1), it is also used for DNA vaccination. RNA interference (RNAi) has become a powerful tool for the knockdown of target gene expression and subsequent phenotypic analysis of gene function in mammalian cells in culture. Critical to the success of any small interfering RNA (siRNA) (synthetic double-stranded RNA sequences of 19-23 nucleotides) knockdown in cells is the efficient delivery of the siRNA to those cells. As a result, there has recently been a significant surge of interest in the application of siRNA in functional genomics programmes as a means of deciphering specific gene function.

For a gene or an siRNA to be a medicine giving the desired therapeutic effect it should be formulated and delivered to its site of action. For DNA this is the nucleus, and for siRNA the cytoplasm of the cells. There are two major methods for delivery of genes. One method utilizes viral vectors and is generally an efficient tool of transfection. Attempts, however, to resolve drawbacks with viral vectors (e.g., high risk of mutagenicity, immunogenicity, low production yield, limited gene payload size, oncogene activation, etc.), led to the development of an alternative method which makes use of non-viral vectors. Non-viral delivery systems include the use of DNA alone, so called “naked DNA”, or complexed with synthetic cationic lipids (lipoplexes) or cationic polymers (polyplexes). These vectors not only circumvent the drawbacks of viral vectors, but also have the advantages of simplicity of use and the

ease of large-scale production. They can be classified as liposomal and non-liposomal non-viral delivery vectors. Liposomal delivery vectors usually contain two types of lipids, a cationic lipid (a positively charged amphiphile) for DNA condensation and cellular membrane interaction, and a neutral helper lipid (phospholipid), to increase transfection efficiency as it has a membrane fusion promoting ability (2-4). Non-liposomal cationic-lipid delivery vectors (lipopolyamines) combine both the characteristics of cationic and helper lipids. Although lipopolyamines are less efficient in comparison with viral vectors, their promising lower toxicity than viral vectors means that it is important to design novel lipopolyamines with improved transfection efficiency based on unmet medical need.

Our considerations are of structure-activity relationships (SAR) within naturally occurring and synthetic polyamines. The covalent addition of a lipid moiety, typically one or two alkyl or alkenyl chains, or a steroid, allows much greater efficiency in DNA condensation and in the cellular transfection achieved. Thus, efficient DNA or siRNA condensation and subsequently drug delivery (i.e., with DNA or siRNA as the drug) can be brought about using novel polyamine conjugates.

Cationic lipid-mediated gene transfer is an attractive technique. It is of general use with respect to cell type and DNA size, as it is entirely driven by non-specific ionic interactions. It may be of low toxicity if the carrier is designed to be biodegradable. It can be prepared in significant quantities with relative ease (compared to viral vectors) and extensively characterised. Furthermore, each of the constituent parts can be modified, thereby facilitating the elucidation of the much needed SAR.

It may be foreseen that in order to be successful, incorporating the various functions is required in order to perform the different steps involved in gene transfection. Such self-assembly nanosystems are a current challenge in molecular pharmaceutics (5-10). Thus, the aims of our research are to understand, design, prepare and evaluate small-molecule lipopolyamines for non-viral gene therapy (NVGT). These novel lipopolyamine conjugates mimic the positive charge distribution found in the tri-amine spermidine and the tetra-amine spermine alkaloids. After optimizing their SAR, these probes will be useful in monitoring gene delivery by NVGT, and in early experiments to validate siRNA delivery, in vitro. Then, in the future, in vivo studies can be considered (7-12).

1.2. GENE THERAPY CLINICAL TRIALS UPDATE IN MARCH 2008

The *J. Gene Medicine* Clinical Trials site, the most comprehensive source of information on worldwide gene therapy clinical trials available on the internet (www.wiley.co.uk/genmed/clinical/) gives a clear idea about recent updates in gene therapy clinical trials from different aspects e.g., therapeutic strategies based on the addition of genes to compensate for faulty genes, addition of genes with new functions, or disruption of gene expression. From the point of view of possible target disease states, we find most of the clinical trials are for the treatment of cancer diseases (66.5%, Table 1.1) which include the strategy of introducing genetic materials into cells for the production of therapeutic proteins or blocking the synthesis of harmful proteins (e.g., melanoma, leukaemia, breast cancer, cervical carcinoma, ovarian cancer, lung cancer, prostate cancer, lymphoma, pancreatic carcinoma, gliogblastoma and squamous cell carcinoma), followed by cardiovascular (e.g., myocardial angiogenesis, severe peripheral artery occlusive disease, critical limb ischaemia, chronic granulomatosis coronary heart disease and peripheral arterial occlusive disease PAOD) and monogenic diseases (e.g., severe combined immuno-deficiency syndromes SCID, cystic fibrosis, haemophilia, sickle cell anaemia, β-thalassemia, muscular dystrophy).

Table 1.1. Gene Therapy Clinical Trials (Indications, 1989-2007) from *J. Gene Medicine*.

Indications	**Gene Therapy Clinical Trials**	
	Number	**%**
Cancer diseases	896	66.5
Cardiovascular diseases	121	9
Gene marking	50	3.7
Healthy volunteers	26	1.9
Infectious diseases	89	6.6
Monogenic diseases	110	8.2
Neurological diseases	17	1.3
Ocular diseases	12	0.9
Others	26	1.9
Total	1347	100

The number of approved clinical trials increased significantly in the last ten years (Table 1.2). Even though these trials started 20 years ago, in 1989, there was only a 2.7% in Phase III (Table 1.3). Viral vectors are the majority of these trials (66.9%) followed by naked DNA (17.8%), lipofection (7.4%), and siRNA (1.4%) trials.

Table 1.2. Gene Therapy Clinical Trials (Year of clinical trial, 1989-2007) from *J. Gene Medicine*.

Years	**Gene Therapy Clinical Trials**	
	Number	**%**
1989-1993	62	4.6
1994-1998	306	22.7
1999-2003	489	36.3
2004-2007	358	26.6
unknown	132	9.8
	1347	100

Table 1.3. Gene Therapy Clinical Trials (Phase of clinical trial, 1989-2007) from *J. Gene Medicine*.

Phase	**Gene Therapy Clinical Trials**	
	Number	**%**
Phase I	820	60.9
Phase I/II	262	19.5
Phase II	216	16
Phase II/III	13	1
Phase III	36	2.7
	1347	100

Therefore, the development of safe and efficient vectors for gene (plasmid DNA) and siRNA formulation and delivery is still a major challenge in order for them to become real medicines. We urgently need to meet this challenge to enable gene therapy, DNA vaccination, or RNA silencing to become a clinical reality. An understanding of the background to these problems is provided by two literature reviews on gene and siRNA polynucleic acid delivery.

1.3. GENE DELIVERY – AN INTRODUCTION

Treatment with traditional drugs is based on molecular substitution, which involves the chemical modification of various compounds that are then subjected to screening programmes. An increasing array of inherited and acquired diseases is now understood by an "inside out" approach involving the identification and targeting of the underlying genetic cause. As a result, therapeutic strategies based on the addition of genes to compensate for faulty genes, addition of genes with new functions, or disruption of gene expression have been developed and they are rapidly growing in diversity and scope to treats diseases caused by the malfunction of a gene. Gene therapy is a method to introduce genetic materials into cells for the production of therapeutic proteins or blocking the synthesis of harmful proteins. The former includes correction of genetic defects in target cells. This strategy is exploited for the treatment of diseases with single gene disorders (e.g., severe combined immuno-deficiency syndromes, cystic fibrosis, haemophilia, sickle cell anaemia, β-thalassemia, muscular dystrophy) and malignant tumours, including ovarian carcinoma. The latter strategy includes destruction of target cells using a cytotoxic pathway. This strategy is used for treatment of uterine leiomyomata and of malignant tumours, including ovarian, breast, and endometrial carcinoma (1,13). During the past decade, gene therapy technologies have progressed remarkably, and many clinical trials have been reported. Intracellular delivery of genetic material is the key step in gene therapy.

Gene therapy research is divided into two major research fields. One is to develop a therapeutic gene. This research includes development of an effective therapeutic gene for a specific disease and a tissue specific or regulated gene expression system. The other is to develop an efficient and safe delivery system. Optimization of delivery vectors is of major importance for turning gene therapy into a successful therapeutic method, so the development of safe and effective gene delivery methods is a major challenge to enable gene therapy or DNA vaccines to become a reality (14). Gene delivery systems are divided into viral vectors including retroviruses, lentivirus and adenoviruses and non-viral vectors including physical methods (naked DNA) and chemical methods including complexed with synthetic cationic lipids (lipoplexes) or cationic polymers (polyplexes) (5,15). They can be classified as liposomal and non-liposomal non-viral delivery vectors. Liposomal delivery vectors usually contain two types of lipids, a cationic lipid (a positively charged amphiphile based upon a polyamine or at least a cationic skeleton) for DNA

condensation and cellular membrane interaction, and a neutral helper lipid (phospholipid), to increase transfection efficiency as it has a membrane fusion promoting ability (2-4). Non-liposomal cationic-lipid delivery vectors combine both the characteristics of cationic and helper lipids (lipopolyamines). Although lipopolyamines are less efficient in comparison with viral vectors, their promising significantly lower toxicity than viral vectors ensures a continuous effort to design novel lipopolyamines with improved transfection efficiency.

The choice of the delivery system is determined by the nature of the disease to be treated and the need for long-term vs. transient and low vs. high expression of the gene of interest. Although at present viral systems dominate in clinical trials for gene therapy, cationic lipids have been studied in several clinical trials for treatment of cystic fibrosis, cancer, and, more recently, cardiovascular diseases at this point, some positive results have been attained, but the overall outcome indicates that a crucial requirement for successful gene therapy is the use of more efficient vectors (9,16).

Non-viral vectors have many advantages over viral gene vectors, although viral vectors are currently the most efficient way to deliver genes to cells. Unlike viral vectors, non-viral vectors have low cytotoxicity, low immunogenicity, no size limit, low cost, and reproducibility added to the practical issues of large scale production and quality control.

The ideal vector for gene delivery would have at least the following characteristics: 1) safety with low cytotoxicity and low immunogenicity, 2) high gene delivery efficiency with the ability to express, in an appropriately regulated fashion, the therapeutic gene for as long as required, 3) specificity for delivery of genes to target organs and 4) resistance to metabolic degradation and/or attack by the immune system. Until now, many gene carriers have been developed to meet the requirements of gene delivery to humans. These carriers were able to condense and protect plasmid DNA from DNase enzyme, resulting in the enhancement of gene delivery efficiency. However, there still remain drawbacks such as low biocompatibility and transfection efficiency (14,17). Most gene carriers have positive charges at their amine groups. The positive charges of the carriers interact with negative charges of phosphate groups in plasmid DNA, resulting in condensation of plasmid DNA. The lipoplex/plasmid DNA complexes are usually prepared in the presence of an excess amount of lipoplex, and the complex has a net positive charge. The positively charged complexes interact with negatively charged cell membranes, facilitating cellular uptake of the

lipoplex/plasmid DNA complexes via endocytosis. The lipoplex/plasmid DNA complexes have small particle size of around 100-200 nm. Although there is no size limit for the transfection, it was suggested that lipoplex/ plasmid DNA complex with diameters of around 100-200 nm corresponds to the diameter of the coated pits in endocytosis. Degradation of DNA by nucleases is a problem for gene therapy. Degradation of plasmid DNA by nucleases results in loss of gene expression. Therefore, carriers must protect plasmid DNA from nucleases. Condensation of plasmid DNA by carriers prevents the access of nucleases to plasmid DNA, improving resistance of plasmid DNA against enzymatic degradation (18).

For drug formulators, it is difficult to deliver a drug molecule of 3.3 kDa molecular weight carrying 10 negative charges, but in the case of the (pro-drug) DNA, a 5 kbp plasmid has a molecular weight of about 3.3 megaDaltons and carries 10,000 negative charges. So the first key step in gene formulation is DNA condensation into a nanoparticle form, through masking the negative charges of the phosphate backbone which causes alleviation of charge repulsion between remote phosphates on the DNA helix leading to collapse into a more compact structure (11,19). The importance of DNA condensation is attributed to the correlation of the transfection efficiency with the formation of DNA nanoparticles that are essential for the delivery of DNA through the cell membrane. Cationic lipids are considered to be the major gene carriers among the non-viral delivery systems. They have the ability to condense DNA into particles that can be readily endocytosed by (cultured) cells, and facilitate endosomal escape leading to efficient delivery to the nucleus.

We are studying how these polyamine conjugates interact with circular plasmids in order to produce nanometre-sized particles suitable for transfecting cells. Our main considerations are of structure-activity relationships (SAR) within naturally occurring and synthetic polyamines. The covalent addition of a lipid moiety, typically one or two alkyl or alkenyl chains, or a steroid, allows much greater efficiency in DNA condensation and in the cellular transfection achieved. Thus, efficient DNA or RNA condensation and subsequently drug delivery (e.g., with DNA or RNA as the drug) can be brought about using novel polyamine conjugates. The current aims of our research are to understand, design, prepare and evaluate small-molecule lipopolyamines for non-viral gene therapy (NVGT). These novel lipopolyamine conjugates mimic the positive charge distribution found in the tri-amine spermidine

and the tetra-amine spermine alkaloids. After optimizing their SAR, these probes will be useful in monitoring NVGT in vitro and then in vivo (7-10,12,14).

1.3.1. Mechanisms in NVGT

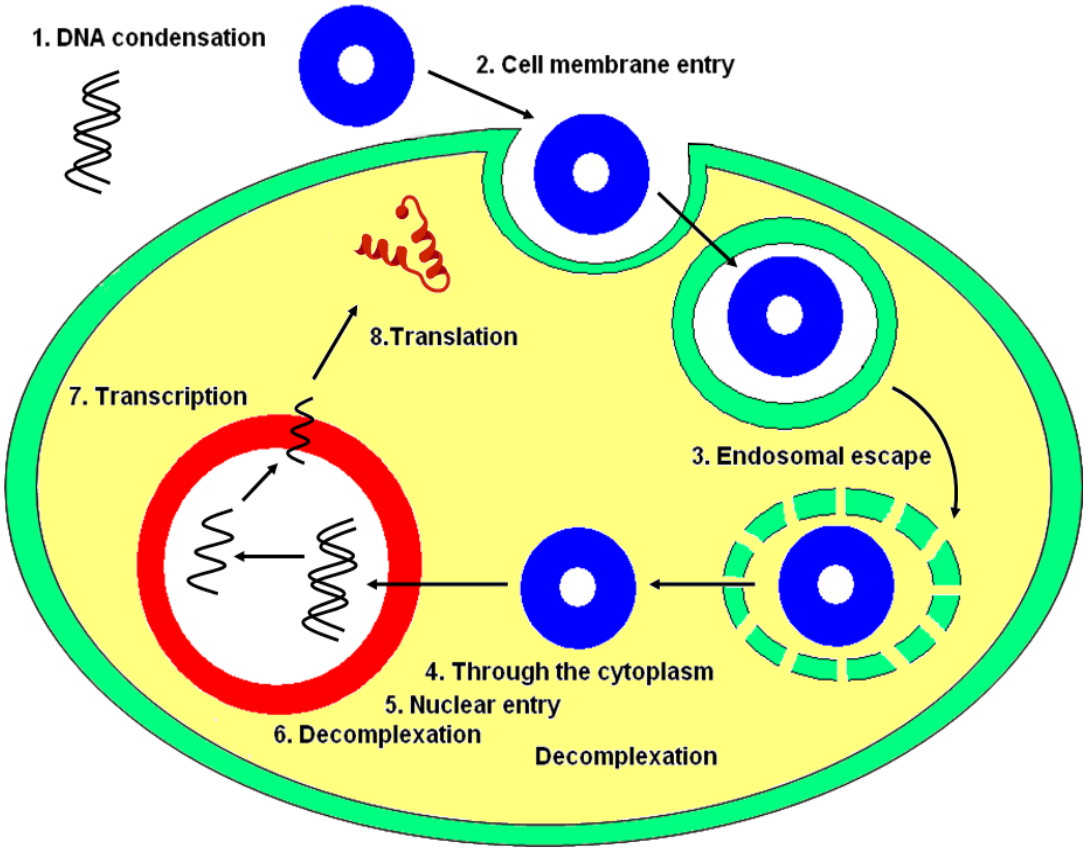

Fig. 1.1. Steps in the process of non-viral gene therapy by endocytosis showing the barriers for DNA nanoparticles, from the formation of the DNA complex (lipoplex) to gene delivery.

There is a need for a better understanding of the mechanism of gene delivery to targeted cells and more detailed understanding of the barriers for non-viral gene delivery to achieve efficient formulation (Fig. 1.1) (20,21). The barriers that hinder the delivery of DNA to its physical site of action (the nucleus) have been summarized as follows:

1. DNA condensation

Cationic lipids and polymers have the ability to condense DNA into particles that can be readily endocytosed. The formed nanoparticles and their size are essential for the

development of gene delivery vehicles (22-24). In addition, the cationic polymers or lipids increase the stability of DNA in serum (25). DNA is condensed by naturally occurring positively charged polyamines spermine and spermidine working together with the basic proteins, histones (11,19).

2. Cell membrane entry

The mammalian cell membrane is selectively and/or passively permeable, even to charged molecules. It is a phospholipid bilayer which contains many proteins including enzymes and selective ion channels. It allows the transport of macromolecules by endocytosis. Neutralization of the many negative charges on DNA by lipopolyamines will enable the delivery of DNA through the cell membrane as there are negative charges on both DNA and cell membrane. Also, the positively charged lipid complex (the nanobioparticle) will mediate transfection by fusion with cell membranes. Several trials have linked a DNA lipoplex to a targeting ligand in order to improve the efficiency of transfection, where the lipoplex is internalized by efficient receptor-mediated endocytosis in cells that present receptors for the target ligand (26-31).

3. Endosomal escape

Major barriers to the efficient delivery of DNA into the nucleus are located in the cytoplasm. Although the DNA complex is efficiently internalized in the cell, only a small fraction is transferred to the nucleus and expressed. As the DNA complex is internalized, it is retained inside the early endosomes, then in the late endosomes that are characterized by increased acidity (low pH values, about 5.5). At this stage, the efficient escape of DNA from the endosome is an important factor for successful gene delivery, before any further trafficking of the trapped DNA to the lysosomal compartment where the DNA is subjected to degradation by the nucleases found in the lysosomes (32-35). The possible mechanisms for endosomal escape are:

1. Disruption of endosomal membrane through mixing with the cationic lipid vector (36).
2. Cationic lipid interaction with the negatively charged endosomal membrane (37).
3. Proton sponge hypothesis, where a cationic lipid, has the ability of endosomal pH buffering that leads to chloride ion influx together with water molecules (H_3O^+) that leads to membrane swelling and disruption (38).

4. Membrane destabilising peptides, which includes fusogenic or lytic peptides, such as the basic peptide KALA (39), acidic peptide EGLA (40), or the uncharged peptides at neutral pH such as H5WYG (41). These peptides have the ability to disrupt the endosomal membrane and increase the release of DNA to the cytosol.

4. Through the cytoplasm

While ribozymes and antisense oligonucleotides may already be active in the cytosol, plasmid DNA has (typically) to be transported into the nucleus, in order to exhibit the desired gene expression. The cytoplasm is a critical place with respect to the stability of DNA and RNA, due to the presence of nucleases that reduce their half-life dramatically. Naked plasmid DNA, for example, exhibits a half-life as short as 50–90 mins. As the majority of plasmid DNA enters the nucleus during cell division, it must remain stable until the next disassembly of the nuclear envelope. Another factor that plays an important role in nucleic acid transit through the cytoplasm is the rate of mobility which depends on both the size and spherical structure of the molecule. The mobility of large molecules, e.g., plasmid DNA, is extremely low in the cytoplasm (42). Low mobility means a longer trafficking time to the nucleus and thus prolonged exposure to (aggressive) nucleases (34,35,43).

Increased cytosolic mobility result from complexation of DNA with cationic carriers (DNA condensation into a compacted state) (44,45), compared to naked DNA (46). Another reason for the higher level of gene expression of complexes (compared to naked DNA) could be the protection of DNA from cytoplasmic nuclease degradation. Several studies have demonstrated excellent stabilization using cationic complexes (47), when comparing the stability of naked and complexed DNA/RNA in the presence of DNases or RNases. It was demonstrated that cationic carriers could interact with F-actin fibres altering the structure of the cytoskeleton and thus enhancing the permeability for large molecules (48).

5. Nuclear entry

One of the crucial steps for successful delivery of DNA into its site of action is crossing the nuclear membrane. The entry of macromolecules to the nucleus occurs through the nuclear pore complex (NPC) which allows a passive diffusion of molecules of up to 50 kDa molecular weight or about 10 nm in diameter, but in the case of larger molecules NPC is capable of actively transporting particles of about 25-

50 MDa or about 25 nm diameter (49). Nuclear localization signals (NLS), due to their characteristics to target macromolecules to the nucleus and increase transfection efficiency, are being actively investigated (50). The other way for DNA to enter to the nucleus is during mitosis where the nuclear membrane is broken down so that DNA and macromolecules can easily gain access.

6. Decomplexation

The dissociation of DNA from the condensing agent is an important step for the host transcription factors to initiate the transcription reaction. The decomplexation process may occur after endosomal escape in the cytoplasm (36) or after nuclear entry (44) (see: Fig. 1.1).

7. Transcription and translation

Inside the nucleus, the next step for gene therapy is the transcription process which depends on the promoter strength and presence of an enhancer in the vector which effects on transfection efficiency (51). The successful transcription process leads to the translation and formation of the desired protein (the active form of the required drug, achieved by delivering of the prodrug DNA).

1.3.2. Naked Plasmid DNA Transfection

1. Mechanical methods

1. **Microinjection:** The most direct method to introduce DNA into cells is microinjection, either into the cytoplasm or into the nucleus.
2. **Particle bombardment - the "gene gun":** The idea behind gene-mediated particle bombardment (or use of the so-called "gene gun") is to move naked DNA plasmid into target cells on an accelerated particle carrier. Biolistic (a contraction of biological and ballistic) delivery utilises heavy metal particles propelled at a sufficient velocity into the target cell. Acceleration is achieved by a high-voltage electric spark, or a helium discharge.

3. **Naked DNA transfer by transient occlusion of blood flow:** The strategy for this approach is to increase the retention time of plasmid DNA by transiently blocks the blood flow through the target organ. Due to the technical difficulty in blocking blood

flow through the lung, trials started with the liver. In this approach, satisfactory gene transfer can be achieved by a simple occlusion of blood flow through the liver following intravenous administration of naked plasmid DNA (4).

2. Physical methods

1. **Electroporation:** This technique, termed electroporation or electropermeabilization, exposes the cell membrane to high-intensity electrical pulses that can cause transient and localized destabilization of the barrier. During this perturbation, the cell membrane becomes highly permeable to exogenous molecules, e.g., DNA, present in the surrounding medium.
2. **Sonoporation:** Sonoporation enhances cell permeability via the application of ultrasound, using sinusoidal probes at MHz frequencies.
3. **Laser irradiation**: The laser beam is commonly focused onto the target cell via a lens. Predictably, the permeability of the cell membrane is modified at the site of the beam impact (probably) by a local thermal effect.
4. **Magnetic field-enhanced transfection-magnetofection:** The idea is to associate magnetic nanoparticles with DNA and either its transfection reagent or its viral vector. The magnetic nanoparticles are made of iron oxide, which is biodegradable, with a polymer coating. The magnetic particles are then concentrated preferentially into the target cells by the influence of an external magnetic field. This technology allows delivery of genetic material to the target cell surface (52,53).

1.3.3. Complexed Plasmid DNA Transfection

1. Cationic polymers (Polyplexes) for gene delivery

Since the cellular membrane is negatively charged, cationic polymers have received most of the attention as potential carriers for genes. The Coulombic forces governing the interaction between plasma membrane and polycations are so strong that the influence of other properties of the polymers (e.g., hydrophilicity) is drastically diminished. However, the cationic polymers do not constitute the ideal solution. Cationic carriers must contain enough charge to neutralise the DNA and also to provide sufficient residual charge for interaction with the membrane of cells. On the other hand, in conditions of contact with serum, the positive charge of the carrier

might be never enough to counterbalance the negatively charged serum components. The internalisation of conjugates can be prohibited (2).

1. **Cationic polypeptides**

The interaction of nucleic acids with basic polyelectrolytes is a process that has been known for a long time. An early application of polycations was the development of a standard procedure for assaying infectious viral nucleic acids, based on the observation that cationic polyelectrolytes such as PL, polyornithine, or diethylaminoethyl dextran, application of cationic polypeptides (PL, polyornithine, polyarginine) included their use as model compounds in the investigation of interaction between nucleic acids and histone species, which plays an important role in the regulation of genetic process. These studies suggested that the binding reaction is more than a simple electrostatic neutralisation, involving steric selectivity and inducing stabilisation of DNA. these polymers have been used so far in the gene delivery (54).

2. **Dendritic polyamidoamines**

The dendrimers are highly branched polymers with a globular architecture. Polyamidoamine (PAMAM) dendrimers can be synthesised with a well-defined diameter and a precise number of terminal amino groups at each branching level ("generation"). Haensler and Szoka (55) were the first to investigate their use as carriers for DNA in gene therapy. Subsequent studies demonstrated that PAMAM–DNA complexes were able to mediate an efficient transfer of plasmid DNA into various cell types in vitro. So far, PAMAM dendrimers have been applied as carriers for gene delivery (55,56).

3. **Polyethylenimine**

Polyethylenimine (PEI) is produced by the acid-catalysed polymerisation of aziridine, involving propagation through cyclic ammonium cations. Due to end-group reactions and to the high reactivity of the intermediate ammonium species, the resulting polymer is usually branched. PEI is very soluble in water and has a high capacity to carry positive charges, as every third atom is ionisable nitrogen (1,13). PEI has been proposed as a carrier for plasmid DNA, but the larger molecular weight PEIs are often found to be too toxic to target cells (38). This together with its inherent inhomogeneity makes it an unsuitable vector.

4. **Cationic block copolymers**

Cationic block (or graft) copolymers have been developed as carriers for DNA or antisense phosphorothioate oligonucleotides (PS-ODN), from polyspermine and polyethylene glycol (PEG, polyethylene oxide), by Kabanov and co-workers (57-59). Such a block copolymer cationic carrier architecture contains both the water soluble polycations of spermine and the water-soluble non-ionic PEG moieties. They delivered antisense ODNs to achieve increased antiviral activity in vitro (57-59).

5. **Polyethylene glycol**

PEG is the term used for the polyoxyethylene polymers with low molecular weight, while the term polyethylene oxide is preferred to designate polyoxyethylenes with high molecular weight. This convention is rather obscure and generally overlooked. PEGs constitute a class of water-soluble polymers with many applications (60). When crosslinked, PEGs behave like typical hydrogels, a form in which they were employed as carriers in various drug delivery formulations. However, their use in the delivery of genes is not based on hydrogels. PEG chains were incorporated covalently as chemical modifiers in order to (a) mask the identity of genes, protecting them from recognition by nucleases, and (b) enhance cellular penetration, due probably to the chain structure of PEG (1,18).

6. **Cyclodextrins**

Cyclodextrins (CDs) comprise a group of water-soluble cyclic polysaccharides containing glucose units with (1,4)-linkages. α-CD, β-CD, and γ-CD have respectively 6, 7, and 8 glucose units and they are all available commercially. Their cyclic structure provides an internal hydrophobic cone-shaped cavity that is surrounded by a hydrophilic shell containing a large number of hydroxyl groups. Due to this conformation, CDs and their derivatives readily form complexes with a large variety of compounds, and consequently they have been investigated as carriers for drugs (61).

7. **Electrically conductive polymers**

Polymers possessing conjugated p-electron backbone chains have unusual electronic properties. The application of these materials in oligonucleotide chemistry originated in the development of an electrochemically controlled synthesis of conductive polymer films containing genes. Copolymerisation of pyrrole and pyrrole-ODN covalent conjugates was performed electrochemically and resulted in deposition on an electrode of solid films.

2. Cationic lipids (Lipoplexes)

Cationic lipids are especially attractive as they can be easily prepared and extensively characterised. Further, each of their constituent parts can be modified, thereby facilitating the elucidation of structure-activity relationships. A great number and an impressive variety of synthetic vectors have been prepared and their transfection efficiency evaluated not only in experimental studies, but also in clinical trials for treatment of diseases such as cancer (62,63) and cystic fibrosis (64,65). At this point, some positive results have been attained, but the overall outcome indicates that a crucial requirement for successful gene therapy is the use of more efficient vectors (66). Their three fundamental constituent parts are: the cationic headgroup, hydrophobic domain and connecting linker. There are possible correlations between the length, saturation, and type of hydrophobic moiety and transfection efficiency. Intracellular DNA-release strategies that can be triggered as a function of the incorporation of cellular environmentally-sensitive groups (pH-, redox- and enzyme-sensitive) within the linker moiety are also under investigation.

The length and type of the aliphatic chains incorporated into cationic lipids significantly affect their transfection efficiency. Thus, vectors are often prepared in a series differing in their hydrophobic domain. The hydrophobic domain has also been functionally modified by the inclusion of highly fluorinated alkyl chains which are both hydrophobic and lipophobic, a characteristic which may better protect the lipoplex from unwanted interactions. At first, a series of close fluorinated analogues of DOGS (with either both chains fluorinated to varying degrees or just a single chain fluorinated with the other remaining a regular alkyl chain) were prepared in order to chart the effect of the hydrophobic/lipophobic balance on the transfection efficiency (67).

1.3.4. Basic Principles of Cationic Lipid-Mediated Gene Transfection

The first step in the preparation of vector/DNA aggregates suitable for gene transfer is the condensation of the DNA, which is driven by an electrostatic interaction between the cationic lipid and the polyanionic DNA. Spontaneous self-assembly into nanometre-scale particles (lipoplexes, nanobioparticles) results, leading to shielding of the DNA from the nucleases of the extracellular medium. Use of an excess of cationic amphiphile (quantified by the lipid/DNA ratio resulting in a mean theoretical charge ratio of the lipoplex (+/-)) gives the lipoplex surface a positive charge, which is

presumed to mediate subsequent cellular uptake by interaction with negative cell surface structures such as heparin sulfates.

As a result of non-specific endocytosis, the lipoplex is encapsulated in intracellular vesicles, though fusion-based cellular uptake is not totally excluded. The DNA must then avoid degradation in the late endosome/lysosome compartment by escaping from the (early) endosome into the cytoplasm. Trafficking of the DNA through the cytoplasm precedes uptake by the nucleus of the target cell, and then transgene expression occurs. In the nucleus, the DNA appears to be separated from its vector. Microinjection experiments have suggested that gene expression does not occur if the DNA remains condensed in intact lipoplexes (68). The efficiency of cationic lipids for gene transfection can be evaluated in terms of gene delivery (percentage of transfected cells) or gene expression (amount of transgene protein produced). The efficiency of any transfection reagent also strongly depends on the cell system chosen for its evaluation (transformed cell lines or primary cells in vitro, in vivo administration), efficiency gains in vitro do not therefore automatically lead to higher efficiencies in vivo. How the relative efficiency of cationic lipids is compared is crucial, so quantifying the efficiency of cationic lipid systems needs to take into account their intended use, i.e., on the experimental or clinical setting.

Cationic lipids were first introduced by Felgner *et al*. (2,69), following early attempts to transfer DNA via encapsulation in liposomes (70,71). Thus, the first reported lipid was DOTMA (*N*-(1-(2,3-dioleyloxy)propyl)-*N*,*N*,*N*-trimethylammonium chloride), which consists of a quaternary amine connected to two unsaturated aliphatic hydrocarbon chains via ether groups (2). Synthesis of the multivalent lipopolyamine DOGS (dioctadecylamido-glycylspermine) was reported soon afterwards (72) and the efficiency of the vector DC-Chol (3β-(*N*-(*N*',*N*'-dimethylaminoethyl)carbamoyl) cholesterol) with cholesterol as the hydrophobic portion closely followed (73). The transfection activity of cationic lipids (especially those which cannot form bilayers alone) can be increased by their formulation as stable liposomes with the neutral colipid DOPE (dioleoyl phosphatidylethanolamine) (3). Inclusion of DOPE is presumed to enhance endosomal escape of the lipoplexes into the cytoplasm as DOPE is thought to have fusogenic properties important for endosomal membrane disruption (74). The use of these initial lipids demonstrated the transfection ability of cationic lipids. However, this “proof of principle” stage has been followed by a highly challenging period. Indeed, progress in improving the level

of transfection efficiency up to that required for therapeutic use has been slow. This is possibly linked to an unclear structure-activity relationship in vector design, and to the related incomplete understanding of the highly complex series of steps involved in transfection. Thus, the development of novel lipids is justified, a novel cationic lipid being not just a "me too" addition, but rather opening new possibilities for differently influencing those steps (9). Accordingly, numerous novel vectors were developed, representing a wide variety in structures and thus numerous potential mechanisms by which better transfection levels might be obtained (9,75-79).

1.3.5. Basic Structural Features of Cationic Lipids

A cationic lipid is a positively charged amphiphile, which generally contains the three following structural domains (Fig. 1.2): i) a hydrophilic headgroup which is positively charged, usually *via* the protonation of one (monovalent lipid) or several (multivalent lipid) amino groups; ii) a hydrophobic portion composed of a steroid or of alkyl chains (saturated or unsaturated); and iii) a linker (connecting the cationic headgroup with the hydrophobic anchor) whose nature and length may impact on the stability and the biodegradability of the vector. Modifications of the hydrophobic domain have shown that optimal vector structure is often dependant on this moiety, which can fall into various structural classes and variants. Finally, labile linkers have been introduced which are sensitive to various biological stimuli, inducing DNA release at defined time-points during the intracellular trafficking of the lipoplex. The following sections will therefore successively cover the important advances made to these three fundamental functional domains of any cationic lipid.

Cationic Headgroup Design

Monovalent lipids and the hydration/packing issue

DNA binding by the vector requires a headgroup which is capable of sustaining a positive charge at physiological pH (Fig. 1.2). The charge is most often located on amino groups, as was the case for the 'early' vectors. However, other charged groups have been employed. The vast majority of cationic lipids for gene delivery rely on the charge accommodated on a nitrogen atom, and there appears to be a relationship between the hydration of such mono-ammonium headgroups and the transfection activity. Figuratively, the greater the imbalance between the cross-

sectional area of the headgroup (small end) and the hydrophobic moiety (large end) i.e., the more cone-shaped the cationic lipid - the more unstable the resulting lipid assembly and so the greater the likeliness to undergo fusion with anionic vesicles. Lipoplex instability is presumed to result in improved transfection as fusion between the cationic lipoplex and the endosomal membrane leads to DNA release into the cytoplasm (36,80-82).

Spermine

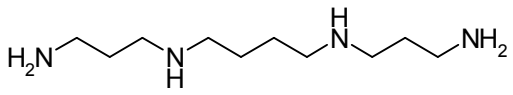

DOPE, a helper lipid

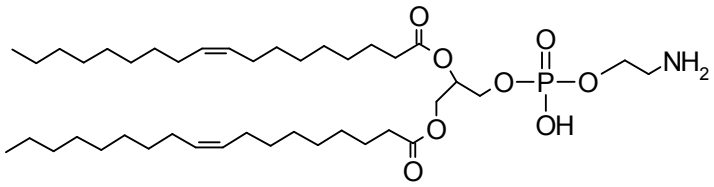

DOTMA

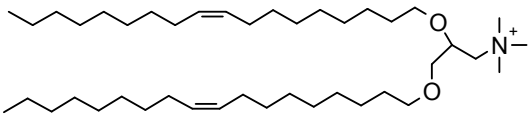

Lipofectin® is a 1:1 (w/w) liposome formulation of DOTMA and DOPE

DOSPA

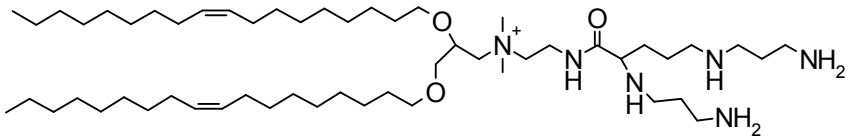

Lipofectamine™ is a 3:1 (w/w) liposome formulation of DOSPA and DOPE

Transfectam (DOGS) (72)

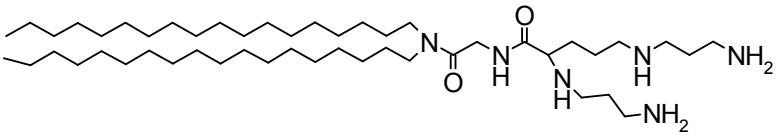

Fig. 1.2. Typical vector molecules for gene delivery.

Multivalent headgroups

As multivalent cationic lipids may form liposomes with a greater surface charge density than their monovalent counterparts, they are generally expected to be better at DNA binding and delivery. A rational approach was the incorporation of natural polyamines e.g., spermidine and spermine with their ability to interact with the minor groove of B-DNA (83). Triamine spermidine in cholesteryl-spermidine (84), and tetraamine spermine in the lipid DOGS (72) are early representative examples. The presence of protonation sites with different pK_a values in DOGS may actually result in buffering of the endosomal acidification, thereby protecting the DNA from degradation and facilitating its escape from the endosome. The results suggested that the tetramethylene portion of spermine might be able to bridge between the complementary strands of DNA, whereas a polyamine with a trimethylene central spacer would only interact with adjacent phosphate groups on the same DNA strand. As these branched structures have the advantage of avoiding the folding problems of linear polyamine chains, they can include additional protonation sites without affecting DNA binding. Importantly, with more protonation sites per molecule, the resulting lipoplexes can thus achieve the same charge density with lesser amounts of the cationic lipid in the formulation. This may lessen the drawback of cationic lipid-associated cytotoxicity. Indeed, as cationic lipids exhibit some degree of cytotoxicity, an optimal set of conditions resulting in high transgene expression and acceptable toxicity need to be found (15,85,86).

The hydrophobic and hydrophilic moieties of cationic lipids are commonly linked using carbamate, amide, ester or ether bonds. The linking bond mediates the stability of the cationic amphiphile, there is a balance between a vector's persistence and its toxicity which is likely to be related to its half-life in the cell. Although no particular bond emerges as consistently optimal in structure-activity studies across different vector types, ether linked vectors are stable (87); consequently, they are expected to be more toxic than ester linked lipids which may be more easily cleaved within the cell (80,81). Carbamates are thought to achieve a reasonable balance between stability and toxicity and are therefore often used (73).

The multivalent polycationic headgroups can be used for pDNA delivery. What of siRNA delivery (siFection)? There are initial similarities between pDNA and siRNA with regard to double stranded (ds) nucleic acid chains, rich in phosphate anions. Can we utilise existing non-viral gene delivery vectors for siRNA delivery?

1.4. siRNA DELIVERY – AN INTRODUCTION

The development of efficient vectors for siRNA formulation and delivery, in order for them to become real medicines is a challenge for formulation which needs an understanding of the background provided by a literature review. Many vectors used for gene delivery can be selected for the delivery of siRNA. The initial selection was based on established gene delivery and pDNA formulation (88). The emphasis hereinafter is given to the delivery of siRNA as there exist many differences between pDNA formulation and obtaining results for an optimized siRNA formulation (88).

RNA interference (RNAi) is a recently discovered gene-silencing tool that has generated remarkable excitement in biomedical research. The phenomenon of specific RNA inactivation was first discovered in fungi and plants as a defence mechanism against virus infection. Over a decade ago, this gene-silencing phenomenon was first described in plants and fungi (89). In 1998, Fire and colleagues demonstrated that RNAi could also be invoked in animals (90). Its physiologic function appears to lie in viral defence, transposon silencing, and regulation of developmental pathways. In experimental settings, RNAi was readily appreciated as a powerful tool in gene function validation (91). In addition to its use in functional genomics, RNAi holds a promise as a novel therapeutic strategy. Its attractive properties include a strong knockdown of the targeted gene for a relatively prolonged period of time and presumed high sequence specificity. Single nucleotide difference between targets can result in dramatic differences in the RNAi-mediated gene silencing, which is an interesting quality for treatment of several dominant-negative disorders by targeting specific alleles with single nucleotide mutations compared to the wild type (92). Challenging diseases failing conventional therapeutics could become treatable by specific silencing of key pathogenic genes. More specifically, therapeutic targets previously deemed “undruggable” by small molecules, are now coming within reach of RNAi based therapy. For RNAi to be effective and elicit a gene silencing response, the ds RNA molecules must be delivered to the target cell. Unfortunately, delivery of these RNA duplexes has been challenging, halting rapid development of RNAi-based therapies. The advantages of RNAi over other therapeutic modalities include its high specificity (in some cases, a single point mutation can abolish silencing effect), versatility (interfering RNA can be designed against virtually any gene), and efficiency (in many cases, genes can be silenced by over 90%) (93,94).

1.4.1. Mechanisms in RNAi

mRNA is produced by cells when the cellular metabolism is in need of a specific protein, and subject to degradation thereafter. RNAi is triggered by the presence of double-stranded RNA (dsRNA) in the cell and results in the rapid destruction of the mRNA containing identical or nearly identical sequence. Use of RNAi by means of long dsRNAs (greater than 50 bp) has been limited in mammalian systems (95). The mechanism of siRNA is not completely understood. However, the generally proposed model is that a double stranded (ds) RNA, which is targeted against a homologous mRNA, binds to the mRNA and mediates its degradation, causing the silencing of the corresponding gene (92). Between intracellular introduction of the dsRNA and the silencing of the gene, several steps occur inside the cell. The dsRNA is cleaved into smaller duplexes by an RNase III-like activity involving an endogenous ribonuclease enzyme, dicer. These shorter fragments consist of 19–21 nucleotide duplexes with two nucleotide overhangs on the 3'-position and are known as small interfering RNAs (siRNAs). Subsequently, siRNAs associate with several proteins that together form a nuclease complex known as the RNA-induced silencing complex (RISC). As the siRNA unwinds, probably through the action of a helicase, the RISC becomes activated, and the antisense siRNA strand "guides" the RISC to the complementary target mRNA through Watson-Crick base pairing interactions between the siRNA antisense strand and the mRNA. Finally, the mRNA is cleaved approximately 12 nucleotides from the 3'-terminus of the complementary siRNA strand, thereby silencing the corresponding gene (96-98).

Gene downregulation by siRNA was initially studied in *Caenorhabditis elegans, Drosophila melanogaster*, and other non-vertebrates, but RNAi-mediated gene knockdown in mammalian cells has been demonstrated (99,100). The difficulty in showing a sequence-specific siRNA mediated gene silencing in most mammalian cell types lies in a nonspecific protein production shutdown, partly mediated by the RNA-dependent protein kinase pathway, by introduction of long (>30 nucleotides) dsRNA molecules. Only by introducing the smaller siRNA can a sequence specific gene silencing effect be observed (100). siRNA, in mammalian cells, is both transient and confined to the cells in which it was introduced (100).

siRNA can be introduced in two forms into mammalian cells: 1) via transfection from the extracellular compartment as a chemically or enzymatically synthesized product or 2) as a product of intracellularly transcribed DNA upon transfection,

transduction, or infection with the transcript-encoding genetic material. Tuschl and colleagues have identified many of the requirements and preferred characteristics of siRNA with regard to silencing efficacy (100,101). siRNAs preferably consist of 19 nucleotide duplexes with 2 nucleotide overhangs on each 3'-position. The overhang sequence does not appear to be critical and can even include 2'-deoxynucleotides (like TT) which are thought to be more resistant to the action of nucleases (100,101). However, replacement of either strand with a strand composed of 2'-deoxynucleotides obliterates siRNA activity. In general, modifications to the 3'-position are better tolerated than modifications to the 5'-positions with regard to preserving silencing efficacy (101,102). The phosphorylation of the 5'-end of the siRNA, needed for activity, may explain this difference. Although base modifications may offer the prospect of increased siRNA stability, modified bases may distort normal cell metabolism, with possible toxic sequelae. Due to its high target sequence specificity, mismatches between mRNA and the siRNA duplex have been shown strongly to reduce activity (100-104). Tuschl and colleagues have identified many of the requirements and preferred characteristics of siRNA with regard to silencing efficacy (100,101). The complementary regions are connected in shRNA, produced by plasmids containing the RNA polymerase III dependent promoter (H1-RNA) region, consist of 19-nucleotide inverted repeats (forming the hairpin-stem) and a, not strictly regulated, number of spacer nucleotides forming the loop (105,106). The 3'-overhang is generally composed of 4 uridine nucleotides. By cotransfecting such a vector with a gene conferring puromycin-resistance, stable expression can be achieved (107).

1.4.2. Methods of Delivery

The therapeutic application of siRNA is largely dependent on the development of a delivery vehicle that can efficiently deliver the siRNA to target cells (108). In addition, such delivery vehicles must be administered efficiently, safely and repeatedly (109). Employed in the field of gene therapy research for over a decade, and now in some clinical trials, viral vectors have been applied to RNAi. The five types of viral vectors that are currently in use for RNAi include: retrovirus, lentivirus, adenovirus, adeno-associated-virus (AAV), and baculovirus.

Retroviruses have serious safety concerns and limitations in efficiency. Lentiviruses, a subclass of retroviruses, may find in vivo applications and are widely used for proof of concept experiments. While safety concerns still exist, lentiviruses

are free of some of the major disadvantages of retroviruses. Adenoviral vectors are found in ~25% of current clinical gene therapy trials. These are vectors of choice for tumour-targeting gene therapy, where a relatively short duration of action is sufficient, unlike the need for long-term gene replacement therapy in treatment of genetic disorders (e.g., cystic fibrosis). A major disadvantage of adenoviral vectors, however, is the lack of clear tissue tropism and dependence on defined surface receptors of the target cell, which are often absent in the tissues of interest (especially tumour cells), but adenovirus hepatotoxicity is significant and can be dose-limiting, so reducing possible therapeutic effects in the target tissue (110).

Delivery of RNAi without viral vectors has been tried with a wide variety of agents: injection of pure, unmodified ("naked") siRNA, chemically stabilized or modified RNA, encapsulating the siRNA in microparticles or liposomes, and binding siRNA to cationic or other particulate (nanoparticle) carriers (111).

1.4.3. Chemically Modified siRNA Molecules

Duration of siRNA activity in vivo and any possible therapeutic effect will depend on its stability in the serum. Double stranded RNA is more stable than single strand RNA in serum, but it is still degraded within a few hours by RNase. Chemical modifications may increase siRNA stability in serum without affecting the RNAi effect. Ideally, these chemical modifications could also contribute to increase thermal stability, cellular tropism, silencing activity and the pharmacokinetic properties of the siRNA (112). Other chemical alterations include modifications of residues added at the 2' position of the ribose: 2'-*O*-Me, 2'-*O*-allyl, and 2'-deoxyfluorouridine modifications. These modifications were based on early reports showing that the 2'-OH group is not required for silencing in siRNA (113,114).

1.4.4. Liposomes and Nanoparticles

Research into delivery of siRNA is at quite a preliminary level. One reason for this may be the apparent misconception that all poly-nucleic acids are much alike and should be delivered to cells in comparable ways using comparable delivery systems. Superficially this is true. Both pDNA and siRNA have anionic phosphodiester backbones with identical negative charge:nucleotide ratios and should therefore interact electrostatically with cationic lipids to form lipoplex nanoparticles that are able to transfer the nucleic acids into cells. However, pDNA and siRNA are otherwise

very different from each other in molecular weight and molecular topography with potentially important consequences (115).

Unmodified siRNA has a half-life of less than an hour in human plasma, and circulating siRNAs are rapidly excreted by kidneys thanks to their small size. To address the concerns of low stability in serum and rapid renal excretion, several different approaches have been developed to deliver envelope packaged siRNA. The most popular envelopes included liposomes and other nanoparticles, both as simple packages, but also in combination with specific homing signals designed to direct the preferential uptake by a specific target tissue or a group of target cells. Some research groups have used liposomes for in vivo delivery with good results. Sorensen *et al*. (116) used cationic DOTAP liposomes to inject RNAi against TNF-α, and were able to suppress lethal reaction to LPS injection in a mouse model of sepsis. In the same publication, they report successful silencing of a marker gene (GFP) in liver after intravenous injection of liposomes (116).

1.4.5. Cationic Lipids

Cationic lipids, the most used non-viral vectors, are composed of positively charged lipid bilayers and can be complexed to negatively charged siRNA duplexes (116,117). Cationic lipids are routinely used for delivery of poly-nucleic acids into mammalian cells in vitro, and systemic *i.v*. administration of lipoplexes (composed of cationic lipid, neutral helper lipid and nucleic acid) has been applied for gene and siRNA delivery in vivo. The development of novel siRNA formulations for the systemic in vivo application of siRNAs is a current challenging area of research. In contrast to "naked" or non-formulated siRNA molecules, the siRNA-lipoplexes are strongly taken up by the vascular endothelium in the liver, heart, and lung (118). Vectors are being developed based on cationic polymers or lipids that contain functional groups to mediate appropriate interactions with the extracellular environment or to bind to specific cellular macromolecules. siRNA delivery decreases target protein production (119). However, the efficacy of RNAi depends upon efficient delivery of the intermediates of RNAi, short interfering RNA (siRNA) and short hairpin RNA (shRNA) oligonucleotides. The delivery challenge is even greater when the aim is to inhibit the expression of target genes in animal models (120).

While there is a great deal of structural variation in lipid molecules that are able to mediate transfection, all have a number of common features. First, there is a

positively charged head group that usually contains one or more positively charged nitrogen atoms to allow interaction between the transfection reagent and the negatively charged sugar–phosphate backbone of a nucleic acid molecule. A spacer usually links the charged head group to one, two or three hydrocarbon chains. In some instances, this spacer may play a role in promoting contact between the cationic lipid and the nucleic acid. The hydrocarbon chains are often 14 or more carbon atoms in length. The degree of saturation and the presence of *cis*- or *trans*-isomers introduce more potential for structural variation (109).

RNAi is being exploited for a variety of laboratory applications in biology and as a promising therapeutic product. The clinical use of siRNA is hindered by three major problems: 1) rapid enzymatic degradation resulting in a short half-life in the blood; 2) poor cellular uptake; 3) insufficient tissue bioavailability. In general, these problems can be partly overcome by mixing siRNAs with cationic lipids or cationic polymers to form complexes, which could be additionally surface-modified with specific ligands allowing for targeting of required tissues (97).

1.4.6. siRNA Delivery Steps

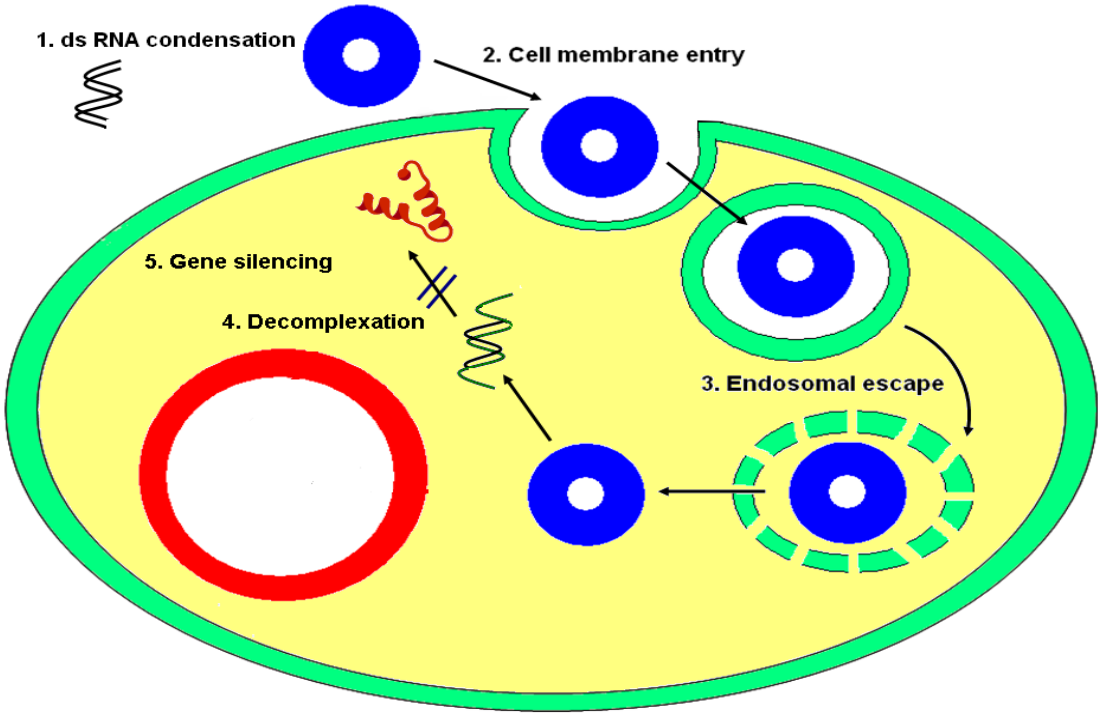

Fig. 1.3. Steps in the process of non-viral siFection by endocytosis showing the barriers for RNA nanoparticles, from the RNA-lipoplex formation to gene silencing.

There is a need for a better understanding of the mechanism of gene silencing to targeted cells and detailed understanding of the barriers for siRNA delivery to achieve efficient formulation (Fig. 1.3). These barriers that hinder the delivery of siRNA to its physical site of action (the cytoplasm) are summarized, and they follow after RNA condensation, cell membrane entry, and endosomal escape as outlined above for DNA delivery. The dissociation of RNA from the condensing agent, decomplexation, is an important step for the host transcription factors to initiate the transcription reaction. This decomplexation process occurs after endosomal escape in the cytoplasm. It can be compared with the dissociation of DNA from its condensing agent, a step that must occur for the host transcription factors to initiate transcription. DNA decomplexation may occur after endosomal escape in the cytoplasm (36) or after nuclear entry (44). A sufficient amount of synthetic siRNA must be delivered to cells to show an RNAi effect, gene silencing

1.4.7. In Vitro Use of siRNA

In vitro use simplify many of the problems associated with targeted cell delivery, target selectivity, homeostasis mechanisms, and possible non-target cell toxicity encountered in vivo. Yet, the cellular membrane is still an important physical barrier to the efficient intracellular introduction of nucleic acids. Similarly as in gene and antisense studies, passage through the cell membrane of nucleic acids is difficult to achieve as a result of their hydrophilic and polyanionic nature. Experience with DNA and antisense oligonucleotides has provided a variety of chemical and physical techniques that would allow the transfection or infection of cells with extracellularly synthesized siRNA, as reviewed recently (16,33,121). The chemical techniques are generally based on the use of (poly)cations. The cationic compounds condense the siRNA, resulting in the formation of particles. These particles generally have a net positive charge, as an excess of the cation provides efficient condensation and prevents particle aggregation. The net positive charge of the particle additionally promotes electrostatic interaction with the overall negative charge of the cell membrane. Both by condensing the siRNA and promoting cell membrane interaction, relatively efficient cell transfection can be achieved. A whole range of cations exists that have been shown to promote the intracellular delivery of nucleic acids (16,33,121). Of these, the cationic lipids, cationic polyamines and combinations of both are the most prominent.

The ultimate in vitro transfection-efficiency of a cationic compound appears to be dependent on the characteristics of the cell e.g., cell type, confluency, and passage number, as well as the properties of the cationic particle, e.g., cell medium compatibility, cell toxicity, cation structure, strength of electrostatic interaction, and particle size. It appears that the most popular cationic agents possess an ability to influence the intracellular processing of the particle in addition to their nucleic acid condensing ability. Although interaction between the cell surface and the delivery system promotes siRNA uptake, appropriate intracellular trafficking should still follow the interaction. The cationic lipoplexes are likely to be taken into cells by endocytosis. Therefore, the lipoplex and/or its siRNA should be able to escape the endosomal vesicle to evade lysosomal degradation and allow RNAi effects to occur.

Although, systematic studies evaluating the efficiency of siRNA introduction into cells by various transfection reagents are lacking thus far, it is conceivable that some polycations will have a more suitable structure for the introduction of small siRNA than others. Physical techniques to overcome the cellular membrane barrier either force the nucleic acid into the cell (like gene gun, magnetofection) or lower the cell membrane barrier (electroporation, or ultrasound) (121). For transfection of genetic material encoding for transcript siRNAs or shRNAs the same considerations are valid. Recent research suggests that nuclear localization of siRNA produced by transcription may be required for efficient gene silencing (66), although another study reports cytoplasmic degradation of mRNA by externally applied siRNA (122). It has been suggested that the intracellular processing of externally applied siRNA or intracellularly transcribed siRNA may be different (66). For transcript-encoding DNA, additionally, viruses can be used to deliver the genetic material. The viral techniques make use of the evolutionary adaptations of virions for efficient cell attachment and correct intracellular processing for high-level transcription of delivered genetic material. From gene therapy studies, useful viruses have been identified: the retrovirus, adenovirus, herpes virus, lentivirus, and baculovirus, each having its own advantages and disadvantages. These viral systems can also be attractive for the delivery of transcript-encoding DNA in vitro. Taken together, these systems could provide means for studying loss-of-function phenotypes, target identification and validation, and identifying possible therapeutic strategies for siRNA in vitro. Still, to assess a protein's importance and potential in disease-control, which is in the ultimate interest of pharmaceutical applications, in vivo studies are needed.

The production of gene-specific synthetic siRNA sequences useful in functional genomics programs and, more intriguingly, potentially as drugs to treat disease is now feasible. siFection with siRNA requires a delivery system displaying the capability to mediate the RNA sequence to the intracellular environment. Cationic lipids carriers have long been used to mediate the transfer of DNA into cells; since the nature of their interactions with DNA and RNA is identical (charge/charge), it seems obvious to adapt formulations that were developed for pDNA to the delivery of siRNA. However, a closer look at this process reveals problems. One particularity of DNA formulation with a cationic entity such as peptides, proteins, polymers, or cationic lipids is the occurrence of the so-called bDNA condensation process. This phenomenon is triggered when 70–90% of the DNA phosphodiester charge is neutralized, and is manifested by the collapse of DNA into nanostructures of differential morphology due to the predominant hydrophobic nature of the DNA nanoparticle. A minimal length of the DNA of about 800 bp is required for a DNA condensation process to occur. This finding has important consequences: short double-stranded siRNAs are devoid of such a condensation process. While the volume occupied by a condensed DNA nanoparticle is about 10,000-times smaller than of its uncondensed counterpart, short double-stranded siRNA stretches retain their initial volume when complexed to a cationic entity. As a result, several copies of siRNA are complexed/incorporated per liposome rather than one single entity of condensed DNA (11).

Interestingly, pDNAs delivered to cultured cells by a transfection reagent naturally localize to the nucleus within short time after transfection, whereas their carrier molecules remain in perinuclear area. In sharp contrast, synthetic siRNAs localize to perinuclear regions and not to the nucleus after siFection, even after extended periods of time (108). These differences in uptake, intracellular trafficking, and storage have important consequences: firstly, the formulation parameters of synthetic siRNA need to be carefully established prior to use. In other words, a delivery reagent developed for DNA is most likely not suitable for siRNA. Secondly, siRNA delivery must be devoid of any toxic effects which come with the siFection reagent. We have shown that certain widely used transfection reagents induce a degree of cellular toxicity that severely interferes with the outcome of the gene down-regulation study.

1.4.8. Delivering siRNA In Vivo Using Non-viral Carriers

Many non-viral carriers used in the delivery of DNA for gene therapy have been adopted for siRNA delivery. As RNAi is active in the cytoplasm, delivery of siRNA is relatively easier than delivery of plasmid or viral DNA, which has to be in the nucleus for expression. Non-viral siRNA delivery to the disease tissue does not elicit an immune response, which has a great advantage for its application in drug target validation and also allows multiple administrations of siRNA, which are crucial for siRNA therapeutic applications. Cationic lipids and polymers are two major classes of non-viral siRNA delivery carriers and both are positively charged and can form complexes with negatively charged siRNA. The siRNA–carrier complex can be condensed into nanoparticles of ~100 nm, allowing very efficient cellular uptake of the siRNA agent through endocytosis. Several studies, reviewed in (120), have shown that cationic lipids and polymers can enhance siRNA delivery in vivo through systemic routes either intravenously (*i.v.*) or *i.p*. Carrier-administered siRNA agents were efficiently knocking down the target genes and achieved antitumor efficacies. Some ligand-targeted siRNA delivery systems have been developed using the cationic liposome complex and polymer complex systems. Recent successes using ligand-targeted complexes (123-125) to deliver therapeutic siRNA into tumour tissues and liver tissues suggest that targeted systemic delivery for siRNA therapeutics is promising (126,127). Systemic siRNA delivery requires stability in the blood and in the local environment to enter the target cells. Recent studies showed that tumour-targeting siRNA delivery was achieved by using a cyclic RGD-tripeptide ligand-directed nanoparticle and that its application in antiangiogenic treatment for cancer was obtained by systemic siRNA delivery (128). Antibody-mediated delivery of siRNA was reported for tumour targeting via cell-surface receptors (124). This antibody-mediated binding to artificial tumour cells is interesting for a proof of concept, but it might well have limitations for clinical-viable delivery (120).

1.4.9. Delivering siRNA In Vivo Using Local Administration

The choice between local and systemic delivery depends on what tissues and cell types are targeted. Skin and muscle are better accessed using local siRNA delivery, but lung and tumours are reached efficiently by local or systemic siRNA deliveries. Different approaches show that siRNA can be efficiently delivered to various tissue types (103).

Intranasal

Airway delivery of siRNA is a very useful method for target validation and therapeutic development because of the relevance of the respiratory system in various diseases (129,130).

Intraocular

An increasing number of clinical protocols have been approved for treating eye diseases with nucleic acid drugs, such as antisense oligonucleotides or RNA aptamers (131).

Intracerebral

The brain tissue is the foundation of the central nervous system (CNS), obviously a very important biological system that draws interest for functional genomics research and therapeutic development. A recent study showed that infusion of an aqueous solution of chemically protected siRNA oligonucleotides directly into the brain was able to selectively inhibit gene expression (132).

Intramuscular

The skeletal-muscle tissue is accessible for local siRNA administration. Direct injection of siRNA formulated with cationic lipids or polymers can be considered for local delivery, although inflammation caused by the injection is a common problem. A recent study with non-formulated siRNA delivered by direct injection into mouse muscle followed by electroporation demonstrated a significant gene silencing that lasted for 11 days (133).

Intratumoural

Intratumoural delivery of siRNA is a very attractive approach for functional validation of tumourigenic genes. Inhibition of tumour growth in two human breast cancer xenografts using intratumoural delivery of VEGF specific siRNA was observed (134).

1.4.10. siRNA Delivery In Vivo Using Systemic Administration

Usually, the purpose of systemic administration is not to deliver siRNA throughout the entire body, but to reach specific diseased tissues. Two tissue types have been of particular interest for many siRNA delivery efforts: liver and tumour.

Malignant tumours grow fast and spread throughout the body via the blood or the lymphatic system. Metastatic tumours established at distant locations are usually not encapsulated and thus, more amenable for systemic delivery. The local siRNA administration methods discussed above can meet the requirements for most functional genomics studies by acting on primary tumours or xenograft models, which

form the basis of most cancer biology research. However, systemic delivery of siRNA is needed not only for studies related to gene functions, but also for siRNA-based cancer therapeutics, targeting the tumour and the neovasculature. Systemic siRNA delivery imposes several requirements and greater hurdles than local siRNA delivery, the stablety of oligonucleotides in the blood and in the local environment are needed to enter the target cells, and the siRNA needs to pass through multiple tissue barriers to reach the target cell (107).

1.5. AIMS

The aims of this thesis are to design and develop non-toxic, non-viral vectors for in vitro and then possible in vivo applications. These vectors are based upon our novel spermine conjugates, and we have made systematic changes to the length, type, and position of the hydrophobic anchor. These lipospermine verctors (cationic lipids) probably assist in the self-assembling of polycationic scaffolds as well as facilitating absorptive endocytosis and/or fusion with cell membranes. These lipospermines form spontaneous complexes with negatively charged poly-nucleic acids leading to the formation of nanoparticles after removal of small counterions from both the cationic carriers and the nucleic acids in a thermodynamically favoured step which drives and stabilizes complex formation. Thus, these formed nanoparticles are suitable for gene or siRNA delivery. We have chosen pEGFP as the reporter gene and a commercially available fluorescein-labelled model siRNA. The formed complexes will be monitored using: ethidium bromide (EthBr) fluorescence quenching assay for DNA, RiboGreen intercalation assay for siRNA, a light scattering assay, gel-shift (gel electrophoresis) assays (including DNase protection), particle size measurement by laser-light scattering, zeta-potential measurement, and confocal microscopy visualization.

The transfection efficiency of these novel lipopolyamine vectors will then be investigated in an immortalized cancer cell line (HtTA) and in a primary (hard-to-transfect) skin cell line (FEK4). Furthermore, we will achieve a key aim if we are able to deliver efficiently in the presence of serum, i.e., in the presence of DNase and RNase. Also, the cytotoxicity of these compounds will be investigated using the MTT cytotoxicity assay for the comparison between structure and function versus cytotoxicity for both DNA and siRNA delivery.

CHAPTER 2

Materials and Methods

2.1. CHEMICALS

N^1,N^{12}-Dimyristoleoyl spermine, N^1,N^{12}-dimyristoyl spermine, N^1,N^{12}-dioleoyl spermine, N^1,N^{12}-distearoyl spermine, N^4-cholesteryl,N^9-oleoyl spermine N^4-decanoyl,N^9-stearoyl spermine, N^4-decanoyl,N^9-oleoyl spermine, N^4,N^9-diarachidonoyl spermine, N^4,N^9-diarachidoyl spermine, N^4,N^9-didecanoyl spermine, N^4,N^9-dieicosenoyl spermine, N^4,N^9-dierucoyl spermine, N^4,N^9-dimyristoyl spermine, N^4,N^9-dinervonoyl spermine, N^4,N^9-dioleoyl spermine, and N^4-lithocholoyl,N^9-oleoyl spermine were kindly provided by Shi Li, Department of Pharmacy and Pharmacology, University of Bath, UK. N^4,N^9-Dilauroyl spermine, N^4,N^9-dimyristoleoyl spermine, N^4,N^9-dioleoyl spermine, N^4,N^9-dioleyl spermine, N^4,N^9-dipalmitoyl spermine, N^4,N^9-diretinoyl spermine, N^4,N^9-distearoyl spermine, N^4,N^9-distearyl spermine, N^4-myristoleoyl,N^9-myristoylspermine, N^4-oleoyl,N^9-retinoyl spermine, N^4-oleoyl,N^9-stearoyl spermine N^4-palmitoyl,N^9-retinoyl spermine and twelve heterocyclic N^4,N^9-diacyl spermines were kindly provided by Mostafa Khamis, Department of Pharmacy and Pharmacology, University of Bath, UK.

Ethidium bromide (EthBr), (4-(2-hydroxyethyl)-1-piperazineethanesulfonic acid) (HEPES), ethylenediaminetetraacetic (EDTA) sodium salt, tris-acetate-EDTA (TAE 1x), 3-(4,5-dimethylthiazol-2-yl)-2,5-diphenyltetrazolium bromide (MTT), dimethyl sulfoxide (DMSO) were routinely purchased from Sigma-Aldrich unless otherwise stated and used without purification. *Luria Bertani* (LB) broth, LB agar and ampicillin were purchased from Sigma-Aldrich. *Escherichia coli* competent cells JM109, high efficiency (>10^8 cfu/μg) were purchased from Promega.

LB broth and LB agar were prepared by dissolving the specified amount of powder in 1 L milliQ water according to the formula shown below. Both LB agar and LB broth were autoclaved (121 °C, 15 lb/inch^2) for 30 mins, then both media were allowed to cool to 40 °C.

LB broth is composed of:

Tryptone (pancreatic digest of casein)	2 parts (10 g/L)*
Yeast extract	1 part (5 g/L)
NaCl	1 part (5 g/L)

*(g/L) is the concentration of each ingredient after preparation of 20 g/L milliQ water as recommended by the manufacturer.

LB agar is composed of :

Agar	3 parts (15 g/L)*
Tryptone (pancreatic digest of casein)	2 parts (10 g/L)
Yeast extract	1 part (5 g/L)
NaCl	1 part (5 g/L)

*(g/L) is the concentration of each ingredient after preparation of 35 g/L milliQ water as recommended by the manufacturer.

Cell culture chemicals used for media preparation were purchased from Gibco used without further purification. Cell culture plates, flasks and Pipettes from fisher. Sterile Falcon polypropylene tubes (15 and 50 ml) and FACS polystyrene test tubes from Falcon. Ultracentrifuge tubes obtained from Eppendorf Ltd. Lipofectin and Lipofectamine were purchased from Invitrogen, Transfectam® was from Promega and Foetal Calf Serum FCS was from PAA laboratories. Autoclaved (sterile) phosphate-buffered saline (PBS) pH 7.3 contains 10 mM phosphate buffer, 2.7 mM KCl and 137 mM NaCl in MilliQ water. Trypsin was diluted to a working concentration of 0.25 % w/v with PBS.

pEGFP vector (4.7 kbp) was purchased from Clontech, and deoxyribonucleic acid (DNA) from calf thymus, activated and lyophilized powder was purchased from Sigma-Aldrich. Plasmids were isolated and purified using HiSpeed™ plasmid Maxi kit, obtained from Qiagen. MilliQ water was obtained from a MilliQ PF plus system with ultra-filtration cartridge, Millipore Ltd., free of DNase and RNase. Label IT® RNAi Delivery Controls (Fluorescently labelled RNAi duplexes) and TransIT-TKO® Transfection Reagent were purchased from Mirus.

2.2. BUFFERS AND MEDIA

EMEM Earle's Minimal Essential Medium

FCS Foetal Calf Serum

HEPES buffer (20 mM NaCl, 2 mM HEPES,10 μM EDTA, pH 7.4)

PBS Phosphate-buffered saline

TE buffer (50 μl, 200mM Tris-HCl, 20 mM EDTA, pH 7.5, in DEPC-treated water)

TAE buffer (Tris-Acetate-EDTA, 40 mM Tris-Acetate and 1 mM EDTA)

2.3. SUPPLIERS

Chemicals, reagents, kits, solvents, plasmids, disposables, instruments were obtained from UK suppliers (unless otherwise stated):

1. **Beckman Coulter**, Oakley Court, Kingsmead Business Park, London Road, High Wycombe, Buckinghamshire.
2. **Becton Dickinson Biosciences**, 21 Towns Road, Cowley, Oxford.
3. **Biochrom Ltd**, Cambridge Science Park, Milton Road, Cambridge.
4. **Bio-Rad Laboratories Ltd**., Bio-Rad House, Maxted Road, Hemel Hempstead, Hertfordshire.
5. **BMG LABTECH GmbH**, Hanns-Martin-Schleyer-Str. Offenburg/Germany.
6. **Calbiochem,** Merck Chemicals Limited, Padge Road, Nottingham,
7. **Carl Zeiss Ltd.** Woodfield Road, Welwyn Garden City, Hertfordshire
8. **Clontech**, Clontech BD Biosciences, Between Towns Road, Cowley Oxford.
9. **Corning Ltd**., Fisher Scientific UK Ltd., Bishop Meadow Road, Loughborough, Leicestershire.
10. **Dharmacon RNAi Technologies,** Perbio Science UK Ltd, Unit 9 Atley Way, North Nelson Industrial Estate, Cramlington, Northumberland**.**
11. **Eppendorf**, Fisher Scientific UK Ltd., Bishop Meadow Road, Loughborough, Leicestershire.
12. **Falcon**, Fisher Scientific UK Ltd., Bishop Meadow Road, Loughborough, Leicestershire.
13. **Fisher**, Fisher Scientific UK Ltd., Bishop Meadow Road, Loughborough, Leicestershire.
14. **Gibco**, Gibco-Invitrogen Ltd, 3 Fountain Drive, Inchinnan Business Park, Paisley.
15. **Grant**, Keison Products, Chelmsford, Essex.
16. **Heraeus**, Kendro Laboratory Products Plc, Stortford Hall Park, Bishop's Stortford, Hertfordshire.
17. **Intermed MDH Ltd.**, Kenn Road, Clevedon, Somerset.
18. **Invitrogen Ltd**, 3 Fountain Drive, Inchinnan Business Park, Paisley.
19. **Kodak**, Hemel Hempstead, Hertfordshire.
20. **Malvern Instruments Ltd**, Enigma Business Park, Grovewood Road, Malvern, Worcestershire.

21. **Merck**, VWR International Ltd., Merck House, Poole, Dorset.
22. **Millipore UK Ltd**., Units 3&5 the Courtyards, Hatters Lane, Watford.
23. **Mirus,** Cambridge BioScience 24-25 Signet Court Newmarket Road Cambridge
24. **NanoSight Ltd**., 2 Centre One, Lysander Way, Old Sarum Park, Salisbury, Wiltshire.
25. **New Brunswick Scientific**, 17 Alban Park, Hatfield Road, St. Albans, Hertfordshire.
26. **NUNC**, Fisher Scientific UK Ltd Bishop Meadow Road, Loughborough, Leicestershire.
27. **PAA laboratories Ltd,** 1 Technine, Guard Avenue, Houndstone Business Park, Yeovil, Somerset.
28. **Promega**, Delta House, Southampton Science Park, Southampton.
29. **Qiagen Ltd.**, Qiagen House, Fleming Way, Crawley, West Sussex.
30. **Rank Brothers Ltd.**, 56 High Street, Bottisham, Cambridge
31. **Sanyo**, Integrated Services TCP Inc., Palisades Park, New Jersey, USA.
32. **Sigma-Aldrich Company Ltd**. The Old Brickyard, New Road, Gillingham, Dorset.
33. **Syngene**, Beacon House, Nuffield Rd., Cambridge.
34. **Wilovert Hund,** the Helmut Hund Ltd. Company, Helmut Hund GmbH, Wilhelm-Will-Str. 7, Wetzlar, Germany.

2.4. METHODS

2.4.1. Amplification and Purification of Plasmid DNA

pEGFP plasmids

pDNA (EGFP) under CMV promoter, obtained from Clontech, was used as reporter gene in this study and DNA condensation studies. DNA can amplify in a large scale (up to 750 μg) using Qiagen HiSpeed™ plasmid Maxi kit (Qiagen Ltd.). Large-scale preparation of plasmids DNA protocol, described below, is based on a modified method described by Sambrook et al. (135) and using Qiagen anion-exchange resin. A positively charged diethylaminoethanol (DEAE) resin was used to separate negatively charged phosphate groups of DNA, by properly adjusting the

NaCl concentration of the elution solution. Aqueous NaCl solution (1.2-1.6 M) was used to elute DNA and separate the plasmid.

2.4.1.1. Plasmid amplification

The plasmid, pEGFP was transformed into *E. coli* JM 109 bacterial host strain. The transformed cells were grown in larger quantities (0.2–0.3 l) of LB broth supplemented with 100 mg/L ampicillin as follows:

LB broth was prepared by dissolving LB broth base powder (10 g) in 500 ml milliQ water. LB agar, for the preparation of agar plates, was prepared by dissolving LB agar powder (17.5 g) in 500 ml milliQ water. Both LB agar and LB broth were autoclaved (121 °C, 15 lb/inch^2) for 30 mins. Then, both media were left to cool to 40 °C. Ampicillin solution (0.1 g/ml in milliQ water, 500 µl) was added to both (500 ml) media and mixed well.

Sterile LB broth can be kept at 20 °C in a tightly closed bottle for one month. To prepare LB agar plates, about 10 ml of warm LB agar was poured in a 9 cm plate, using aseptic techniques. LB agar was then left for 30 mins to cool. LB agar plates were then incubated for 20 mins in a hot room (37 °C) upside down until dry. The solidified agar plates were kept in a cold room (4 °C) for use within 3 months.

2.4.1.2. Transformation of competent cells and plasmid propagation

Heat shock technique was used for *E. coli* JM 109 transformation. Sterile Falcon polypropylene tubes (50 ml) were chilled on ice one per transformation. Competent cells (*E. coli* JM 109) were thawed from -80 °C on ice. The thawed competent cells were gently mixed by flicking, and then 100 µl were transferred to each chilled tube. For each 100 µl competent cells, 50-100 ng of DNA was added and mixed by flicking. Tubes were placed on ice for 10 mins. Cells were heat-shocked for 45-50 s in a temperature controlled water bath (Grant) at 42 °C without shaking. Tubes were then immediately put on ice for 2 mins. Cold (4 °C) LB broth (900 µl) was added and the tubes were incubated for 60 mins at 37 °C with shaking (200 rpm) using a temperature-controlled flask shaker (New Brunswick Scientific).

For each transformation, 100 µl transformed cells were plated on LB agar medium containing 100 µg/ml ampicillin. Plates were then incubated upside down for 18 h in an incubator (Heraeus Instruments) at 37 °C. A single colony was isolated

from LB plate and incubated in 2 ml of LB broth containing ampicillin (100 μg/ml) in a 50 ml Falcon tube. The culture was grown for 8 h at 37 °C with shaking (200 rpm). The culture was then scaled-up by the addition of the starter culture (2 ml) into a flask (of at least 1 l size flask) containing LB broth (250 ml) with ampicillin (100 μg/ml). The flask was then incubated for 18 h at 37 °C with shaking (200 rpm) using a temperature-controlled flask shaker.

2.4.1.3. Long term storage of transformed cells

A single colony was isolated from each LB plate and incubated in LB broth (1-2 ml) containing ampicillin. The culture was grown for 8 h. Glycerol solution (30 % v/v) was prepared and sterile filtered. The culture (0.5 ml) was mixed with sterile glycerol (0.5 ml) solution and transferred to a cryo-preservation vial, obtained from Corning Ltd., then stored at -80 °C.

2.4.1.4. Plasmid isolation and purification

After incubating the 250 ml bacterial culture flask for 18 h at 37 °C with shaking (200 rpm) using a temperature-controlled flask shaker, cells were harvested by centrifugation, using Beckman floor centrifuge model J2-MC (Beckman Coulter) at 6,000 rpm using Beckman JA-10 rotor for 15 mins at 4 °C. Cell pellets, obtained after completely removing the supernatant liquid, were resuspended in 10 ml ice-cooled P1 buffer (50 mM Tris-Cl, 10 mM EDTA and 100 μg/ml RNase A, pH 8.0), complete mixing was allowed by vortexing until no cell clumps remained. Then, 10 ml of P2 lysis buffer (200 mM aqueous NaOH, 1 % w/v sodium dodecyl sulfate) was added to the cell suspension. The tube was then inverted gently 4 times and incubated at 20 °C for 5 mins. Ice-cooled P3 neutralisation buffer (10 ml, 3.0 M potassium acetate, pH 5.5) was added into the cell lysates and the mixture was inverted gently 4 times. The lysate was poured into the barrel of the Qiafilter cartridge and incubated for 10 mins, with the outlet nozzle closed.

The HiSpeed Maxi Tip (a syringe column with a filtration unit) was equilibrated with 10 ml buffer QBT (750 mM NaCl, 50 mM 3-[*N*-morpholino] propanesulfonic acid (MOPS), 15 % isopropanol v/v, 0.15 % Triton X-100 v/v) and the column was allowed to empty by gravity flow. The outlet nozzle cap of the Qiafilter cartridge was removed and the plunger was gently inserted into the cartridge.

The filtrate was collected into the equilibrated Maxi Tip and allowed to be filtered through the resin. After that, 60 ml of buffer QC (1.0 M NaCl, 50 mM MOPS, 15 % isopropanol v/v, pH 7.0) was added to wash the HiSpeed Maxi Tip. Entrapped DNA in the resin was eluted by adding 15 ml of buffer QF (1.25 M NaCl, 50 mM Tris-Cl, 15 % isopropanol v/v, pH 8.5) into the tip. The eluted solution was kept in a 50 ml Falcon tube. Isopropanol (10.5 ml) was then added and mixed well to precipitate the DNA, then the mixture was incubated for 5 mins at 20 °C.

A DNA collection unit (QIA precipitator tip) was attached to the nozzle of a 30 ml syringe from which a plunger was removed. Then, the eluate/isopropanol mixture that has the precipitated DNA was added to the precipitator unit, and the plunger was inserted into the syringe using constant pressure. DNA was entrapped in the precipitator unit. Then, the tip and the plunger were removed from the syringe. After that, the tip was reconnected again to the syringe nozzle and 2 ml of 70 % EtOH v/v was added into the syringe. DNA was washed by pressing EtOH through the QIA precipitator using inserted plunger at a constant pressure. The tip and the plunger were removed from the syringe and DNA was dried by pushing air through the precipitator 2-3 times and the outlet nozzle of the precipitator was dried with absorbent paper.

To elute the DNA in the tip, 1 ml of buffer TE (10mM Tris-HCl, 1mM EDTA, pH 8) was added into a new 5 ml syringe to which the precipitator tip was connected. The plunger was attached and pushed gently. The eluted solution was collected in an ultracentrifuge tube (1.5 ml). The previous step was repeated by the transfer of the eluate in the 1.5 ml ultracentrifuge tube to the 5 ml syringe to which the precipitator tip was connected and eluted again in the same 1.5 ml tube. DNA solution was stored at -20 °C.

2.4.1.5. Analysis of the purification procedure

The DNA obtained can be quantified by the maximum UV absorption at 260 nm. This wavelength is an average of the absorption of the individual nucleotides which vary between 256 – 281 nm. DNA was determined by measuring the maximum absorption at 260 nm for nucleic acids and 280 nm for proteins. Ratios of A_{260}/A_{280} between 1.75–1.90 are considered acceptable for DNA purity (136,137).

Plasmid DNA yields and quality were analyzed spectrophotometrically using Gene Quant II RNA/DNA calculator (Biochrom Ltd). Plasmid DNA sample 5 μl was diluted to 100 μl with TE buffer, in a microcuvette. The absorbance was measured at 260 nm (A_{260}) and 280 nm (A_{280}). TE buffer (100 μl) was used as a standard reference. The calculation for DNA concentration by dilution factor 20, and a conversion factor for double stranded dsDNA, 50 μg/ml/A_{260}.

2.4.2. DNA Condensation Studies

DNA condensation was carried out to investigate the neutralization of the negative charges of the phosphate groups on the DNA backbone. These studies include:

1. Ethidium bromide fluorescence quenching assay
2. Light scattering assay
3. Gel electrophoresis study

2.4.2.1. Ethidium bromide fluorescence quenching assay

Each concentration of the DNA (pEGFP) stock solutions (approximately 1 μg/μl) was determined spectroscopically and 6 μg (approximately 6 μl) of DNA was diluted to 3 ml with HEPES buffer in a glass cuvette stirred with a micro-flea. Immediately prior to analysis, EthBr solution (3 μl, 0.5 mg/ml) was added to the stirring solution and allowed to equilibrate for 10 mins.

Aliquots (5 μl) of spermine (10 x 0.04 mg/ml, and then 5 x 0.2 mg/ml) were then added to the stirring solution and the fluorescence measured after 1 min equilibration using Perkin-Elmer LS 50B luminescent spectrometer (λ_{ex} = 260 nm and λ_{em} = 600 nm with slit width 5 nm) while stirring using an electronic stirrer (Rank Brothers Ltd.). The total polyamine solution added to the DNA solution did not exceed 5 % of the total volume of the solution, so no correction was made for sample dilution. The fluorescence was expressed as the percentage of the maximum fluorescence when EthBr was bound to the DNA in the absence of competition for binding and was corrected for background fluorescence of free EthBr in solution as optimized by Geall and Blagbrough (138). This correction and the subsequent normalization were performed using an Excel spreadsheet.

For synthesized lipopolyamines, commercially available transfecting agents, Lipofectin, Lipofectamine (available as liposomal formulations) and the non-liposomal formulation Transfectam®, the lipopolyamines were prepared as stock solutions using absolute EtOH as solvent and diluted with HEPES buffer to the specified concentrations directly before use. Aliquots were added to the stirring solution of 3 ml HEPES buffer in a glass cuvette containing DNA (6 μg) and EthBr (1.5 μg). The fluorescence was measured after 1 min equilibration using Perkin-Elmer LS 50B luminescent spectrometer (λ_{ex} = 260 nm and λ_{em} = 600 nm with slit width 5 nm) while stirring using an electronic stirrer (Rank Brothers Ltd.). The total lipopolyamine solution added to the DNA solution did not exceed 5 % of the total volume of the solution, so no correction was made for sample dilution. The fluorescence was expressed as the percentage of the maximum fluorescence when EthBr was bound to the DNA in the absence of competition for binding and was corrected for background fluorescence of free EthBr in solution. This correction and the subsequent normalization were performed using an Excel spreadsheet.

The DNA polyamine complex composition is expressed as N/P (ammonium/phosphate) as follows:

$$\text{N/P} = \frac{Ammonium\ \ equivalents\ of\ \ the\ \ cationic\ compound}{Phosphate\ \ equivalents\ of\ the\ DNA\ \ used} \qquad \text{eq.[1]}$$

Ammonium equivalents of the polyamine were determined from pK_a value of each amino group at pH 7.4 (HEPES buffer) according to the Henderson-Hasselbach equation:

$$\text{pH} = \text{p}K_a + \log_{10} \frac{[conjugate\ base]}{[conjugate\ acid]} \qquad \text{eq. [2]}$$

The N/P charge ratio was calculated according to the ammonium/phosphate, (+/-) charge ratio of the investigated lipopolyamines to DNA. For DNA it was calculated as 330 g/mole of DNA that contains one negative charge (139). In the case of N^4,N^9-diacyl spermines and N^1,N^{12}-diacyl spermines it was calculated as 1 mole contains two amino groups that are (fully) protonated (positively charged) at pH 7.4.

In the case of N^4,N^9-dialkyl spermine it was calculated as 1 mole (molecular weight) contains four amino groups (2 primary and 2 tertiary) that are fully protonated at pH 7.4.

In the case of the commercially available lipopolyamine (DOGS, Transfectam®) it was calculated as 1263 g/mole (trifluoroacetate salt) that contains three are fully protonated nitrogens (more accurately 2.92) at pH 7.4, although Transfectam® has four nitrogens (two secondary amines and two primary amines, ignoring the two neutral amides) that can be protonated in strong acid.

In the liposomal formulation Lipofectin, the cationic lipid DOTMA carries 1 positive charge (ammonium eq/mole) (2)while the cationic lipid DOSPA in the Lipofectamine formulation and carries 4 positive charges (ammonium eq/mole) (15). In the non-liposomal formulations, Transfectam® carries 3 positive charges (139).

Binding constant calculation

From EthBr fluorescence quenching results for DNA interaction with the condensing agent, the binding constant of the DNA condensing agent (vector) to DNA can be calculated and compared with the loss of EthBr fluorescence as a function of DNA condensing agent concentration. The drug concentration producing 50 % inhibition of fluorescence is approximately inversely proportional to the binding constant (140). Denny and co-workers (141) established the binding equations of DNA to both EthBr and vectors as follows:

$$[DNA] + [vector] \leftrightarrow [DNA\text{–}vector] \qquad \text{eq. [3]}$$

$$[DNA] + [EthBr] \leftrightarrow [DNA\text{–}EthBr] \qquad \text{eq. [4]}$$

$$K_b \text{ (vector)} = \frac{[DNA\text{–}vector]}{[DNA] \times [vector]} \qquad \text{eq. [5]}$$

$$K_b \text{ (EthBr)} = \frac{[DNA\text{–}EthBr]}{[DNA] \times [EthBr]} \qquad \text{eq. [6]}$$

$$K_b \text{ (vector)} = \frac{[DNA\text{–}vector] \times [EthBr] \times K_b\,(EthBr)}{[DNA\text{–}EthBr] \times [vector]} \qquad \text{eq. [7]}$$

At 50 % residual fluorescence, the ratio of [DNA-vector] to [DNA-EthBr] is equal to 1. Therefore, the "apparent" equilibrium constant (K_b) of polyamine binding was calculated, taking into account that Morgan et al. (140) reported that the binding constant of ethidium bromide K_b *(EthBr)* was 10^7 M^{-1}, as follows:

$$K_b \text{ (vector)} = \frac{[EthBr] \times 10^7}{[vector]} \qquad \text{eq. [8]}$$

The concentration of the condensing agent producing 50 % intercalated EthBr fluorescence inhibition was calculated experimentally.

2.4.2.2. Light scattering assay

A light scattering experiment was designed to investigate particle formation as a result of DNA condensation by polyamines and lipopolyamines. The apparent UV absorbance at 320 nm, where there is no DNA absorbance interference above 300 nm, was measured showing light scattering (i.e., decreased light transmission) (23). All DNA (linear calf thymus) solutions were diluted using TE buffer and their concentrations were measured by GeneQuant II spectrophotometer. HEPES buffer was made of 2 mM HEPES, 20 mM NaCl, 10 μM EDTA, and MilliQ water, the pH was adjusted to 7.4 with aqueous NaOH solution. HEPES buffer was filtered through a 0.22 μm membrane prior to use.

Spermine (17 mg) was dissolved in MilliQ water (1 ml as a stock solution). DNA 60 μg (of 1 mg/ml solution) diluted to 3 ml with HEPES buffer in a cuvette with a micro-flea, and the concentration determined spectroscopically (Milton Roy Spectronic 601 spectrometer, 1 cm path length, 3 ml cuvette). UV measurement of DNA in buffer was performed and adjusted to zero. Then, aliquots (5 μl) of spermine (10 x 0.4 mg/ml, and then 5 x 2.0 mg/ml) were then added to the stirring solution and the absorbance (light scattering) at 320 nm measured after 1 min stirring to allow the mixture to reach equilibrium. The Apparent UV absorbance values were then plotted against N/P ratios.

2.4.2.3. Gel electrophoresis study

Agarose (1 g, electrophoresis grade, Gibco) was added to 100 ml of 1x TAE (Tris-Acetate-EDTA, 40 mM Tris-Acetate and 1 mM EDTA) buffer. The mixture was then heated in a microwave oven at the max power to boiling for 2 mins with swirling the flask 3-4 times while boiling to dissolve the agarose. When the agarose was completely dissolved, the solution was then allowed to cool to a consistency that can be poured. Then EthBr was added to a concentration of 1.0 μg/ml. When the gel was cooling down, the gel tray was securely sealed at the ends with tape strips to form a fluid-tight seal. The comb was placed over the gel tray. After that, when the agarose had been cooled to about 60°C, it was poured into the gel tray to a depth of 4-8 mm. Then the gel was allowed to set at 20 ºC for 30 mins followed by refrigeration for further 15 mins for complete solidification of the gel. The comb was removed from the solidified gel as well as the tape from the edges of the gel tray. The gel was then transferred to the electrophoresis chamber, Kodak Biomax QS 710 (Kodak), and submerged into the electrophoresis buffer (TAE buffer).

For pEGFP lipoplex formation, two solutions were prepared for each well, solution A (DNA) and solution B (lipopolyamine). Solution A was prepared by diluting DNA solution (0.5-1 μg/well) to 5 μl using 1x TAE buffer, in a sterile 1.5 ml micro-centrifuge tube, gently mixed using a vortex, for 2 s and incubated for 30 mins at 20 ºC. Solution B was prepared by diluting the lipopolyamine solution to 10 μl using 1x TAE buffer, in a sterile 1.5 ml micro-centrifuge tube, gently mixed using a vortex, for 2 s and incubated for 30 mins at 20 ºC. The complex was then prepared by mixing solution A and B (brief vortex, 1 s) then incubated for 20 mins at 20 ºC.

Each lipopolyamine used in solution B was at a different volume according to the required N/P ratio for 0.5-1 μg DNA/well, as described above in the N/P determination section for EthBr assay.

Samples (15 μl) of plasmid DNA (0.5 μg), either free or complexed with the lipopolyamine (according to the charge ratio) were mixed with the loading dye (blue/orange loading dye 6X, Promega) and loaded into the wells. The loading dye was used at a 1X final concentration and contains 0.03 % xylene cyanol FF (4 kbp migration), 0.03 % bromophenol blue (300 bp migration), 0.4 % orange G (50 bp migration), 10mM Tris-HCl (pH 7.5) and 50mM EDTA (pH 8). Electrophoresis at 75 V/cm (Bio-Rad Power Pack 300, Bio-Rad Laboratories Ltd) was carried out for 1 h.

The gel was removed and the (unbound) free DNA in the agarose gel was visualized under UV using GeneGenius (Syngene).

2.4.3. DNase I Sensitivity Assay

Briefly, in a typical assay, pEGFP plasmid (1μg) was complexed with the varying amounts of the lipospermines using the indicated charge ratios in a total volume of 30 μl in HEPES buffer, pH 7.4, and incubated at 20 ºC for 30 mins on a rotary shaker. Subsequently, the complexes were treated with 10 μl DNase I (Qiagen, at a final concentration of 1 μg/ml) in presence of 20 mM $MgCl_2$ and incubated for 20 mins at 37°C. The reactions were then halted by adding EDTA (to a final concentration of 50 mM) and incubated at 60°C for 10 mins in a water bath. The aqueous layer was washed with 50 μl of phenol:chloroform:isoamylalcohol (25:24:1 mixture, v/v) and centrifuged at 10,000 rpm for 5 mins. The aqueous supernatants were separated, loaded (15 μl) with loading dye on a 1% agarose gel (pre-stained with ethidium bromide1.0 μg/ml) and electrophoresed at 100 V for 1 h as described above in the gel electrophoresis study.

2.4.4. RiboGreen Intercalation Assay

RiboGreen solution (Invitrogen, 50 μl dil. 1 to 20) was added to each well of a 96-well plates (opaque bottom), containing 50 ng of siGENOME Non-Targeting siRNA #1 (Dharmacon) either free or complexed with different amounts Trans-IT or lipospermines according to the N/P ratio containing in TE buffer, and the fluorescence measured after 5 mins equilibration using FLUOstar Optima Microplate Reader (BMG-LABTECH), λ_{ex} = 480 nm, λ_{em} = 520 nm. The fluorescence was expressed as the percentage of the maximum fluorescence when RiboGreen was bound to the RNA in the absence of competition for binding and was corrected for background fluorescence of free RiboGreen in solution. This correction and the subsequent normalization were performed using an Excel spreadsheet. The amount of siRNA available to interact with the probe was expressed as a percentage of the control that contained naked siRNA only, according to the following formula: % free siRNA = 100 x RiboGreen $\text{fluorescence}_{\text{complexes}}$ /RiboGreen $\text{fluorescence}_{\text{naked siRNA}}$.

2.4.5. Tissue Culture and Transfection Experiments

2.4.5.1. Primary skin cell line FEK4

A primary skin cell line was used in the transfection experiments. FEK4 cells are human primary fibroblasts derived from newborn foreskin explants (142-144), which were used as a model for human primary cells (passage dependent cell line). FEK4 cells were kindly provided by Prof. R. M. Tyrrell, Department of Pharmacy and Pharmacology, University of Bath, UK. Cells were cultured in Earle's Minimal Essential Medium (EMEM) with a final Foetal Calf Serum (FCS) concentration of 15 % v/v according to the following formula (for 500 ml):

10X EMEM	50 ml
7.5 % $NaHCO_3$	13.5 ml
200 mM L-glutamine	5 ml
Penicillin (10,000 IU/ml)/Streptomycin (10,000 IU/ml)	2.5 ml
Foetal calf serum (FCS)	75 ml
Autoclaved MilliQ Water	354 ml

FCS was heat inactivated before use by defrosting at 37 ^{o}C and heating at 56 ^{o}C for 45 mins in a temperature-controlled water bath (Grant). Sterile PBS solution was used in all transfection experiments to wash cells and contains 0.01 M phosphate buffer, 0.0027 M KCl and 0.137 M NaCl in MilliQ water at pH 7.4. Trypsin was diluted to a working concentration at 0.25 % w/v with PBS.

Cells were visually assessed daily for evidence of microbial contamination under an inverted light microscope (Wilovert Hund). All aseptic techniques for cell culture were carried out in a laminar flow cabinet (Intermed MDH Ltd.) designed for vertical re-circulation of air. A temperature-controlled water bath (Grant) was used to warm the media for cell culture experiments. A monolayer of primary skin cell lines was grown in 25 ml EMEM supplemented with 15 % FCS v/v in 150 cm^2 (T_{150}) flasks from NUNC. Cell lines were incubated at 37 ^{o}C, 5 % CO_2, 95 % air and humidified atmosphere using an LEEC PF2 incubator (Sanyo). Primary skin cells were passaged twice (minimum once) a week and used between passages 9-16.

Primary cells were passaged (subcultured) by trypsinisation technique. The growth medium was aspirated from the flasks. Then, cells were washed twice with

PBS solution (10 ml/T_{150} flask). PBS solution was then removed by aspiration. Cells were treated with trypsin 0.25 % w/v (3 ml/T_{150} flask) and incubated for 5-10 mins at 37 ^{o}C and 5 % CO_2 v/v for trypsinisation reaction. After that, the flasks were gently tapped to assess the detachment of the cells, which were checked under a light microscope to ensure at least 85 % cell detachment. To stop trypsinisation, 10 ml of 15 % FCS v/v EMEM was added to the flask. The cell suspension was then transferred to a 15 ml Falcon tube, obtained from Falcon, for separation of cells by centrifugation at1,200 rpm for 5 mins using a cells centrifuge, Falcon 6/300 MSE (Sanyo). Cells were re-suspended in 6 ml of 15 % FCS v/v EMEM and seeded at a concentration of 1 x 10^6 cells/flask (T_{150}) containing 25 ml 15 % FCS v/v EMEM for next passage.

To determine the concentration of cells in a sample, a viable count was carried out using a haematocytometer slide. A stained cell suspension was prepared by mixing trypsinized cells (50 µl) with the same volume of nigrosin or trypan blue (50 µl) 0.4 % (w/v) solution in PBS. The cell sample was loaded into the raised sides of the glass chambers (top and bottom) covered with a coverslip 0.1 mm above the chamber floor until the whole chamber was fully loaded. The slide was then placed under an inverted light microscope. Viable cells were detected using a bright halo light around their cell membrane. On the other hand, dead cells were permeabilized by the dye and appeared as black spheres under the microscope. The viable cell number in the four squares surrounding the central square and this was repeated for the other side of the haemocytometer chamber. The viable cell concentration in the original cell suspension was calculated using the following equation:

$$Cell\ conc.\ (cells/ml) = \frac{total\ cell\ count\ in\ 4\ squares}{4} \times dilution\ \ factor \times 10^4 \qquad \text{eq. [9]}$$

For cell storage, cells were detached from a confluent monolayer by trypsinisation as described before followed by centrifugation at 1,200 rpm for 5 mins. The supernatant was then discarded and the cell pellets were re-suspended in the growth media at a concentration of 2 x 10^5 cells/ml. A cell freezing solution (10 % v/v) of growth media with a filter-sterilized solution of dimethylsulfoxide (DMSO) as a cryopreservative was prepared. Cell suspension (0.4 ml) was dispensed with 0.6 ml of cell freezing solution into cryotubes and stored at -70 ^{o}C overnight. After that,

tubes were fitted into a Union Carbide LR-40 liquid nitrogen freezer where they were stored at approximately -150 ^{o}C (long-term, years).

For cell recovery, the contents of the cryotube were thawed rapidly by brief incubation at 37 ^{o}C in a water bath, followed by dilution with 10 ml of fresh growth medium. Cells were centrifuged for 5 mins at 1200 rpm and the supernatant was discarded. Cell pellets were then re-suspended in 10 ml of fresh medium, and then 1 x 10^6 cells were transferred to a flask (T_{150}) containing 25 ml of growth medium and incubated under standard culture conditions. Cells were cultured for at least two passages in order to establish them before any experiments were carried out.

Transfection experiments were carried out using pEGFP, encoding for enhanced green fluorescent protein as a reporter gene, either complexed with DNA condensing agents, or free (naked DNA) as a negative control. Cells were seeded in 12-well plates, obtained from NUNC. DNA was used at a concentration of 1 μg/well. DNA condensing agents used for FEK4 primary cells transfection were the liposomal formulations Lipofectin (DOTMA/DOPE 1:1 w/w) and Lipofectamine (DOSPA/DOPE 3:1 w/w), and the non-liposomal formulations Transfectam® (DOGS) and all designed and synthesized lipospermines.

For the DNA-vector complex formation experiment, two solutions were prepared for each well (12-well plate), solution A (DNA) and solution B (condensing agent). Solution A was prepared by diluting DNA solution (1 μg/well) to 50 μl using Opti-MEM, a serum free media (Gibco), in a sterile 1.5 ml micro-centrifuge tube, gently mixed using a vortex, for 2 s and incubated for 30 mins at 20 ºC. Solution B was prepared by diluting transfection agents solution to 50 μl using Opti-MEM, serum free media, in a sterile 1.5 ml micro-centrifuge tube, gently mixed using a vortex, for 2 s and incubated for 30 mins at 20 ºC. The complex was then prepared by mixing solution A and B with vortex for 1 s then incubated for 20 mins at 20 ºC.

Each transfection agent used in solution B was at a different volume according to the required N/P ratio for 1 μg DNA/well, as described before in the N/P determination section for EthBr assay.

For FEK4 transfection, 5x 10^4 cells/well were seeded in 12-well plates in 2 ml of 15 % FCS v/v EMEM. Cells were incubated at 37 ^{o}C and 5 % CO_2 v/v in a CO_2 incubator for 24 h to reach 50-60 % confluency. Prior to transfection, the media were replaced with 400 μl of the 15 % FCS v/v EMEM to which 100 μl of the transfection

complex, as a result of mixing solution A and B, was added to the plates for the total volume of 500 µl/well except for control cells where Opti-MEM 500 µl was added (no DNA complex solution). The transfected plates were incubated for 4 h at 37 ^{o}C in an atmosphere of 5 % CO_2 v/v. After that, the 15 % FCS v/v EMEM with DNA complex in the incubated plates was aspirated and replaced with 2 ml of 15 % FCS v/v EMEM media and incubated for a further 44 h at 37 ^{o}C in an atmosphere of 5 % CO_2 v/v.

The study using naked DNA was performed to assess if there was any transfection efficiency from naked DNA compared to the lipoplexes. The same transfection protocol used before was applied, except for solution B that contains only serum free media without any DNA condensing agent to be added. For all transfection studies, each data point represents the mean ± standard deviation (± SD) of triplicate samples and each experiment was repeated three times.

2.4.5.2. HtTA cell transfection

Human cervix carcinoma, HeLa derivative and transformed cell line (HtTA) (145,146) was used as a model for carcinoma cells (an immortal cell line). The HtTA cells being stably transfected with a tetracycline-controlled transactivator (tTA) consisting of the tet repressor fused with the activating domain of virion protein 16 of the herpes simplex virus (HSV). HtTA cells were kindly provided by Prof. R. M. Tyrrell, Department of Pharmacy and Pharmacology, University of Bath, UK. Cells were cultured in Earle's Minimal Essential Medium (EMEM) with a final FCS concentration of 10 % v/v according to the following formula (for 500 ml):

10X EMEM	50 ml
7.5 % $NaHCO_3$	13.5 ml
200 mM L-glutamine	5 ml
Penicillin (10,000 IU/ml)/Streptomycin (10,000 IU/ml)	2.5 ml
Foetal calf serum (FCS)	50 ml
Autoclaved MilliQ Water	379 ml

FCS was heat inactivated before use by defrosting at 37 ^{o}C and heating at 56 ^{o}C for 45 mins in a temperature-controlled water bath (Grant). Trypsinisation procedures were carried out using the same protocol for FEK4 sub-culturing. The culture was incubated at 37 ^{o}C in an atmosphere of 5 % CO_2 v/v. HtTA cells were passaged every 3 days.

For the transfection (gene delivery) and the resultant gene activity (transfection efficiency) the same protocol for HtTA transfection was used as described above for FEK4. Briefly, HtTA cells were seeded at 50,000 cell/well in 12 well plates in 1 ml EMEM media with 10 % FCS v/v for 24 h to reach a plate confluency of 50-60 % on the day of transfection. The complex was prepared by mixing pEGFP (1 μg) with the cationic liposomes or lipopolyamine in serum free media Opti-MEM according to the charge ratio at 20 ºC for 30 m, and then incubated with the cells in EMEM media with 10 % FCS v/v for 4 h at 37 ^{o}C in 5 % CO_2 v/v, then the cells were cultured for a further 44 h in growth medium at 37 ^{o}C in 5 % CO_2 v/v before the assay.

2.4.5.3. Transfection experiments in the absence of serum for FEK4 and HtTA cells

For the transfection (gene delivery) and the resultant gene activity (transfection efficiency), the same seeding protocol for FEK4 and HtTA transfection was used as described above. Then, in the transfection step, the cells were incubated in serum-free media Opti-MEM (instead of full-growth media) for 4 h at 37 ^{o}C in 5 % CO_2 v/v, then the cells were cultured for further 44 h in full-growth media (15 % FCS for FEK4 and 10 % FCS for HtTA) at 37 ^{o}C in 5 % CO_2 v/v before the assay.

2.4.6. Fluorescence Activated Cell Sorting Experiment

To analyse the transfection efficiency of the delivered pEGFP, levels of green fluorescent protein (GFP positive cells) in the transfected cells were detected using a fluorescence activated cell sorting (FACS) machine (147) Becton Dickinson FACS Vantage dual Laser Instrument, (argon ion laser 488 nm) (Becton Dickinson Biosciences). FACS is used to determine the fluorescent molecules (or biomolecules) inside studied cells. Individual cells pass through a laser beam allowing the light scatter and fluorescence characteristics of each cell to be measured. Filter lens (F) for

emission detection was chosen based on the fluorophore used. In our experiment, EGFP is detected by F1 (λ_{ex} = 488 nm, λ_{em} = 530 nm).

2.4.7. siRNA Transfection Experiments in the Presence of Serum for FEK4 and HtTA Cells

We used Label IT® RNAi Delivery Control (Mirus) which consists of a fluorescein-labelled double-stranded RNA duplex that has the same length (ds 21-mer), charge, and configuration as standard siRNA used in RNAi studies.

For the siRNA-vector complex formation experiment, two solutions were prepared for each well (12-well plate), solution A (RNA) and solution B (condensing agent). Solution A was prepared by diluting 1.25 µl solution siRNA (12.5 pmol/well) to 12.5 µl using 10X RNAi Dilution Buffer (Mirus, diluted by RNase and DNase free water), in a sterile 1.5 ml micro-centrifuge tube, gently mixed using a vortex, for 2 s and incubated for 30 mins at 20 ºC. Solution B was prepared by diluting transfection agents solution to 50 µl using Opti-MEM, serum free media, in a sterile 1.5 ml micro-centrifuge tube, gently mixed using a vortex, for 2 s and incubated for 30 mins at 20 ºC. The complex was then prepared by mixing solution A and B with vortex for 1 s then incubated for 20 mins at 20 ºC.

Each transfection agent used in solution B was at a different volume according to the required concentration using broad-spectrum TransIT-TKO® Transfection Reagent as a positive control and naked Label IT® RNAi as a negative control.

For transfection, 50,000 cells/well were seeded in 12-well plates in 2 ml of 15 % FCS v/v EMEM and 10 % FCS v/v EMEM for FEK4 and HtTA Cells respectively were incubated at 37 ^{o}C and 5 % CO_2 v/v in a CO_2 incubator for 24 h to reach 50-60 % confluency. Prior to transfection, the media replaced with 437.5 µl of the 15 % FCS v/v EMEM in case of FEK4 cells and the10 % FCS v/v EMEM in case of HtTA cells to which 62.5 µl of the transfection complex, as a result of mixing solution A and B, was added to the plates for final volume of 500 µl/well except for control cells where 500 µl of Opti-MEM with serum was added (no RNA complex solution). The transfected plates were incubated for 4 h at 37 ^{o}C in an atmosphere of 5 % CO_2 v/v. After that, the FCS EMEM with RNA complex in the incubated plates was aspirated and replaced with 2 ml of FCS EMEM media and incubated for a further 44 h at 37 ^{o}C in an atmosphere of 5 % CO_2 v/v.

The study using naked RNA was performed to assess if there was any transfection efficiency from naked RNA compared to the lipoplexes. The same transfection protocol used before was applied, except for solution B that contains only serum free media without any RNA condensing agent to be added. For all transfection studies, each data point represents the mean ± standard deviation (± SD) of triplicate samples and each experiment was repeated three times.

2.4.8. Preparation of Cell Samples for FACS Analysis for both DNA and siRNA

After transfection (4 h), and then incubation (44 h), for either DNA or siRNA, the cells were detached through aspiration of the media from 12-well plates. Then, cells were washed twice with PBS solution (1 ml/well). PBS buffer was removed by aspiration. Cells were treated with trypsin 0.25 % w/v (0.5 ml/well) and incubated for 5 mins at 37 ^{o}C and 5 % CO_2 v/v for trypsinisation reaction. After that, the plates were gently tapped to assess the detachment of the cells, which were checked under microscope to ensure at least 85 % of cells were detached. To stop trypsinisation The cell suspension was then transferred to FACS polystyrene test tubes (12 x 75 mm), obtained from Falcon, filled with 1 ml of 15 % FCS EMEM for separation of cells by centrifugation at 1,200 rpm for 5 mins 20 ºC using a cells centrifuge, Falcon 6/300 MSE (Sanyo). Cells were re-suspended in PBS (1 ml/tube) for further centrifugation at 1,200 rpm for 5 mins at 20 ºC. Cell suspension for FACS analysis was obtained by dissolving the pellet in 500 µl PBS/tube. Untreated (untransfected) cell sample was used as a control in the measurement.

CELLQuest v.1.0 software (Becton Dickinson Biosciences) was used to analyse FACS data. Typically, 10,000 events were collected. Recordings were made at green fluorescence (FL1) and data were expressed as histograms. Only a subset of the data obtained from healthy cells data (major population) was analysed through a gate setting. This gating was determined from the dot plots between forward-scattered light (FSC) and side-scattered light (SSC). FSC is a parameter proportional to cell size and SSC indicates the cell granularity or internal complexity. In the histogram of events at different fluorescence intensity control group, the fluorescence intensity range (M_1) was set as a constant range throughout the experiments. For EGFP detection, the % fluorescence cells sorting events in the established range (M_1) was

reported with the correction of the background fluorescence of the control sample. The same for fluorescein-tagged RNA which has λ_{ex} = 495 nm and λ_{em} = 518 nm.

2.4.9. Cytotoxicity (MTT) Assay of the Formed DNA-Lipoplexes on Transfected Cell Lines

The MTT assay is a colorimetric assay to evaluate the metabolic activity of viable cells to convert a soluble tetrazolium salt [3-(4,5-dimethylthiazol-2-yl)-2,5-diphenyltetrazolium bromide (MTT)] into an insoluble formazan crystal (148). This assay is used to investigate the cytotoxic effects of lipopolyamines and lipoplexes (pEGFP complexes). primary cell line was used in the cytotoxicity experiments, FEK4 cells are human primary fibroblasts derived from newborn foreskin explants, which were used as a model for human primary cells (mortal cell line), and these cells were cultured in EMEM with a final serum concentration of 15 % v/v. HtTA was used as a model for carcinoma cells (an immortal cell line), and these HtTA cells were cultured in EMEM with a final FCS concentration of 10 % v/v. Lipopolyamines used in the MTT assay were the liposomal formulations Lipofectin (DOTMA/DOPE 1:1 w/w) and Lipofectamine (DOSPA/DOPE 3:1 w/w) and the non-liposomal formulations Transfectam® (DOGS), and all our synthetic lipospermines.

For DNA-vector complex formation, two solutions were prepared for each well (96-well plate), solution A (DNA) and solution B (condensing agent). Solution A was prepared by diluting DNA solution (0.2 μg/well) to 10 μl using Opti-MEM, a serum free media, in a sterile 1.5 ml micro-centrifuge tube, gently mixed using a vortex (2 s) and incubated for 30 mins 20 ºC. Solution B was prepared by diluting transfection agent solution to 10 μl/well using Opti-MEM, serum free media, in a sterile 1.5 ml micro-centrifuge tube, gently mixed using a vortex (2 s) and incubated for 30 mins at 20 ºC. The complex was then prepared by mixing solution A and B with vortex for 1 s then incubated for 20 mins at 20 ºC. Each transfection agent used in solution B was at a different volume according to the required N/P ratio for 0.2 μg DNA/well, as described before in the N/P determination section for EthBr assay.

For primary fibroblasts and carcinoma cells toxicity study, 8,000 cells/well were seeded in 96-well plates, obtained from NUNC, in 200 μl of 15 % FCS v/v EMEM and 10 % FCS v/v EMEM in the case of primary fibroblasts and HtTA, respectively. Cells were incubated at 37 ^{o}C and 5 % CO_2 v/v in a CO_2 incubator for 24

h to reach 50-60 % confluency. The medium was removed and replaced with 80 µl of 15 % FCS v/v EMEM and 10 % FCS v/v EMEM in the case of primary fibroblasts and HtTA, respectively to which 20 µl of either the transfection complex (lipoplex), the free lipopolyamine, or the free DNA (naked DNA) was added to the plates except for control cells where FCS EMEM (100 µl) was added (no DNA complex solution). The plates were incubated for 4 h at 37 ^{o}C in an atmosphere of 5 % CO_2 v/v. After that, the FCS EMEM complex containing media in the incubated plates was aspirated and replaced with 200 µl of 15 % FCS v/v EMEM and 10 % FCS v/v EMEM in the case of primary fibroblasts and HtTA, respectively. Then, incubated for a further 44 h at 37 ^{o}C in an atmosphere of 5 % CO_2 v/v.

After incubation for 44 h, the media was replaced with 90 µl of fresh media and 10 µl of sterile filtered MTT solution (Sigma-Aldrich) (5 mg/ml) to reach a final concentration of 0.5 mg/ml. Then the plates were incubated for a further 4 h at 37 ^{o}C in an atmosphere of 5 % CO_2 v/v. After incubation, the media and the un-reacted dye were aspirated and the formed blue formazan crystals were dissolved in 200 µl/well of DMSO. The produced colour was measured using a plate-reader (VERSAmax™) at wavelength 570 nm. The % viability related to control wells containing cells without DNA and/or polymer and is calculated as follow (149):

$$\%\ cell\ viability = \left(\frac{A_{570}\ sample}{A_{570}\ control} \right) \times 100 \qquad \text{eq. [10]}$$

For all cytotoxicity (MTT) studies, each data point represents the mean ± standard deviation (± SD) of triplicate samples and each experiment was repeated three times.

2.4.10. Cytotoxicity (MTT) Assay of the Formed siRNA-Lipoplexes

The same assay as detailed above, but for RNA-vector complex formation. Two solutions were prepared for each well (96-well plate), solution A (siRNA) and solution B (condensing agent). Solution A was prepared by diluting 0.25 µl solution siRNA (2.5 pmol/well) to 2.5 µl using 10X RNAi Dilution Buffer (diluted by RNase and DNase free water), in a sterile 1.5 ml micro-centrifuge tube, gently mixed using a vortex, for 2 s and incubated for 30 mins at 20 ºC. Solution B was prepared by diluting transfection agents solution to 10 µl using Opti-MEM, serum free media, in a

sterile 1.5 ml micro-centrifuge tube, gently mixed using a vortex, for 2 s and incubated for 30 mins at 20 ºC. The complex was then prepared by mixing solution A and B with vortex for 1 s then incubated for 20 mins at 20 ºC. Each transfection agent used in solution B was at a different concentration, as described above in the transfection experiments.

For the primary fibroblasts and carcinoma cells toxicity study, 8,000 cells/well were seeded in 96-well plates, obtained from NUNC, in 200 µl of 15 % FCS v/v EMEM and 10 % FCS v/v EMEM in the case of primary fibroblasts and HtTA, respectively. Cells were incubated at 37 ^{o}C and 5 % CO_2 v/v in a CO_2 incubator for 24 h to reach 50-60 % confluency. The medium was removed and replaced with 87.5 µl of 15 % FCS v/v EMEM and 10 % FCS v/v EMEM in the case of primary fibroblasts and HtTA, respectively to which 12.5 µl of either the transfection complex (lipoplex), the free lipopolyamine, or the free RNA (naked RNA) was added to the plates for final volume of 100 µl except for control cells where 100 µl of serum Opti-MEM was added (no RNA complex solution). The plates were incubated for 4 h at 37 ^{o}C in an atmosphere of 5 % CO_2 v/v. After that, media in the incubated plates were aspirated and replaced with 200 µl of 15 % FCS v/v EMEM and 10 % FCS v/v EMEM in the case of primary fibroblasts and HtTA, respectively. The plates were then incubated for a further 44 h at 37 ^{o}C in an atmosphere of 5 % CO_2 v/v. The same procedures and calculations were followed as for the DNA cytotoxicity assay described above.

2.4.11. Characterization of the Formed Nanoparticles

2.4.11.1. Particle size

Particle size of the lipoplexes was measured by laser light scattering using a NANOSIGHT LM10 (NANOSIGHT, Salisbury, UK). The samples containing 1 µg of DNA or 332 ng (25 pmoles) siRNA were prepared at the effective concentration of lipospermine and diluted to a final volume of 200 µl with PBS. The mean particle sizes were determined in at least two independent experiments, each with five independent measurements, using NTA Analytical Software

The average particle size for the lipoplexes formed (at their effective concentration of transfection), after mixing with a vortex mixer, was determined using a laserlight scattering using a NANOSIGHT LM10 (NANOSIGHT, Salisbury, UK)

(nano-particle analysis range: 10-1,000 nm, Laser output: 20 mW at 650 nm, Real-time dynamic nano-particle visualization, particle-by-particle analysis, particle counting and sizing, and particle size distributions displayed as histograms). All measurements were carried out on lipoplexes with 1 μg/200 μl plasmid DNA or 25 pmol/200 μl siRNA in HEPES buffer at pH 7.4 and 20 °C.

For pEGFP lipoplex formation, two solutions were prepared for each sample, solution A (DNA) and solution B (lipopolyamine). Solution A was prepared by diluting DNA solution (1 μg/100 μl) in 1.5 ml micro-centrifuge tube, gently mixed using a vortex for 2 s, and then incubated for 30 mins at 20 ºC. Solution B was prepared by diluting the lipopolyamine solution to 100 μl using HEPES buffer, in 1.5 ml micro-centrifuge tube, gently mixed using a vortex for 2 s, and then incubated for 30 mins at 20 ºC. The complex was then prepared by mixing solutions A and B (brief vortex, 1 s), incubated for 20 mins at 20 ºC and then injected in the machine using a 1 ml sterile syringe.

Each lipopolyamine used in solution B was at a different concentration for the required N/P ratio for 1 μg DNA/200 μl as described above in the N/P determination section for the EthBr fluorescence quenching assay.

For siRNA lipoplex formation, two solutions were prepared for each sample, solution A (RNA) and solution B (lipopolyamine). Solution A was prepared by diluting RNA solution (332 ng/25 μl) in 1.5 ml micro-centrifuge tube, gently mixed using a vortex (2 s), and then incubated for 30 mins at 20 ºC. Solution B was prepared by diluting the lipopolyamine solution (at its effective concentration) to 175 μl using HEPES buffer, in 1.5 ml micro-centrifuge tube, gently mixed using a vortex for 2 s, and then incubated for 30 mins at 20 ºC. The complex was then prepared by mixing solutions A and B (brief vortex, 1 s), and then incubated for 20 mins at 20 ºC and then injected in the machine using 1 ml sterile syringe.

2.4.11.2. Zeta potential

ζ-Potential measurements were determined using a Delsa™Nano Zeta Potential and Submicron Particle Size Analyzer (Beckman Coulter) which determines particle size by measuring the rate of fluctuations in laser light intensity scattered by particles as they diffuse through a fluid, for size analysis measurements and/or electrophoretic light scattering (ELS), which determines electrophoretic movement of

charged particles under an applied electric field from the Doppler shift of scattered light, for zeta potential determination. All measurements were carried out on lipoplexes with 6 μg/ml plasmid DNA in HEPES buffer at pH 7.4 and 20 °C.

For pEGFP lipoplex formation, two solutions were prepared for each well, solution A (DNA) and solution B (lipopolyamine). Solution A was prepared by diluting DNA solution (6 μg/ml) in 1.5 ml micro-centrifuge tube, gently mixed using a vortex for 2 s, and then incubated for 30 mins at 20 ºC. Solution B was prepared by diluting the lipopolyamine solution to 1.0 ml using HEPES buffer, in sterile 2 ml micro-centrifuge tube gently mixed using a vortex for 2 s, and incubated for 30 mins at 20 ºC. The complex was then prepared by mixing solutions A and B (brief vortex 1 s) then incubated for 20 mins at 20 ºC. Each lipopolyamine used in solution B was at the required N/P ratio for 6 μg, as described above in the N/P determination for the particle size and the EthBr experimental sections.

For siRNA lipoplex formation, two solutions were prepared for each sample, solution A (RNA) and solution B (lipopolyamine). Solution A was prepared by diluting RNA solution (75 pmol /75 μl) in 1.5 ml micro-centrifuge tube, gently mixed using a vortex for 2 s, and then incubated for 30 mins at 20 ºC. Solution B was prepared by diluting the lipopolyamine solution (at its effective concentration) to 300 μl using HEPES buffer, in 1.5 ml micro-centrifuge tube, gently mixed using a vortex for 2 s, and then incubated for 30 mins at 20 ºC. The complex was then prepared by mixing solutions A and B by brief vortex (1 s), and then incubated for 20 mins at 20 ºC, diluted to 2 ml, and then injected into the machine using a 3 ml sterile syringe. The ζ-potential measurements of the nanoparticles were computed from the electrophoretic mobility using the software package based on the Henry equation:

$$U_E = \frac{2\varepsilon\zeta f(\kappa a)}{3\eta} \qquad \text{eq. [11]}$$

where U_E is the electrophoretic mobility (velocity of the nanoparticles in a unit electric field), ζ is the zeta potential, ε is the dielectric constant, η is the solvent viscosity and f (κa) is Henry's function, which in aqueous media and electrolyte is equal to 1.5, known as the Smoluchowski approximation.

2.4.12. Confocal Microscopy Studies

2.4.12.1. Preparation of Mowiol coverslip mounting solution

For the preparation of mounting media we used Mowiol (Mowiol 4.88, Calbiochem catalogue number 475904) a solution of polyvinyl alcohol which normally hardens overnight after slide preparation. For preparation, Mowiol (2.4 g) was added to glycerol (6 g) in a 50 ml plastic centrifuge tube equipped with a small stirrer-bar. While stirring, distilled water (6 ml) was added and left for 2 h at 20 ºC then 2M Tris (12 ml, pH 8.5) was added and the tube was incubated in warm water (50–60 ºC) for 10 mins to dissolve the Mowiol, then centrifuged at 5,000 rpm for 15 mins to remove any undissolved solids, and stored as 1 ml aliquots in Eppendorf tubes at -20 ºC. On the day of the experiment, the tubes were thawed at 20 ºC prior to use.

2.4.12.2. Preparation of slides for confocal microscopy visualization

For both DNA and RNA we used the same transfection protocol for both FEK4 and HtTA using 6-well plates with a sterile round coverslip in the bottom of each well, and double the amount of DNA (2 μg/well) or fluorescein-tagged siRNA (25 pmol/well) and the transfecting agents at their optimum amount. At the end of transfection procedures (48 h), we prepared fresh 4% formaldehyde in PBS (w/v) from stocks of formalin 37% (w/v) (Sigma Aldrich). The transfected cells were washed twice with PBS, cells were fixed in 1 ml per well 4% formaldehyde/PBS at 20 ºC for 20 mins, then the formaldehyde PBS solution was aspirated and the cells gently washed 3 times with PBS. After formaldehyde fixing, cells adhering to coverslip(s) were labelled with labelling solution according to the manufacturer's protocol. Labelling solution contains both Alexa Fluor 594 wheat germ agglutinin for cell membrane labelling, ($\lambda_{ex}/\lambda_{em}$ 591/618 nm) and Hoechst 33342 for nuclei labelling ($\lambda_{ex}/\lambda_{em}$ 350/461 nm) mixed in one solution (from Invitrogen, Image-iT live plasma membrane and nuclear labelling kit). We prepared a solution with concentrations of Alexa Fluor 594 wheat germ agglutinin at 5.0 μg/ml and Hoechst 33342 stain at 2 μM. Both combined in a single staining solution in PBS, then we applied 1 ml of labelling solution to cover cells adhering to coverslip(s) and incubated for 10 mins at 20 ºC, then the labelling solution was removed and the cells were washed with PBS (2 x 1 ml).

For slide preparation we used a Pap pen for immunostaining 2 mm tip width (Sigma-Aldrich), to draw a complete circle on the glass slide (the diameter of the circle was less than the diameter of the coverslip that will cover it). We placed a drop (20 µl) of mounting solution Mowiol (Calbiochem) in the centre of each marked circle. The coverslip was removed with forceps and the underside (non-cell side) was gently wiped with a Kimwipe® tissue. Then the coverslip was carefully mounted, cell-side down, onto the mounting solution, we then used capillary action to drain the excess of mounting solution from under the coverslip with a Kimwipe® tissue and left it in the dark (16 h) to solidify in order to be ready for confocal microscopy visualization.

2.4.12.3. Confocal microscopy visualization

Following the DNA and siRNA transfection protocols, cells were seeded on a sterile coverslip at the bottom of each well. After 48 h, media were aspirated and cells were fixed with freshly prepared 4% formaldehyde solution in PBS (1 ml/well) for 15 mins at 37 ^{o}C. After formaldehyde fixing, cells adhering to coverslips were labelled with labelling solution according to the manufacturer's protocol. Labelling solution contained both Alexa Fluor 594 wheat germ agglutinin for cell membrane labelling, λ_{ex} 591 nm and λ_{em} 618 nm, and Hoechst 33342 for nuclei labelling, λ_{ex} 350 nm and λ_{em} 461 nm, mixed in one solution purchased from Invitrogen (Image-iT live plasma membrane and nuclear labelling kit), cell labelling with Alexa Fluor WGA (5 µg/ml) and Hoechst 33342 (2 µl, 2 µM). After that, labelled cells were mounted using mounting liquid (20 µl, Mow-Iol, Merck) and left for 16 h. Then, mounted cells in the coverslips were visualized using a confocal laser scanning microscope (LSM510META, Carl Zeiss) under the 60× oil immersion objective, with filters. The ZeissLSM510 Meta system consists of a Zeiss Axiovert 200M microscope Meta detector head (range 410-750 nm), Fujitsu/Siemens Computer, LSM Software Version 4.0 and the high power objectives are Zeiss: EC Plan- 63x/1.4 Oil DIC. For blue, green and red fluorescence, we used blue: Violet Diode Laser (λ_{ex} = 405 nm and λ_{em} 420-480 nm) + BP 420-480 nm filter; green: Argon Laser (λ_{ex} = 488 nm and λ_{em} 505-530 nm) + BP 505-530 nm filter; red: HeNe543 Laser (λ_{ex} = 543 nm and λ_{em} 560-615 nm) + Meta 550-615 nm detection.

CHAPTER 3

Design and Development of Pharmaceutical Dosage Forms for Gene Delivery

3.1. INTRODUCTION

For gene therapy to realise its potential and become an efficient medicine for the treatment of diseases such as cancer, cystic fibrosis, inflammation, or for vaccination, key obstacles must be overcome. The essential requirements for gene delivery are the transport of DNA through the cell membrane and ultimately to the nucleus. The design of an efficient formula for the delivery of genetic material requires a detailed understanding of the barriers that hinder this process. Thus, efficient formulations of lipoplexes (150) or polyplexes (151-153) must be able to deliver safely the required DNA across the various cellular barriers to the nucleus. Barriers to DNA delivery also include complex formation between the DNA and the lipopolyamine leading to DNA nanoparticle formation by electrostatic charge neutralisation (to about 90 % of the total negative charge) and overall packing as condensed DNA nanoparticles (154). So, a key first step in this method of gene formulation is masking the phosphate negative charges. This anion titration with a lipopolyamine causes alleviation of charge repulsion between remote phosphates along the DNA helix leading to collapse into a more compact structure that facilitates cell entry.

For NVGT, except for naked (free, uncomplexed) DNA being trapped inside cells by direct association with the chromatin during mitosis, the (prodrug) DNA must be formulated. Small molecule synthetic cationic lipids are one of the major gene carriers for NVGT, often classified as liposomal and non-liposomal non-viral delivery vectors. They condense DNA into nanoparticles that are readily endocytosed by cultured cells, and facilitate endosomal escape leading to efficient nuclear delivery presumably entering through the nuclear pore complex (NPC). After nuclear entry, the payload DNA should ultimately be able to give the desired protein through transcription and translation.

The possibility of reaching the goal of intracellular protein levels at therapeutic concentrations moves even more towards utilising non-viral gene therapy (NVGT). Since the design and formulation of Lipofectin by Felgner and co-workers, reported in 1987 (2), the focus on non-viral vectors for DNA delivery has shown a remarkable increase worldwide (34,155). Cationic lipids are considered to be the major gene carriers among the non-viral delivery systems (156). They have the ability to condense DNA into particles that can be readily endocytosed by cultured cells, and facilitate endosomal escape leading to efficient delivery to the nucleus. Liposomal delivery vectors usually contain two types of lipids, a cationic lipid (positively charged

amphiphile) for DNA condensation and cellular membrane interaction, and a neutral helper lipid (phospholipid), most use dioleoylphosphatidyl ethanolamine (DOPE) (Fig. 3.1) to increase transfection efficiency as it has a membrane fusion promoting ability (2,3). Non-liposomal cationic-lipid delivery vectors combine both the characteristics of cationic and helper lipids e.g., Transfectam® (dioctadecylamido-glycyl spermine, DOGS) formulation (Fig. 3.1) (15,72) whose synthesis by Behr and co-workers (72) as a promising transfecting agent, encouraged several laboratories to focus on the synthesis of novel cationic lipids based on the naturally occurring polyamine spermine.

One of the important factors to improve the release of free DNA or the lipoplex into the cytoplasm is the influence of the cationic lipid chain. Xu and Szoka (36) have reported that unsaturated hydrocarbon chains increase the transfection efficiency of the lipoplex by decreasing the rigidity of the bilayer and favouring a higher inter-membrane transfer rate and lipid mixing, compared to their saturated counterparts. However, Engberts, Hoekstra and co-workers recently reported that, in certain cases, saturated fatty chains afforded better results than unsaturated chains (157). Also, Heyes et al. (93) showed that, among the cationic lipid analogues they synthesized with variation in the degree of saturation, the saturated C18 conjugates were internalized in to the cells more, although they are less efficient in gene silencing (siRNA delivery).

In liposomal formulations, DOPE (Fig. 3.1) is often used as a helper lipid for liposomal formulation and for its fusogenic ability as it has the characteristics of non-bilayer forming activity leading to destabilisation of the lipid bilayer (3). Oleoyl and oleyl chains have also been bound as esters and ethers in liposomal formulations: 1,3-dioleoyloxy-2-(6-carboxyspermine) DOSPER (158), of 2,3-dioleyloxy-*N*-[2(spermine-carboxamido)ethyl]-*N,N*-dimethyl-1-propanaminium trifluoroacetate (DOSPA)-DOPE (3/1 w/w, Lipofectamine™), *N*-[1-(2,3-dioleyloxy)propyl]-*N*,*N*,*N*-trimethylammonium chloride (DOTMA)-DOPE (1/1 w/w, Lipofectin®) (Fig. 3.1). The use of cationic liposomes in poly-nucleic acid delivery was pioneered by Felgner and co-workers who developed the cationic liposome now commercially available as Lipofectin (2). Lipofectin is a 1:1 ratio of the cytofectin DOTMA and the naturally occurring, neutral lipid DOPE; Lipofectamine is a 3:1 (w/w) liposome formulation DOSPA and DOPE.

3.1.1. Methods for Cationic Liposome Formulation

The formulation of cationic liposomes, with or without a neutral co-lipid, has involved a number of different possible procedures. Broadly speaking these are:

1. Sonication and/or vortex-mixing of an aqueous solution,
2. Reverse-phase evaporation,
3. Aqueous dilution of an ethanolic stock solution.

The method of formulation is undoubtedly important, but the extent to which it affects the efficiency of poly-nucleic acid transfer has yet to be properly investigated. DOTMA and its analogues are usually formulated into cationic liposomes with the neutral colipid DOPE. Liposomes are typically prepared by vortex-mixing of equimolar amounts of a cationic lipid and a neutral lipid at room temperature to produce large multilamellar vesicles (MLVs) which are then sonicated to produce small unilamellar vesicles (SUVs) suitable for gene transfection (159). Alternatively, rotary evaporation of the lipid mix (e.g., from chloroform or dichloromethane) to yield a film, which is evaporated for 1 h and then rehydrated in PBS at pH 7.4. Size-reduction can be carried out by repeatedly passing through a thermobarrel extruder with a sub-micron filter (160). However, cationic amphiphile DOGS (Transfectam) is non-liposomal and is formulated simply by ten-fold dilution of an aqueous ethanol stock solution into an aqueous buffer (72).

In this study we are concentrating on lipopolyamines composed either of two symmetric or unsymmetrical (i.e., different) carbon chain, or lipophilic steroid attached (12,23,161-163), covalently bound to a polyamine e.g., spermine (1,12-diamino-4,9-diazadodecane) (164). The first cellular barrier for the delivery of the DNA nanoparticles is the eukaryotic cell membrane which is composed mainly of phospholipids (50-90 % of total lipid content, most phospholipids are derivatives of diacyl-glycerol-3-phosphate), sterols (5-25 %), and glycol-lipids (usually less than 5 %). The diacyl-glycerol chains (C14 to C24) are derived from linear fatty acids with varying degrees of unsaturation (165). In NVGT, cationic lipids which interact with the DNA payload also mediate cell-membrane transport, typically through adsorptive endocytosis or mediated by cations (166-168), both routes leading to internalization of the DNA complex nanoparticles. Such endocytosis is via the clathrin-coated pits (diameter 250-300 nm) (169), followed by fusion of the early endosome and sorting to the late endosomal compartment, hence avoiding degradation in the lysosome.

In this study, the effects on DNA formulation of a circular plasmid are investigated with variation in the position, length, saturation or the symmetry of the two fatty chains (diacyl or dialkyl) in our lipospermines or the attachment of a heterocyclic group on the two primary amines of lipospermines to increase its pK_a these lipid chains are linked by amide bonds at the secondary amino groups of spermine to form N^4,N^9-diacyl spermine or the primary amino groups of spermine to form N^1,N^{12}-diacyl spermine. This study includes the physicochemical characterisation of the lipoplexes nanoparticles formed, transfection results and cytotoxicity effects with the synthesized lipospermine formulations. The ability of this synthetic lipopolyamine to condense DNA was studied using ethidium bromide (EthBr) fluorescence quenching, light scattering assays and gel electrophoresis assay. The physicochemical characterization includes the particle size measurements and zeta potential studies. The ability of these formed complexes to protect DNA from degradation by DNase enzyme studied by the gel electrophoresis.

Transfection efficiency was studied in an immortalized cancer cell line (HtTA), and in primary skin cells (FEK4) in presence and absence of serum to test the ability of these novel transfecting agents to work efficiently in the presence of serum which open the door for successful ones for further in vivo investigations, and compare these results with those obtained with the (liposomal) transfection formulations, Lipofectin® and Lipofectamine™ that incorporate such oleoyl or oleyl (C18) chains and non-liposomal lipospermine Transfectam and Lipogen™ (InvivoGen) (170,171).

Lipofectamine™ is available as a mixture of the cationic lipid DOSPA and the neutral helper lipid DOPE as 3/1 w/w, respectively. While Lipofectin® is available as a mixture of the cationic lipid DOTMA and the helper lipid DOPE as 1/1 w/w, respectively. The cytotoxicity of these compounds was studied in both primary skin and immortalised cancer cell lines using the MTT assay. Two commercially available liposomal transfection formulations, Lipofectin® and Lipofectamine™ and then the non-liposomal lipospermine Transfectam and N^4,N^9-dioleoyl spermine (Lipogen™, InvivoGen) were the starting point for these investigations.

Spermine

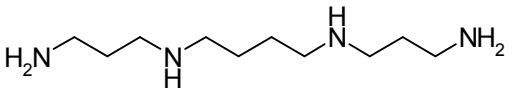

DOPE, Helper lipid (3,69)

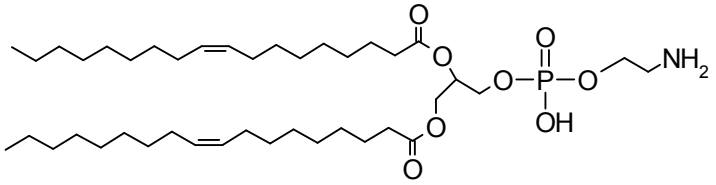

DOTMA

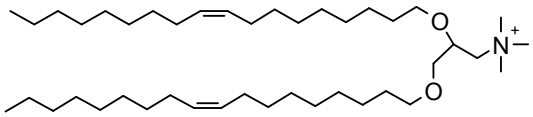

Lipofectin® is a 1:1 (w/w) liposome formulation of DOTMA and DOPE (2)

DOSPA

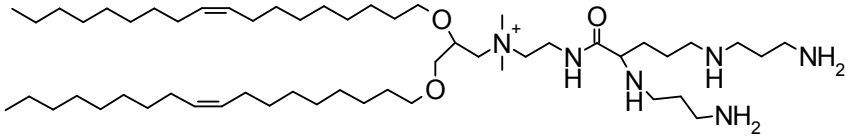

Lipofectamine™ is a 3:1 (w/w) liposome formulation of DOSPA and DOPE (Life technology-Invitrogen)

Transfectam (DOGS) (72)

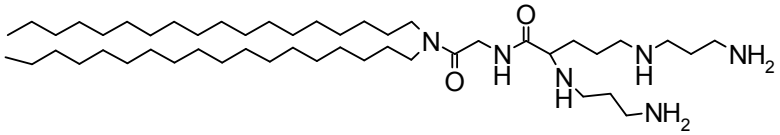

Mol. Wt 807.40

***N*^{4},*N*^{9}-Dioleoyl spermine** (170,171)

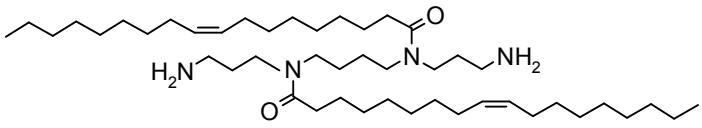

Lipogen™ (InvivoGen), Mol. Wt 731.26

Fig. 3.1. DNA condensing and delivering lipopolyamines cationic lipids

3.1.2. DNA Condensation

The use of an efficient carrier for poly-nucleic acid delivery is a determinant factor for the successful application of gene delivery (172). This carrier is responsible for the complex process of gene delivery to the nucleus (154). Within the prerequisites for delivery of DNA across intact cytoplasmic membrane are condensation and masking the negative charges of the phosphate backbone. Condensation of DNA occurs when 90 % of the charge on DNA is neutralised (11,173). To investigate the neutralization of these negative charges along the DNA backbone that leads to collapse of the DNA into a more compact structure (nanoparticles), three experiments were carried out:

1. Ethidium bromide fluorescence quenching assay,
2. Light scattering assay,
3. Gel electrophoresis study.

The ability of spermine to condense calf thymus DNA, also Lipofectin, Lipofectamine, Transfectam and synthesized lipospermines to condense circular plasmids DNA pEGFP was investigated (pEGFP encoding for enhanced green fluorescent protein (4.7 kbp) under CMV promoter). Also, the ability of N^4,N^9-dioleoyl spermine to condense DNA, leading to the formation of nanoparticles (that are suitable for gene delivery), was compared with the commercially available liposomal transfection formulations Lipofectin and Lipofectamine and non liposomal Transfectam.

3.1.3. Ethidium Bromide Fluorescence Quenching Assay

EthBr (2,7-diamino-9-phenylphenanthridinium-10-ethyl bromide, Fig. 3.2) a cationic dye that displays a marked increase in the fluorescence upon binding with DNA and RNA through the intercalation between the EthBr phenanthridinium moiety and adjacent base pairs of specific DNA sequences (174-176). The increase in the fluorescence of EthBr upon binding with DNA making EthBr a useful probe to measure drug-DNA interactions (164,174,175). The binding of cationic molecules with DNA is not entirely responsible for the release of EthBr, but alteration of the molecular flexibility of DNA through cationic compaction facilitated the release of bound EthBr (163,175,176).

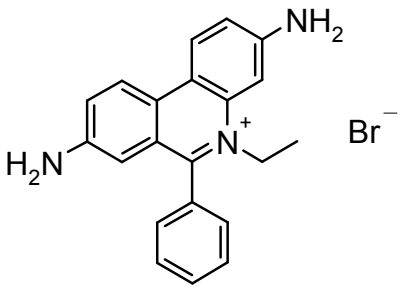

Fig. 3.2. Ethidium bromide (Eth Br)

The significant enhancement of fluorescence when EthBr intercalates DNA is attributed to the hydrophobic environment surrounding the EthBr molecule leading to longer life time for the excited state (174,177). On the other hand, free EthBr (in solution) is strongly quenched by aqueous solvent, so it exhibits a weak fluorescence relative to that from intercalated dye (177). The fluorescence intensity of free EthBr (no DNA) in HEPES buffer solution (20 mM NaCl, 2 mM HEPES, 10 μM EDTA, pH 7.4) was usually small (background). On the other hand, the fluorescence intensity of the EthBr solution was significantly increased after the addition of DNA solution, as a result of EthBr intercalation between DNA base-pairs. The fluorescence was expressed as the percentage of the maximum fluorescence when EthBr was bound to the DNA in the absence of competition for binding and was corrected for background fluorescence of free EthBr in solution.

DNA condensation studies were started through investigating the effect of spermine to condense calf thymus DNA (Fig. 3.3). The charge ratio was calculated according to the ammonium/phosphate (+/-) charge ratio for spermine as 202.35 g/mole spermine contains four nitrogens that can be protonated. Spermine has pK_a values of 10.9, 10.1, 8.9 and 8.1, and according to Henderson-Hasselbach equation, spermine has 3.8 charges / molecule at pH 7.4 (23). Fig. 3.3 shows that the fluorescence of EthBr decrease as a function of increasing the N/P ratio of spermine.

These results confirmed that, both the number of positive charges and their distribution on the surface of the molecule have profound effects on DNA condensation as indicated in previous studies (161,178,179).

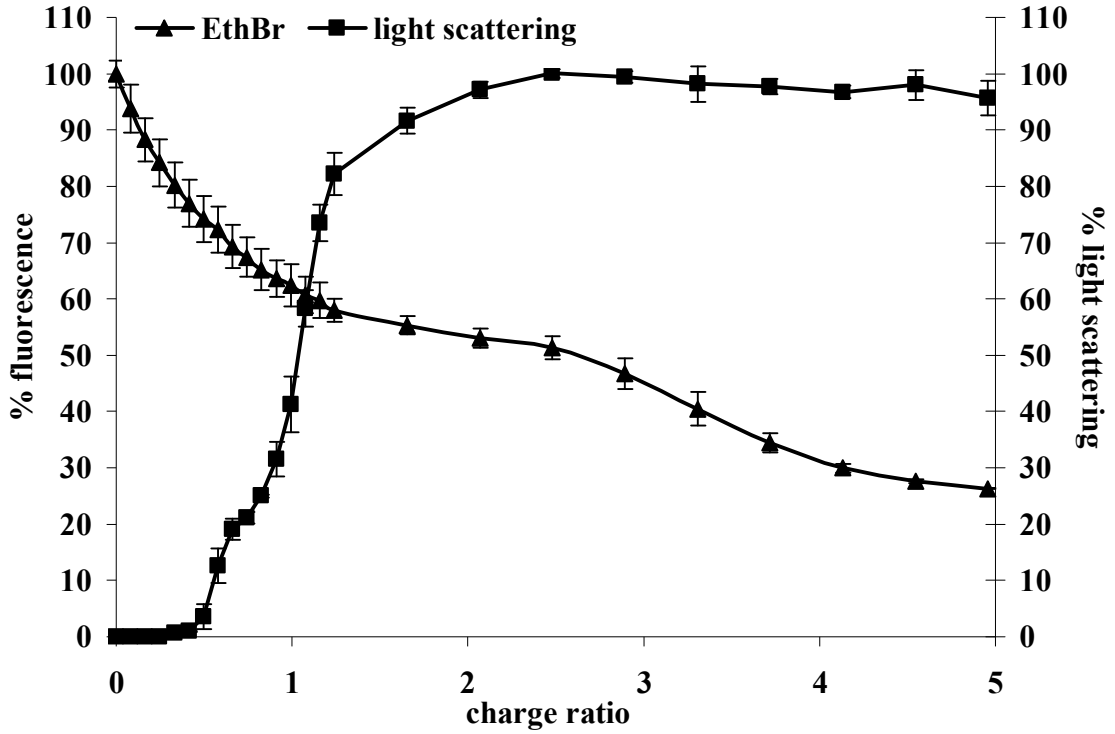

Fig. 3.3. Plot of EthBr displacement assay and light scattering assay (relative maximum apparent absorbance at λ =320nm) of calf thymus DNA complexed with spermine

The ability of the commercially available liposomal cationic lipids (Lipofectin, and Lipofectamine) and non-liposomal (Transfectam and N^4,N^9-dioleoyl spermine) to condense pEGFP was investigated. Fig. 3.4 shows DNA condensation ability of N^4,N^9-dioleoyl spermine in comparison with the commercially available, liposomal cationic lipid formulations Lipofectin® and Lipofectamine™ and non liposomal Transfectam. All cationic lipid formulations have the ability to condense completely DNA through the displacement of EthBr leading to fluorescence quenching. At lower charge ratios, and Transfectam and Lipofectamine has better ability to suppress fluorescence, which produces 50 % fluorescence decrease at N/P charge ratio 0.6 and 1.23 respectively, than N^4,N^9-dioleoyl spermine and Lipofectin®, which produces 50 % fluorescence decrease at N/P charge ratio 1.35 and 1.85, respectively.

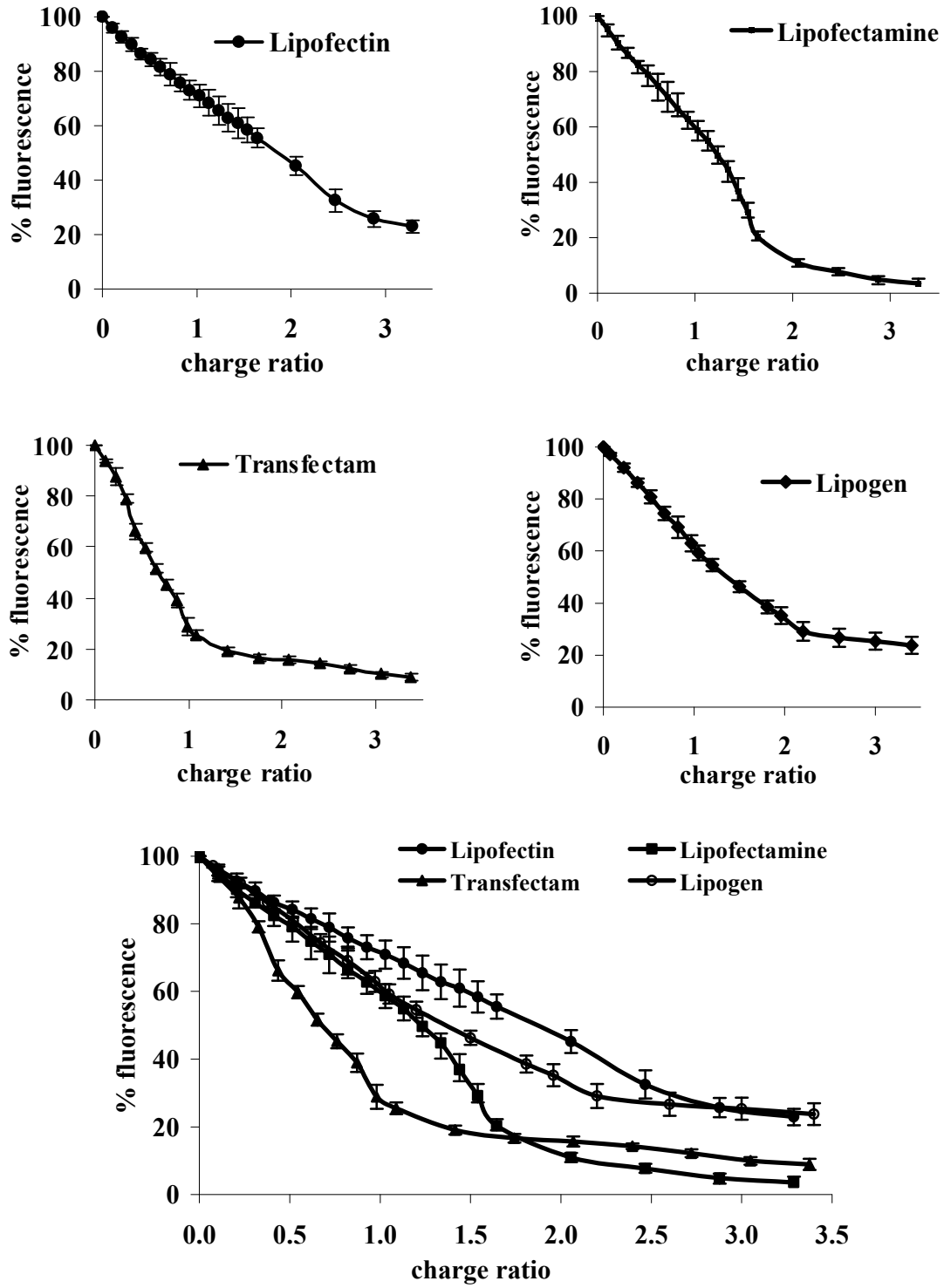

Fig. 3.4. Plot of EthBr fluorescence quenching assay of pEGFP DNA complexed with Lipofectin, Lipofectamine, Transfectam and Lipogen (N^4,N^9-dioleoyl spermine).

Table 3.1. pEGFP DNA binding data

Condensing agent	Drug concentration at 50 % fluorescence quenching (μM)	K_{app*}
Spermine	0.68	$1.9x10^7$ M^{-1}
Lipofectin	1.85	$7x10^6$ M^{-1}
Lipofectamine	0.31	$4.2x10^7$ M^{-1}
Transfectam	0.22	$5.8x10^7$ M^{-1}
N^4,N^9-Dioleoyl spermine	0.68	$1.9x10^7$ M^{-1}

* "apparent" equilibrium binding constant of condensing agent to pEGFP DNA

To quantify the ability of the investigated polyamines in condensing DNA, the binding constant of these polyamines with DNA was estimated (Table 3.1) and compared using EthBr assay that has been shown to be a valid method for comparison of DNA binding affinity (175). The drug concentration producing 50 % inhibition of fluorescence is approximately inversely proportional to the binding constant.

From Table 3.1 data, the concentrations of condensing agents producing 50 % fluorescence inhibition were calculated (equation 1) as shown in the experimental chapter. The "apparent" equilibrium constant (K_{app}) of polyamine binding was calculated taking into account that the binding constant of ethidium to be 10^7 M^{-1} (140) and the concentration of EthBr is 1.3 μM. From these results it was found that Transfectam has the highest binding affinity (K_{app} $5.8x10^7$ M^{-1}) between the compared polyamines and Lipofectin the lowest with binding affinity (K_{app} $7x\ 10^6$ M^{-1}) which could be attributed to the higher number of positive charges and the charge distribution on other polyamines because in Lipofectin the cationic lipid DOTMA carries 1 positive charge (ammonium eq/mole) (2) while the cationic lipid DOSPA in the Lipofectamine formulation and carries 4 positive charges (ammonium eq/mole) (15). In the non-liposomal formulations, N^4,N^9-dioleoyl spermine carries 2 positive charges, Transfectam® carries 3 positive charges (139), and spermine carries 4 positive charges at physiological pH.

$$K_b \text{ (vector)} = \frac{[EthBr]\times 10^7}{[vector]} \qquad \text{eq. [1]}$$

DNA is condensed by neutralizing the DNA phosphate negative charges by the two primary amines that are positively charged at pH 7.4 and coated by the dioleoyl lipophilic moiety of N^4,N^9-dioleoyl spermine. In addition, the formation of N^4,N^9-dioleoyl spermine-DNA lipoplex at lower charge ratio decreases the toxicity of the DNA delivering lipopolyamine. In addition, as the mammalian cell membrane is a semi-permeable membrane formed of phospholipids bilayer that allows the transport of macromolecules by endocytosis, neutralization of the negative charges on the DNA by polycations will improve the delivery of DNA through the cell membrane because of the presence of negative charges on both DNA and cell membrane. Also, the positively charged lipid complex will mediate transfection by fusion with cell membrane (36,150).

3.1.4. Light Scattering Assay

This experiment has been carried out to investigate the condensation of DNA by polyamines and the formation of particles (180). The apparent UV absorbance at 320 nm (where there is no DNA absorbance above 300 nm) was measured (19,161) showing light scattering. The formation of DNA nanoparticles causes scattering of light that reduces light intensity at the UV detector. The results from Fig. 3.3 indicated the formation of particles upon interaction of spermine maximum at N/P ratio 2.5.

In addition, Fig. 3.3 shows that the light scattering due to particle formation increases with the increase in the displaced EthBr and reaches the maximum at approximately the same charge ratio at which there is a maximum EthBr displacement, although the concentration of DNA used in light scattering experiments is ten times the concentration used in fluorescence quenching experiments which is related to the lack of sensitivity of the light scattering experiment in comparison with EthBr fluorescence assay. Also, from light scattering results, there is a decrease in the % relative maximal apparent absorbance (% rel. max. app. abs.) after reaching the maximum absorbance, which could be attributed to the formation of polyamine-DNA aggregates as reported by Gosule and Schellman (181) where any DNA intra-chain binding agents will also act as inter-chain segment binders. The formation of aggregates at high charge ratio, at the relatively high concentration of DNA in comparison with EthBr assay, will decrease the scattering light that will decrease the apparent absorption value. As this light scattering assay is much less sensitive than the EthBr fluorescence quenching assay, we decided not to use it anymore, and we

depended only on both the EthBr assay and agarose gel electrophoresis experiments for verification of pDNA condensation as found in many recent gene delivery publications.

3.1.5. Agarose Gel Electrophoresis

The complex formation of lipopolyamines polyanionic DNA (pEGFP) was examined by analysis of the electrophoretic mobility of the circular plasmid DNA-lipopolyamine complex within an agarose gel (1 %) stained with EthBr. The unbound free DNA in the agarose gel was visualized under UV using GeneGenius (Syngene).

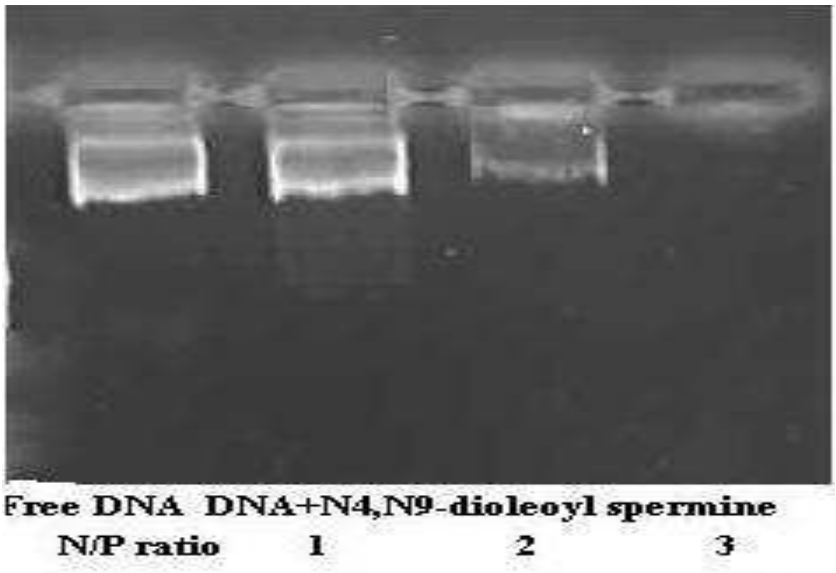

Fig. 3.5. Gel retardation assay of pEGFP either free (pEGFP lane) or complexed with N^4,N^9-dioleoyl spermine at different N/P ratios.

N^4,N^9-Dioleoyl spermine was able to condense pEGFP DNA efficiently (as a result of the interactions between the lipopolyamine ammonium ions and the DNA phosphate charges) at the optimised respective charge ratios (N/P) of transfection leads to immobilization and reduction of EthBr intercalation with DNA. Fig. 3.5 shows that N^4,N^9-dioleoyl spermine was able to completely inhibit the migration of the circular plasmid DNA from lipoplexes in the agarose gel at charge ratio of transfection. The results revealed the ability of N^4,N^9-dioleoyl spermine to completely immobilize pEGFP at higher charge ratios (charge ratio 3). While at lower charge ratios (≤ 2) a moderate inhibition of pEGFP in the agarose gel was observed (Fig. 3.5). These results were in agreement with the EthBr fluorescence intensity (DNA

condensation) results (Fig. 3.4) that showed more than 80 % fluorescence quenching was achieved by pEGFP- N^4,N^9-dioleoyl spermine charge ratio of 3.

3.1.6. Cell Culture and Transfection Experiments

Two cell lines were used in the transfection experiment, FEK4 cells (143,144,182), are human primary fibroblasts derived from newborn foreskin explants (144) and HtTA cells are a human cervical carcinoma, HeLa derived and transformed cell line. Cells were cultured in Earle's Minimal Essential Medium (EMEM) supplemented with foetal calf serum (FCS) 15 % in the case of FEK4 cells and 10 % in the case of HtTA cells, penicillin and streptomycin (50 IU/ml each), glutamine (2 mM), and sodium bicarbonate (0.2 %). Primary cells were passaged once a week, and used between passages 7-15.

For the transfection (gene delivery) and the resultant gene activity (transfection efficiency), cells were seeded in 12-well plates at a density of 5 x 10^4 cells/well (in 1 ml EMEM with FCS) for 24 h to reach a 50-60 % confluency on the day of transfection. The complex was prepared by mixing pEGFP (1 μg/ml/well) with each lipopolyamine in Opti-MEM (serum free media, Gibco BRL) according to the charge ratio at 20 ^oC for 30 mins, and then incubated with the cells for 4 h at 37 ^oC in 5 % CO_2. Then the cells were washed and cultured for a further 44 h in growth medium at 37 ^oC in 5 % CO_2.

Levels of EGFP in the transfected cells were detected and corrected for background fluorescence of the control cells using a fluorescence activated cell sorting (FACS) machine (Becton Dickinson FACS Vantage dual Laser Instrument, argon ion laser 488 nm). The transfection efficiency was calculated based on the percentage of the viable cells that expressed EGFP (positive cells) in the total number of cells.

The tested lipopolyamines were investigated for their gene delivery ability in cells using pEGFP as a reporter gene.

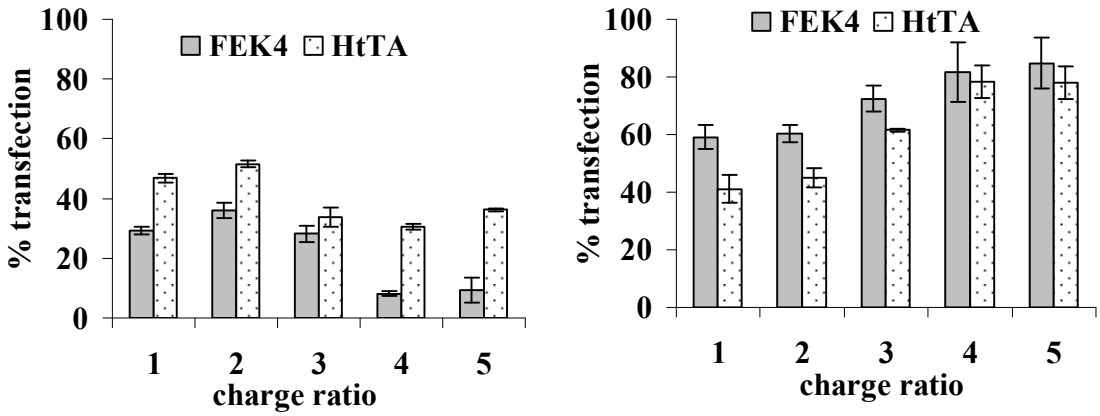

Fig. 3.6. Lipofection of primary skin cell line (FEK4) and cancer cell line (HtTA) transfected with pEGFP complexed with different concentrations of Lipofectin (left) and Lipofectamine (right) at different N/P ratios. The data show 3 different experiments (3 replicates each) and the error bars are the standard deviation.

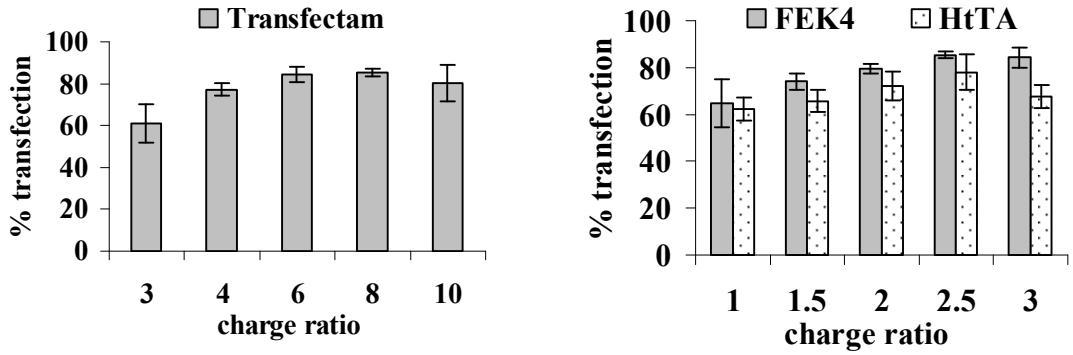

Fig. 3.7. Lipofection of primary skin cell line (FEK4) transfected with pEGFP complexed with different concentrations of Transfectam (left) and of primary skin cell line (FEK4) and cancer cell line (HtTA) transfected with pEGFP complexed with different concentrations of N^4,N^9-dioleoyl spermine (right). The data show 3 different experiments (3 replicates each) and the error bars are the standard deviation.

Fig. 3.6 shows the transfection results of pEGFP into FEK4 and HtTA using Lipofectin and Lipofectamine at different charge ratios. These results show that Lipofectin is unable to achieve high transfection efficiency in FEK4 and HtTA cell lines up to charge ratio 5, it shows that Lipofectin achieves a maximum of 36% for FEK4 and 52% for HtTA transfection efficiency from charge ratio 2, while Lipofectamine results show 85% for FEK4 and 78% for HtTA transfection efficiency from charge ratio 5. In the case of Transfectam®, it shows a significant improvement

in the transfection levels of the primary cell line FEK4 at different charge ratios, from 61 % at charge ratio 3 to up to 85 % transfection levels at charge ratio 8 with optimum transfection efficiency 84% at N/P ratio 6. N^4,N^9-Dioleoyl spermine achieves 85 %for FEK4 and 78% for HtTA transfection efficiency at the optimum charge ratio of transfection 2.5 (Fig. 3.7).

3.1.7. In Vitro Cytotoxicity

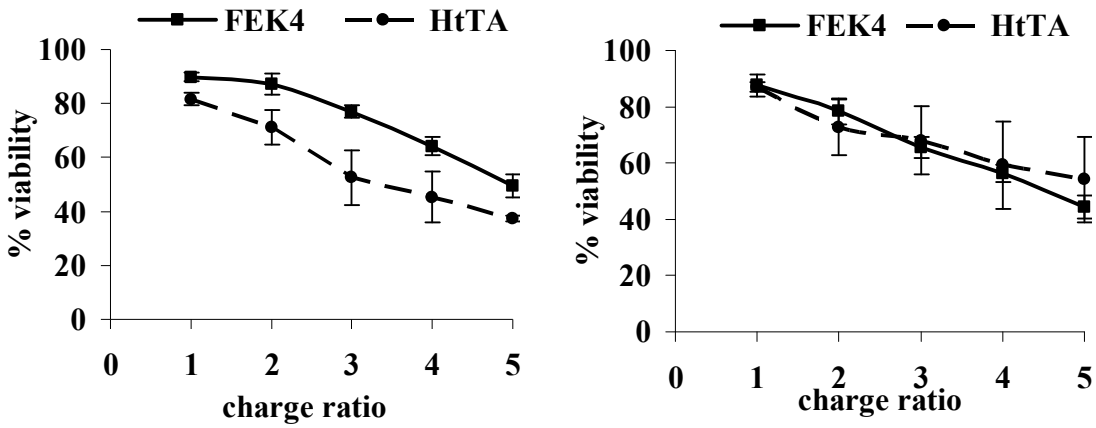

Fig. 3.8. Viability of primary skin cell line (FEK4) and cancer cell line (HtTA) transfected with pEGFP complexed with different concentrations of Lipofectin (left) and Lipofectamine (right) at different N/P ratios The data show 3 different experiments (3 replicates each) and the error bars are the standard deviation.

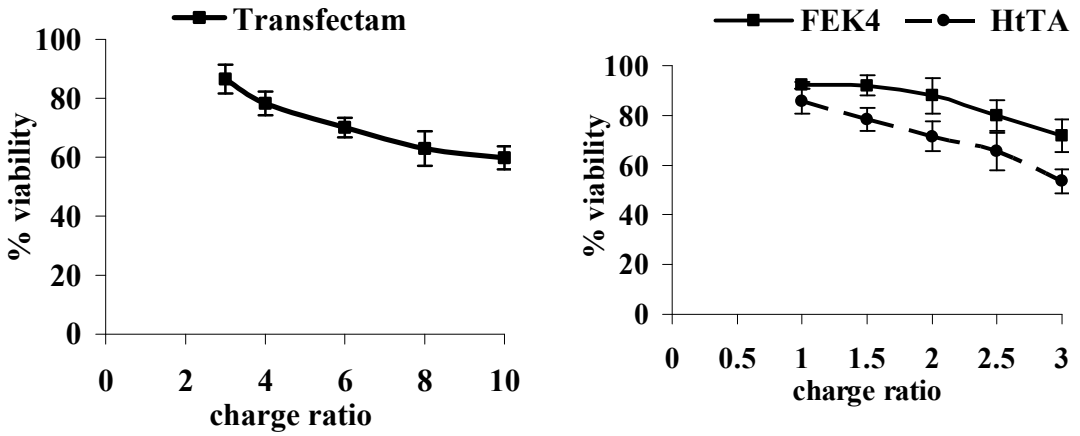

Fig. 3.9. Viability of primary skin cell line (FEK4) transfected with pEGFP complexed with different concentrations of Transfectam (left) and of primary skin cell line (FEK4) and cancer cell line (HtTA) transfected with pEGFP complexed with

different concentrations of N^4,N^9-dioleoyl spermine (right). The data show 3 different experiments (3 replicates each) and the error bars are the standard deviation.

Two cell lines were used in the transfection experiment; primary cell line FEK4 cells and cancer cell line HtTA were used for the cytotoxicity studies too.

Lipofectin achieves a viability range from 90% to 50 % for FEK4 and 82% to 38% for HtTA viability from charge ratio ascending from 1 to 5 with viability of 87% for FEK4 and 71% for HtTA at its maximum transfection efficiency at N/P ratio 2, while Lipofectamine results show viability range from 87% to 55% for FEK4 and 78% to 45% for HtTA from charge ratio ascending from 1 to 5 which is the max transfection efficient ratio (Fig. 3.8). In the case of Transfectam®, it shows reduction in the viability of the primary cell line FEK4 from 87 % at charge ratio 3 to 60 % at charge ratio 8 with cell viability 70% at the maximum transfection level at N/P ratio 6 (Fig. 3.9). N^4,N^9-Dioleoyl spermine (Fig. 3.9) achieves cell viability 92% to 72 % for FEK4 and 85% to 54% for HtTA with cell viability 83%for FEK4 and 65% for HtTA at the optimum charge ratio of transfection 2.5.

The increased toxicity levels of the lipoplex could be attributed to the high efficiency of the lipopolyamine in transfecting the primary and cancer cell lines investigated.

3.1.8. Characterization of the Lipoplex Formulations

Lipoplex Particle Size and Zeta-Potential Measurement

Condensation of DNA into nanoparticles is a way to decrease the size of the delivered gene in order to facilitate cellular membrane entry by endocytosis and subsequent trafficking to the nucleus. Zeta potential characterizes the stability of the formulation. Romoren et al. (183) investigated the long-term stability of chitosan-based polyplex solutions (25 mM sodium acetate buffer, pH 5.5) at different temperatures (4 °C, 25 °C, 45 °C) over a period of up to 1 year. They showed the relation between the change in the physicochemical characteristics of the polyplexes (particle size and zeta potential) and the change in the transfection efficiency.

3.1.8.1. Lipoplex Particle Size Measurement

The average particle size for the lipoplexes formed (at their optimum charge ratio of transfection) between plasmid DNA and lipopolyamines, after mixing with vortex mixer was determined using Nanosight LM10 (Nanosight). All measurements were carried out on lipoplexes having a 2 μg DNA/200μl in HEPES buffer at pH 7.4 at 20 ºC.

The characterization of particle size revealed that the average particle size of Transfectam® lipoplexes was considerably smaller (65 nm) than that obtained with N^4,N^9-dioleoyl spermine (150 nm). Lipoplexes with liposomal reagents, Lipofectin and Lipofectamine showed larger average particle sizes of 200 and 245 nm, respectively, as indicated in Table 3.2. All the particle size measurements were carried out on the lipoplexes at their optimum charge ratio of transfection.

The results of pEGFP (4.7 kbp) condensation and formation of 65 nm nanoparticles with Transfectam® were in agreement with the results found by Dunlap et al. in their study of the commercial lipospermine condensation of plasmid DNA (5–7 kbp) that induced condensates of 50–70 nm in diameter (184).

Table 3.2. Particle size of DNA lipoplexes of Lipofectin, Lipofectamine, Transfectam and N^4,N^9-dioleoyl spermine at their optimum charge ratio for transfection.

Lipopolyamine	Charge ratio (N/P)	Lipoplex diameter (nm)
Lipofectin	2.0	245 (15)
Lipofectamine	4.5	200 (34)
Transfectam	8.0	65 (5)
N^4,N^9-Dioleoyl spermine	2.5	150 (12)

Each lipoplex diameter value shows the mean ± S.D.

3.1.8.2. Zeta-Potential Measurement

Zeta- (ζ–) potential is an important parameter helping to predict the stability of the formulation as well as the ability of the positively charged particles to interact with cell membranes (185). Zeta potential depends on several factors including: pH, ionic charge, ion size, and concentration of ions in solution (186). The interaction of DNA with cationic lipids leads to the formation of net charge on the surface of the

formed nanoparticles, either positive or negative according to the DNA- cationic lipid charge ratio, which attracts counter ions close to the surface of the formed nanoparticles (an electrical double layer). Ions close to the surface of the particle are bound relatively strongly to the surface until the hydrodynamic plane of shear. After this plane, ion distribution is determined by a balance of electrostatic forces and random thermal motion. The potential in this region, therefore, decays as the distance from the surface increases until, at sufficient distance, it reaches the bulk solution value (zero). The potential at this imaginary surface, the hydrodynamic plane of shear, which separates the thin layer of liquid bound to the solid surface and showing elastic behaviour from the rest of the liquid is the ζ-potential. The formed nanoparticles are considered to be stable when they have pronounced ζ-potential values, either positive or negative, but the tendency to aggregate is higher when the ζ-potential is close to zero.

The average ζ-potential measurement for the lipoplexes formed (at their optimum charge ratio of transfection), after mixing with vortex mixer, was determined using a Delsa™Nano Zeta Potential and Submicron Particle Size Analyzer (Beckman Coulter). All measurements were carried out on 2 ml of lipoplexes solution with 3 μg/ml plasmid DNA in HEPES buffer at pH 7.4 and 20 °C. The results revealed that the surface charge, as determined by ζ-potential measurements, was +2.17 for N^4,N^9-dioleoyl spermine (at N/P charge ratio of 2.5), while the measured ζ-potential for naked DNA is -1.02 mV. After these preliminary studies we started to test our novel lipospermine and based on the change of the position of diacyl fatty chains (N^1,N^{12}-diacyl spermines), change the length (C18 and C14) and degree of saturation (saturated and mono unsaturated) of the fatty chain. In the next section, we will study N^1,N^{12}-dimyristoleoyl spermine, N^1,N^{12}-dimyristoyl spermine, N^1,N^{12}-dioleoyl spermine and N^1,N^{12}-distearoyl spermine and compare them with N^4,N^9-dioleoyl spermine.

3.2. N^1,N^{12}-DIACYL SPERMINES: SAR STUDIES ON NON-VIRAL LIPOPOLYAMINE VECTORS FOR pDNA FORMULATION

Four long chain N^1,N^{12}-diacyl lipopolyamines: N^1,N^{12}-[dimyristoyl, dimyristoleoyl, distearoyl and dioleoyl]-1,12-diamino-4,9-diazadodecane were synthesized from the naturally occurring polyamine spermine (Fig. 3.10). Their abilities to condense DNA and to form nanoparticles were characterized. Transfection efficiencies were studied in FEK4 primary skin cells and in an immortalized cancer cell line (HtTA), and compared with N^4,N^9-regioisomers.

N^1,N^{12}-dimyristoyl spermine

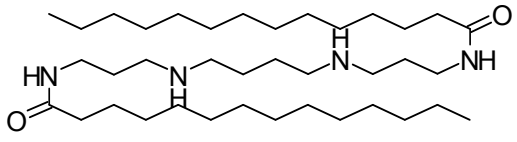

Mol. Wt 623.07

N^1,N^{12}-dimyristoleoyl spermine

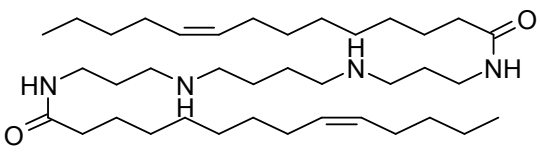

Mol. Wt 619.04

N^1,N^{12}-distearoyl spermine

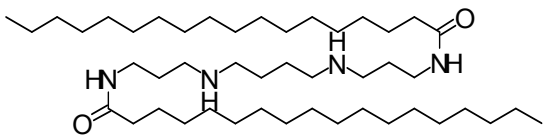

Mol. Wt 735.29

N^1,N^{12}-dioleoyl spermine

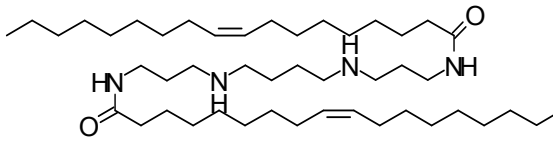

Mol. Wt 731.26

Fig. 3.10. Lipopolyamines - cationic lipids (N^1,N^{12}-diacyl spermines)

3.2.1. DNA Condensation

Fig. 3.11 shows the DNA condensation ability of the synthesized lipopolyamines in an EthBr fluorescence quenching assay. It shows that N^1,N^{12}-dimyristoleoyl spermine and N^1,N^{12}-dioleoyl spermine have the best DNA condensing ability, more than 90% EthBr fluorescence quenching at N/P charge ratio 6, while N^1,N^{12}-dimyristoyl spermine shows 75% and N^1,N^{12}-distearoyl spermine 60% fluorescence quenching at the same N/P ratio.

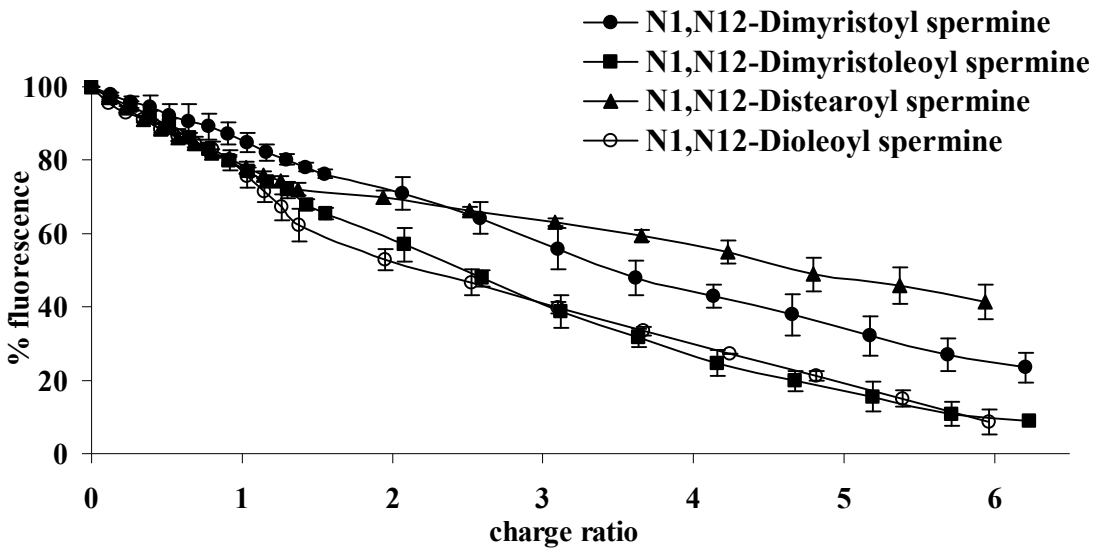

Fig. 3.11. Plot of EthBr fluorescence quenching assay of pEGFP complexed with different N^1,N^{12}-diacyl spermine.

The gel electrophoresis results (Fig. 3.12) show that N^1,N^{12}-dimyristoyl spermine was able to condense pEGFP DNA efficiently (as a result of neutralization of DNA phosphate negative charges by the lipopolyamine ammonium positive charges) at its optimised N/P charge ratio of transfection by inhibiting the electrophoretic mobility of plasmid DNA.

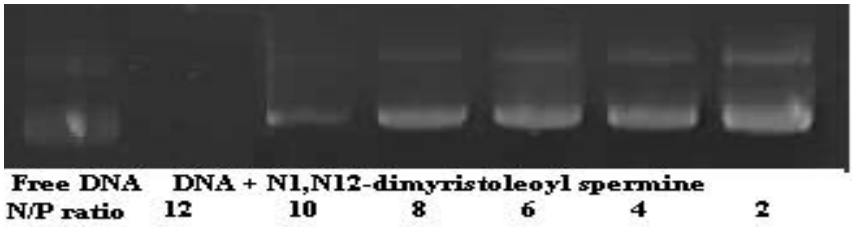

Fig. 3.12. Typical 1% agarose gel assay of fluorescent EthBr intercalated in pEGFP, DNA gel permeation on complexation (lipoplex formation) with N^1,N^{12}-dimyristoyl spermine at N/P ratios 2-12.

3.2.2. Lipoplex Particle Size and ζ-Potential

The particle size measurements were carried out on the lipoplexes at their optimum concentration for transfection (Table 3.3). Particle size characterization by laser diffraction showed that the nanoscale particle size of the formed DNA complexes ranged from 170 nm (N^1,N^{12}-dioleoyl spermine) to 250 nm (N^1,N^{12}-dimyristoleoyl spermine) with an average particle size of 205 nm, compared with

N^4,N^9-dioleoyl spermine pEGFP lipoplex particle size of 150 nm (Table 3.3). Two representative ζ-potential measurements for the lipoplexes formed (at their optimum charge ratio of transfection with 3 μg/ml pEGFP) were measured with a Delsa™Nano Zeta Potential instrument showing N^4,N^9-dioleoyl spermine +2.17 mV and N^1,N^{12}-dioleoyl spermine +3.69 mV.

Table 3.3. Particle size (mean ± S.D.) pEGFP complexes with the studied lipopolyamines.

Lipospermine	Charge ratio (N/P)	Lipoplex diameter (nm)
N^4,N^9-Dioleoyl spermine	2.5	150 (12)
N^1,N^{12}-Dioleoyl spermine	3	170 (30)
N^1,N^{12}-Distearoyl spermine	30	210 (35)
N^1,N^{12}-Dimyristoleoyl spermine	12	250 (49)
N^1,N^{12}-Dimyristoyl spermine.	12	190 (39)

3.2.3. pEGFP Transfection and In Vitro Cytotoxicity

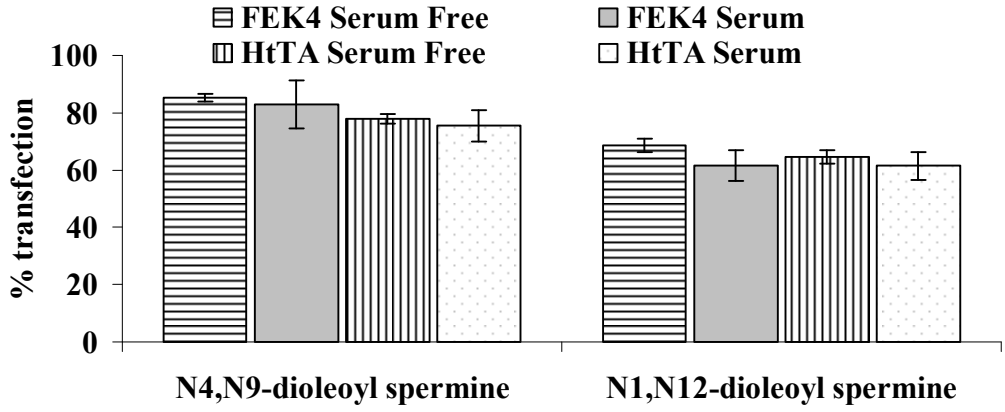

Fig. 3.13. Lipofection effects of pEGFP (1 μg) complexed with N^4,N^9-dioleoyl spermine (2.8 μg/ml), N^1,N^{12}-dioleoyl spermine (3.32 μg) on the primary skin cell line FEK4 and the HeLa derived cancer cell line HtTA in the absence and presence of serum.

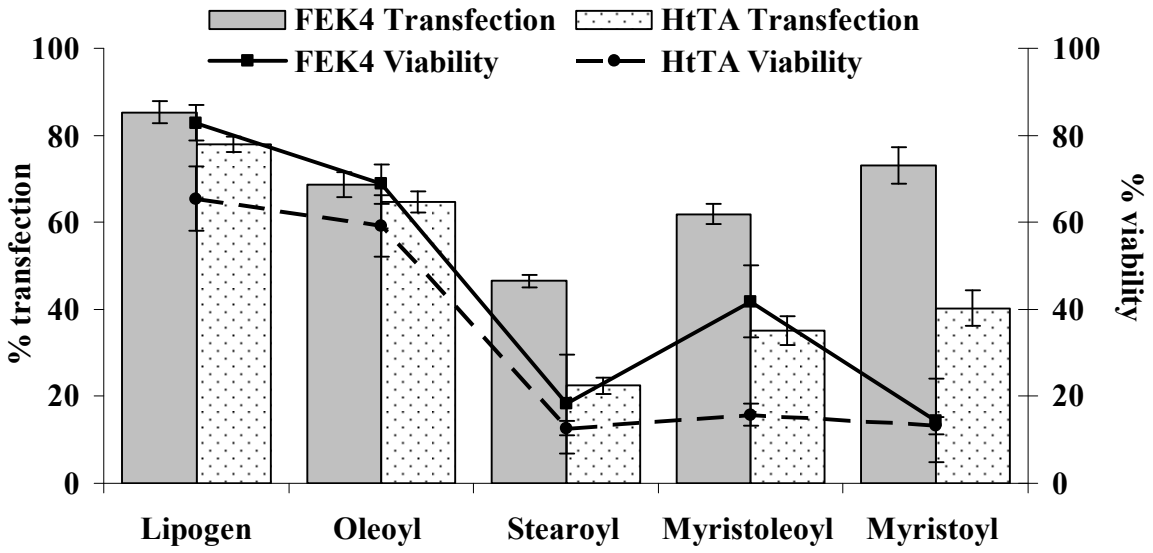

Fig. 3.14. Lipofection and cytotoxicity effects of pEGFP (1 μg) complexed with Lipogen (N^4,N^9-dioleoyl spermine) (2.77 μg), Oleoyl (N^1,N^{12}-dioleoyl spermine) (3.32 μg), Stearoyl (N^1,N^{12}-distearoyl spermine) (33.36 μg), Myristoleoyl (N^1,N^{12}-dimyristoleoyl spermine) (11.24 μg) and Myristoyl (N^1,N^{12}-dimyristoyl spermine) (11.31 μg) on the primary skin cell line FEK4and the HeLa derived cancer cell line HtTA.

The transduction of EGFP into a primary skin cell line FEK4 and a cancer cell line (HeLa-derived HtTA) was investigated in presence and absence of serum (Fig. 3.13) and we found that there was no significant difference in the transfection levels in the presence of serum for N^4,N^9-dioleoyl spermine and N^1,N^{12}-dioleoyl spermine. Encouraged by these positive results, all our subsequent transfection experiments are performed in the presence of serum. The optimum concentrations (in a final volume of 0.5 ml) and their corresponding N/P charge ratios for transfection were experimentally determined by using ascending N/P ratios of lipospermines from 2, 4, 6 etc. until we reached around 80% transfection and there was not a further step-up in transfection efficiency at the next highest N/P ratio. So the optimum amounts (and corresponding N/P charge ratios) for transfection with pEGFP (1 μg in 50 μl) were found to be: N^4,N^9-dioleoyl spermine (2.77 μg, N/P = 2.5), N^1,N^{12}-dioleoyl spermine (3.32 μg, N/P = 3), N^1,N^{12}-distearoyl spermine (33.36 μg, N/P = 30.0), N^1,N^{12}-dimyristoleoyl spermine (11.24 μg, N/P = 12.0), and N^1,N^{12}-dimyristoyl spermine (11.31 μg N/P = 12.0). The results (Fig. 3.14) indicate that N^1,N^{12}-dioleoyl spermine typically shows

70% and 65% transfection ability and 70% and 60% cell viability for FEK4 and HtTA cells respectively is the best of the all tested complexes and can be compared with the N^4,N^9 dioleoyl spermine.

In this section, we have investigated the change in the position then length and degree of saturation of the symmetrical diacyl fatty chain formulations of lipospermine on pDNA condensation and cellular delivery. The results from pEGFP condensation (Fig. 3.11), investigated using the EthBr fluorescence quenching assay, revealed that of our synthetic lipopolyamines N^1,N^{12}-dioleoyl spermine and N^1,N^{12}-dimyristoleoyl spermine were able to condense DNA to less than 10% EthBr fluorescence at N/P charge ratio 6, while, N^1,N^{12}-dimyristoyl spermine and N^1,N^{12}-distearoyl spermine show 75% and 60% condensation respectively at the same N/P ratio. The lipid chains make a significant contribution to the DNA condensation, the differences are clear (Fig. 3.11) with respect to position and unsaturation, where pDNA condensation efficiency follows: saturated-1,12< unsaturated-1,12< unsaturated-4,9 regioisomers.

Particle size of the final gene formulation is also an important factor in improving gene delivery (187,188). Particle size results (Table 3.3) for pDNA showed average particle size 205 nm. On the relationship between particle size and transfection efficiency, there are no definite limits to the nanoparticle size that are suitable for transfection (189). Nanoparticles have relatively higher intracellular uptake than microparticles (155). Also, on the nanoscale, smaller-size polyplexes are more able to enter cells and thereby increase the efficiency of transfection (190).

From the combination of both the transfection and viability results we found that N^1,N^{12}-dioleoyl spermine (transfection efficiency FEK4 70%, HtTA 65% and cell viability FEK4 70%, HtTA 60%) was a better vector based on these two factors of transfection efficiency and cell viability. It was superior to the saturated analogue N^1,N^{12}-distearoyl spermine and the shorter analogues, unsaturated N^1,N^{12}-dimyristoleoyl spermine or saturated N^1,N^{12}-dimyristoyl spermine and comparable to the N^4,N^9-regiosisomer N^4,N^9-dioleoyl spermine (Lipogen®). Based on these DNA transfection and cell viability results, we investigated the change in the position and length of the symmetrical diacyl fatty chain formulation of lipospermine on siRNA condensation and cellular delivery.

The DNA compacting properties of polyamines (especially spermine) are well-known, hence the use of spermine as the cationic part in several synthetic DNA

carriers. Clement and his research group recently reported the use lipophosphoramidate as the lipidic part of lipospermines for gene delivery (191). Due to their high net charge at physiological pH, polyamines effectively charge neutralize the phosphodiester backbone of DNA (192). Many pK_a measurements have been made on spermidine, spermine, and their derivatives (193,194) which all indicate their high number of positive charges at physiological pH. Spermidine typically shows pK_a values of: 11.1, 10.0 and 8.6 or 10.9, 9.8 and 8.4 (195) and spermine: pK_1 10.9, pK_2 10.1, pK_3 8.9 and pK_4 8.1 (23) and 10.9, 10.0, 8.8 and 8.4 (196). However, in preparing the N^4,N^9-regioisomeric analogues we have separated the two primary amines from the (significant base-weakening) transient charges on the secondary amines, and the primary amines may therefore be assumed to have pK_a values typical of primary amines, 10.6-10.8, i.e., N^4,N^9-diacyl analogues will carry two positive charges at physiological pH (7.4). Moving the diacyl chains to the N^1,N^{12}-position, means that these analogues will still carry two positive charges at pH = 7.4, but their pK_a values are likely to follow those of putrescine (1,4-diaminobutane) (10.8 and 9.4 or 10.7 and 9.2) (197,198) and we assume that there will not be any significant effect from the γ-amide functional group. Thus, these novel conjugates are dibasic for N/P charge ratio calculations, and their efficient charge neutralisation by phosphate anion titration will be a function of steric more than electronic effects when compared with the 12 atoms (10 C and 2 N) separating the two positive charges in the N^4,N^9 series. We conclude from the above results that the N^1,N^{12}-dioleoyl spermine is the best of the N^1,N^{12}-substituted series for DNA delivery. It is comparable to the commercially available N^4,N^9-regioisomer N^4,N^9-dioleoyl spermine (Lipogen®) for DNA transfection efficiency.

From the above results, N^4,N^9-dioleoyl spermine was shown to be better than all the tested N^1,N^{12}-diacyl spermine analogues, so in the next part we will test the N^4,N^9-diacyl spermines with changes to the length of the fatty chain from C10 to C18 and also using saturated or mono unsaturated when available.

3.3. VARYING THE CHAIN LENGTH IN N^4,N^9-DIACYL SPERMINES: NON-VIRAL LIPOPOLYAMINE VECTORS FOR EFFICIENT pDNA FORMULATION

In this section we study the effect of varying the chain length in synthesized N^4,N^9-diacyl spermines on plasmid DNA (pDNA) condensation and then compare their transfection efficiencies in two cell lines. The eight N^4,N^9-diacyl lipopolyamines: N^4,N^9-[didecanoyl, dilauroyl, dimyristoyl, dimyristoleoyl, dipalmitoyl, distearoyl, dioleoyl and diretinoyl]- and two dialkyl N^4,N^9-[distearyl and dioleyl]-1,12-diamino-4,9-diazadodecane conjugates (Fig. 3.15) are designed to range from C10 to C18, but they also include C20 (diretinoyl) which due to its structure is comparable to C13-C14 in overall length. The abilities of these novel compounds to condense DNA and to form nanoparticles were studied using EthBr fluorescence quenching and nanoparticle characterization techniques. Transfection efficiency was studied in our usual FEK4 primary skin cells and in the cancer cell line (HtTA). The N^4,N^9-diacyl spermine vectors were then compared with two reduced amides, i.e., N^4,N^9-dialkyl spermines, analogues derived by reduction of the best two diacyl compounds, as they can carry up to four positive charges at physiological pH and therefore may have a higher affinity for pDNA.

N^4,N^9-didecanoyl spermine

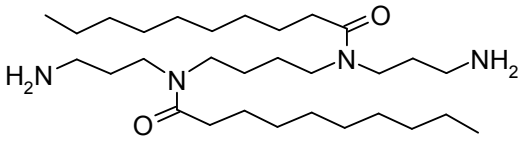

Mol. Wt. 510.85

N^4,N^9-dilauroyl spermine

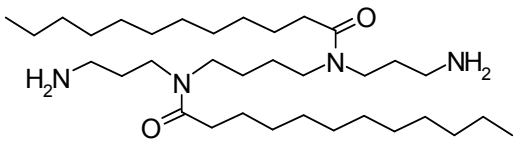

Mol. Wt. 566.96

N^4,N^9-dimyristoyl spermine

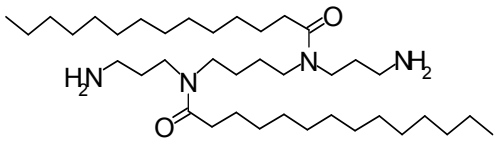

Mol. Wt. 623.07

N^4,N^9-dimyristoleoyl spermine

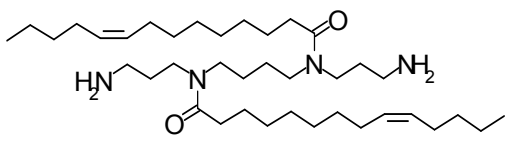

Mol. Wt. 619.04

N^4,N^9-dipalmitoyl spermine

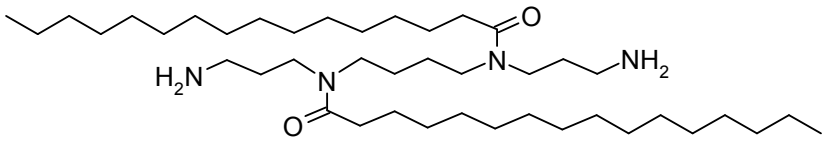

Mol. Wt. 679.18

N^4,N^9-distearoyl spermine

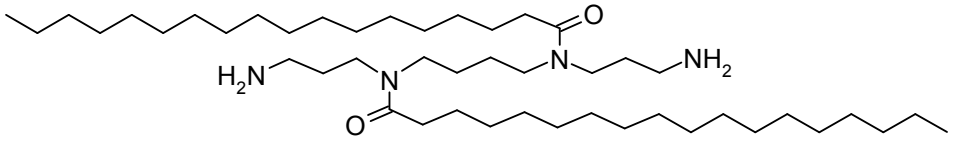

Mol. Wt. 735.29

N^4,N^9-dioleyl spermine

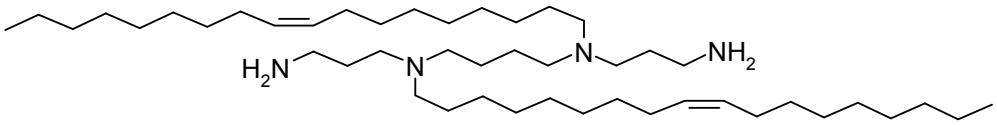

Mol. Wt. 703.29

N^4,N^9-distearyl spermine

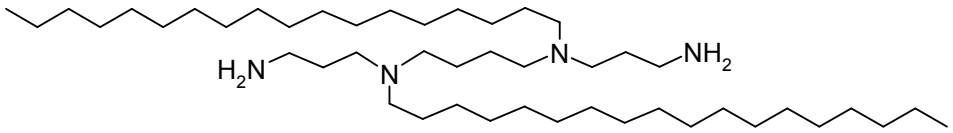

Mol. Wt. 707.32

N^4,N^9-diretinoyl spermine

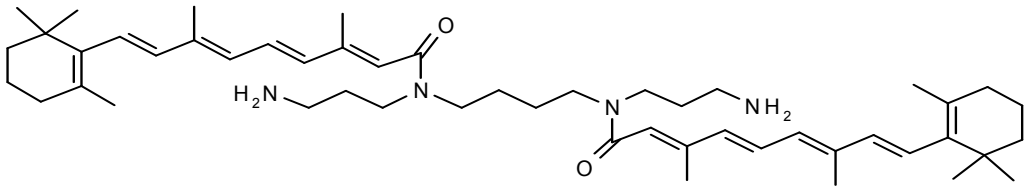

Mol. Wt. 767.20

Fig. 3.15. Symmetric lipopolyamines cationic lipids (N^4,N^9-diacyl spermine and N^4,N^9-dialkyl spermine)

3.3.1. DNA Condensation

In Fig. 3.16, the DNA condensation abilities of the synthesized lipopolyamines in an EthBr fluorescence quenching assay are shown. These results show that N^4,N^9-dimyristoyl spermine and N^4,N^9-dimyristoleoyl spermine have the best DNA condensing ability, more than 90% EthBr fluorescence quenching at N/P charge ratio 2, while N^4,N^9-dipalmitoyl and N^4,N^9-distearoyl show such a result at N/P = 3, then N^4,N^9-didecanoyl spermine and N^4,N^9-dioleoyl spermine show 75% fluorescence quenching at N/P = 4 and lastly N^4,N^9-dilauroyl spermine is only able to achieve about 60% fluorescence quenching at the same N/P charge ratio.

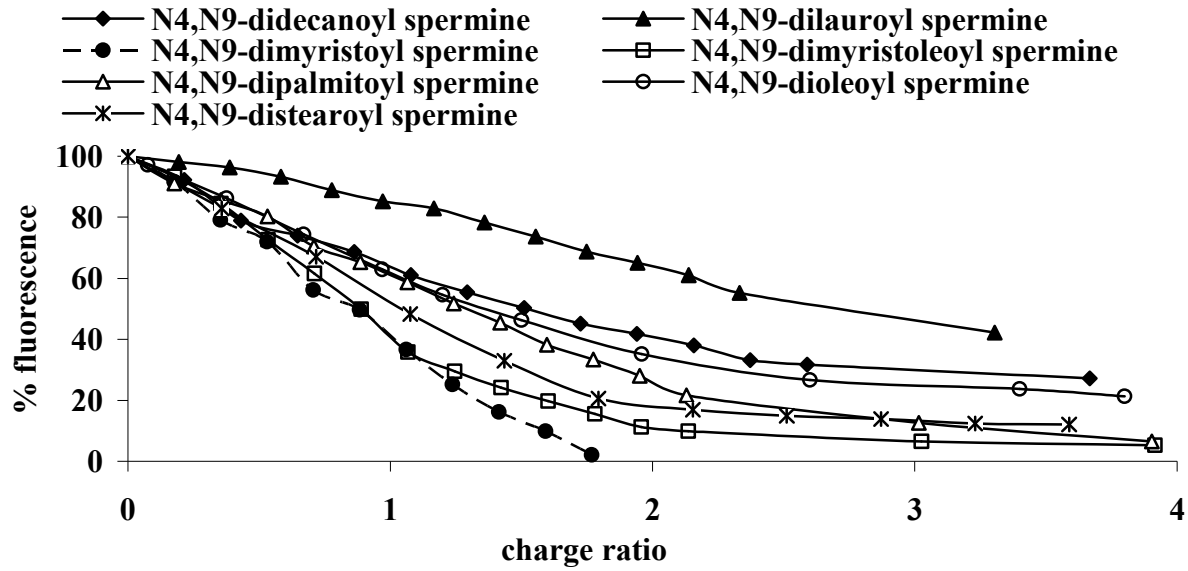

Fig. 3.16. EthBr fluorescence quenching assay of pEGFP complexed with different N^4,N^9-diacyl spermines.

The gel electrophoresis results (Fig. 3.17) show that N^4,N^9-didecanoyl spermine was able to prevent the migration of pEGFP DNA efficiently, as a result of neutralization of DNA phosphate negative charges by the lipopolyamine ammonium positive charges at their optimised respective charge ratios (N/P) of transfection. Thus, by completely inhibiting the electrophoretic mobility of plasmid DNA, we conclude that they are charge neutralised, experimental evidence which supports the pEGFP DNA condensation data that we obtained from the EthBr fluorescence quenching assay (Fig. 3.16). Of course, it is not essential that the DNA is fully condensed, provided that nanoparticles are formed, if entry is via the clathrin coated pit, in comparison with relying upon entry during mitosis as in the use of naked DNA.

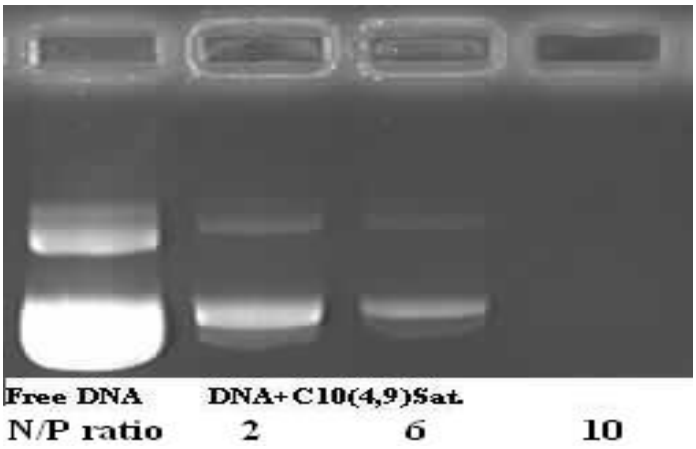

Fig. 3.17. Typical 1% agarose gel assay of fluorescent EthBr intercalated in pEGFP, DNA gel permeation on complexation (lipoplex formation) with N^4,N^9-didecanoyl spermine at N/P ratios 2, 6 and 10.

3.3.2. Lipoplex Particle Size and Zeta-Potential Measurements

Table 3.4. Particle Size (mean ± S.D.) and ζ-Potential of pEGFP Complexes with the Studied Lipopolyamines

Lipospermine	Charge ratio (N/P)	Lipoplex diameter (nm)	ζ-Potential (+) mV
N^4,N^9-Didecanoyl spermine	10	150 (6)	4.77
N^4,N^9-Dilauroyl spermine	20	170 (12)	14.32
N^4,N^9-Dimyristoyl spermine	10	150 (13)	6.78
N^4,N^9-Dimyristoleoyl spermine	12	130 (9)	8.21
N^4,N^9-Dipalmitoyl spermine	20	160 (10)	9.24
N^4,N^9-Disteraroyl spermine	15	220 (21)	
N^4,N^9-Dioleoyl spermine	2.5	150 (12)	2.17

The particle size and ζ-potential characterization measurements were carried out on the lipoplexes at their optimum N/P charge ratio of transfection (Table 3.4). Particle size characterization by laser diffraction showed that the nanoscale particle size of the formed complexes ranged from 130 nm (N^4,N^9-dimyristoleoyl spermine) to

170 nm (N^4,N^9-dilauroyl spermine) and 220 nm (N^4,N^9-distearoyl spermine) with an average particle size of 161 nm (Table 3.4). The particle size of the final pDNA formulation is also an important factor in improving gene delivery (187,188).

The surface charge, as determined by ζ-potential measurements on the lipoplexes at their experimentally determined optimum N/P charge ratios of transfection, show that all values are positive (Table 3.4) and they ranged from +2.17 mV (N^4,N^9-dioleoyl spermine) to +14.32 mV (N^4,N^9-dilauroyl spermine); the measured ζ-potential for naked DNA is -1.02 mV.

3.3.3. DNase I Protection

The DNase I protection assay was carried using plasmid DNA complexed with different N/P charge ratios of the lipopolyamines. Reasonably intense undigested DNA bands were detected in the gel as a control, and there was no band in the lane for uncondensed DNA which was fully digested by DNase I as negative control (Fig. 3.18). we performed the DNase protection assay using different N/P charge ratios of our lipopolyamines e.g., for N^4,N^9-dioleoyl spermine the intense band of undigested DNA appeared at N/P charge ratio 3 (Fig. 3.18) which means that the lipoplex formed from condensed pEGFP DNA with this lipopolyamine is effectively protected from DNase I enzyme, and this may contribute to the lipoplex serum stability.

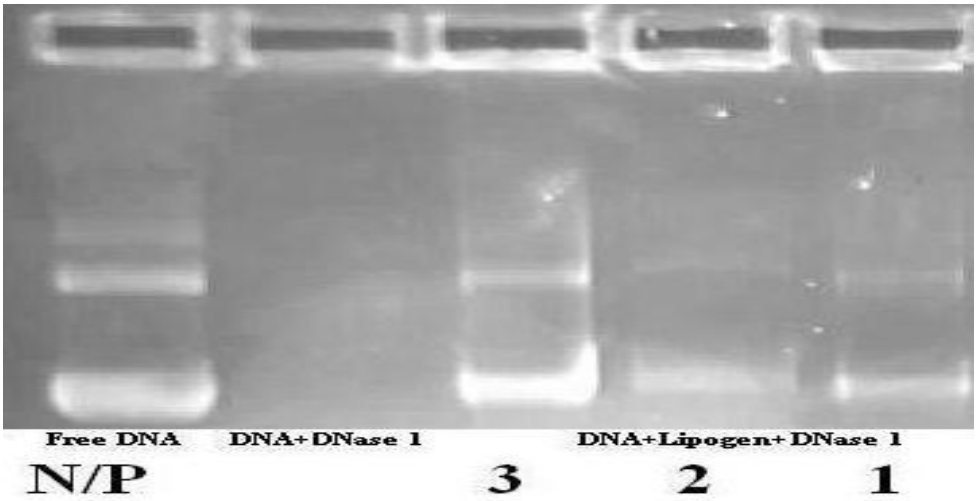

Fig. 3.18. Typical 1% agarose gel of fluorescent EthBr intercalated in pEGFP, assay of DNase I protection on complexation (lipoplex formation) with N^4,N^9-dioleoyl spermine.

3.3.4. Transfection Experiments and In Vitro Cytotoxicity

The transduction of EGFP into a primary skin cell line FEK4 and a cancer cell line (HeLa-derived HtTA) was investigated. The optimum concentrations (in a final volume of 0.5 ml) and their corresponding N/P charge ratios for transfection were experimentally determined by using ascending N/P ratios of lipospermines from 2, 4, 6 etc. until we reached around 80% transfection and there was not a further step-up in transfection efficiency at the next highest N/P ratio.

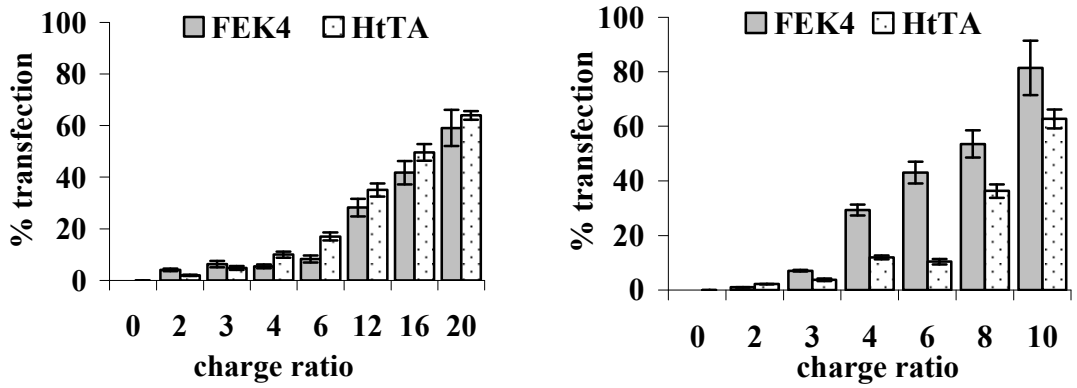

Fig. 3.19. Lipofection of the primary skin cell line FEK4 and the cancer cell line HtTA transfected with pEGFP (1 µg) complexed with N^4,N^9-dilauroyl spermine (left) and N^4,N^9-dimyristoyl spermine (right) at different N/P charge ratios.

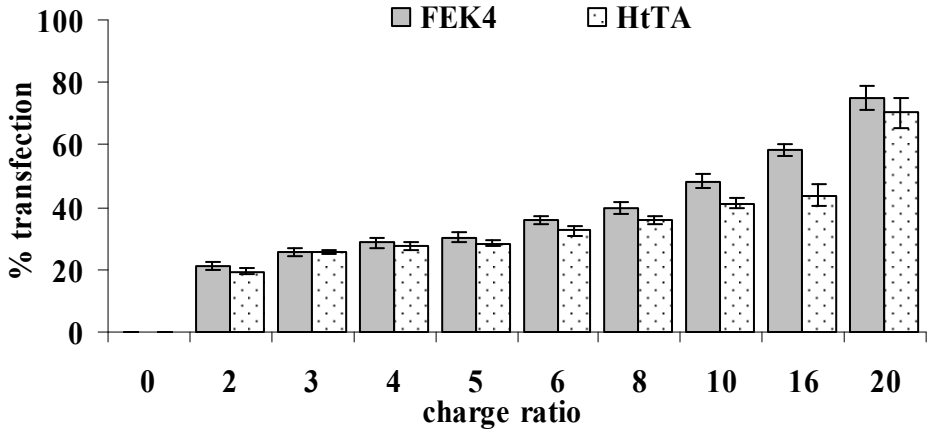

Fig. 3.20. Lipofection and of FEK4 and HtTA cells transfected with of pEGFP (1 µg) complexed with N^4,N^9-dipalmitoyl spermine at different N/P charge ratios.

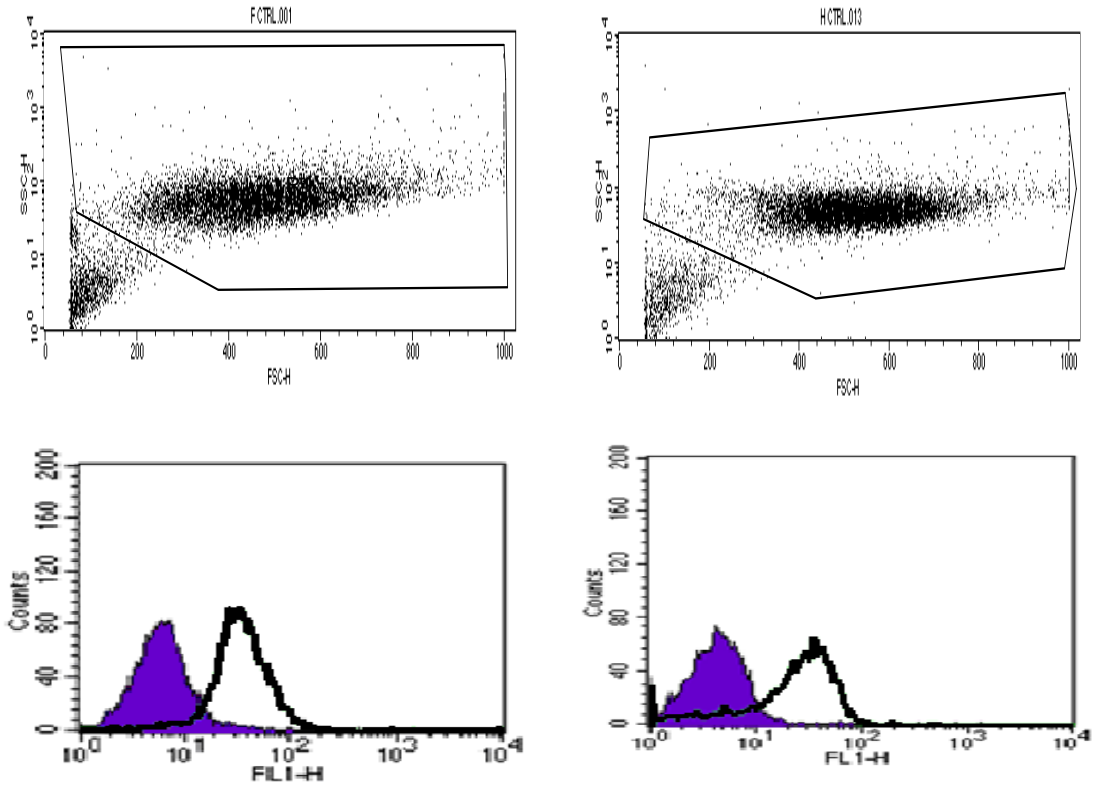

Fig. 3.21. FACS analysis showing the live FEK4 (above left) and HtTA (above right) populations gated, and FEK4 (lower left) and HtTA (lower right) after 48 h transfection of pEFGP complexed with N^4,N^9-dioleoyl spermine: ■ untransduced cells, □ EGFP-positive cells.

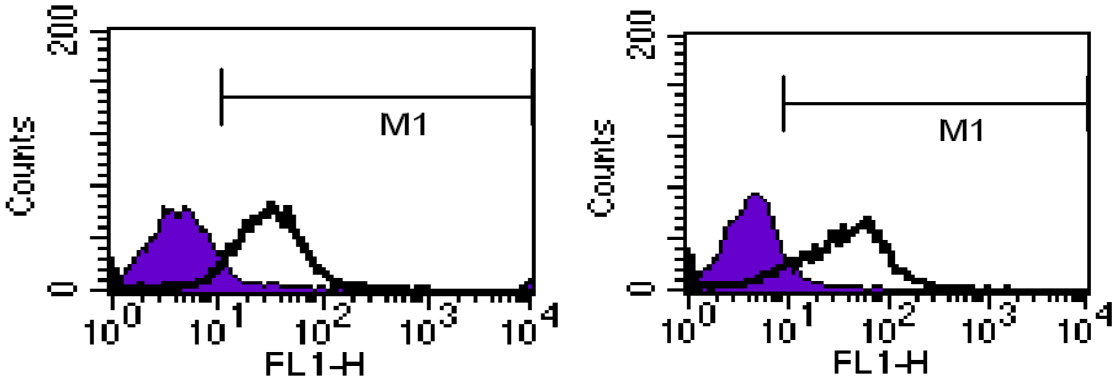

Fig. 3.22. FACS analysis of FEK4 (left) and HtTA (right) after 48 h transfection of pEFGP complexed with N^4,N^9-dimyristoleoyl spermine: ■ untransduced cells, □ EGFP-positive cells.

From our typical results, shown in Figs. 3.19 and 20 (for 2 x C12, 2 x C14, and 2 x C16 saturated chains, respectively), we conclude that for the lipopolyamines that are less efficient than N^4,N^9-dioleoyl spermine, transfection efficiency increases with N/P charge ratio. That these lipopolyamines are pDNA delivery vectors which can achieve high transfection efficiency is immediately seen from our gated FACS analysis with N^4,N^9-dioleoyl spermine and N^4,N^9- dimyristoleoyl spermine in both cell lines (Figs. 3.21 and 3.22). Only a subset of the data obtained from healthy cells (the major population) was analysed through a gate setting. This gating was determined from the dot plots.

Further transfection efficiency studies (carried out in triplicate on 3 separate experiments, n = 9) showed that there was no significant difference between the transfection efficiency in the presence (FEK4 82.9% ± 4.3, HtTA 75.4% ± 5.5) or absence (FEK4 85.3% ± 1.4, HtTA 78.0% ± 1.7) of serum (Fig. 3.13).

Encouraged by these positive results, all our subsequent transfection experiments are performed in the presence of serum. However, the toxicity also increases (decrease in cell viability) as the N/P charge ratio is increased (Fig. 3.23). The required lipopolyamine amounts and the corresponding N/P charge ratios to deliver pEGFP (1 μg in 50 μl, in a total final volume of 0.5 ml) for optimum transfection were found to be: N^4,N^9-didecanoyl spermine (7.7 μg, N/P = 10.0), N^4,N^9-dilauroyl spermine (17.2 μg, N/P = 20.0), N^4,N^9-dimyristoyl spermine (9.4 μg, N/P = 10.0), N^4,N^9-dimyristoleoyl spermine (11.2 μg, N/P = 12.0), N^4,N^9-dipalmitoyl spermine (20.5 μg, N/P = 20), N^4,N^9-distearoyl spermine (16.7 μg, N/P = 15), N^4,N^9-dioleoyl spermine (2.8 μg, N/P = 2.5) and N^4,N^9-diretinoyl spermine (23.2 μg, N/P = 20).

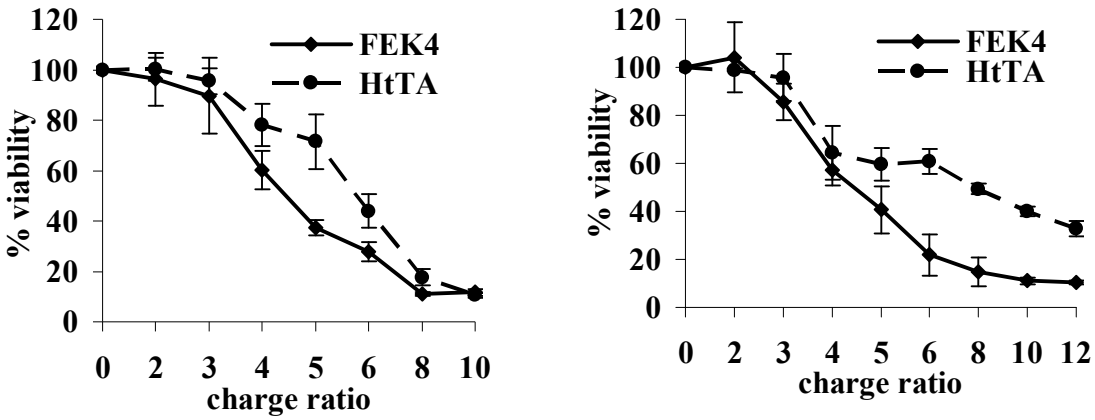

Fig. 3.23. Cytotoxicity effect of pEGFP (1 μg) complexed with N^4,N^9-didecanoyl spermine (left) and N^4,N^9-dimyristoleoyl spermine (right) at different N/P ratios on the primary skin cell line FEK4 and the cancer cell line HtTA.

The transfection results (histograms in Fig. 3.24) indicate that there is no significant difference in the transfection ability of the different lipospermines (at their optimum pDNA delivery N/P charge ratio) on both cell lines except for the N^4,N^9-distearoyl spermine which is much lower. However, the cell viability (MTT assay) results (solid lines on Fig. 3.24) indicate that N^4,N^9-dioleoyl spermine typically shows 83% and 65% cell viability for FEK4 and HtTA cells, respectively. The shorter chain lipospermines, especially di-C14, both saturated and *cis*-mono-unsaturated, whilst efficient at cell transfection, are toxic to both cell lines (viability less than 40%, and often under 20%). It is often proposed that toxicity increases with increasing n-alkyl chain length, e.g., going from C2 to C8 (199-201) and similarly to C10 (202), as such cationic surfactants are known to increase membrane permeability. Although this is not an immutable rule, as was found for C2 to C12 in the 8-alkylberberine chloride series where upon elongating the aliphatic chain, toxicity decreased gradually (203). We are not proposing that these results contradict this, rather that our N^4,N^9-dioleoyl spermine is used at a significantly low N/P charge ratio, and the shorter chain analogues are used at higher N/P ratios.

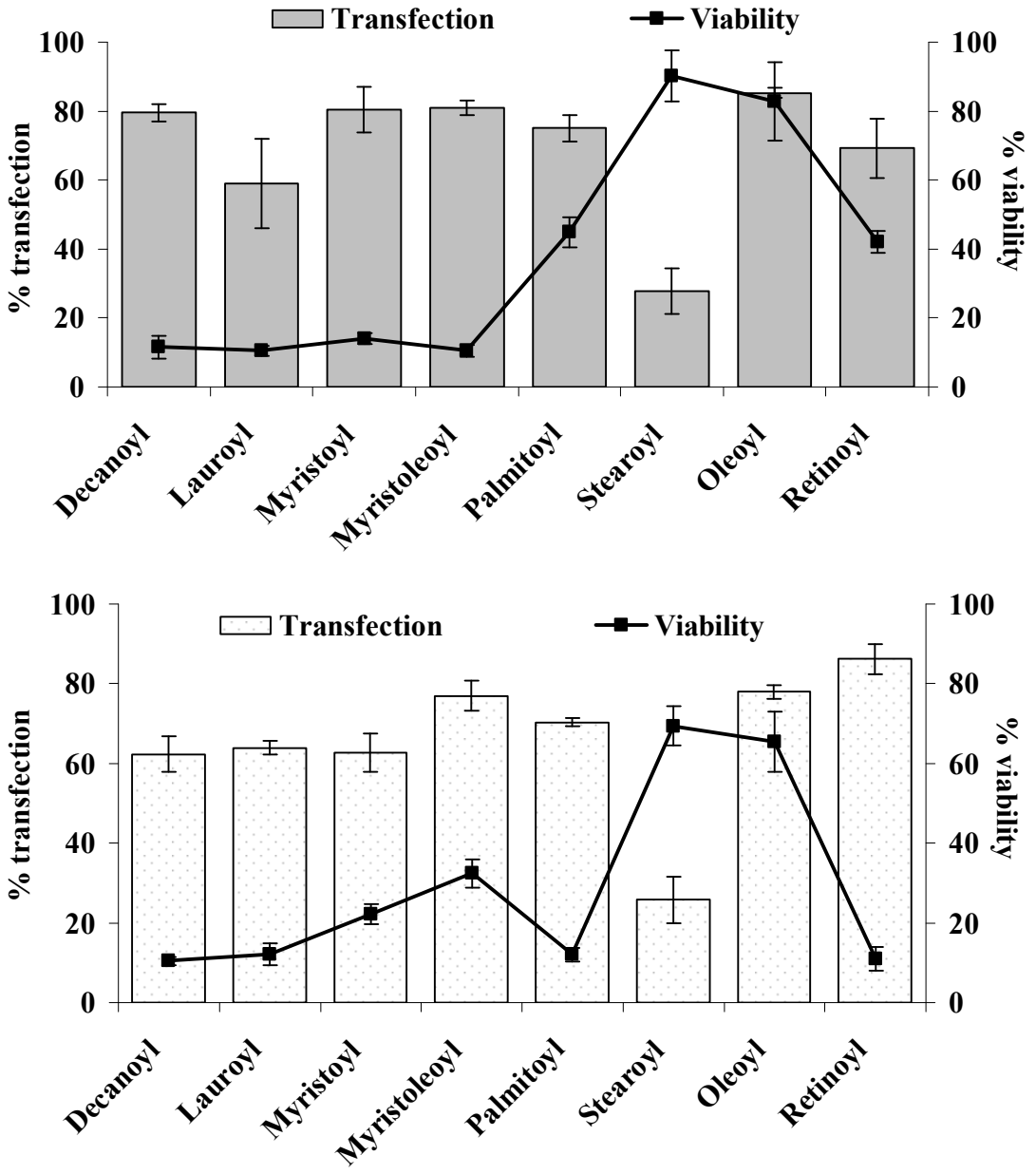

Fig. 3.24. Lipofection and cytotoxicity effects of pEGFP (1 μg) complexed with decanoyl (N^4,N^9-didecanoyl spermine) (7.7 μg), lauroyl (N^4,N^9-dilauroyl spermine) (17.2 μg), myristoyl (N^4,N^9-dimyristoyl spermine) (9.4 μg), myristoleoyl (N^4,N^9-dimyristoleoyl spermine) (11.2 μg), palmitoyl (N^4,N^9-dipalmitoyl spermine) (20.5 μg), stearoyl (N^4,N^9-distearoyl spermine) (16.7 μg), oleoyl (N^4,N^9-dioleoyl spermine) (2.8 μg) and retinoyl (N^4,N^9-diretinoyl spermine) (23.2 μg) on FEK4 (above) and on HtTA cell lines (below) The data represent 3 different experiments (3 replicates each) and the error bars represent the S.D.

The remarkably different results obtained between N^4,N^9-distearoyl and N^4,N^9-dioleoyl spermine, the former with poor transfection and the latter with high

transfection, but both showing good cell viability at practical concentrations for pDNA delivery with N^4,N^9-dioleoyl spermine, made us investigate further these vectors but with four positive charges at physiological pH from amide reduction to the tetraamines. Therefore, the corresponding alkyl analogues N^4,N^9-distearyl spermine and N^4,N^9-dioleyl spermine were compared with the two C18 acyl lipospermines, the saturated N^4,N^9-distearoyl spermine and the mono-*cis*-unsaturated N^4,N^9-dioleoyl spermine. The results (Fig. 3.25) show that there is not a large difference in the transfection efficiency, neither gain nor loss, on doubling the number of positive charges in the conjugate derived from N^4,N^9-dioleoyl spermine, while there is a great gain in the transfection efficiency for the conjugate from N^4,N^9-distearoyl spermine. Thus, N^4,N^9-distearoyl spermine shows transfection efficiencies of 28% and 26% (FEK4 and HtTA respectively), N^4,N^9-distearyl spermine 72% and 87%, N^4,N^9-dioleoyl spermine 85% and 78%, and N^4,N^9-dioleyl spermine 80% and 76%, but the cell viabilities drop from around 65-90% to 10-42%. Therefore, the two alkyl analogues are much more toxic (Fig. 3.25) to both cell lines.

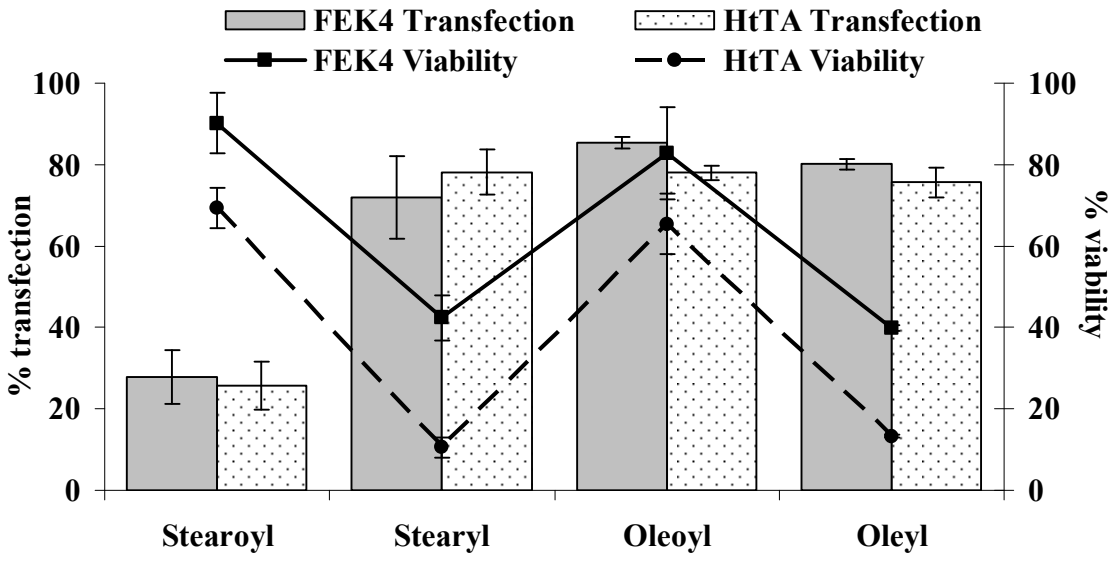

Fig. 3.25. Lipofection and cytotoxicity effects of pEGFP (1 μg) complexed with oleoyl (N^4,N^9-dioleoyl spermine) (2.8 μg), oleyl (N^4,N^9-dioleyl spermine) (4.3 μg), stearoyl (N^4,N^9-distearoyl spermine) (16.7 μg) and stearyl (N^4,N^9-distearyl spermine) (6.7 μg) on the primary skin cell line FEK4 and the HeLa derived cancer cell line HtTA.

3.3.5. Confocal Microscopy Visualization

Using confocal laser scanning microscopy with one labelling solution (Invitrogen) containing both Alexa Fluor 594 wheat germ agglutinin (5 μg/ml) for cell membrane labelling, and Hoechst 33342 (2 μM) for nuclei labelling, we have shown (Fig. 3.26) that FEK4 cells were successfully transfected with pDNA as the cells biosynthesized EGFP by transcription and translation.

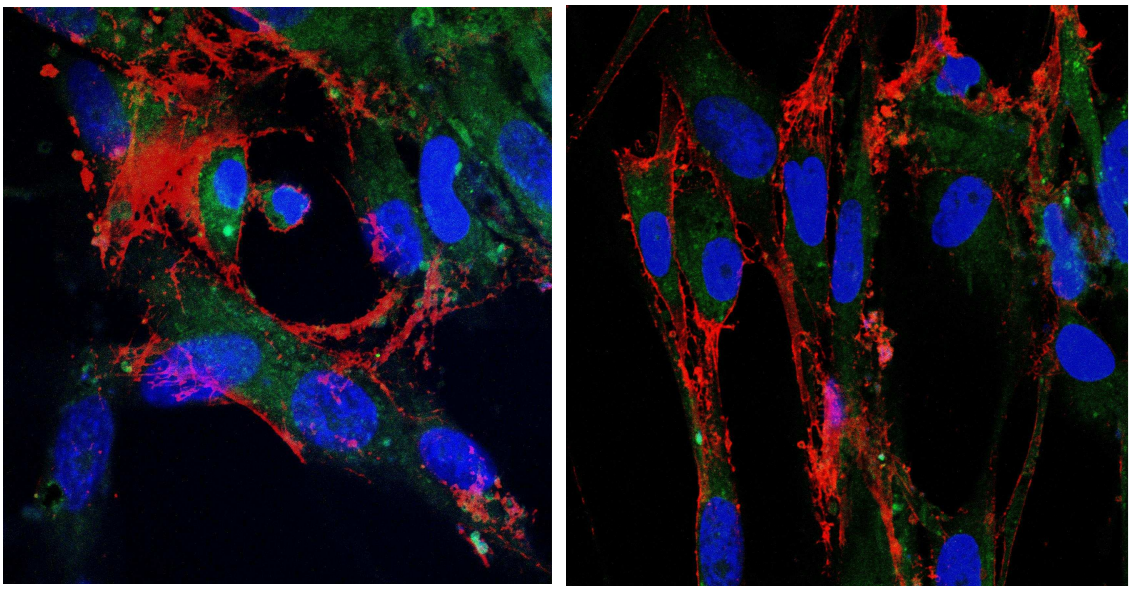

Fig. 3.26. Transfection of the primary skin cell line FEK4 with pEGFP showing cytosolic green fluorescence from EGFP, delivered with N^4,N^9-dioleoyl spermine. The cell lipid bilayers fluoresce red from the Alexa Fluor 594 and the nuclei fluoresce blue from the Hoechst 33342 (LSM510META, under the 60× oil immersion objective).

In this section, we have investigated effects resulting from changes in the length of the symmetrical N^4,N^9- diacyl fatty chain formulations of lipospermines on DNA condensation and cellular delivery. The results from pEGFP condensation, investigated by EthBr fluorescence quenching assay, revealed that five of our synthetic lipopolyamines were able to condense DNA to less than 20% EthBr fluorescence. However, N^4,N^9-dilauroyl spermine had not quenched the EthBr fluorescence to 20% by N/P charge ratio 3.5 (Fig. 3.16). Particle size of the final nanoscale formulation is also an important factor in improving gene delivery (187,188). Particle size results (Table 3.4) showed an average particle size of 161 nm. On the relationship between particle size and transfection efficiency, all our lipoplexes

are in the range 130-220 nm, and they transfected target cell lines efficiently. If internalisation is via a clathrin coated pit, there will be an upper-size limit of 250-300 nm (169), although larger sizes of nanoparticles still do achieve transfection, presumably by a different mechanism (189). Nanoparticles have relatively higher intracellular uptake than microparticles (155). Also, on the nanoscale, smaller-size polyplexes are more able to enter cells and thereby increase the efficiency of transfection (190).

The lipid moiety in our cationic lipids interacts with the phospholipid bilayer of the cell membrane, and that facilitates cell entry, either in crossing the membrane bilayer and/or in helping to weaken the endosomal bilayer and thereby aid escape into the cytosol. DNA, either as a nanoparticle or now free (uncomplexed) from the condensing lipopolyamine, must now traffic to the nucleus and cross the nuclear membrane which is thought to occur through the NPC or by direct association with the chromatin during mitosis. After nuclear entry, the payload DNA should successfully be able to give the desired protein through transcription and translation. The first key step in this gene formulation is DNA condensation into nanoparticles by masking the negative charges of the phosphate backbone. As introduced above, an advantage of cationic lipids is that this titration of the phosphate anions with a lipopolyamine causes alleviation of charge repulsion between remote phosphates along the DNA helix leading to collapse into a more compact structure that facilitates cell entry. Furthermore, the packing of the lipid chains make a significant contribution to this DNA compaction (Fig. 3.16).

It have previously reported the importance of the substituents in the lipid moiety conjugated to the cationic polyamine to achieve improvements in DNA condensation efficiency for non liposomal formulations where the lipid moiety must be considered in shape (volume) and substituent pattern, as well as the polyamine moiety and its pK_a values (12,161,162,170,171). The design and synthesis of novel cationic lipids based on the tetra-amine spermine, as non-liposomal formulations, where the lipid moiety is a long carbon chain, were largely investigated by Behr et al. (72) and Remy et al. (15) with their design and preparation of the highly efficient lipopolyamine DOGS (dioctadecylamido-glycyl spermine, Transfectam®). It is generally agreed that the length and type of the aliphatic chains incorporated into cationic lipids significantly affect their transfection efficiency, but this needs experimental verification. Thus, a series of vectors differing in their hydrophobic

domains have been prepared. Behr and co-workers made a series of lipopolyamines and found that their gene delivery efficiency was independent of chain saturation (oleoyl *vs*. stearoyl lipopolyamines) (15). Further, when comparing saturated chains, McGregor et al. found C18 chains to be optimal in a series of gemini surfactants according to the order C18 > C16 > C14 (204), which was also reported by Scherman and co-workers with a series of linear polyamine-based vectors (205). Results obtained with DMRIE (206) (1,2-dimyristyloxypropyl-3-dimethyl-hydroxyethyl-ammonium bromide, an analogue of DOTMA), alkyl acyl carnitine esters (207) and bis-ether lipids related to DOTAP (208) have shown that a comparison of vectors based solely on the lengths of the two saturated aliphatic chains led to the order C14 > C16 > C18 (in terms of transgene expression). Early liposomal studies therefore led to the proposal that a shorter chain length may facilitate intermembrane mixing, an important factor in endosomal escape (206). A common moiety is the use of *cis*-mono-unsaturated alkyl chains e.g., the oleoyl group (C18). This leads to higher transfection levels than the corresponding saturated e.g., stearoyl (C18) derivatives, a result possibly related to the issues of hydrophobic moiety hydration or packing (206,207).

By incorporating two aliphatic chains and then stepwise changing their length, we have shown that the all our synthesized lipospermines afford transfection results in a similar range (essentially equally efficient), but at different N/P ratios of which N^4,N^9-dioleoyl spermine has the lowest (N/P = 2.5) while the others ranged over N/P ratios 10-20. This may give a lead to their higher toxicity, often more than 60% compared with the ~25% observed for N^4,N^9-dioleoyl spermine which, with its two unsaturated chains, is also much more efficient than the saturated analogue N^4,N^9-distearoyl spermine.

From the above results we can conclude that N^4,N^9-dioleoyl spermine is much better than all the tested shorter N^4,N^9-diacyl spermine (C10-C18) which gave us a reason to test longer N^4,N^9-diacyl spermine (C20-C24) even with different degrees of saturation and to compare the results with N^4,N^9-dioleoyl spermine in order to find the optimum chain length and degree of saturation of N^4,N^9-diacyl spermine.

3.4. VERY LONG CHAIN N^4,N^9-DIACYL SPERMINES: NON-VIRAL LIPOPOLYAMINE VECTORS FOR EFFICIENT pDNA DELIVERY

N^4,N^9-diarachidoyl spermine

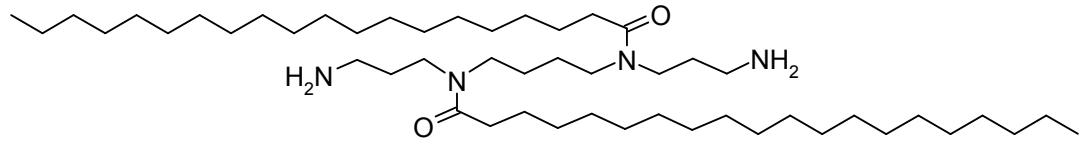

Mol. Wt 791.40

N^4,N^9-dieicosenoyl spermine

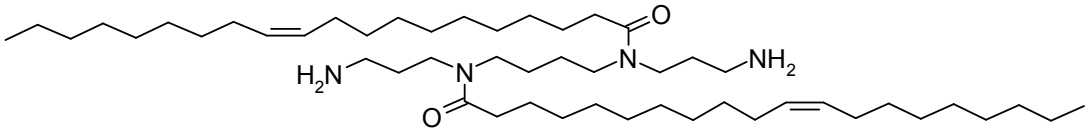

Mol. Wt 787.36

N^4,N^9-diarachidonoyl spermine

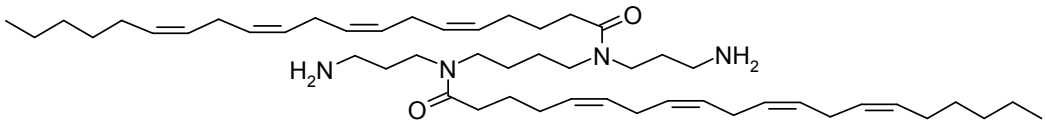

Mol. Wt 775.27

N^4,N^9-dierucoyl spermine

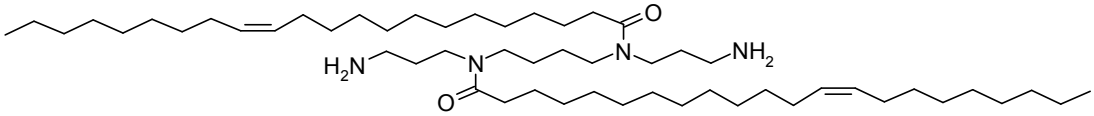

Mol. Wt 843.47

N^4,N^9-dinervonoyl spermine

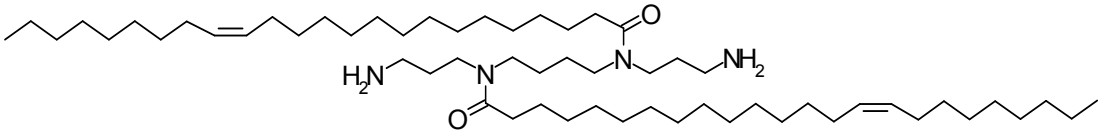

Mol. Wt 899.58.

Fig. 3.27. Very long symmetric lipopolyamines cationic lipids (N^4,N^9-diacyl spermines)

In this section, five novel very long chain N^4,N^9-diacyl polyamines: N^4,N^9-[diarachidoyl, diarachidonoyl, dieicosenoyl, dierucoyl and dinervonoyl]-1,12-diamino-4,9-diazadodecane (Fig. 3.27) were studied. The abilities of these novel compounds to condense DNA and to form nanoparticles were studied using EthBr

fluorescence quenching and nanoparticle characterization techniques. Transfection efficiency was studied in FEK4 primary skin cells and in an immortalized cancer cell line (HtTA), and compared with N^4,N^9-dioleoyl-1,12-diamino-4,9-diazadodecane.

3.4.1. DNA Condensation

In Fig. 28, we show the DNA condensation ability of the synthesized lipopolyamines in an EthBr fluorescence quenching assay. N^4,N^9-Dioleoyl spermine has the best DNA condensing ability, 90% EthBr fluorescence quenched at N/P charge ratio 5.5, while N^4,N^9-dieicosenoyl spermine shows such a result at N/P = 8, and N^4,N^9-dierucoyl spermine is only able to achieve around 60% fluorescence quenching at the same N/P ratio. The gel electrophoresis results (Fig. 3.29) show, by inhibiting the electrophoretic mobility of pDNA, that N^4,N^9-dinervonoyl spermine was able to condense pEGFP efficiently (as a result of neutralization of DNA phosphate negative charges by the ammonium positive charges).

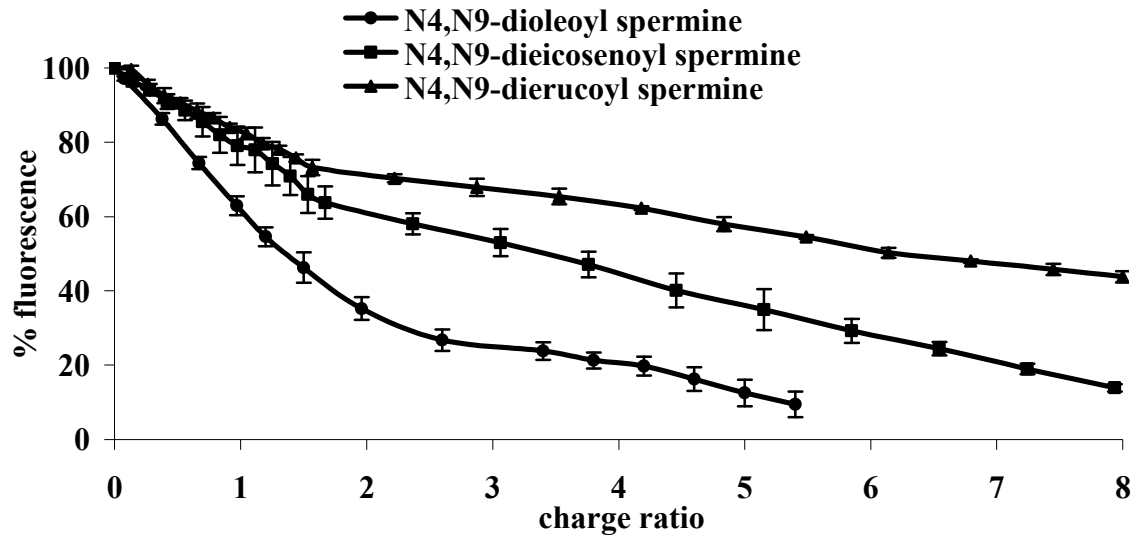

Fig. 3.28. Plot of EthBr fluorescence quenching assay of pEGFP complexed with different very long N^4,N^9-diacyl spermine.

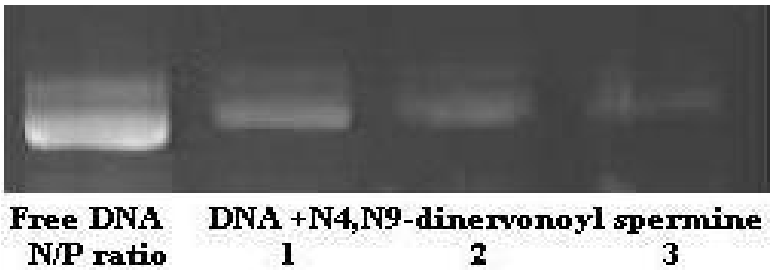

Fig. 3.29. Typical 1% agarose gel of fluorescent EthBr intercalated in pEGFP, assay of DNA gel permeation on complexation (lipoplex formation) with N^4,N^9-dinervonoyl spermine at N/P charge ratios 1, 2, 3.

3.4.2. Lipoplex Particle Size and Zeta-Potential Measurements

The particle size and ζ-potential characterization measurements were carried out on the lipoplexes at their optimum N/P charge ratio for transfection (see: Table 3.5).

Table 3.5. Particle size (mean ± S.D., n = 9) and zeta potential of pEGFP lipoplexes.

Lipospermine	Charge ratio (N/P)	Lipoplex diameter (nm)	ζ-Potential (+) mV
N^4,N^9-Dioleoyl spermine	2.5	150 (12)	2.2
N^4,N^9-Dieicosenoyl spermine	10	170 (22)	16.7
N^4,N^9-Diarachidonoyl spermine	8	170 (42)	
N^4,N^9-Dierucoyl spermine	4	210 (31)	3.6
N^4,N^9-Dinervonoyl spermine	4	190 (30)	

The physicochemically important parameter, ζ-potential helps to predict the stability of the formulation and the ability of the positively charged nanoparticles to interact with cell membranes. The ζ-potential measurements on the lipoplexes, at their optimum concentrations of transfection, show that all values are positive (Table 3.5), therefore there is a net positive charge on the surface. For DNA lipoplexes, ζ-potentials range from +2.2 mV (N^4,N^9-dioleoyl spermine) to +16.7 mV (N^4,N^9-dieicosenoyl spermine) (209-211), the measured ζ-potential for naked DNA is -1.0 mV.

3.4.3. pEGFP Transfection Experiments and In Vitro Cytotoxicity

The transduction of EGFP into a primary skin cell line (FEK4) and a cancer cell line (HeLa-derived HtTA) was investigated. All our polynucleotide delivery experiments are performed in the presence of serum. The optimum concentrations (in a final volume of 0.5 ml) and their corresponding N/P charge ratios for transfection were experimentally determined by using ascending N/P ratios of lipospermines from 2, 4, 6 etc. until we reached around 80% transfection and there was not a further step-up in transfection efficiency at the next highest N/P ratio.

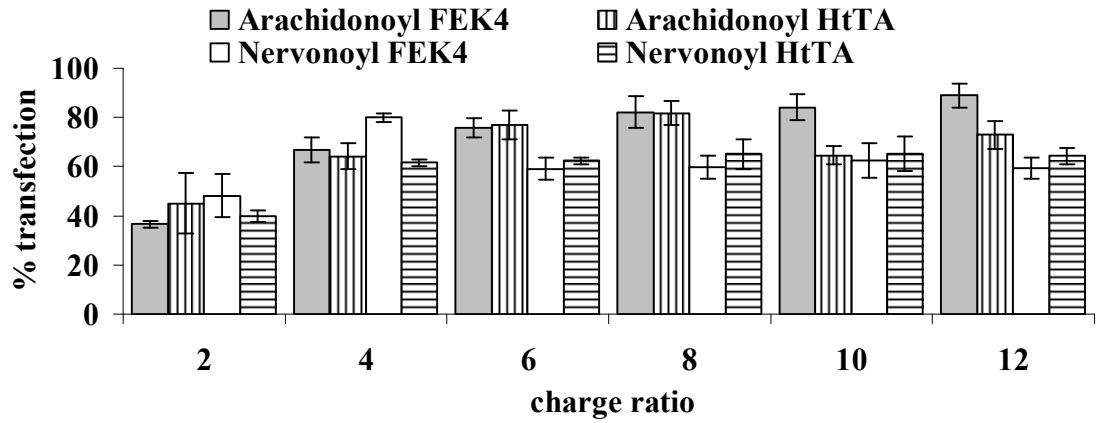

Fig. 3.30. Lipofection of the primary skin cell line FEK4 and the cancer cell line HtTA transfected with pEGFP (1 μg) complexed with N^4,N^9-diarachidonoyl spermine and N^4,N^9-dinervonoyl spermine at different N/P charge ratios.

The results in Fig. 3.30 show that the transfection efficiency is related to the N/P ratio. On the other hand, the toxicity also increases as the N/P ratio is increased (Fig. 3.31). So the optimum concentrations (and corresponding N/P charge ratios) for transfection were found to be N^4,N^9-dioleoyl spermine (2.8 μg, N/P = 2.5), N^4,N^9-diarachidoyl spermine (4.8 μg, N/P = 4.0), N^4,N^9-dieicosenoyl spermine (11.9 μg, N/P = 10.0), N^4,N^9-diarachidonoyl spermine (9.4 μg, N/P = 8.0), N^4,N^9-dierucoyl spermine (5.1 μg, N/P = 4.0), and N^4,N^9-dinervonoyl spermine (5.4 μg, N/P = 4.0).

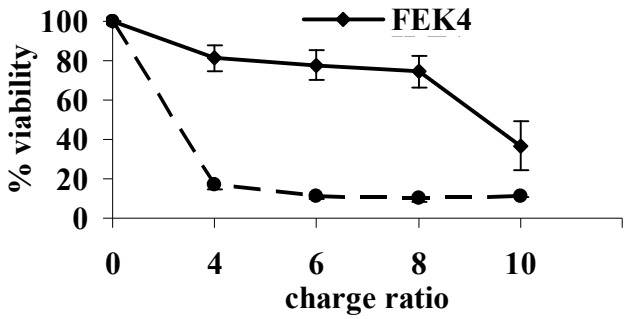

Fig. 3.31. Cytotoxicity effect of pEGFP (1 μg) complexed with N^4,N^9-diarachidonoyl spermine at different N/P ratios on FEK4 and HtTA cell lines.

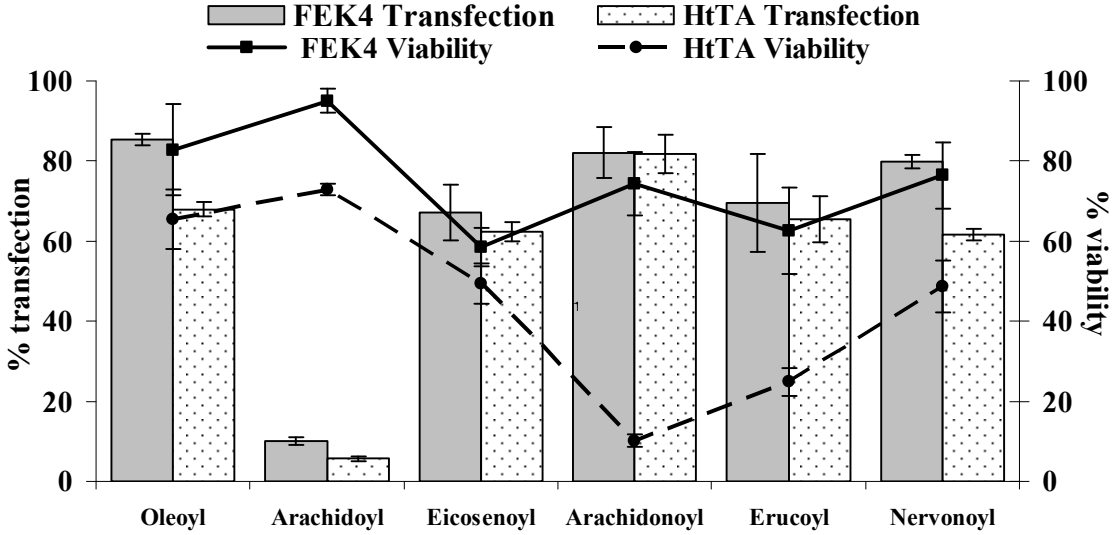

Fig. 3.32. Lipofection and cytotoxicity effects of pEGFP (1 μg) complexed with oleoyl (N^4,N^9-dioleoyl spermine) (2.8 μg), arachidoyl (N^4,N^9-diarachidoyl spermine) (4.8 μg), eicosenoyl (N^4,N^9-dieicosenoyl spermine) (11.9 μg), arachidonoyl (N^4,N^9-diarachidonoyl spermine) (9.4 μg), erucoyl (N^4,N^9-dierucoyl spermine) (5.1 μg) and nervonoyl (N^4,N^9-dinervonoyl spermine) (5.4 μg) on FEK4 and on the HeLa derived HtTA cell lines.

The results (Fig. 3.32) indicate that the transfection ability of the different lipospermines (at their optimum pDNA delivery N/P ratios) on both cell lines lie in the range 70-85% except for N^4,N^9-diarachidoyl spermine (5-10%). The cell viability (MTT assay) results indicate that while there is not a large difference in the viability of FEK4 cells typically (60-80%), the viability of HtTA cancer cells varies from N^4,N^9-dioleoyl spermine (65%), N^4,N^9-dieicosenoyl spermine and N^4,N^9-dinervonoyl spermine (50%), N^4,N^9-dierucoyl spermine (25%), and finally N^4,N^9-diarachidonoyl spermine (10%).

We have investigated the biological effects of increasing the length of the symmetrical diacyl fatty chain formulation of lipospermine on pDNA condensation and cellular delivery. The results from pEGFP condensation (Fig. 3.28), investigated using the EthBr fluorescence quenching assay, revealed that of our synthetic lipopolyamines N^4,N^9-dioleoyl spermine was able to condense DNA to less than 20% EthBr fluorescence at N/P charge ratio 3.5 (11); however, N^4,N^9-dieicosenoyl spermine and N^4,N^9-dierucoyl spermine were not able to quench the EthBr fluorescence by 80% even at N/P charge ratio 6 (Fig. 3.28). The particle size of the final pDNA formulation is also an important factor in improving gene delivery (187,188). Results for pDNA showed particle size around 190 nm, (Table 3.5), e.g., N^4,N^9-dierucoyl spermine showed a pDNA lipoplex particle size of 210 nm (mean value ± S.D. 31, n = 9). As discussed above, these long chain lipid moieties interact with the phospholipid bilayers (206) of cell membranes, facilitating cell entry, either in crossing the membrane bilayer and/or in helping to weaken the endosomal bilayer and thereby aid escape into the cytosol. The lipid chains make a significant contribution to the DNA compaction (Fig. 3.28) (162,164) and this is observable in the agarose gel permeation assay (Fig. 3.29). Heparan sulfate and other cell-surface polyanionic (sulfated) glycosaminoglycans are also involved in the cell binding of cationic lipoplexes and polyplexes leading to non-specific endocytosis. They interact with the net positive charge on the cationic lipoplexes and inhibit cation-mediated gene transfer, probably directing the lipoplexes into intracellular compartments that do not support transcription. Thus, the mechanisms of the uptake and the intracellular fate of lipoplexes are still obscure, but glycosaminoglycans may act as cellular receptors for cationic ligands, rather than only as passive cation binding sites (212-216).

It has been proposed that a shorter chain length may facilitate intermembrane mixing, an important factor in endosomal escape (206). Variation in the acyl chain, longer than the oleoyl group (C18), has led to higher levels of transfection, a result possibly related to the issues of hydrophobic moiety hydration (206-208). Lindner and co-workers reported the use of very long chain lipids e.g., erucoyl and compared them with other shorter chains in their designed cationic lipids (77), while Cullis and co-workers have studied the variation of the length of the acyl chains contained in the hydrophobic anchor from octanoyl to myristoyl to arachidoyl (217-219).

3.4.4. Confocal Microscopy Visualization

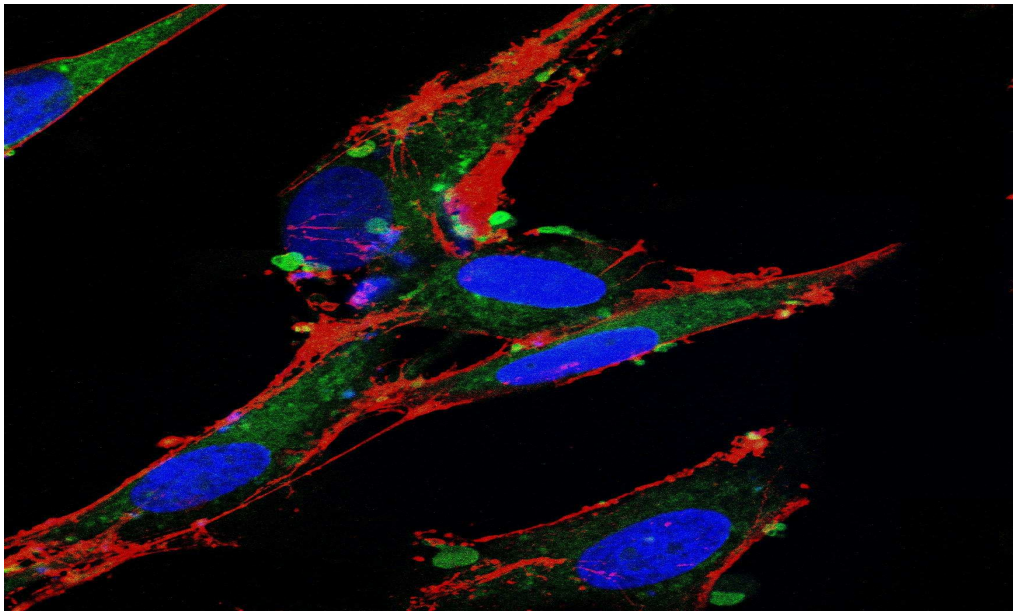

Fig. 3.33. FEK4 cell line transfected with pEGFP showing cytosolic green fluorescence from EGFP, delivered with N^4,N^9-dieicosenoyl spermine. The nuclei fluoresce blue and the cell lipid bilayers red (LSM510META, under the 60× oil immersion objective).

Using confocal laser scanning microscopy with one labelling solution (Invitrogen) containing both Alexa Fluor 594 wheat germ agglutinin (5 μg/ml) for cell membrane (red) labelling, and Hoechst 33342 (2 μM) for nuclei (blue) labelling, we have shown (Fig. 3.33) that FEK4 primary cells were successfully transfected with pDNA as the cells biosynthesized EGFP by transcription and translation.

The cell membranes are more complicated because they contain three classes of amphipathic lipids: phosphplipids, glycolipids, and steroids. The fatty chains in phospholipids and glycolipids usually contain an even number of carbon atoms, typically between 14 and 24. The 16- and 18-carbon fatty acids are the most common. Fatty acids may be saturated or unsaturated, so due to the existence of different fatty chains in naturally occurring phospholipids, we adjusted the focus to target those molecules which have unsymmetric aliphatic chains or steroids on N^4,N^9-positions of the spermine backbone to mimic those naturally occurring phospholipids.

3.5. UNSYMMETRICAL N^4,N^9-DIACYL SPERMINES: NON-VIRAL LIPOPOLYAMINE VECTORS FOR EFFICIENT pDNA DELIVERY

N^4-decanoyl,N^9-oleoyl spermine

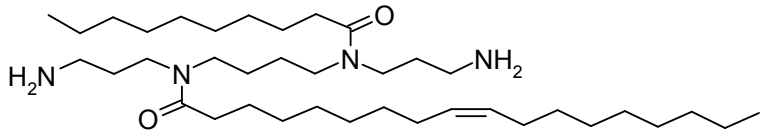

Mol. Wt. 621.06

N^4-decanoyl,N^9-stearoyl spermine

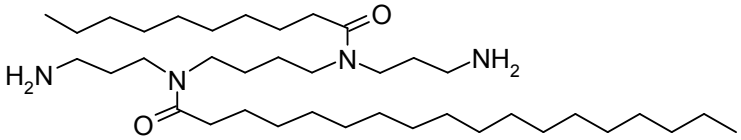

Mol. Wt. 623.07

N^4-myristoleoyl,N^9-myristoyl spermine

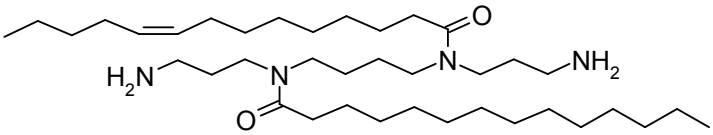

Mol. Wt. 621.06

N^4-oleoyl,N^9-stearoyl spermine

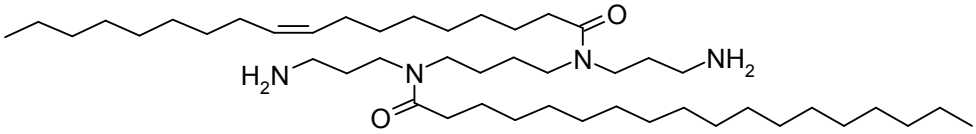

Mol. Wt. 733.27

N^4-cholesteryl,N^9-oleoyl spermine

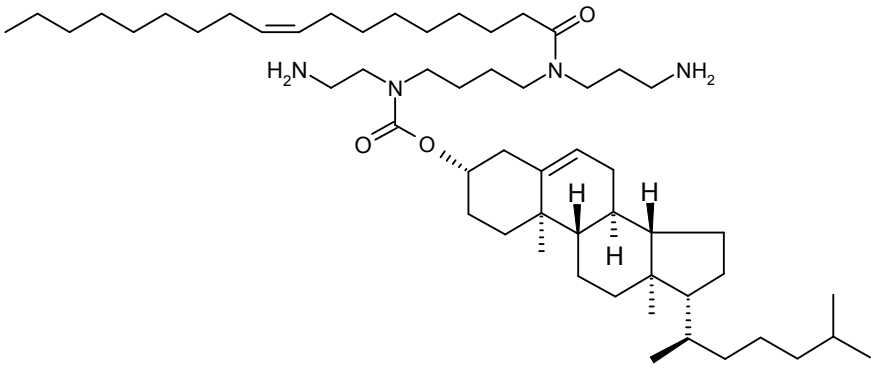

Mol. Wt. 865.44

N^4-lithocholoyl,N^9-oleoyl spermine

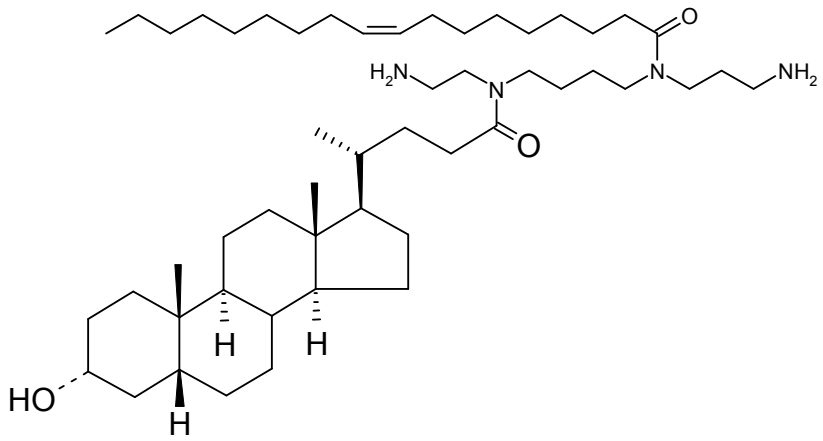

Mol. Wt. 865.44

N^4-palmitoyl,N^9-retinoyl spermine

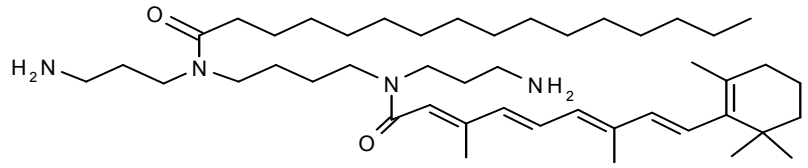

Mol. Wt. 723.19

N^4-oleoyl,N^9-retinoyl spermine

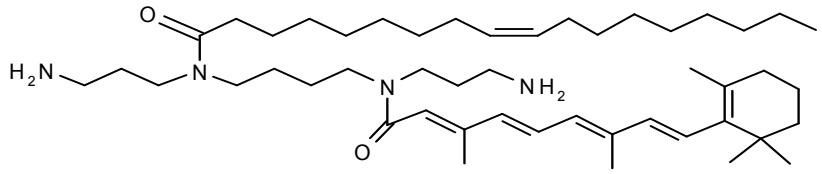

Mol. Wt. 749.23

Fig. 3.34. Unsymmetric lipopolyamine cationic lipids (N^4,N^9-diacyl spermines)

The cell membranes are more complicated because they contain three classes of amphipathic lipids: phosphplipids, glycolipids, and steroids. The fatty chains in phospholipids and glycolipids usually contain an even number of carbon atoms, typically between 14 and 24. The 16- and 18-carbon fatty acids are the most common. Fatty acids may be saturated or unsaturated, so due to the existence of different fatty chains in naturally occurring phospholipids, we adjusted the focus to target those molecules which have unsymmetric aliphatic chains or steroids on N^4,N^9-positions of the spermine backbone to mimic those naturally occurring phospholipids.

Due to the existence of unsymmetric fatty chains on C1 and C2 positions in many natural glycerophospholipids, the focus was changed to investigate those target molecules that have unsymmetrical aliphatic chains on N^4,N^9 positions of spermine backbone to mimic those naturally occurring molecules from the lipid bilayer. So in this section we are testing the N^4,N^9-unsymmetric series. Eight novel unsymmetric N^4,N^9-diacyl polyamines: [N^4-cholesteryl,N^9-oleoyl, N^4-decanoyl,N^9-oleoyl, N^4-decanoyl,N^9-stearoyl, N^4-lithocholoyl,N^9-oleoyl, N^4-myristoleoyl,N^9-myristoyl, N^4-oleoyl,N^9-retinoyl, N^4-oleoyl,N^9-stearoyl and N^4-palmitoyl,N^9-retinoyl]-1,12-diamino-4,9-diazadodecane (Fig. 3.34) were therefore studied. The abilities of these novel compounds to condense DNA and to form nanoparticles were studied using EthBr fluorescence quenching and nanoparticle characterization techniques. Transfection efficiency was studied in FEK4 and in an HtTA cell lines, and compared with the non-liposomal N^4,N^9-dioleoyl-1,12-diamino-4,9-diazadodecane.

3.5.1. DNA Condensation

In Fig. 3.35, the DNA condensation abilities of the synthesized lipopolyamines in an EthBr fluorescence quenching assay are shown. N^4-Decanoyl,N^9-oleoyl spermine has the best DNA condensing ability, 90% EthBr fluorescence quenched at N/P charge ratio 3.5 compared to N^4,N^9-dioleoyl spermine which show 90% at N/P ratio 5.5 while the other tested unsymmetric lipospermines only able to achieve around 70% fluorescence quenching at the N/P ratio 8. The gel electrophoresis results (Fig. 3.36) show, by inhibiting the electrophoretic mobility of pDNA, that N^4-oleoyl,N^9-stearoyl spermine was able to condense pEGFP efficiently (as a result of neutralization of DNA phosphate negative charges by the ammonium positive charges).

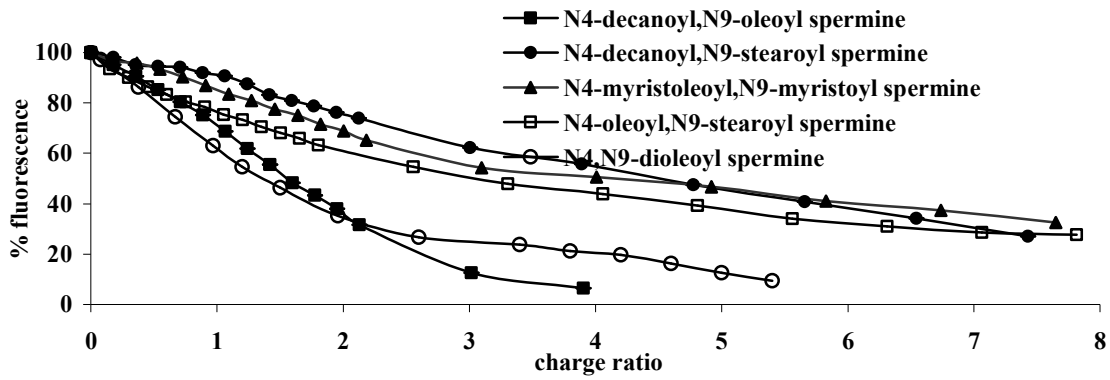

Fig. 3.35. EthBr fluorescence quenching assay of pEGFP DNA complexed with four unsymmetrical lipospermines and N^4,N^9-dioleoyl spermine.

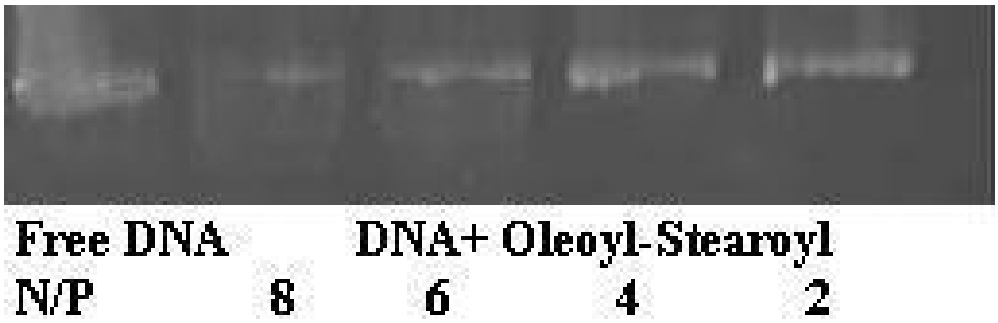

Fig. 3.36. Typical 1% agarose gel of fluorescent EthBr intercalated in pEGFP, assay of DNA gel permeation on complexation (lipoplex formation) with N^4-oleoyl,N^9-stearoyl spermine at N/P ratios 2, 4, 6 and 8.

3.5.2. Lipoplex Particle Size and Zeta-Potential Measurements

The particle size and ζ-potential characterization measurements were carried out on the lipoplexes at their optimum concentration for transfection (see: Table 3.6). Particle size characterization by laser diffraction showed that the nanoscale particle size of the formed DNA complexes ranged from 90 nm (N^4-decanoyl,N^9-oleoyl spermine) to 210 nm (N^4-myristoleoyl,N^9-myristoyl spermine) with an average particle size of 165 nm, (Table 3.6).

The pharmaceutically important ζ-potential helps to predict the stability of the formulation as well as the ability of the positively charged nanoparticles to interact with (phosphate containing, negatively charged) cell membranes(185). Nanoparticles are considered to be stable when they have pronounced ζ-potential values, either positive or negative; the tendency for particles to aggregate is higher when the ζ-

potential is close to zero (171). The surface charge, as determined by ζ-potential measurements on the lipoplexes at their optimum N/P charge ratio of transfection, show that all values are positive (Table 3.6) and they ranged from +2.47 mV (N^4-oleoyl,N^9-stearoyl spermine) to +19.05 mV (N^4-decanoyl,N^9-oleoyl spermine); the measured ζ-potential for naked DNA is -1.02 mV.

Table 3.6. Particle size (mean ± S.D.) and zeta potential of DNA complexes with the studied lipopolyamines.

Lipospermine	Charge ratio (N/P)	Lipoplex diameter (nm)	ζ-Potential (+) mV
N^4-Myristoleoyl,N^9-myristoyl spermine	20	210 (37)	14.58
N^4-Decanoyl,N^9-stearoyl spermine	30	190 (35)	17.90
N^4-Decanoyl,N^9-oleoyl spermine	8	90 (18)	19.05
N^4-Oleoyl,N^9-stearoyl spermine	8	170 (24)	2.47

3.5.3. pEGFP Transfection Experiments and In Vitro Cytotoxicity

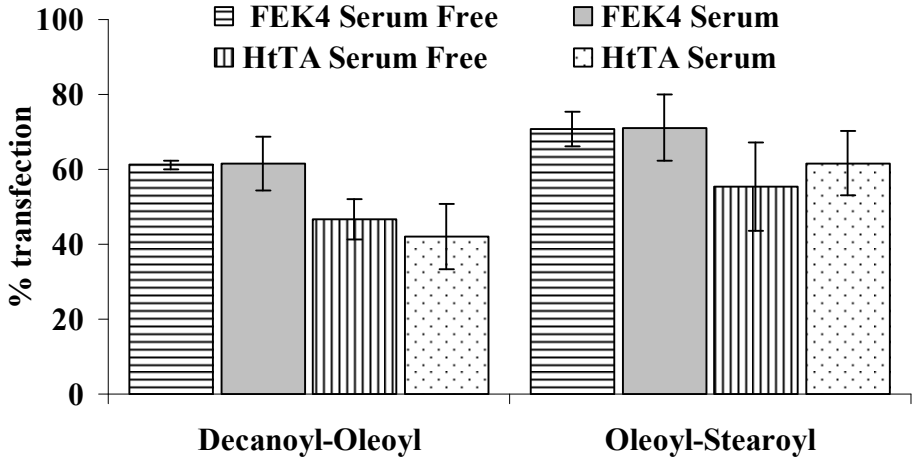

Fig. 3.37. Lipofection effects of pEGFP (1 μg) complexed with Decanoyl-Oleoyl (N^4-decanoyl,N^9-oleoyl spermine) (7.52 μg) N/P ratio 8 and Oleoyl-Stearoyl (N^4-oleoyl,N^9-stearoyl spermine) (8.87 μg) N/P ratio 8 on the primary skin cell line FEK4 and the HeLa derived cancer cell line HtTA in the absence and presence of serum.

The transduction of pEGFP into the primary skin cell line FEK4 and the cancer cell line (HeLa-derived HtTA) was investigated in both the presence and absence of serum (Fig. 3.37). Most pleasingly, we found that there was no significant difference in the transfection levels in the presence of serum for N^4-decanoyl,N^9-oleoyl spermine and N^4-oleoyl,N^9-stearoyl spermine. Encouraged by these positive results, all our subsequent transfection experiments are performed in the presence of serum and this is a significant step for all modern formulations moving towards clinical trials.

The optimum concentrations (in a final volume of 0.5 ml) and their corresponding N/P charge ratios for transfection were experimentally determined by using ascending N/P ratios of lipospermines from 2, 4, 6 etc. until we reached around 80% transfection and there was not a further step-up in transfection efficiency at the next highest N/P ratio. Results in Figs. 3.38 and 3.39 show that the transfection efficiency is related to the N/P ratio, increasing with higher N/P ratios. On the other hand, the toxicity also increases as with increasing N/P ratio, but it is not linear (Fig. 3.40). These data show that N^4-decanoyl,N^9-stearoyl spermine and N^4-myristoleoyl,N^9-myristoyl spermine have a very slight increase in their toxicity, at extreme N/P charge ratios near 20. While N^4-oleoyl,N^9-stearoyl spermine and N^4-decanoyl,N^9-oleoyl spermine show high toxicity at N/P charge ratio over 10. The transfection efficiency can be immediately seen from our FACS analyses in both cell lines (Fig. 3.41) with gating to measure mainly live cells. So the optimum concentrations (and corresponding N/P charge ratios) for transfection (in 0.5 ml) were found to be N^4,N^9-dioleoyl spermine (2.77 μg, N/P = 2.5), N^4-oleoyl,N^9-stearoyl spermine (8.87 μg, N/P = 8), N^4-decanoyl,N^9-oleoyl spermine (7.52 μg, N/P = 8), N^4-decanoyl,N^9-stearoyl spermine (28.27 μg, N/P = 30), N^4-myristoleoyl,N^9-myristoyl spermine (18.30 μg, N/P = 20), N^4-cholesteryl,N^9-oleoyl spermine (15.96 μg, N/P = 12), N^4-lithocholoyl,N^9-oleoyl spermine (14.98 μg, N/P = 12), N^4-palmitoyl,N^9-retinoyl spermine (4.28 μg, N/P = 4) and N^4-oleoyl,N^9-retinoyl spermine (11.33 μg, N/P = 10). In summary, the pEGFP delivery results (Fig. 3.42, histograms) indicate that the transfection ability of N^4-oleoyl,N^9-stearoyl spermine, N^4-lithocholoyl,N^9-oleoyl spermine and N^4-palmitoyl,N^9-retinoyl spermine are as good as N^4,N^9-dioleoyl spermine (at their optimum pDNA delivery N/P ratios) on both cell lines while the other five unsymmetric lipospermines are less efficient.

The cell viability (MTT assay) results (Fig. 3.42, lines) indicate that while there is not a large difference in the viability between N^4,N^9-dioleoyl spermine and most of the tested unsymmetric lipospermines, typically (60-85%) except for those with viability at or below 20%, N^4-cholesteryl,N^9-oleoyl spermine, then N^4-oleoyl,N^9-retinoyl spermine in HtTA cancer cells, and finally N^4-lithocholoyl,N^9-oleoyl spermine which is extremely toxic in both cell lines (viability only 9%).

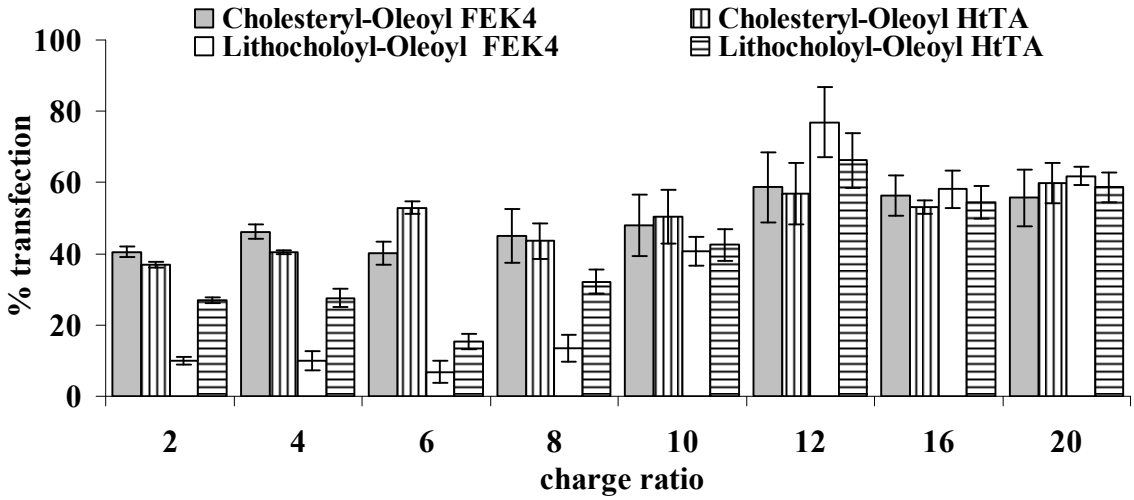

Fig. 3.38. Lipofection of the primary skin cell line FEK4 and the cancer cell line HtTA transfected with pEGFP (1 μg) complexed with N^4-cholesteryl,N^9-oleoyl spermine and N^4-lithocholoyl,N^9-oleoyl spermine at different N/P charge ratios.

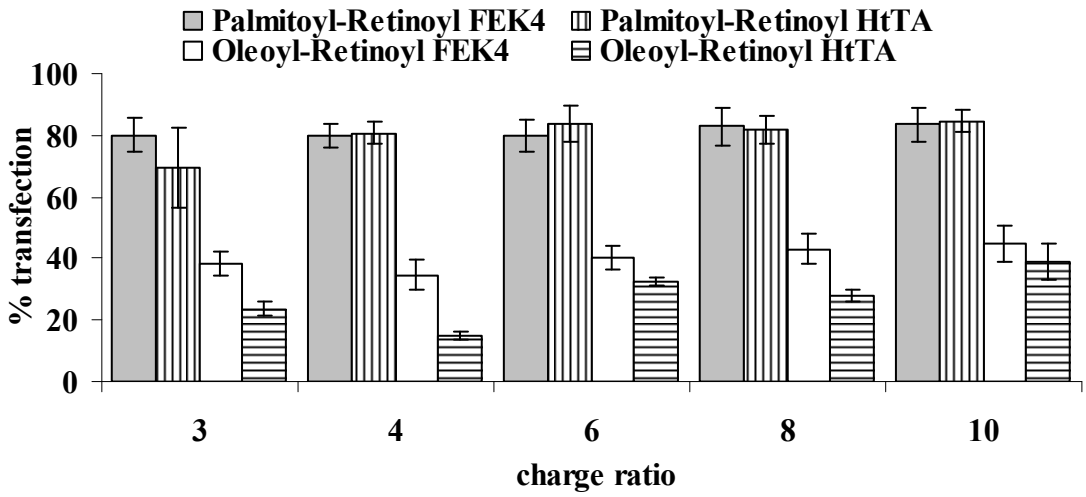

Fig. 3.39. Lipofection of the primary skin cell line FEK4 and the cancer cell line HtTA transfected with pEGFP (1 μg) complexed with N^4-palmitoyl,N^9-retinoyl spermine and N^4-oleoyl,N^9-retinoyl spermine at different N/P charge ratios.

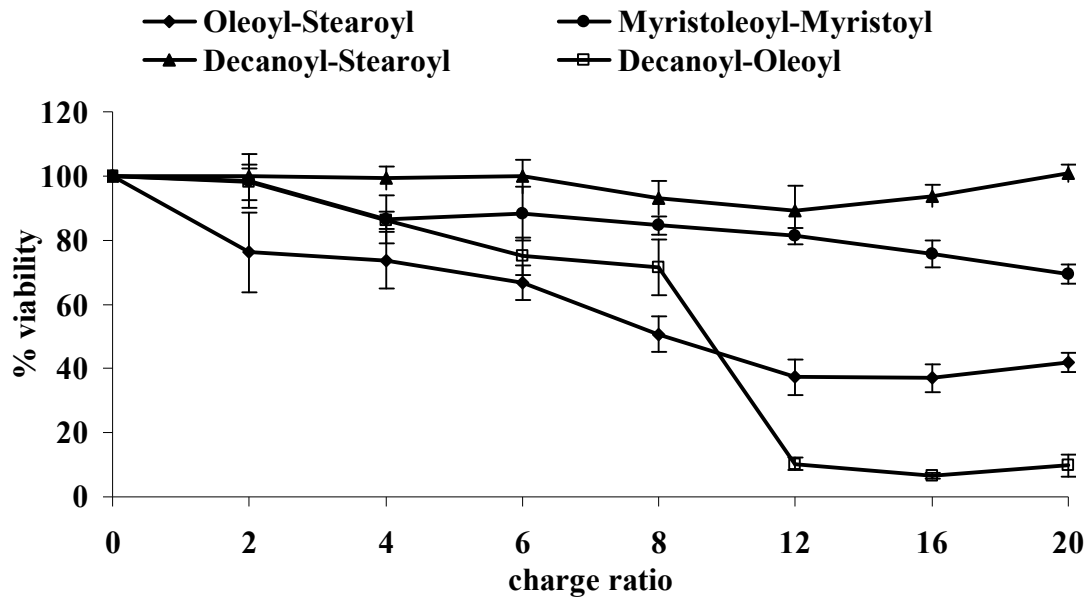

Fig. 3.40. Cytotoxicity effect of pEGFP (1 μg) complexed with different lipospermines at different N/P ratios on the primary skin cell line FEK4.

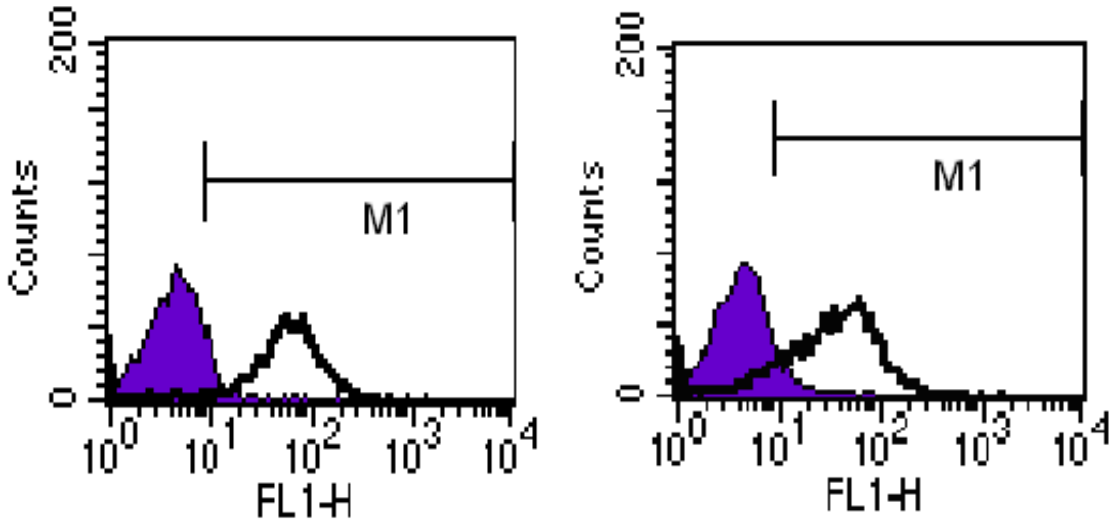

Fig. 3.41. FACS analysis of FEK4 (left) and HtTA (right) after 48 h transfection of pEGFP complexed with N^4-oleoyl,N^9-stearoyl spermine: ■ untransduced cells, □ EGFP-positive cells.

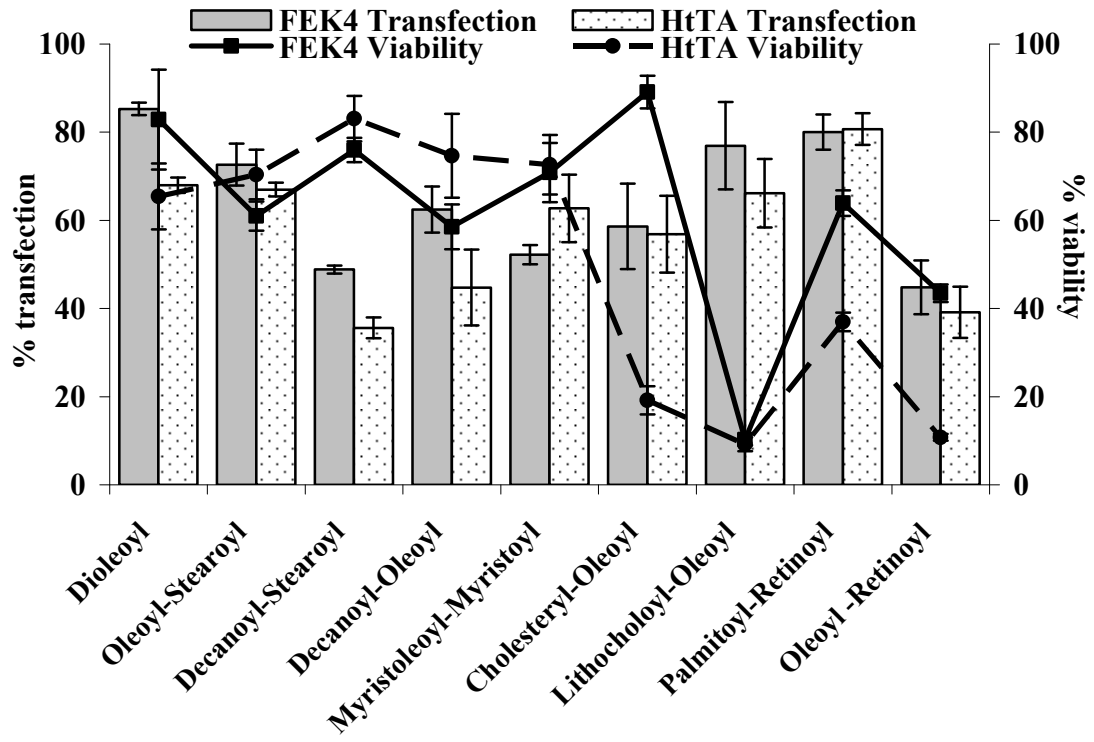

Fig. 3.42. Lipofection and cytotoxicity effects of pEGFP (1 μg) complexed with Dioleoyl (N^4,N^9-dioleoyl spermine) (2.77 μg), Oleoyl-Stearoyl (N^4-oleoyl,N^9-stearoyl spermine) (8.87 μg), Decanoyl-Oleoyl (N^4-decanoyl,N^9-oleoyl spermine) (7.52 μg), Decanoyl-Stearoyl (N^4-decanoyl,N^9-stearoyl spermine) (28.27 μg), Myristoleoyl-Myristoyl (N^4-myristoleoyl,N^9-myristoyl spermine) (18.30 μg), Cholesteryl-Oleoyl (N^4-cholesteryl,N^9-oleoyl spermine) (15.96 μg), Lithocholoyl-Oleoyl (N^4-lithocholoyl,N^9-oleoyl spermine) (14.98 μg), Palmitoyl-Retinoyl (N^4-palmitoyl,N^9-retinoyl spermine) (4.28 μg) and Oleoyl-Retinoyl (N^4-oleoyl,N^9-retinoyl spermine) (11.33 μg) on the primary skin cell line FEK4 and the HeLa derived cancer cell line HtTA.

3.5.4. Confocal Microscopy Visualization

Using confocal laser scanning microscopy with one labelling solution (Invitrogen) containing both Alexa Fluor 594 wheat germ agglutinin (5 μg/ml) for cell membrane labelling, and Hoechst 33342 (2 μM) for nuclei labelling, we have shown (Fig. 3.43) that FEK4 cells were successfully transfected with pDNA as the cells biosynthesized EGFP by transcription and translation. In this section, we have investigated effects resulting from using of the unsymmetrical diacyl fatty chain with different length or degree of saturation, cholesterol, lithocholic acid and retinoic acid formulations of lipospermines on DNA condensation and cellular delivery.

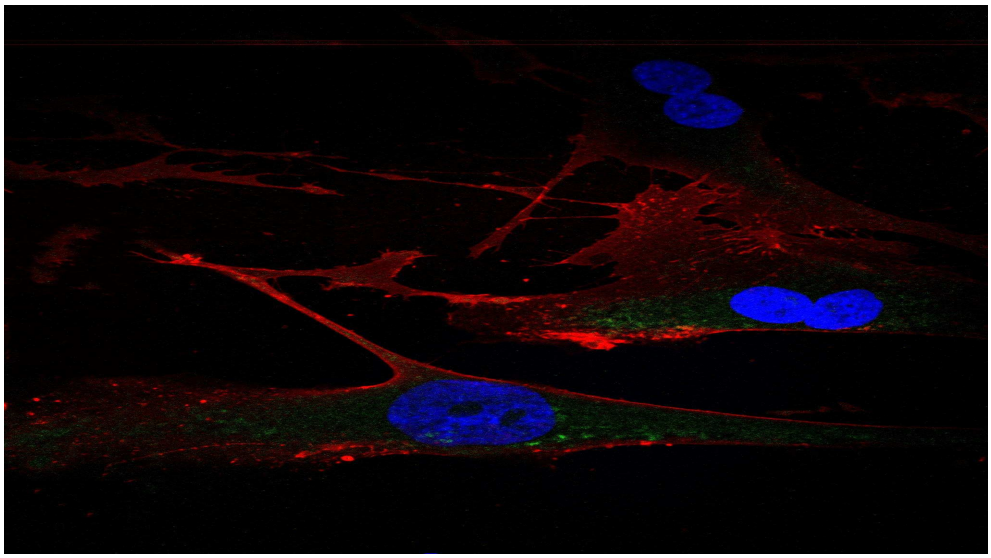

Fig. 3.43. The FEK4 primary cell line transfected with pEGFP showing cytosolic green fluorescence from EGFP, delivered with N^4-decanoyl,N^9-oleoyl spermine. The nuclei fluoresce blue from the Hoechst 33342 and the cell lipid bilayers fluoresce red from the Alexa Fluor 594 (LSM510META, under the 60× oil immersion objective).

The results from pEGFP condensation, investigated by EthBr fluorescence quenching assay, revealed that N^4-decanoyl,N^9-oleoyl spermine is the best condensing result (90% at N/P 3.5) while three of our synthetic lipopolyamines were able to condense DNA to less than 30% EthBr fluorescence at N/P ratio 8 (Fig. 3.35) (11). Particle size of the final nanoscale formulation is also an important factor in improving gene delivery (187,188). Particle size results (Table 3.6) showed an average particle size of 165 nm. On the relationship between particle size and transfection efficiency, all our lipoplexes are in the range 90-210 nm, and they transfected target cell lines efficiently. With regard to the mechanism for this cell entry, it is known that nanoparticles have relatively higher intracellular uptake than microparticles (155) although larger sizes of nanoparticles still do achieve transfection, presumably by a different mechanism (189). Further, when comparing the composition of the phospholipid bilayer of the cell membrane we find a high percentage of unsymmetrical fatty chains, so we try to mimic the nature by characterize ansymmetrical diacyl spermine as transfecting agents. So we are trying to take the advantage of having short and long fatty chains in the same molecules, saturated and unsaturated fatty chain or fatty Acid with cholesterol. Early liposomal studies therefore led to the proposal that a shorter chain length may facilitate

intermembrane mixing, an important factor in endosomal escape (206). A common moiety is the use of *cis*-mono-unsaturated alkyl chains e.g., the oleoyl group (C18). This leads to higher transfection levels than the corresponding saturated e.g., stearoyl (C18) derivatives, a result possibly related to the issues of hydrophobic moiety hydration or packing (206,207). by incorporating two different lipid moieties, we have shown that all our synthesized lipospermines afford transfection results varying in range, and at different N/P ratios and also most of the tested unsymmetric diacyl spermines are not toxic except N^4-lithocholoyl,N^9-oleoyl spermine, so by combination of the transfection efficiency results and viability we found that N^4-oleoyl,N^9-stearoyl spermine is an excellent vector for NVGT.

As lipopolyamines possess substantial buffering capacity below physiological pH, they are efficient transfection agents without the addition of (further) membrane-disruption agents. This observation led us to test heterocyclic substituted lipospermines for their gene delivery potential because it will increase the pK_a of the vector by increasing the number of nitrogen atoms in the lipospermines that can be protonated in the endosome as the pH drops to 5.5, i.e., their pK_as are around 5-7. Indeed, it makes the polymeric network an effective proton sponge at virtually any physiological pH (38). Our idea is that its efficiency relies on extensive lysosome buffering that protects DNA from nuclease (DNase) degradation, and consequently lysosomal swelling and rupture provide an escape mechanism for the particles, based on the hypothesis that a causal relationship exists between the protonation reservoir of a molecule below neutral pH and its transfection efficiency. This relationship may be the basis for the design of new synthetic vectors. Endosome buffering may protect DNA from lysosomal nucleases, but it may also perturb either the trafficking of endosomes or their osmolarity. For instance, massive vesicular ATPase-driven proton accumulation followed by passive chloride influx into endosomes buffered with lipospermine should cause osmotic swelling and subsequent endosome disruption. Furthermore, because the monomeric unit has such low molecular mass, the whole molecule will behave as an extensive proton sponge (38).

3.6. VARYING THE HETEROCYCLIC ENDGROUPS IN N^4,N^9-DIACYL SPERMINES FOR EFFICIENT pDNA FORMULATION

Di-4-imidazolylmethyl N^4,N^9-dimyristoyl spermine

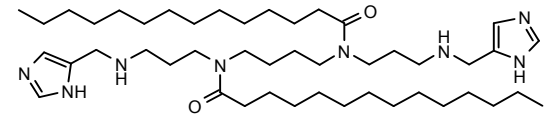

Di-2-pyridinylmethyl N^4,N^9-dimyristoyl spermine

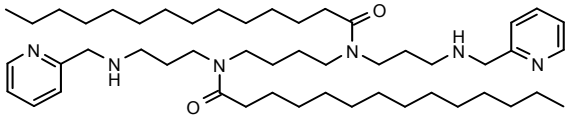

Di-2-quinolinylmethyl N^4,N^9-dimyristoyl spermine

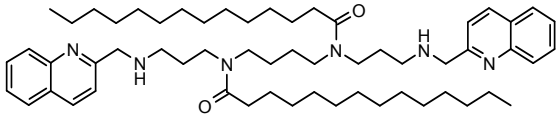

Di-4-imidazolylmethyl N^4,N^9-dipalmitoyl spermine

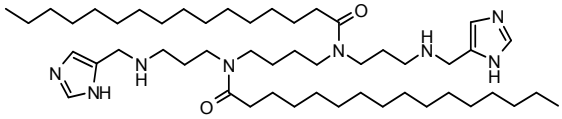

Di-2-pyridinylmethyl N^4,N^9-dipalmitoyl spermine

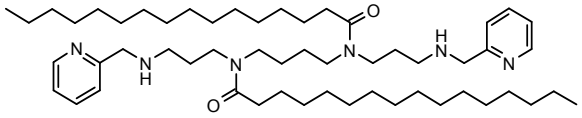

Di-2-quinolinylmethyl N^4,N^9-dipalmitoyl spermine

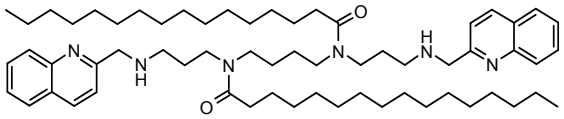

Di-4-imidazolylmethyl N^4,N^9-distearoyl spermine

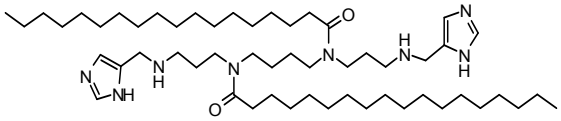

Di-2-pyridinylmethyl N^4,N^9-distearoyl spermine

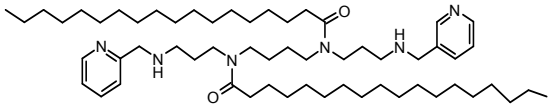

Di-2-quinolinylmethyl N^4,N^9-distearoyl spermine

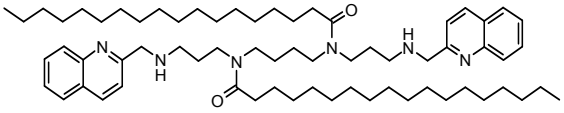

Di-4-imidazolylmethyl N^4,N^9-dioleoyl spermine

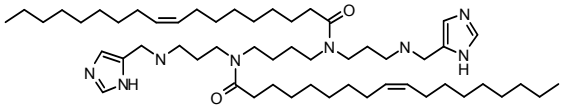

Di-2-pyridinylmethyl N^4,N^9-dioleoyl spermine

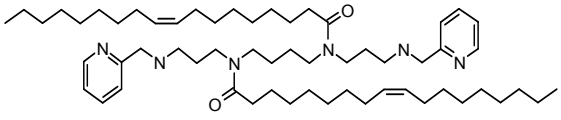

Di-2-quinolinylmethyl N^4,N^9-dioleoyl spermine

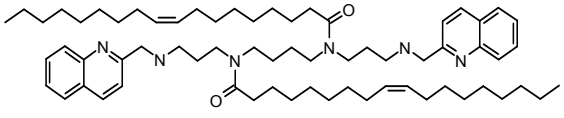

Fig. 3.44. Heterocyclic lipopolyamines cationic lipids (N^4,N^9-diacyl spermines)

3.6.1. pEGFP Transfection Experiments and In Vitro Cytotoxicity

In this study, we have investigated the formulation effects resulting from changes in a series of four N^4,N^9-diacyl spermines (myristoyl, palmitoyl, stearoyl, and oleoyl) each end-capped with the (weakly basic) nitrogen-containing heterocycles: imidazole, pyridine and quinoline. The surface charge, as determined by ζ-potential measurements on the lipoplexes at their optimum N/P charge ratio of transfection, for di-4-imidazolylmethyl N^4,N^9-dioleoyl spermine was found to be + 17.55 mV.

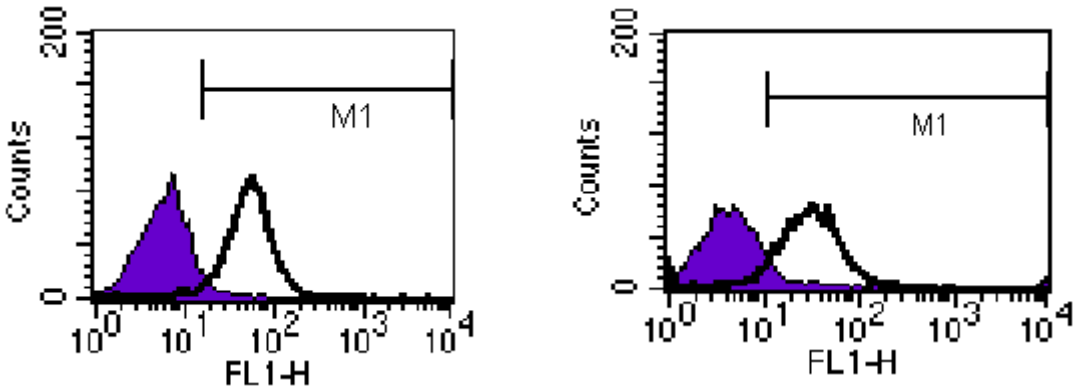

Fig. 3.45. FACS analysis of FEK4 (left) and HtTA (right) after 48 h transfection of pEFGP complexed with Stear-Quino: ■ untransduced cells, □ EGFP-positive cells.

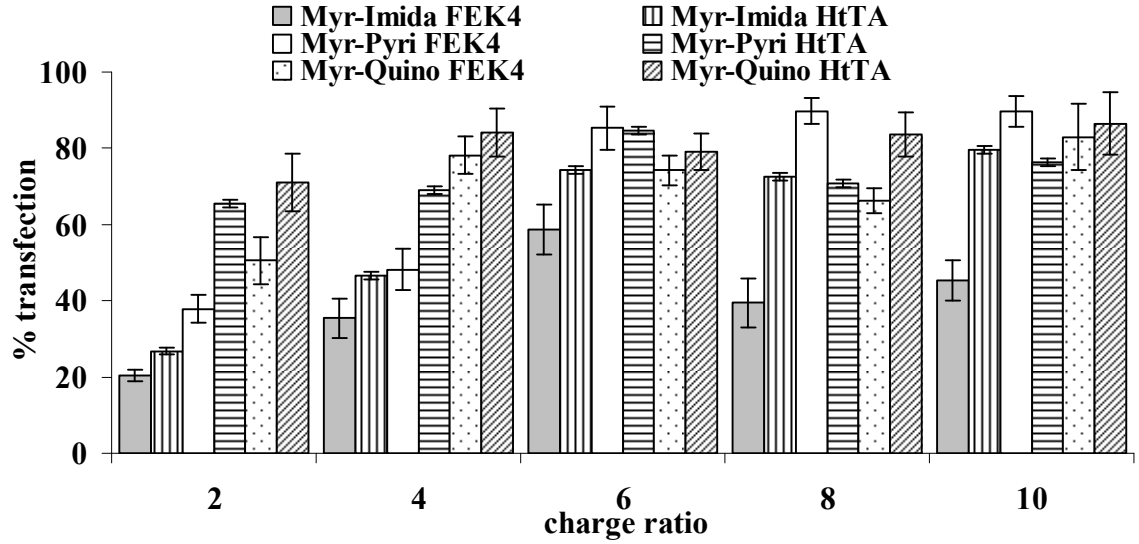

Fig. 3.46. Lipofection of the primary skin cell line FEK4 and the cancer cell line HtTA transfected with pEGFP (1 µg) complexed with different heterocyclic substituted N^4,N^9-dimyristoyl spermine at different N/P charge ratios.

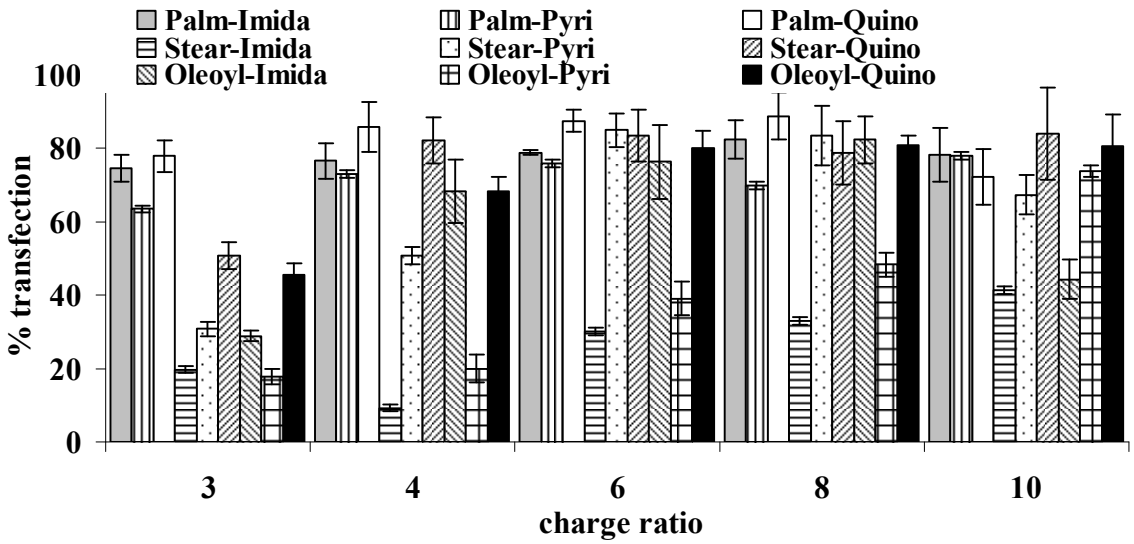

Fig. 3.47. Lipofection of the primary skin cell line FEK4 transfected with pEGFP (1 µg) complexed with different heterocyclic substituted N^4,N^9-diacyl spermine at different N/P charge ratios.

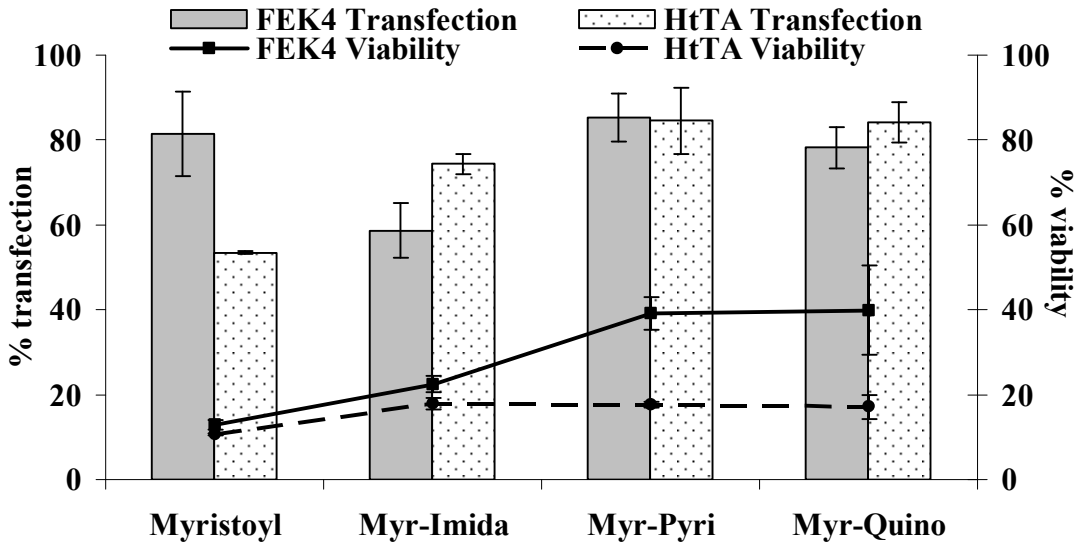

Fig. 3.48. Lipofection and cytotoxicity effects of pEGFP (1 µg) complexed with Myristoyl (9.4 µg), Myr-Imida (7.11 µg), Myr-Pyri (7.31 µg) and Myr-Quino (5.48 µg) on the primary skin cell line FEK4 and the HeLa derived cancer cell line HtTA.

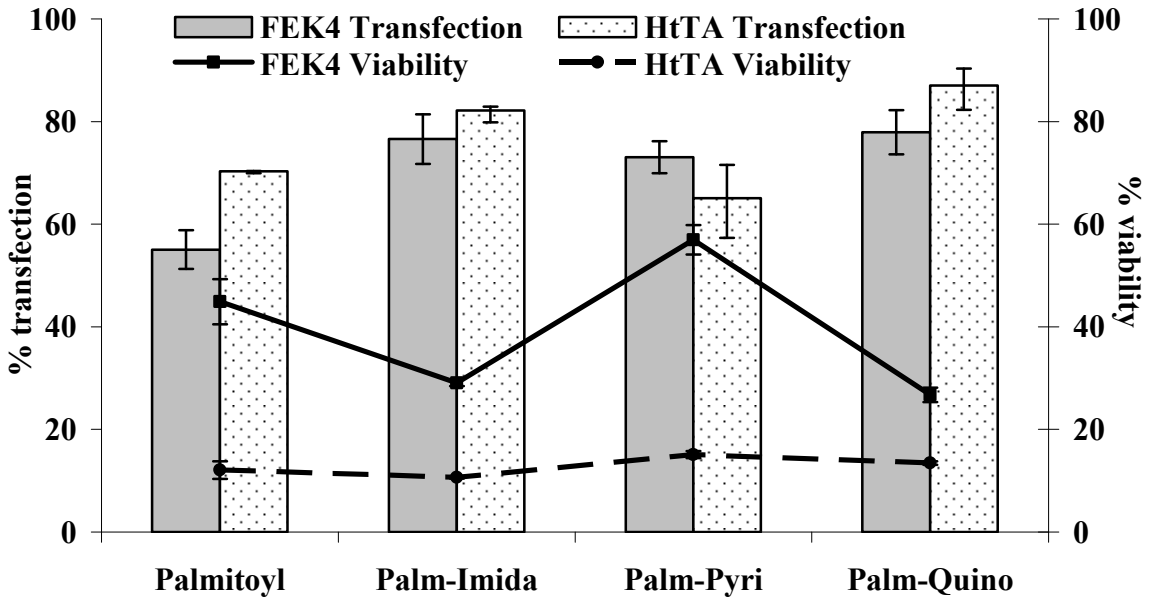

Fig. 3.49. Lipofection and cytotoxicity effects of pEGFP (1 µg) complexed with Palmitoyl (20.50 µg), Palm-Imida (5.08 µg), Palm-Pyri (5.21 µg) and Palm-Quino (4.36 µg) on the primary skin cell line FEK4 and the HeLa derived cancer cell line HtTA.

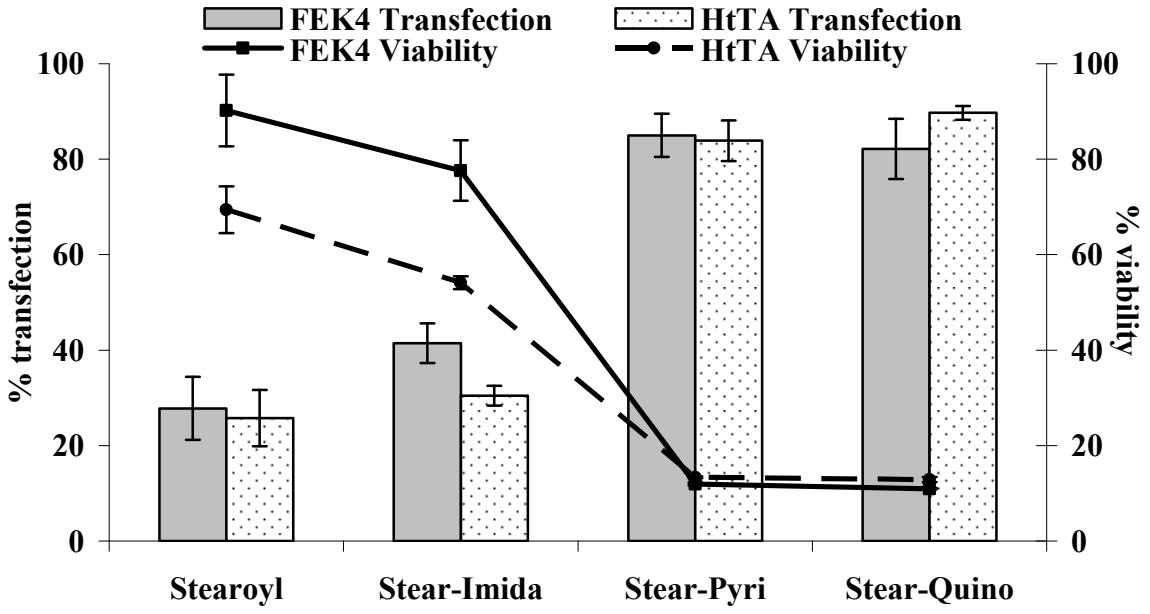

Fig. 3.50. Lipofection and cytotoxicity effects of pEGFP (1 µg) complexed with Stearoyl (16.70 µg), Stear-Imida (13.55 µg), Stear-Pyri (8.33 µg) and Stear-Quino (6.16 µg) on the primary skin cell line FEK4 and the HeLa derived cancer cell line HtTA.

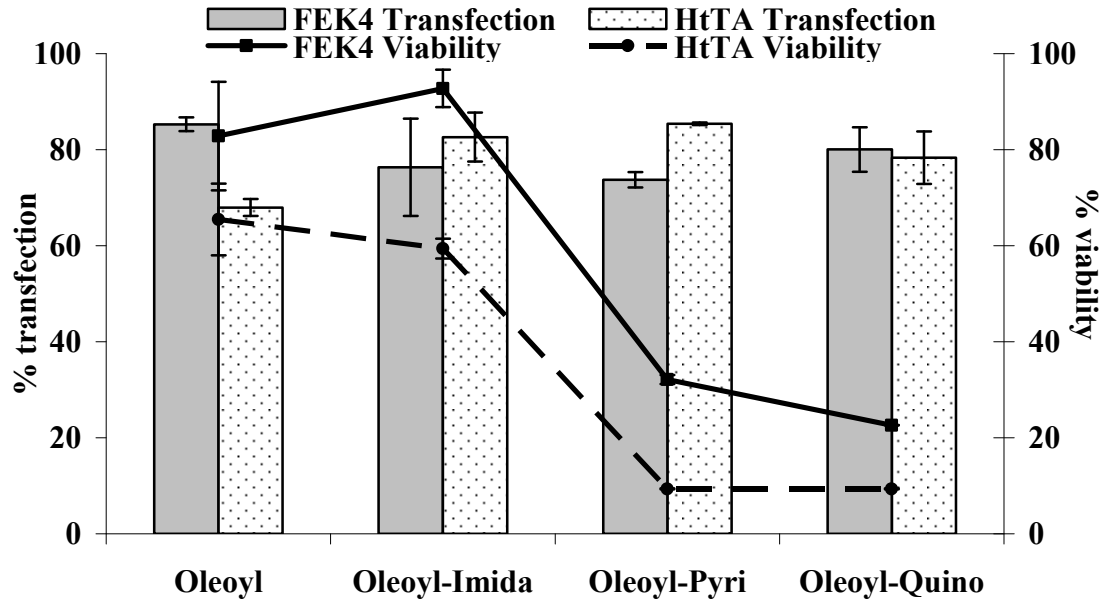

Fig. 3.51. Lipofection and cytotoxicity effects of pEGFP (1 μg) complexed with Oleoyl (2.77 μg), Oleoyl-Imida (8.09 μg), Oleoyl-Pyri (13.82 μg) and Oleoyl-Quino (9.20 μg) on the primary skin cell line FEK4 and the HeLa derived cancer cell line HtTA.

The transduction of EGFP into a primary skin cell line (FEK4) and a cancer cell line (HeLa-derived HtTA) was investigated. All our polynucleotide delivery experiments are performed in the presence of serum and can achieve high transfection efficiency is immediately seen from our FACS analysis with di-2-quinolinylmethyl N^4,N^9-distearoyl spermine in both cell lines (Fig. 3.45) The optimum concentrations (in a final volume of 0.5 ml) and their corresponding N/P charge ratios for transfection were experimentally determined by using ascending N/P ratios of lipospermines from 2, 4, 6 etc. until we reached around 80% transfection and there was not a further step-up in transfection efficiency at the next highest N/P ratio. Results in Figs. 3.46 and 3.47 show that the transfection efficiency is related to the N/P ratio. So the optimum concentrations (and corresponding N/P charge ratios) for transfection (Figs. 3.48-3.51)were found to be di-4-imidazolyl-methyl N^4,N^9-dimyristoyl spermine (7.11 μg, N/P = 6), di-2-pyridinylmethyl N^4,N^9-dimyristoyl spermine (7.31 μg, N/P = 6), di-2-quinolinylmethyl N^4,N^9-dimyristoyl spermine (5.48 μg, N/P = 4), di-4-imidazolylmethyl N^4,N^9-dipalmitoyl spermine (5.08 μg, N/P = 4), di-2-pyridinylmethyl N^4,N^9-dipalmitoyl spermine (5.21 μg, N/P = 4), di-2-quinolinyl-

methyl N^4,N^9-dipalmitoyl spermine (4.36 μg, N/P = 3), di-4-imidazolylmethyl N^4,N^9-distearoyl spermin (13.55 μg, N/P = 10), di-2-pyridinylmethyl N^4,N^9-distearoyl spermine (8.33 μg, N/P = 6), di-2-quinolinylmethyl N^4,N^9-distearoyl spermine (6.16 μg, N/P = 4), di-4-imidazolylmethyl N^4,N^9-dioleoyl spermine (8.09 μg, N/P = 6), di-2-pyridinylmethyl N^4,N^9-dioleoyl spermine (13.82 μg, N/P = 10) and di-2-quinolinyl-methyl N^4,N^9-dioleoyl spermine (9.20 μg, N/P = 6).

The transfection and cell viability results (Fig. 3.48) indicate that for N^4,N^9-dimyristoyl spermine heterocyclic derivatives (at their optimum pDNA delivery N/P ratios) there is no improvement, neither in the transfection ability nor the cell viability, over that achieved with N^4,N^9-dimyristoyl spermine on both cell lines, but there was a significant decrease in the amount of transfecting agent required to achieve this comparably efficient transfection (lower N/P charge ratio). In the N^4,N^9-dipalmitoyl spermine series (Fig. 3.49), there is a slight improvement in the transfection ability, still the same high level of toxicity, but also with a significant decrease in the amount of transfecting agent required for efficient transfection (i.e., lower N/P charge ratios). In the N^4,N^9-distearoyl spermine series (Fig. 3.50), the imidazole derivative only achieves the poor transfection results of N^4,N^9-distearoyl spermine, but it is not toxic. While both the distearoyl pyridine and quinoline analogues show much higher transfection efficiencies (82-90 %) than the (25-27 %) achieved with N^4,N^9-distearoyl spermine and di-4-imidazolylmethyl N^4,N^9-distearoyl spermine on both cell lines, but on the other hand both the distearoyl pyridine and quinoline analogues are extremely toxic. In the N^4,N^9-dioleoyl spermine series (Fig. 3.51), the imidazole derivative is as good as N^4,N^9-dioleoyl spermine in both transfection efficiency and cytotoxicity (cell viability). Even the pyridine and quinoline analogues show the same high levels of transfection efficiency, but this is only achieved with a significant level of toxicity. Therefore, in non-viral pDNA delivery, the novel di-imidazole derivative of N^4,N^9-dioleoyl spermine (di-4-imidazolylmethyl N^4,N^9-dioleoyl spermine) is a useful compound, in vitro it is comparable to, but not significantly better than N^4,N^9-dioleoyl spermine. No other research groups have reported efficient pDNA delivery with such nitrogen-containing heterocyclic analogues of cationic lipids.

3.6.2. Confocal Microscopy Visualization

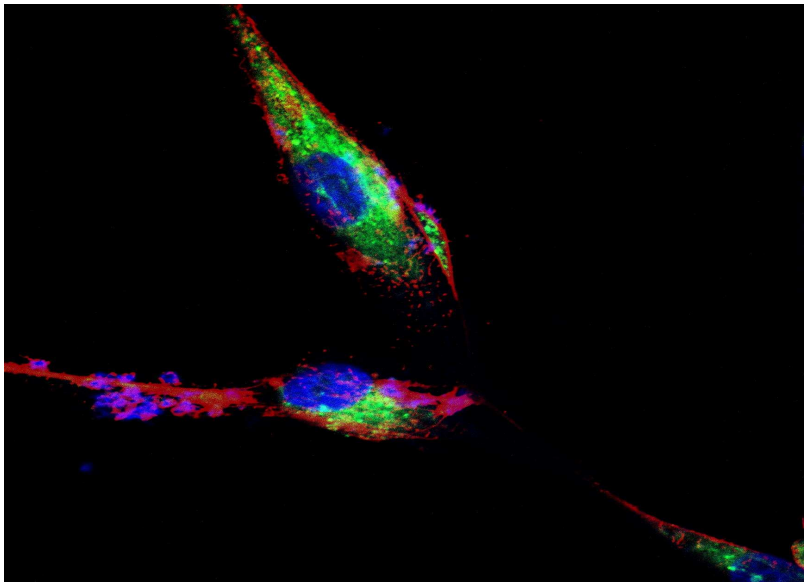

Fig. 3.52. Transfection of the primary skin cell line FEK4 with pEGFP showing cytosolic green fluorescence from EGFP, delivered with di-4-imidazolylmethyl-N^4,N^9-dioleoyl spermine. The cell lipid bilayers fluoresce red from the Alexa Fluor 594 and the nuclei fluoresce blue from the Hoechst 33342 (LSM510META, under the 60× oil immersion objective).

Using confocal laser scanning microscopy with one labelling solution (Invitrogen) containing both Alexa Fluor 594 wheat germ agglutinin (5 μg/ml) for cell membrane labelling (red), and Hoechst 33342 (2 μM) for nuclei labelling (blue), we have shown (Fig. 3.52) that FEK4 cells were successfully transfected with pEGFP using di-4-imidazolylmethyl N^4,N^9-dioleoyl spermine as the vector, as the cells biosynthesized EGFP by transcription and translation. This was the best result from the heterocyclic series, at least comparable with N^4,N^9-dioleoyl spermine in both transfection efficiency and high cell viability.

We now turn our focus to the important topic of efficient non-viral formulations for siRNA delivery. Can we deliver siRNA to our two chosen cell lines using any of these pDNA delivery agents? Many research groups are actively searching for a non-viral vector that will give a high yield of siRNA delivery without paying the price in high cellular toxicity.

CHAPTER 4

Design and Development of Pharmaceutical Dosage Forms for siRNA Delivery

4.1. INTRODUCTION

RNA interference (RNAi) is a naturally occurring phenomenon by which small interfering RNA (siRNA) can use enzymatic cleavage of a target mRNA to reduce or inhibit gene expression into proteins mediated by RNA induced silencing complex (RISC) (90,100,104). RNAi is initiated by short double-stranded RNA (dsRNA) molecules in the cytoplasm where they interact with the catalytic RISC component. The dsRNA can be both exogenous or endogenous whose pathways converge at the RISC complex (220). siRNAs form a class of 19-23 nucleotide-long RNA molecules that play a variety of roles in biology, most notably in the RNAi pathway where each siRNA interferes with (blocks) the expression of a specific gene (104). RNAi is commonly achieved with chemically synthesized siRNA 19-23-mers.

Efficient delivery of siRNA to targeted cells will also be important for the successful treatment of a variety of diseases. Modifications to synthetic siRNA can increase the half-life of circulating siRNA in animal models. Yet it is not enough to enhance siRNA stability if siRNA can not penetrate cells and tissues in vivo in a sufficient concentration to achieve efficient therapy. As siRNAs are ds molecules, delivery and cellular uptake are more difficult than for single-stranded (poly-nucleotide) antisense agents, which bind to serum proteins and are taken up by cells and tissues in vivo. There are a few reports of functional RNAi being obtained by systematic delivery of antisense agents that have never reached a clinical trial. So a better understanding of the mechanism by which backbone modifications might help to enhance cellular and tissue uptake of naked RNAs, or how to develop alternative carriers for systemic delivery of siRNAs is still required. The essentially specific ability of synthetic siRNA to inhibit targeted genes, makes it an extremely powerful tool for functional genomics, it has attracted considerable interest recently (221).

The biological usefulness of spermine (1,12-diamino-4,9-diazadodecane) and its conjugates (12,222-224) encouraged us to focus on the synthesis of novel cationic lipids based on the naturally occurring polyamine spermine (170,171,225,226). In an effort to improve the efficiency and control of siRNA delivery, these novel spermine based cationic lipid formulations have been investigated within our SAR approach to molecular pharmaceutics for molecular medicine.

As has been shown above for gene therapy, methods to deliver poly-nucleic acids fall into two classes. The first employs genetically altered viruses that, in most cases, have had their genome altered or “gutted” to prevent viral replication, reduce

cytotoxicity, and permit incorporation of the therapeutic transgene. These vectors can be extremely efficient at producing expression, with essentially only a single viral particle necessary to induce a measurable effect. However, problems of low virus titre, an inability to transfect non-dividing cells, induction of strong immune responses, and significant toxicity must still be overcome (227). The second class of delivery systems is collectively referred to as non-viral and involves the use complexes with synthetic carrier molecules e.g., cationic lipids or polymers. Such non-viral delivery systems can potentially have considerable advantages over their viral counterparts e.g., greater control of their molecular composition for simplified manufacturing and analysis (228,229), and relatively lower immunogenicity (230-233), but these non viral systems are still significantly less efficient than viral systems. Despite the early hopes and predictions, there is no correlation between pDNA and siRNA delivery, and therefore SAR studies need to be undertaken of the non-viral formulations of siRNA.

In vitro uses simplify many of the problems associated with target cell delivery, target selectivity, homeostasis mechanisms and possible non-target cell toxicity encountered in vivo. Yet, the cellular membrane is still an important physical barrier to the efficient intracellular introduction of nucleic acids. Similarly as in gene delivery, passage through the cell membrane of nucleic acids is difficult to achieve as a result of their hydrophilic and polyanionic nature. Experience with DNA has provided a variety of chemical and physical techniques that should allow the transfection or infection of cells with extracellularly synthesized siRNA. The different techniques currently available for intracellular introduction of siRNA. The chemical techniques are generally based on the use of (poly)cations (107). Liposomes, and lipid complexes or conjugates with small molecules, polymers, proteins and antibodies, have all been used to facilitate delivery of siRNAs to target cells. With these delivery partners, more robust efficacy can be achieved with doses of siRNA that are substantially lower, less frequent or both (234). The cationic compounds condense the siRNA, resulting in the formation of particles. These particles generally bear a net positive charge, as an excess of the cation provides efficient condensation and prevents particle aggregation. The net positive charge of the particle additionally promotes electrostatic interaction with the overall negative charge of the cell membrane. Both by condensing the siRNA and promoting cell membrane interaction, relatively efficient cell transfection can be achieved. A range of cations exists that have been shown to promote the intracellular delivery of nucleic acids. Of these, the

cationic lipids, cationic lipopolyamines are the most prominent. The ultimate in vitro transfection-efficiency of a cationic compound appears to be dependent on the characteristics of the cells, as well as the properties of the cationic particle, e.g., cell medium compatibility, cell toxicity, strength of electrostatic interaction, cation structure, and particle size. Although interaction between the cell surface and the delivery system promotes siRNA uptake, appropriate intracellular trafficking should still follow the interaction (107). The cationic particles are likely taken up by cells through endocytosis. Therefore, the cationic particle and/or its siRNA should be able to escape the endosomal vesicle to evade lysosomal degradation to allow the RNAi effects to occur through cytoplasmic degradation of mRNA by externally applied siRNA, which is in the ultimate interest of pharmaceutical applications.

Lipids and polymers can have cytotoxic effects that might limit their use in siRNA delivery for particular disease indications and dosing paradigms. However, it seems to be possible to identify lipid-based formulations and dosing regimens for which cytotoxicity is minimal and the risk of histopathology is reduced. With advances in pharmaceutical development, these approaches may provide marked enhancements to siRNA delivery with acceptable biological and manufacturing considerations (234). Variations in chemical composition of cationic lipids can have a large impact on the functional properties of cationic lipid with decreased toxicity that are more compatible with administration (94,115).

As many cells and cell lines are either refractory to or adversely affected by transfection, and due to the transient nature of this methodology, more efficient (and less toxic) siRNA delivery vectors are required. The effect of the degree of saturation of certain mono-cationic lipid analogues was investigated to identify the fusogenic and transfection ability of these compounds by Heyes and co-workers (93). The saturated cationic lipid (1,2-distearyloxy-*N*,*N*-dimethyl-3-aminopropane (DSDMA)) was readily internalized in cells, despite it achieving almost no ability of gene silencing (siRNA delivery). Gene silencing increased with the degree of unsaturation as a result of the increase in the fusogenic ability of the cationic lipid, a lower transition temperature from L_α (lamellar organization) to H_{II} (two-dimensional hexagonal state) (93). For this aspect of our research, we formulated a model siRNA 21-mer with novel lipospermines in which the tetra-amine spermine (the cationic moiety) and fatty chains (the lipophilic moiety) that have been reported to improve transfection efficiency by fusion with cellular membranes, are covalently bound

together. We examine the non-viral siRNA delivery efficiency and compare it with the cell viability for self-assembled nanoparticles of siRNA (lipoplexes) formed by these new cationic lipids in order to develop vectors for siRNA delivery make comparisons with pDNA delivery using the same vectors although at different concentrations.

Our model siRNA incorporates the Label IT® RNAi Delivery Control which is designed as a tool to facilitate visualization and optimization of dsRNA oligonucleotide delivery during RNAi experiments, both in vitro and in vivo. The Label IT® RNAi Delivery Control is a fluorescein-labelled RNA duplex that has the same length, charge, and configuration as standard siRNA. The sequence of the duplex (below) is not homologous to any known mammalian gene and is not known to affect any cellular events. It is also suitable for co-delivery with functional target-gene specific siRNA and should not affect the RNAi-mediated inhibition of the target gene. The non-enzymatic Label IT labelling reagent attaches to any reactive heteroatom on any nucleotide residue of DNA or RNA. This direct covalent attachment is made possible by a reactive alkylating agent with strong nucleic acid binding capability facilitated via electrostatic interactions. As the Label IT labelling technology will bind to any nucleotide, we cannot be sure where the fluorophore was attached exactly, but because the reaction is controlled we know that there are 1-2 labels per duplex. The delivered siRNA is a 21-nucleotide "target" sequence with UG-3' overhangs:

GAGGCUCAACUGGCUGACCUG

GUCUCCGAGUUGACCGACUGG

That there is no obvious correlation between the successful transfecting agents for pDNA and those investigated for siRNA delivery, with non-viral vectors, means that this is an important area in current formulation research for poly-nucleic acid delivery. In the previous chapter, we discussed and characterized gene delivery using N^4,N^9-dioleoyl spermine and other diacyl spermine analogues. Therefore, we are carrying further these investigations in order to characterize a successful siRNA delivery agent using the same basis, diacyl spermine derivatives. Although superficially similar, i.e., ds poly-anionic chains are to be delivered, the most immediate difference is the molecular size (length, and therefore weight) which will significantly vary the amount of cationic lipid to be used and therefore the toxicity (cell viability) of the formulation. Based on our successful use of lipospermines in gene delivery (above), the corresponding siRNA formulations are investigated using

our novel lipospermines with variation in the: position, length, saturation, oxidation level or the symmetry of the two fatty chains (diacyl, dialkyl, and steroids) or the attachment of heterocyclic groups on the two primary amines of lipospermines to modulate their pK_a. These lipid chains are linked by amide bonds at the secondary amino groups of spermine to form N^4,N^9-diacyl spermines or the primary amino groups of spermine to form N^1,N^{12}-diacyl spermines, and therefore comparisons (SAR studies) can be made between pDNA and siRNA delivery.

It should not be assumed that this will lead to a 100% overlap of results between pDNA and siRNA delivery. Indeed, it is (in part) the absence of such a study that has hampered progress in siRNA delivery. This study therefore also includes the physicochemical characterisation of the lipoplex nanoparticles formed, including the ability of the synthetic lipopolyamines to bind to siRNA studied using the RiboGreen fluorescence quenching assay. The physicochemical characterization includes the particle size measurements and zeta-potential studies.

Transfection efficiency was studied in an immortalized cancer cell line (HtTA), and in primary skin cells (FEK4), always in the presence of serum to test the ability of these novel transfecting agents to work efficiently in the presence of serum RNase which opens the door for the successful vectors to be considered further with in vivo investigations. Indeed, if these non-viral formulations are not stable in the presence of serum, there is little or no point to studying them further. Furthermore, the results are compared with those obtained with an siRNA delivery market leader Trans-IT™ (Mirus).

The cytotoxicity of the lipoplexes was studied in both primary skin and immortalised cancer cell lines using the MTT assay, but with significantly different concentrations of the cationic lipid lipospermine formulations from those used previously to delivery pDNA, hence we cannot predict the toxicological outcomes.

Cellular delivery of fluorescent-siRNA was also studied using confocal laser scanning microscopy with one labelling solution for both cell membrane and nuclei labelling in order to see if the payload was delivered successfully to the cytosol.

4.2. N^1,N^{12}-DIACYL SPERMINES: SAR STUDIES OF NON-VIRAL LIPOPOLYAMINE VECTORS FOR siRNA FORMULATION

4.2.1. RNA Binding (RiboGreen Intercalation Assay)

This assay is comparable with the EthBr fluorescence quenching assay widely used for initial pDNA formulation studies. RiboGreen solution (Invitrogen, 50 µl diluted 1 to 20) was added to each well of an opaque bottomed 96-well plate containing free siRNA (50 ng) or complexed with lipospermines at different ratios in TE buffer (50 µl, 10 mM Tris-HCl, 1 mM EDTA, pH 7.5, in diethyl pyrocarbonate)- (DEPC) treated water using FLUOstar Optima Microplate Reader (BMG-LABTECH), λ_{ex} = 480 nm, λ_{em} = 520 nm. The amount of siRNA available to interact with the probe was calculated by subtracting the values of the residual fluorescence (RiboGreen without siRNA) from those obtained for each measurement, and expressed as a percentage of the control that contained naked siRNA only, according to the following formula: % free siRNA = 100 x RiboGreen fluorescence$_{complexes}$/RiboGreen fluorescence$_{naked\ siRNA}$.

The siRNA binding results from the RiboGreen intercalation assay, show that efficient fluorescence quenching occurs by N/P charge ratio 4 for all four lipopolyamines (Fig. 4.1). However, the N^4,N^9-regioisomer pattern is preferred, as N^4,N^9-dioleoyl spermine (Lipogen®) and N^4,N^9-dimyristoleoyl spermine achieved 80% fluorescence quenching by N/P = 2.5.

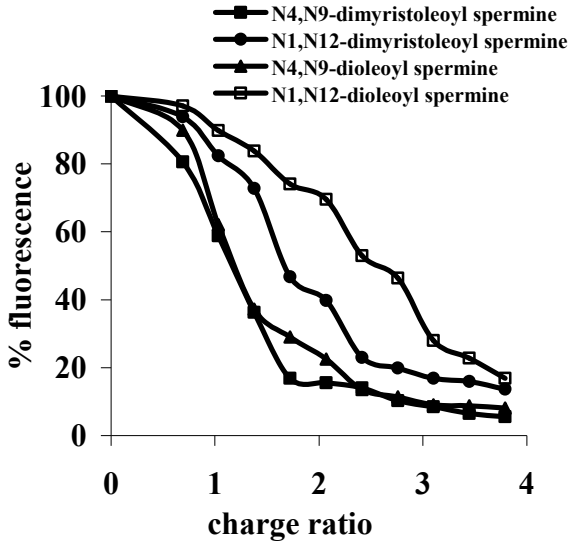

Fig. 4.1. Plot of RiboGreen intercalation assay of siRNA complexed with different lipospermines.

4.2.2. Lipoplex Particle Size and ζ-Potential

The particle size measurements were carried out on the lipoplexes at their optimum concentration for transfection after mixing with a vortex mixer and was determined using a NanoSight LM10 (NanoSight Ltd, Salisbury, UK). All measurements were carried out on lipoplexes with 25 pmol of siRNA (fluorescein-labelled Label IT® RNAi Delivery Control, Mirus) in HEPES buffer (0.2 ml) at pH 7.4 and 20 ^{o}C. Results were analysed with the Nanoparticle Tracking Analysis (NTA) software. Particle size characterization by laser diffraction showed that the nanoscale particle size of the two siRNA lipoplexes measured 150 nm (N^1,N^{12}-dioleoyl spermine) and 170 nm (N^1,N^{12}-dimyristoleoyl spermine), compared with N^4,N^9-dioleoyl spermine siRNA lipoplex particle size of 110 nm (Table 4.1).

Table 4.1. Particle size (mean ± S.D., n = 9) of siRNA lipoplexes.

Lipospermine	siRNA-Lipoplex diameter (nm)
N^4,N^9-Dioleoyl spermine	110 (12)
N^1,N^{12}-Dioleoyl spermine	150 (28)
N^1,N^{12}-Dimyristoleoyl spermine	170 (34)

Our siRNA lipoplexes are 110 and 170 nm in diameter, and they transfected target cell lines efficiently. Two representative ζ-potential measurements for the lipoplexes formed (at their optimum charge ratio of transfection with 75 pmol siRNA) were measured with a Delsa™Nano Zeta Potential instrument showing N^4,N^9-dioleoyl spermine +2.17 mV and N^1,N^{12}-dioleoyl spermine +3.69 mV. The formed nanoparticles are considered to be stable when they have pronounced ζ-potential values, either positive or negative, but the tendency to aggregate is higher when the ζ-potential is close to zero (171).

4.2.3. siRNA Delivery and In Vitro Cytotoxicity in the Presence of Serum

Two cell lines were used in the transfection experiments, a human primary skin fibroblast cells FEK4 derived from a foreskin explant, and a human cervix carcinoma HeLa derivative and transformed cell line (HtTA) (145,146). The HtTA cells being stably transfected with a tetracycline-controlled transactivator (tTA) consisting of the tet repressor fused with the activating domain of virion protein 16 of the herpes simplex virus (HSV). Cells were cultured in Earle's minimal essential medium (EMEM) supplemented with foetal calf serum (FCS) (15% in the case of FEK4 and 10% in the case of HtTA cells), penicillin and streptomycin (50 IU/ml each), glutamine (2 mM), and sodium bicarbonate (0.2%).

We used fluorescein-labelled Label IT® RNAi Delivery Control (Mirus). FEK4 and HtTA cells were seeded at 50,000 cells/well in 12-well plates in EMEM (2 ml) containing FCS (15% in the case of FEK4 and 10% in the case of HtTA cells) for 24 h to reach a plate confluency of 50-60% on the day of transfection. Then the media were replaced by 437.5 μl fresh media. The lipoplex was prepared by mixing siRNA (12.5 pmol in 12.5 μl) with the different amounts of the lipopolyamines in Opti-MEM (typically 2-20 μg in 50 μl) at 20 °C for 30 mins and then incubated with the cells (final volume of 0.5 ml) for 4 h at 37 °C in 5% CO_2 in full growth medium (in the presence of serum). Then the media were replaced by 2 ml of fresh media and cultured for 44 h in full growth media at 37 °C in 5% CO_2 before the assay.

Levels of fluorescein-labelled siRNA in the transfected cells were detected and corrected for background fluorescence of the control cells using a fluorescence activated cell sorting (FACS) machine (Becton Dickinson FACS Vantage dual Laser Instrument, argon ion laser 488 nm). The transfection efficiency was calculated based on the percentage of fluorescein-positive cells in the total number of cells with λ_{ex} = 495 nm and λ_{em} = 518 nm.

The transduction of fluorescein tagged siRNA into a primary skin cell line FEK4 and a cancer cell line (HeLa-derived HtTA) was investigated. We aimed for transfection efficiency about 80% (or higher), but also with a view to minimal toxicity (high cell viability), minimum effective concentrations. These optimum transfection concentrations were experimentally determined by using ascending amounts of lipopolyamines (Figs. 4.2 and 4.3).

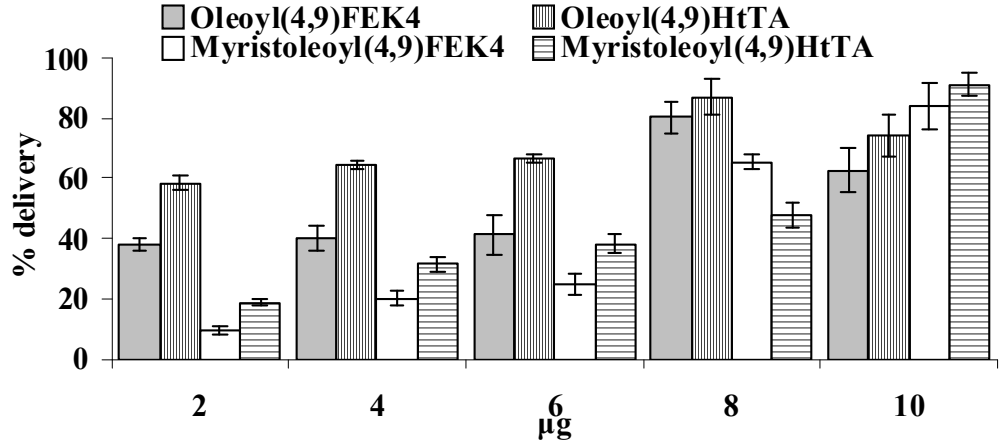

Fig. 4.2. Lipofection of the primary skin cell line FEK4 and the cancer cell line HtTA transfected with siRNA (12.5 pmol) complexed with N^4,N^9-dioleoyl spermine and N^4,N^9-dimyristoleoyl spermine at different ratios.

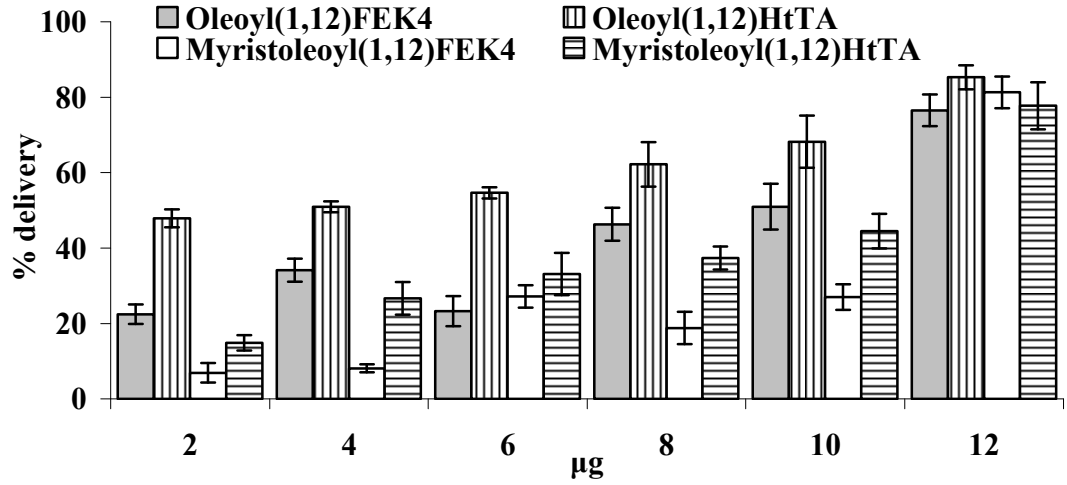

Fig. 4.3. Lipofection of the primary skin cell line FEK4 and the cancer cell line HtTA transfected with siRNA (12.5 pmol) complexed with N^1,N^{12}-dioleoyl spermine and N^1,N^{12}-dimyristoleoyl spermine at different ratios.

FACS analysis (Fig. 4.4) of both cell lines, after 48 h transfection with fluorescein-tagged siRNA complexed with N^1,N^{12}-dioleoyl spermine, show high efficiency of transfection. The transfection of FEK4 primary cells (hard to transfect) and a cancer cell line (HtTA) were compared with a market leader TransIT-TKO (Mirus). The results (Fig. 4.5) indicate that the transfection ability of N^4,N^9-dioleoyl spermine, N^1,N^{12}-dioleoyl spermine, N^4,N^9-dimyristoleoyl spermine and N^1,N^{12}-dimyristoleoyl spermine for both cell lines are comparable (e.g., N^1,N^{12}-dioleoyl

spermine 77% FEK4 and 85% HtTA) to the results of TransIT (91% FEK4 and 93% HtTA). The cell viability (MTT assay) results (Fig. 4.5) show that N^4,N^9- and N^1,N^{12}-dioleoyl spermine have high viability of FEK4 (75%) and HtTA (45%) cells, then N^1,N^{12}-dimyristoleoyl spermine, and N^4,N^9-dimyristoleoyl spermine is more toxic.

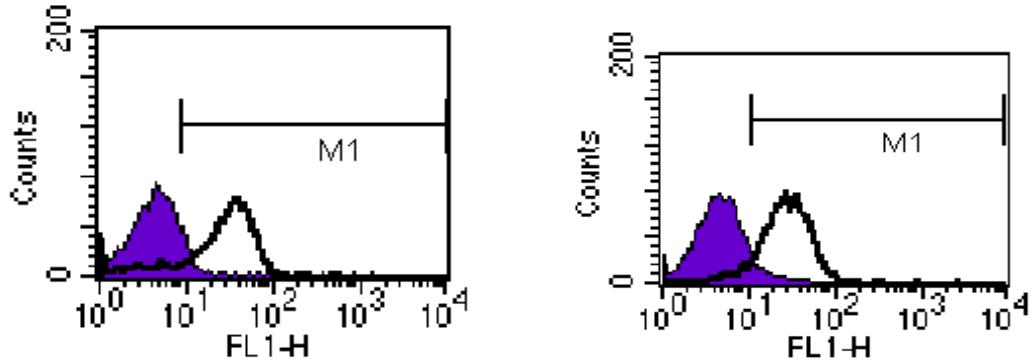

Fig. 4.4. Gated FACS analysis of FEK4 (left) and HtTA (right) after 48 h transfection of fluorescein-tagged siRNA complexed with N^1,N^{12}-dioleoyl spermine
■ untransduced cells, □ fluorescein-positive cells.

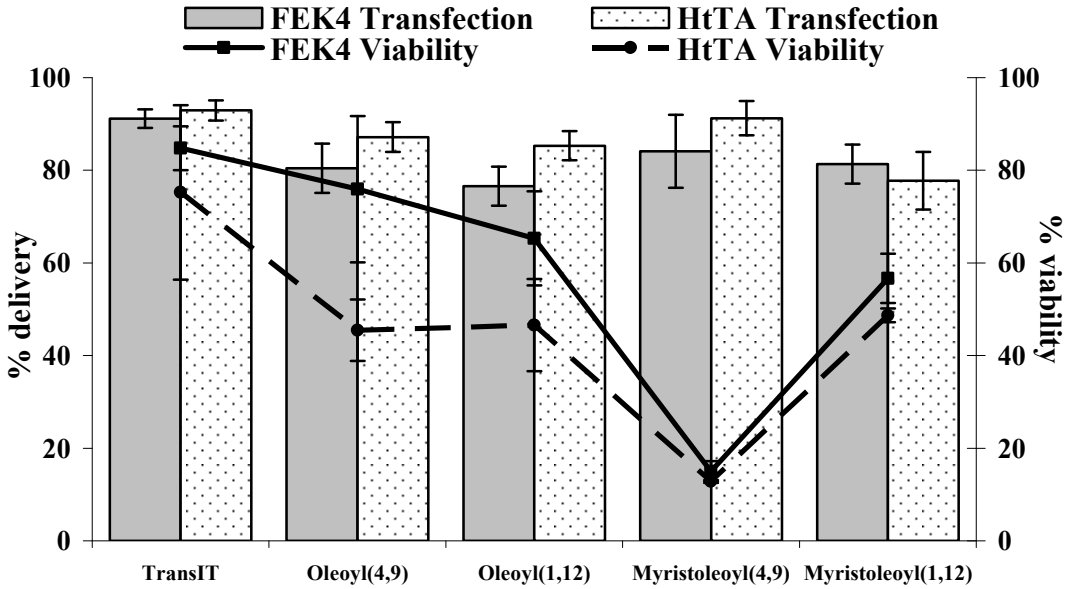

Fig. 4.5. Lipofection and cytotoxicity effects of siRNA (12.5 pmol) complexed with TransIT-TKO (4 µl), Oleoyl(4,9) (N^4,N^9-dioleoyl spermine) (8.0 µg), Oleoyl(1,12) (N^1,N^{12}-dioleoyl spermine) (12.0 µg), Myristoleoyl(4,9) (N^4,N^9-dimyristoleoyl spermine) (10.0 µg) and Myristoleoyl(1,12) (N^1,N^{12}-dimyristoleoyl spermine) (12.0 µg) on the primary skin cell line FEK4 and the HeLa derived cancer cell line HtTA.

In this study, we have investigated the change in the position and length of the symmetrical diacyl fatty chain formulations of lipospermine on siRNA binding and cellular delivery. Particle size of the final gene formulation is also an important factor in improving gene delivery (187,188). Particle size results (Table 4.1) for siRNA are 150 and 170 nm.

From the combination of both the siRNA delivery and viability results we found that the N^1,N^{12}-dioleoyl spermine (transfection efficiency FEK4 77%, HtTA 85% and cell viability FEK4 66%, HtTA 47%) and N^4,N^9-dioleoyl spermine (transfection efficiency FEK4 80%, HtTA 87% and cell viability FEK4 76%, HtTA 46%) are equally active and the best achievements based on these two factors then very close to them the N^1,N^{12} C14, N^1,N^{12}-dimyristoleoyl spermine (transfection efficiency FEK4 81%, HtTA 78% and cell viability FEK 57%, HtTA 49%) and N^4,N^9-dimyristoleoyl spermine came last because it is very toxic.

The lipid moiety in our cationic lipids interacts with the phospholipid bilayer of the cell membrane, and that facilitates cell entry, either in crossing the membrane bilayer and/or in helping to weaken the endosomal bilayer and thereby aid escape into the cytosol, so the position, length and degree of saturation play an important role in their design and formulation where the lipid moiety must be considered in shape (volume) and substituent pattern, as well as the polyamine moiety and its pK_a values (12,170,171,225). We conclude from the above results that the N^1,N^{12}-dioleoyl spermine and N^1,N^{12}-dimyristoleoyl spermine are effective for siRNA delivery. It is as good as the commercially available TransIT-TKO® for siRNA delivery.

From the above results there are no major gains made in siRNA delivery using the N^1,N^{12}-diacyl spermine vectors over their N^4,N^9-diacyl regioisomers. So, for the next part of the research it was decided to test the N^4,N^9-diacyl spermine with stepwise changes in the length of the fatty chain from C10 to C18. These changes will also be made with variation in the oxidation level, incorporating saturated or mono-unsaturated acyl chains where available. As well as the mono-unsaturated analogues, a novel vitamin A derived (di-)retinoyl lipospermine was designed as a new vector for siRNA delivery.

4.3. N^4,N^9-DIACYL SPERMINES: SAR STUDIES OF NON-VIRAL LIPOPOLYAMINE VECTOR siFECTION EFFICIENCY VERSUS TOXICITY

4.3.1. RNA Binding (RiboGreen Intercalation Assay)

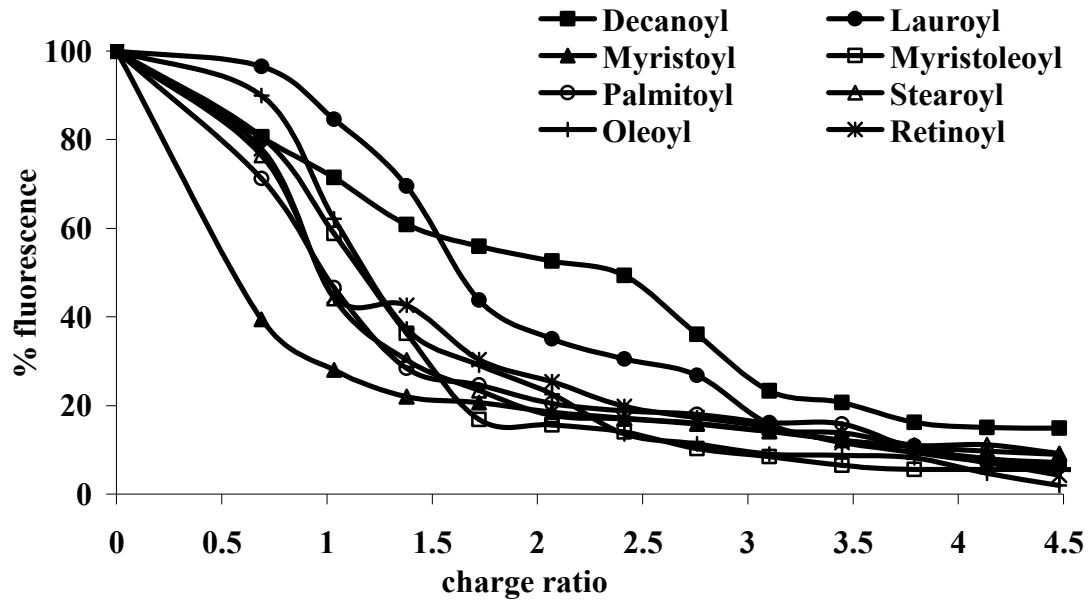

Fig. 4.6. Plot of RiboGreen intercalation assay of siRNA complexed with different lipospermines.

In Fig. 4.6, a measure of the siRNA binding ability of the synthesized N^4,N^9-diacyl lipopolyamines is shown in the RiboGreen intercalation assay which is similar to the PicoGreen assay reported by Wagner and co-workers (235) and to the EthBr fluorescence quenching assay optimized by Geall and Blagbrough (176). These results from siRNA lipoplexes show that all the synthesized lipospermines achieve more than 80% fluorescence quenching at N/P charge ratios below 3, except N^4,N^9-didecanoyl spermine which also achieved 85% fluorescence quenching at N/P = 4.

4.3.2. Lipoplex Particle Size Measurements

The particle size characterization measurements were carried out on the lipoplexes at their optimum concentration for transfection (139). Particle size characterization by laser diffraction showed that the nanoscale particle size of the formed siRNA complexes ranged from 90 nm (N^4,N^9-dimyristoyl spermine and N^4,N^9-dimyristoleoyl spermine) both with C-14 chains to 170 nm (N^4,N^9-didecanoyl spermine) with C10 chain length. These lipoplex nanoparticles were ranged around

140 nm in diameter (Table 4.2). which is typical for such formulations e.g., Schiffelers et al., made polyplexes of PEI-PEG with siRNA of 90-120 nm, (236) and Ishida and co-workers prepared cationic lipoplexes typically of 280-308 nm (237).

Table 4.2. Particle size (mean ± S.D., n = 9) of siRNA lipoplexes

Lipospermine	siRNA-Lipoplex diameter (nm)
***N*^{4},*N*^{9}-Didecanoyl spermine**	170 (29)
***N*^{4},*N*^{9}-Dilauroyl spermine**	150 (21)
***N*^{4},*N*^{9}-Dimyristoyl spermine**	90 (24)
***N*^{4},*N*^{9}-Dimyristoleoyl spermine**	90 (14)
***N*^{4},*N*^{9}-Dioleoyl spermine**	110 (12)

4.3.3. siRNA Delivery and In Vitro Cytotoxicity

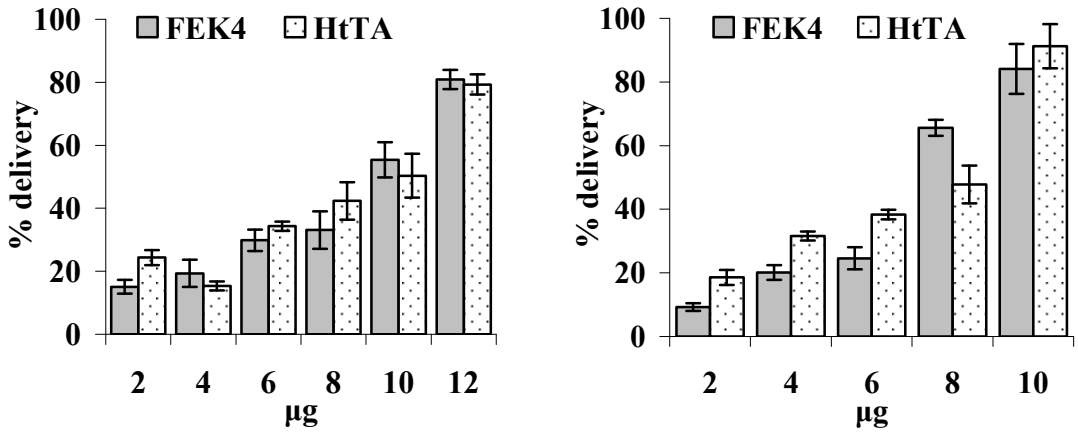

Fig. 4.7. Lipofection of the primary skin cell line FEK4 and the cancer cell line HtTA transfected with siRNA (12.5 pmol) complexed increasing concentrations of *N*^{4},*N*^{9}-didecanoyl spermine (left) and *N*^{4},*N*^{9}-dimyristoleoyl spermine (right).

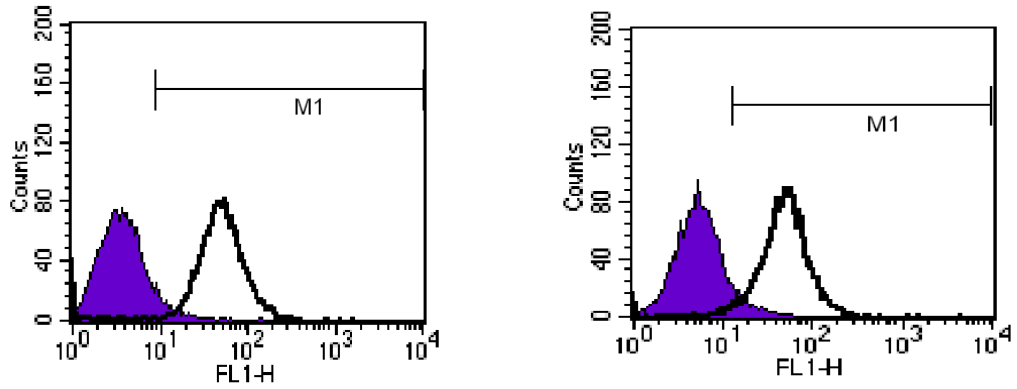

Fig. 4.8. Gated FACS analysis of FEK4 (left) and HtTA (right) after 48 h transfection of fluorescein-tagged siRNA complexed with N^4,N^9-diretinoyl spermine:

■ untransduced cells, □ fluorescein-positive cells.

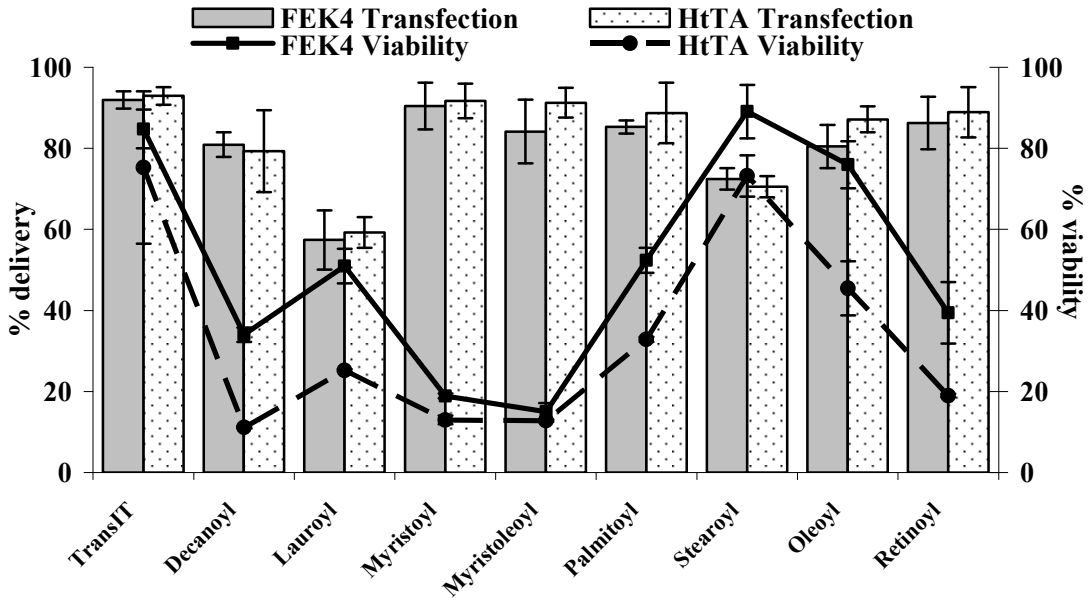

Fig. 4.9. Lipofection and cytotoxicity effects of siRNA (12.5 pmol) complexed with TransIT-TKO (4 µl), decanoyl (N^4,N^9-didecanoyl spermine) (12.0 µg), lauroyl (N^4,N^9-dilauroyl spermine) (4.0 µg), myristoyl (N^4,N^9-dimyristoyl spermine) (12.0 µg), myristoleoyl (N^4,N^9-dimyristoleoyl spermine) (10.0 µg), palmitoyl (N^4,N^9-dipalmitoyl spermine) (12.0 µg), stearoyl (N^4,N^9-distearoyl spermine) (8.0 µg), oleoyl (N^4,N^9-dioleoyl spermine) (8.0 µg), and retinoyl (N^4,N^9-diretinoyl spermine) (12.0 µg) on the primary skin cell line FEK4 and on the HeLa derived cancer cell line HtTA. The data represent 3 different experiments (3 replicates each) and the error bars show the S.D.

The transduction of fluorescein tagged siRNA into a primary skin cell line FEK4 and a cancer cell line (HeLa-derived) HtTA was investigated and compared with a market leader TransIT-TKO (Mirus). The practical concentrations (in a final volume of 0.5 ml) were experimentally determined by using ascending amounts of lipospermines until we reached around 80% transfection and there was not a further step-up in transfection efficiency at the next highest concentration. From our typical results, Fig. 4.7, we conclude that for these lipopolyamines e.g., N^4,N^9-didecanoyl spermine and N^4,N^9-dimyristoleoyl spermine, transfection efficiency increases with lipopolyamine ratio. The gated flow cytometric FACS analysis, Fig. 4.8, of FEK4 and HtTA cell lines after 48 h transfection of fluorescein-tagged siRNA complexed with another representative lipopolyamine, N^4,N^9-diretinoyl spermine, clearly shows a high percentage of live transduced fluorescein-positive cells. The siFection results (Fig. 4.9, histograms) indicate that the transfection ability of the tested lipospermines except N^4,N^9-dilauroyl spermine are comparable with the results obtained with a market leader TransIT, a commercially available reagent (91% FEK4 and 93% HtTA). The highest transfection of primary skin cell line FEK4 cells was found with N^4,N^9-dimyristoyl spermine (90%) and N^4,N^9-dimyristoleoyl spermine (84%), then N^4,N^9-dipalmitoyl spermine (85%) then N^4,N^9-dioleoyl spermine (80%) and the lowest was N^4,N^9-dilauroyl spermine (57%). The transfection results of siRNA delivery into cancer HtTA cells (Fig. 4.9) also follows this pattern from highest with N^4,N^9-dimyristoyl spermine (92%) to lowest with N^4,N^9-dilauroyl spermine (59%).

The cell viability (MTT assay) results (Fig. 4.9, lines) indicate that there is not a large difference in the viability of FEK4 (84%) and HtTA (75%) cells between the commercially available TransIT-TKO, N^4,N^9-distearoyl spermine and N^4,N^9-dioleoyl spermine while all the other shorter lipospermines are more toxic to both cell lines. The cytotoxicity of the siRNA lipoplexes is high, with C-14 (saturated or unsaturated) chains being the most toxic, but C-10, C12, and C16 conjugates are also toxic. The vitamin A derived N^4,N^9-diretinoyl spermine was investigated as it has two C-20 chains, and might therefore show a further improvement over di-C-18 (distearoyl and dioleoyl) which are themselves less toxic than dipalmitoyl (C-16). However, diretinoyl spermine was significantly more toxic to both cell lines than either of the two C-18 compounds, and its shape and structure with its terminal trimethylated cyclohexene ring mean that it is closer in lipid volume to C-12 and C-14 than to C-18.

We considered that by more closely following the positive charge distribution of the naturally occurring tetraamine spermine i.e., mimicking spermine in one of its biologically important roles, that of stabilising condensed DNA wrapped around histones, so with more positive charges we might increase siRNA binding affinity. Or, by increasing the number of basic sites from 2 (diacyl-diamine) to four (tetraamine), we might produce a more efficient proton sponge effect when the early-endosomal pH starts to drop from cytosolic 7.4 to 5.5 on intracellular acidification, as spermine has 3.8 positive charges at pH = 7.4 and can clearly support 4.0 positive charges in acidic milieu. We therefore reduced the two amide functional groups of our two most effective siRNA delivery agents that showed the highest cell viability, to form the analogous tetraamines containing two new (extra) tertiary amines.

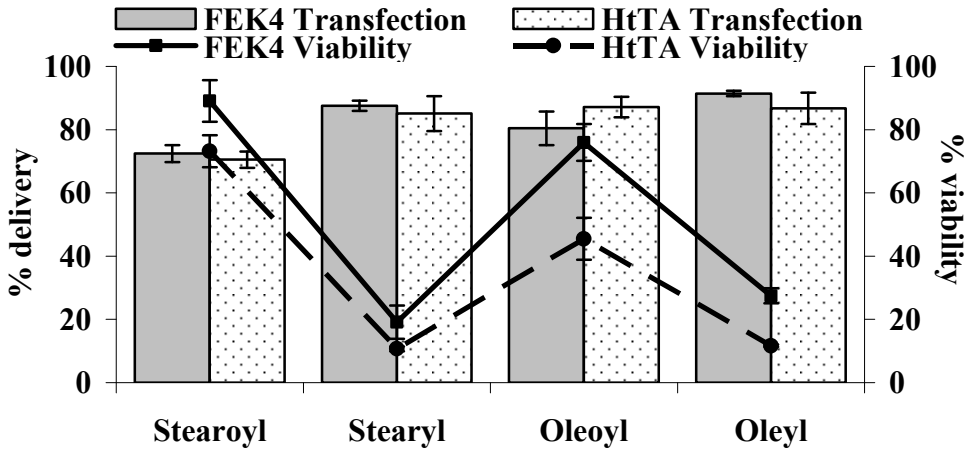

Fig. 4.10. Lipofection and cytotoxicity effects of siRNA (12.5 pmol) complexed with stearoyl (N^4,N^9-distearoyl spermine) (8.0 μg), stearyl (N^4,N^9-distearyl spermine) (6.0 μg), oleoyl (N^4,N^9-dioleoyl spermine) (8.0 μg), and oleyl (N^4,N^9-dioleyl spermine) (4.0 μg) on the primary skin cell line FEK4 and the HeLa derived cancer cell line HtTA.

Comparisons between the two C18 acyl lipospermines, the saturated N^4,N^9-distearoyl spermine and the unsaturated N^4,N^9-dioleoyl spermine and their alkyl analogues N^4,N^9-distearyl spermine and N^4,N^9-dioleyl spermine (Fig. 4.10) show that there is not a large difference in the transfection efficiency, neither gain nor loss, on doubling the number of positive charges in the conjugate. N^4,N^9-Distearoyl spermine shows transfection efficiencies of 72% and 71% (FEK4 and HtTA), N^4,N^9-distearyl spermine 88% and 85%, N^4,N^9-dioleoyl spermine 80% and 87%, and N^4,N^9-dioleyl spermine 91% and 87%, but the cell viabilities drop from around 75% to 10-27%. Therefore, the two alkyl analogues are much more toxic (Fig. 4.10) to both cell lines.

4.3.4. Confocal Microscopy Visualization

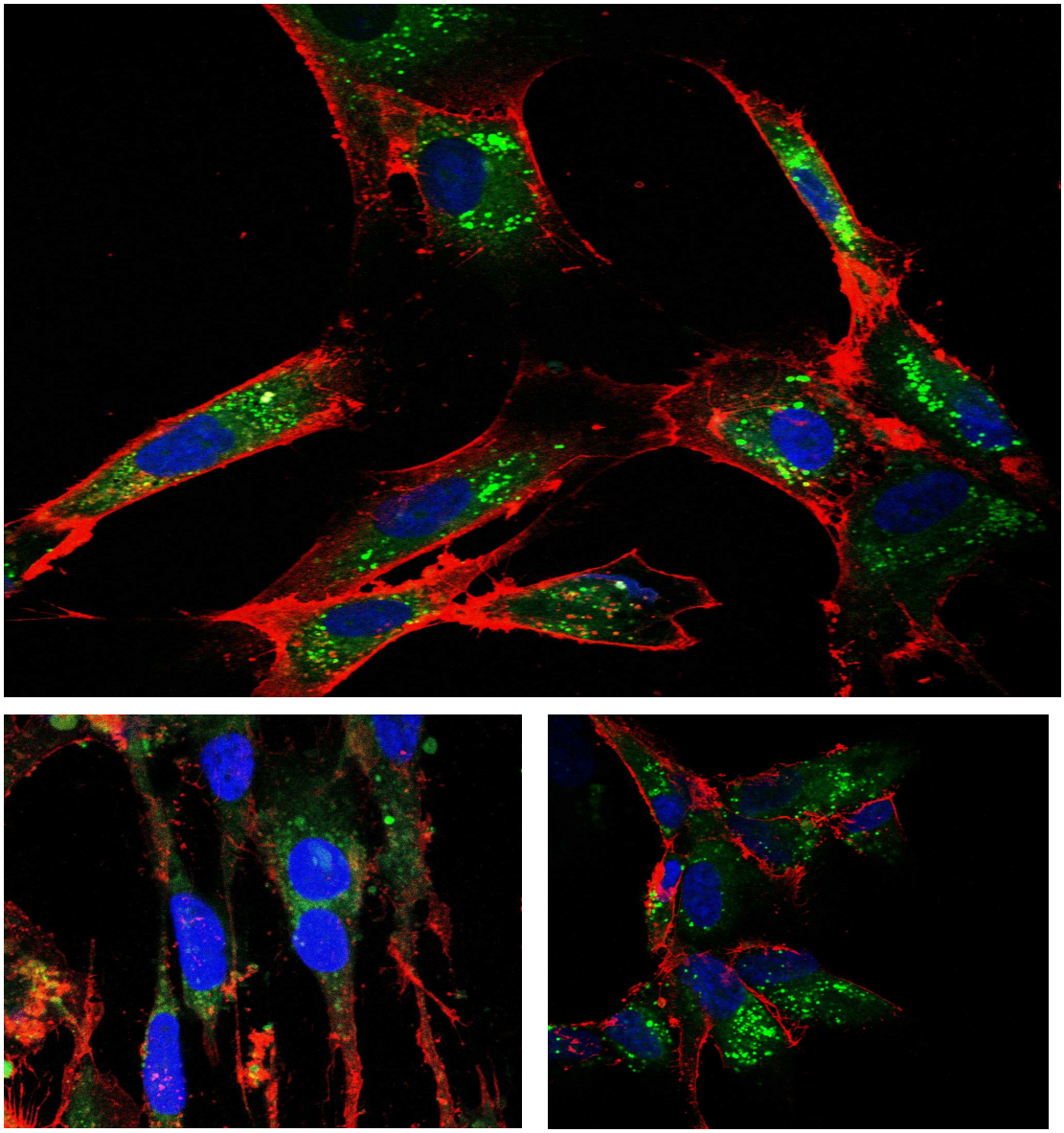

Fig. 4.11. The FEK4 primary cell line transfected with fluorescein-labelled siRNA showing cytosolic green fluorescence from fluorescein, delivered with Trans-IT (above) N^4,N^9-dioleoyl spermine (left) and N^4,N^9-distearoyl spermine (right). The cell lipid bilayers fluoresce red from the Alexa Fluor 594 and the nuclei fluoresce blue from the Hoechst 33342 (LSM510META, under the 60× oil immersion objective).

Following the siRNA transfection protocols, cells were seeded on a sterile cover-slip at the bottom of each well. After 48 h, media were aspirated and cells were fixed with freshly prepared 4% formaldehyde solution in PBS (1 ml/well) for 15 mins at 37 ^{o}C. After formaldehyde fixing, cells adhering to cover-slips were labelled with labelling solution according to the manufacturer's protocol. Labelling solution

contained both Alexa Fluor 594 wheat germ agglutinin for cell membrane labelling, λ_{ex} = 591 nm and λ_{em} = 618 nm, and Hoechst 33342 for nuclei labelling, λ_{ex} = 350 nm and λ_{em} = 461 nm, mixed in one solution purchased from Invitrogen (Image-iT live plasma membrane and nuclear labelling kit), cell labelling with Alexa Fluor WGA (5 μg/ml) and Hoechst 33342 (2 μl, 2 μM). After that, labelled cells were mounted using mounting liquid (20 μl, Mowiol, Merck) and left for 16 h. Then, mounted cover-slips were viewed on a confocal laser scanning microscope (LSM510META,) under the 60× oil immersion objective, with filters: red λ_{ex} = 543 nm and λ_{em} = 560-615 nm, blue λ_{ex} = 405 nm and λ_{em} = 420-480 nm, and green λ_{ex} = 488 nm and λ_{em} = 505-530 nm. Using confocal laser scanning microscopy, it was shown (Fig. 4.11) that N^4,N^9-dioleoyl spermine and N^4,N^9-distearoyl spermine successfully delivered fluorescent-siRNA to the cytosol of FEK4 cells.

These short chain synthetic lipospermines have the ability to deliver siRNA into FEK4 and HtTA cell lines. Whilst increasing the fatty acyl chain length over myristoyl (C-14) does not lead to any further increase in the transfection efficiency (over 92%), it does decrease cytotoxicity. The novel N^4,N^9-diretinoyl spermine lipopolyamine has a similarly long (C-20) carbon chain which does deliver siRNA, but it is too toxic to be considered efficient. Increasing the number of positive charges in the conjugate from 2 to 4 resulted in significantly more toxic compounds. As shorter chain lipopolyamines are too cytotoxic, the most efficient lipopolyamines for siRNA delivery were N^4,N^9-distearoyl spermine and N^4,N^9-dioleoyl spermine. These are practical non-liposomal siFection vectors, comparable with TransIT. From these results we conclude that C18 N^4,N^9-distearoyl spermine and N^4,N^9-dioleoyl spermine achieve the best of all the shorter symmetrical N^4,N^9-diacyl spermines (C10-C18) based on the combination of siRNA delivery and cell cytotoxicity. The vitamin A derived N^4,N^9-diretinoyl spermine with its two C-20 chains was significantly more toxic to both cell lines than the two C-18 compounds. This success with C18 gave us the reason for further characterization and investigation of even longer fatty chains of N^4,N^9-diacyl spermine (C20-C24). We will also change the degree of saturation to find the optimum chain length and degree of saturation of N^4,N^9-diacyl spermines that can achieve maximum in vitro siRNA delivery with minimum cytotoxicity.

4.4. VERY LONG CHAIN N^4,N^9-DIACYL SPERMINES: NON-VIRAL LIPOPOLYAMINE VECTORS FOR EFFICIENT siRNA DELIVERY

4.4.1. Lipoplex Particle Size and Zeta-Potential Measurements

The particle size and ζ-potential characterization measurements were carried out on the lipoplexes at their optimum N/P charge ratio for transfection (see: Table 4.3).

Table 4.3. Particle size (mean ± S.D., n = 9) and zeta-potential of siRNA lipoplexes.

Lipospermine	siRNA-Lipoplex diameter (nm)	siRNA-Lipoplex ζ-potential (+) mV
N^4,N^9-Dieicosenoyl spermine	170 (31)	7.5
N^4,N^9-Diarachidonoyl spermine		8.1
N^4,N^9-Dierucoyl spermine	180 (28)	5.5
N^4,N^9-Dinervonoyl spermine	110 (21)	

The ζ-potential measurements on the lipoplexes, at their optimum concentrations of transfection, show that all values are positive (Table 4.3), therefore there is a net positive charge on the surface. For siRNA lipoplexes, ζ-potentials ranged from +5.5 mV (N^4,N^9-dierucoyl spermine) to +8.1 mV (N^4,N^9-diarachidonoyl spermine); the measured ζ-potential for naked siRNA -0.3, and for the siRNA lipoplex with TransIT-TKO +2.6 mV.

4.4.2. siRNA Delivery and In Vitro Cytotoxicity

The transduction of fluorescein-tagged siRNA (RNAi Delivery Control, Mirus) into a primary skin cell line FEK4 and a cancer cell line (HeLa-derived HtTA) was investigated and compared with a market leader TransIT-TKO (Mirus) which works in the presence of serum.

The optimum concentrations for transfection (in a final volume of 0.5 ml) were experimentally determined by using ascending amounts of lipospermines, as described before, and high transfection efficiency is immediately seen from our FACS analyses in both cell lines (Fig. 4.12) with gating to measure mainly live cells. The siRNA

transfection efficiency results (carried out in triplicate on 3 separate experiments, n = 9, histograms in Fig. 4.13) indicate that the transfection ability of N^4,N^9-dieicosenoyl spermine, N^4,N^9-diarachidonoyl spermine, and N^4,N^9-dierucoyl spermine for both cell lines are comparable (e.g., N^4,N^9-dierucoyl spermine FEK4 88.6% ± 7.2, HtTA 84.9% ± 4.4) to the results of TransIT (91% FEK4 and 93% HtTA) even in the presence of serum. The longer C-24 N^4,N^9-dinervonoyl spermine (63% FEK4 and 68% HtTA) has lower transfection levels and even lower are those for the saturated fat derived N^4,N^9-diarachidoyl spermine (42% FEK4 and 34% HtTA).

The cell viability (MTT assay) results (lines in Fig. 4.13) indicate that there is no significant difference in the viability of FEK4 (85%, p = 0.15) and HtTA (75%, p = 0.42) cells between the commercially available TransIT-TKO and all the tested lipospermines except N^4,N^9-diarachidonoyl spermine which is more toxic to both cell lines and N^4,N^9-dinervonoyl spermine which is significantly less toxic ($p < 0.01$), while N^4,N^9-dieicosenoyl spermine and N^4,N^9-dierucoyl spermine are both equally active as TransIT-TKO and the same viability range.

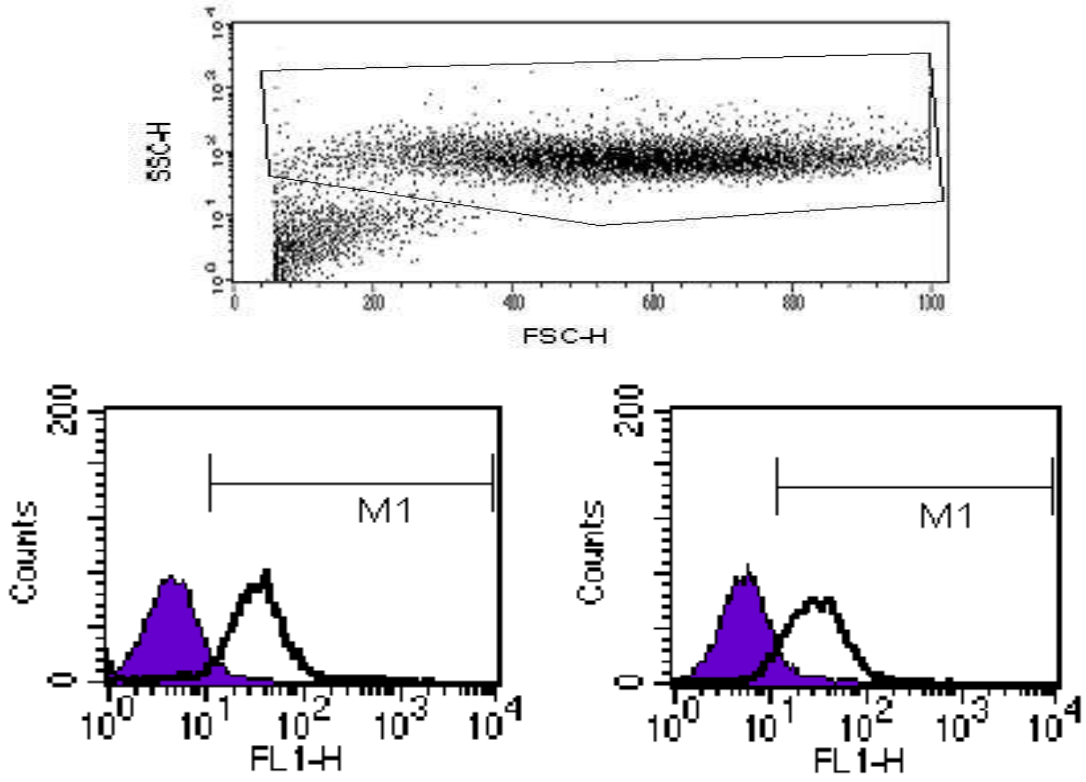

Fig. 4.12. FACS analysis showing the live population gated (above), and of FEK4 (left) and of HtTA (right) after 48 h transfection of fluorescein-tagged siRNA complexed with N^4,N^9-dierucoyl spermine: ■ untransduced cells, □ fluorescein-positive cells.

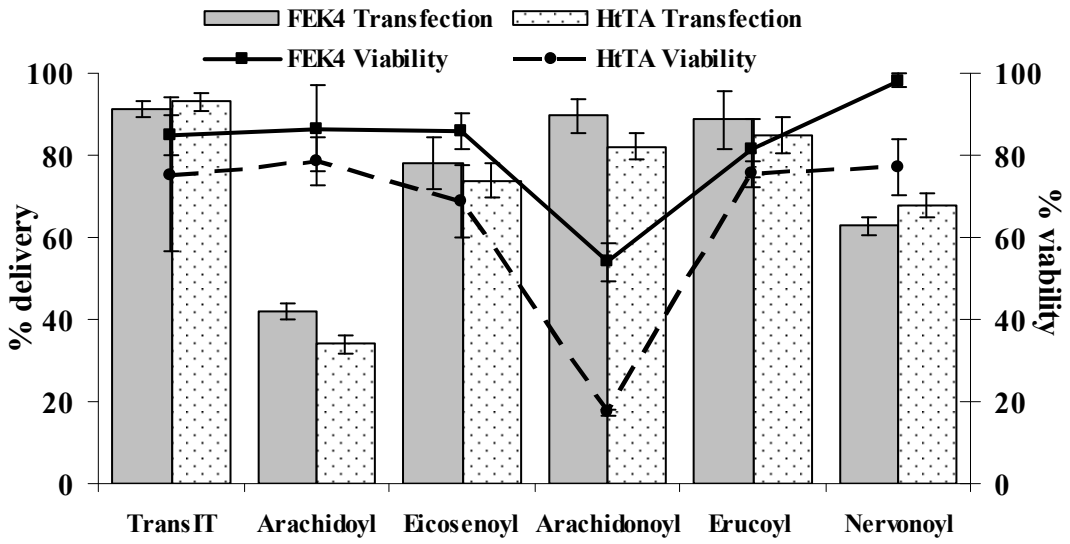

Fig. 4.13. Lipofection and cytotoxicity effects of siRNA (12.5 pmol) complexed with TransIT-TKO (4 µl), arachidoyl (N^4,N^9-diarachidoyl spermine) (6.0 µg), eicosenoyl (N^4,N^9-dieicosenoyl spermine) (4.0 µg), arachidonoyl (N^4,N^9-diarachidonoyl spermine) (6.0 µg), erucoyl (N^4,N^9-dierucoyl spermine) (6.0 µg) and nervonoyl (N^4,N^9-dinervonoyl spermine) (6.0 µg) on FEK4 and HeLa derived HtTA cell lines.

4.4.3. RNA Binding (RiboGreen Intercalation Assay)

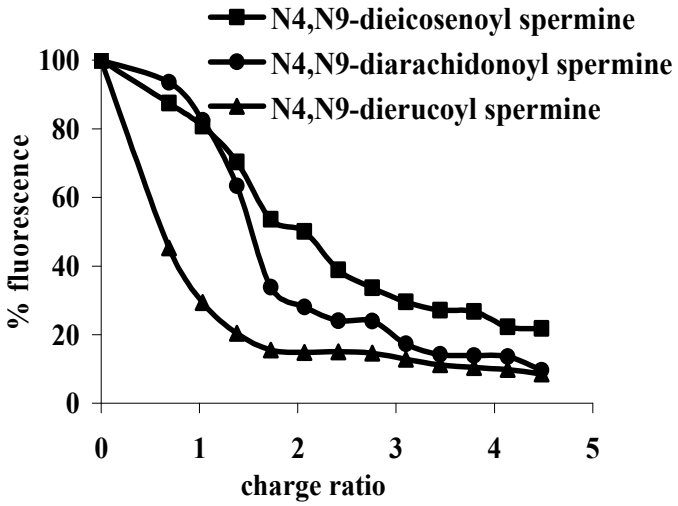

Fig. 4.14. Plot of RiboGreen intercalation assay of siRNA complexed with different lipospermines.

The RiboGreen intercalation assay (Fig. 4.14) was performed on the three most efficient siRNA delivery vectors. Thus, siRNA was complexed with N^4,N^9-dieicosenoyl spermine, N^4,N^9-diarachidonoyl spermine, and N^4,N^9-dierucoyl spermine.

The results show that efficient siRNA binding, as assessed by fluorescence quenching, is occurring by N/P charge ratio 2 for N^4,N^9-dierucoyl spermine, by charge ratio 3 for N^4,N^9-diarachidonoyl spermine, and at charge ratio 4.5 for N^4,N^9-dieicosenoyl spermine. These results give a clear idea about the ability of tested very long chain diacyl spermine to complete condense of siRNA.

We have investigated the biological effects of increasing the length of the symmetrical diacyl fatty chain formulation of lipospermine on siRNA condensation and cellular delivery. Results for siRNA around 155 nm (Table 4.3), e.g., N^4,N^9-dierucoyl spermine showed an siRNA lipoplex particle size of 180 nm (mean value ± S.D. 28, n = 9). All our lipoplexes are in the range 110-180 nm, and they transfected target cell lines efficiently.

In crossing the cell membrane bilayer (i.e., cell entry) and/or in helping to weaken the endosomal bilayer and thereby aiding escape into the cytosol, the lipid moiety in our cationic lipids interacts with the phospholipid bilayer (206). The first key step in this siRNA formulation is nanoparticle formation by masking the negative charges of the phosphate backbone. This titration with a lipopolyamine causes alleviation of charge repulsion between remote phosphates along the RNA helix leading to collapse into a more compact structure that facilitates cell entry.

Using confocal laser scanning microscopy with one labelling solution (Invitrogen) containing both Alexa Fluor 594 wheat germ agglutinin (5 μg/ml) for cell membrane labelling, and Hoechst 33342 (2 μM) for nuclei labelling. Successful delivery of fluorescent-siRNA to the cytosol was also shown (Fig. 4.15).

Incorporating two aliphatic chains and then stepwise increasing their length, our siRNA delivery results (Fig. 4.13) show that of our synthesized very long chain lipospermines, N^4,N^9-dieicosenoyl spermine and N^4,N^9-dierucoyl spermine are two new, efficient delivery vectors that work in primary cell lines even in the presence of serum. They demonstrate efficiencies comparable to the results obtained with TransIT, N^4,N^9-dieicosenoyl spermine typically 78% FEK4 and 74% HtTA, and N^4,N^9-dierucoyl spermine typically 89% FEK4 and 85% HtTA along with cell viability at least as high as TransIT (>80%). These novel very long chain lipopolyamines are remarkably non-toxic and capable of delivering siRNA primary cell lines in the presence of serum and with efficiency equalling a market leader, TransIT-TKO. They are two important new non-viral siRNA delivery vectors.

4.4.4. Confocal Microscopy Visualization

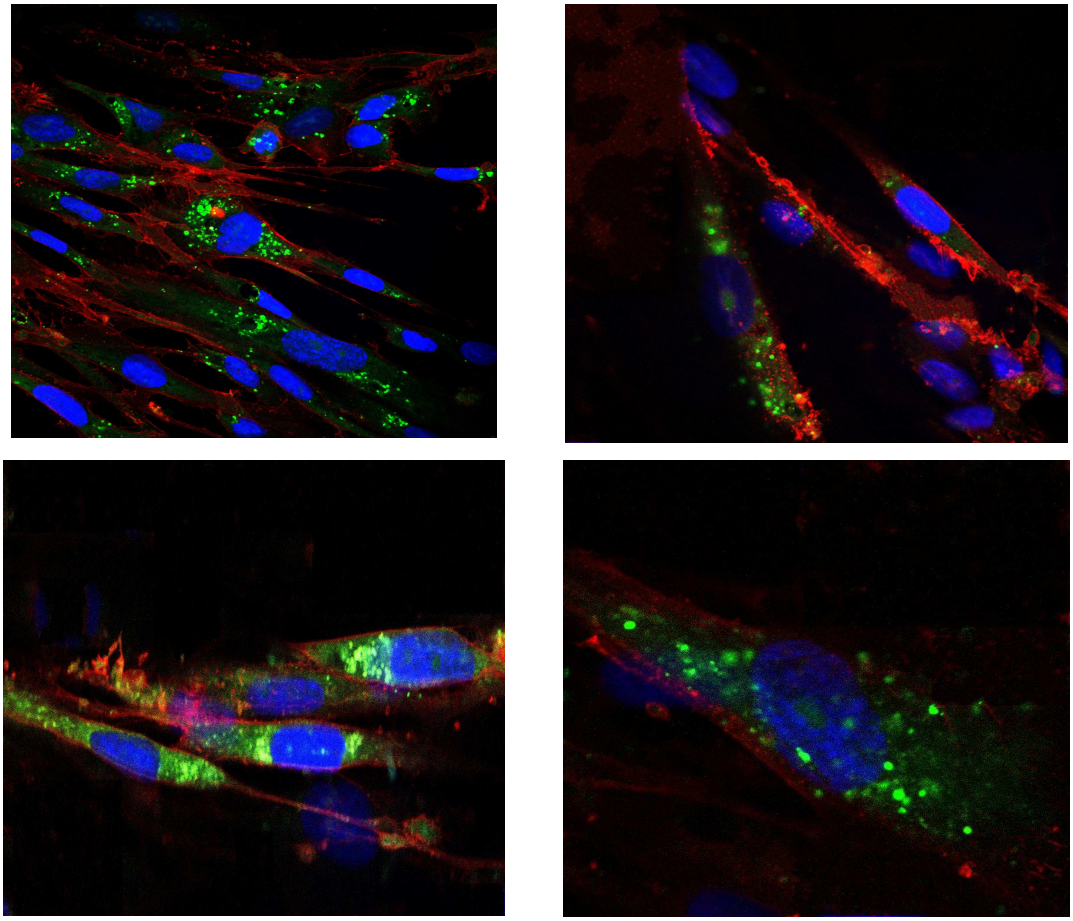

Fig. 4.15. The FEK4 primary cell line transfected with fluorescein-labelled siRNA showing cytosolic green fluorescence from fluorescein, delivered with N^4,N^9-dieicosenoyl spermine (above) and N^4,N^9-dierucoyl spermine (below). The nuclei fluoresce blue from the Hoechst 33342 and the cell lipid bilayers fluoresce red from the Alexa Fluor 594 (LSM510META, under the 60× oil immersion objective).

Cell membranes are complicated as they contain a variety of different classes of lipids. The cell membrane consists of three classes of amphipathic lipids: phospholipids, glycolipids, and steroids, most of the plasma membrane is lipid. The fatty chains in phospholipids and glycolipids usually contain an even number of carbon atoms, typically between 14 and 24, the 16- and 18-carbon fatty acids are the most common. Fatty acids may be saturated or unsaturated, so due to existence of different fatty chains in naturally occurring phospholipids, we adjusted the focus to target those molecules which have unsymmetrical aliphatic chains or steroids on the N^4,N^9-positions of the spermine backbone, mimicking naturally occurring phospholipids, so in the next section we test this N^4,N^9-unsymmetrical series.

4.5. UNSYMMETRICAL N^4,N^9-DIACYL SPERMINES: NON-VIRAL LIPOPOLYAMINE VECTORS FOR EFFICIENT siRNA DELIVERY

4.5.1. Lipoplex Particle Size and Zeta-Potential Measurements

The particle size and ζ-potential characterization measurements were carried out on the lipoplexes at their optimum concentration for transfection (see: Table 4.4). Particle size characterization by laser diffraction showed that the nanoscale particle size of the formed siRNA complexes ranged from 130 nm (N^4-decanoyl,-N^9-stearoyl spermine) to 170 nm (N^4-myristoleoyl,N^9-myristoyl spermine and N^4-oleoyl,N^9-stearoyl spermine) with an average particle size of 155 nm (Table 4.4).

The surface charge, as determined by ζ-potential measurements on the lipoplexes at their optimum N/P charge ratio of transfection, show e.g., that two typical values are positive +2.47 mV (N^4-oleoyl,N^9-stearoyl spermine) and +19.05 mV (N^4-decanoyl,N^9-oleoyl spermine); the measured ζ-potential for naked siRNA -0.3, and for the siRNA lipoplex with TransIT-TKO +2.6 mV.

Table 4.4. Particle size (mean ± S.D. n = 9) of siRNA lipoplexes.

Lipospermine	siRNA-Lipoplex diameter (nm)
N^4-Myristoleoyl,N^9-myristoyl spermine	170 (38)
N^4-Decanoyl,N^9-stearoyl spermine	130 (36)
N^4-Decanoyl,N^9-oleoyl spermine	150 (35)
N^4-Oleoyl,N^9-stearoyl spermine	170 (46)

4.5.2. RNA Binding (RiboGreen Intercalation Assay)

The RiboGreen intercalation assay (Fig. 4.16) was performed on most ot the unsymmetrical synthesized lipospermine delivery vectors. The results show that efficient siRNA binding, as assessed by 90% fluorescence quenching at N/P charge ratio 2-4 for all lipospermines except N^4-myristoleoyl,N^9-myristoyl spermine which show 80% fluorescence quenching at N/P charge ratio 4.5.

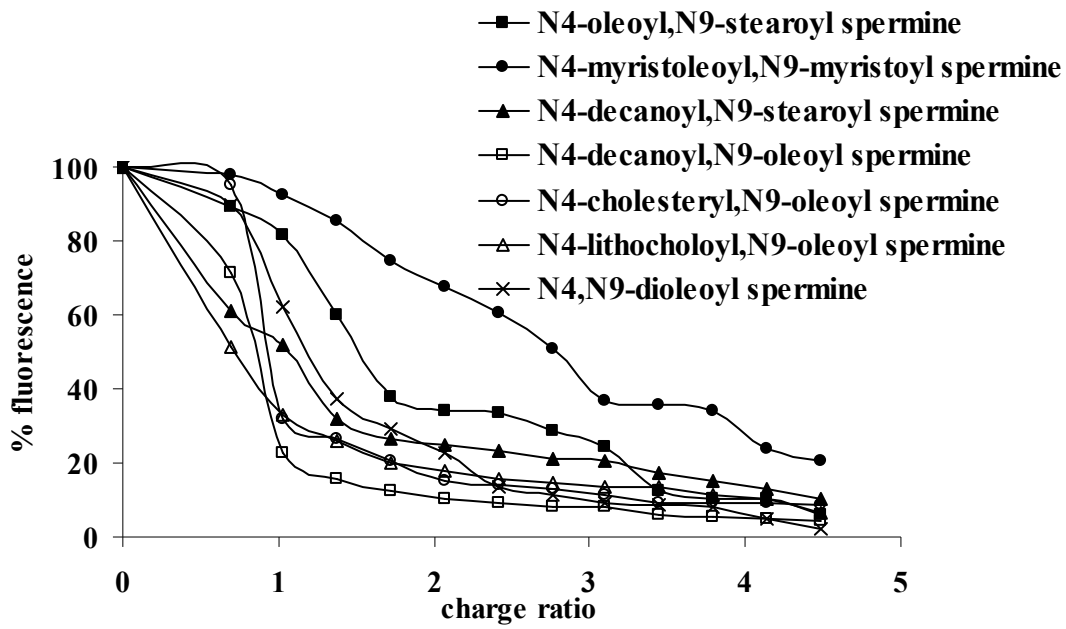

Fig. 4.16. Plot of RiboGreen intercalation assay of siRNA complexed with different unsymmetrical lipospermines.

4.5.3. siRNA Delivery and In Vitro Cytotoxicity

The transduction of fluorescein tagged siRNA into a primary skin cell line FEK4 and a cancer cell line (HeLa-derived) HtTA was investigated and compared with a market leader TransIT-TKO (Mirus). The practical concentrations (in a final volume of 0.5 ml) were experimentally determined by using ascending amounts of lipospermines until we reached around 80% transfection and there was not a further step-up in transfection efficiency at the next highest concentration.

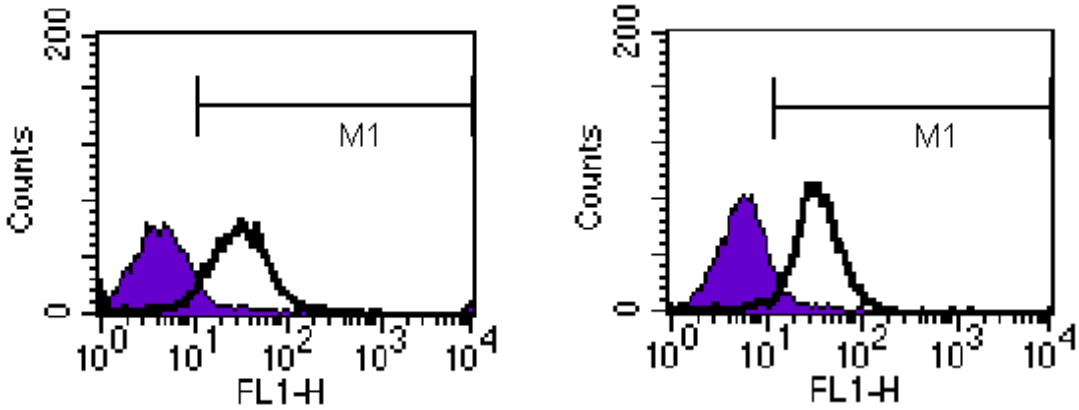

Fig. 4.17. Gated FACS analysis of FEK4 (left) and HtTA (right) after 48 h transfection of fluorescein-tagged siRNA complexed with N^4-decanoyl,N^9-stearoyl spermine ■ untransduced cells, □ fluorescein-positive cells.

The gated flow cytometric FACS analysis, Fig. 4.17, of FEK4 and HtTA cell lines after 48 h transfection of fluorescein-tagged siRNA complexed with another representative lipopolyamine, N^4-decanoyl,N^9-stearoyl spermine, clearly shows a high percentage of transduced fluorescein-positive cells. From our typical results, Figs. 4.18-4.20, we conclude that for these lipopolyamines e.g., N^4-oleoyl,N^9-stearoyl spermine, transfection efficiency increases with increasing lipopolyamine ratio.

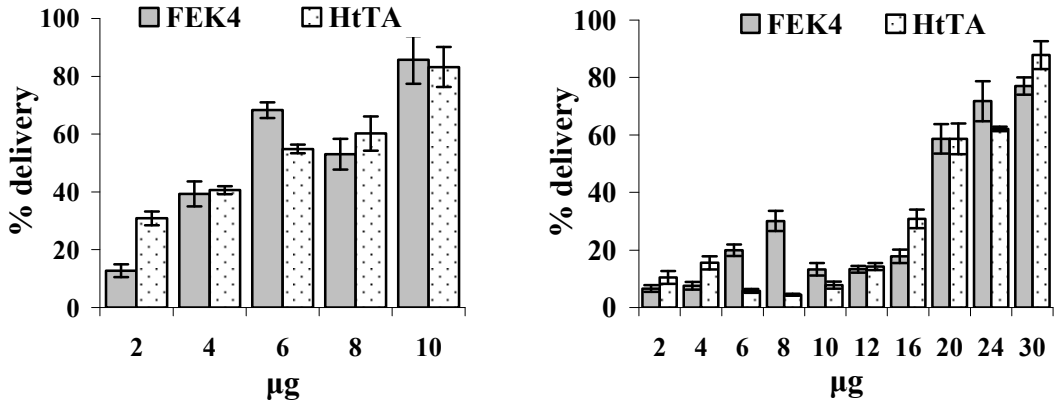

Fig. 4.18. Lipofection of the primary skin cell line FEK4 and the cancer cell line HtTA transfected with siRNA (12.5 pmol) complexed with N^4-decanoyl,N^9-oleoyl spermine (left) and N^4-decanoyl,N^9-stearoyl spermine (right) at different ratios.

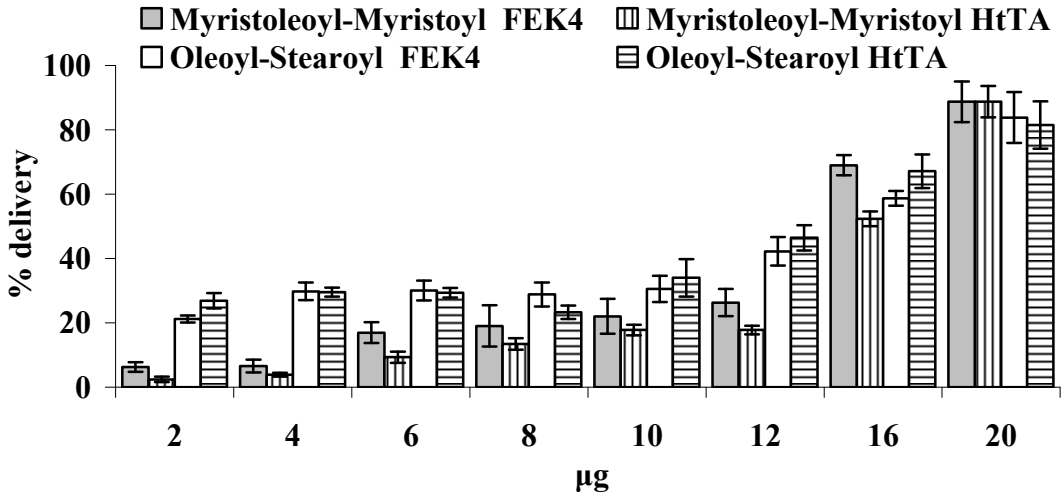

Fig. 4.19. Lipofection of the primary skin cell line FEK4 and the cancer cell line HtTA transfected with siRNA (12.5 pmol) complexed with N^4-myristoleoyl,N^9-myristoyl spermine and N^4-oleoyl,N^9-stearoyl spermine at different ratios.

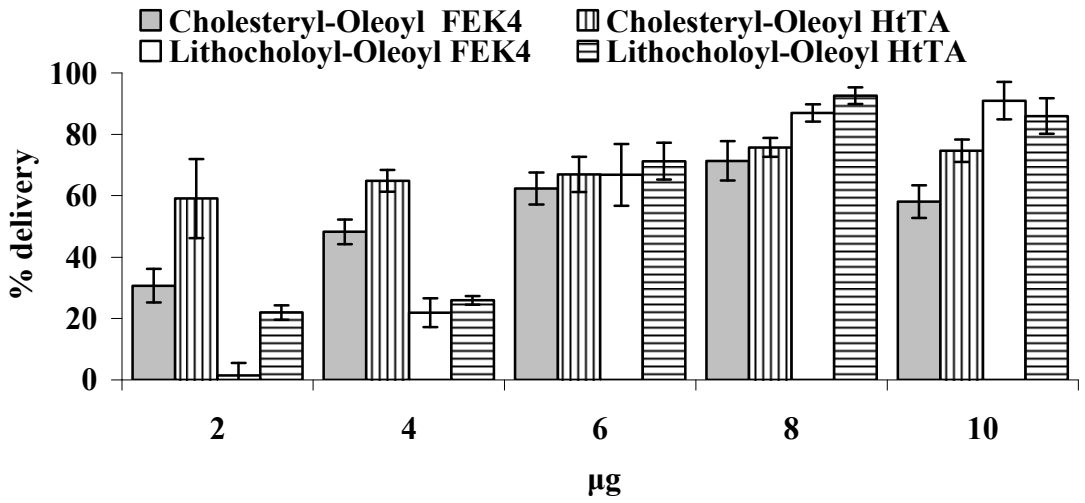

Fig. 4.20. Lipofection of the primary skin cell line FEK4 and the cancer cell line HtTA transfected with siRNA (12.5 pmol) complexed with N^4-cholesteryl,N^9-oleoyl spermine and N^4-lithocholoyl,N^9-oleoyl spermine at different ratios.

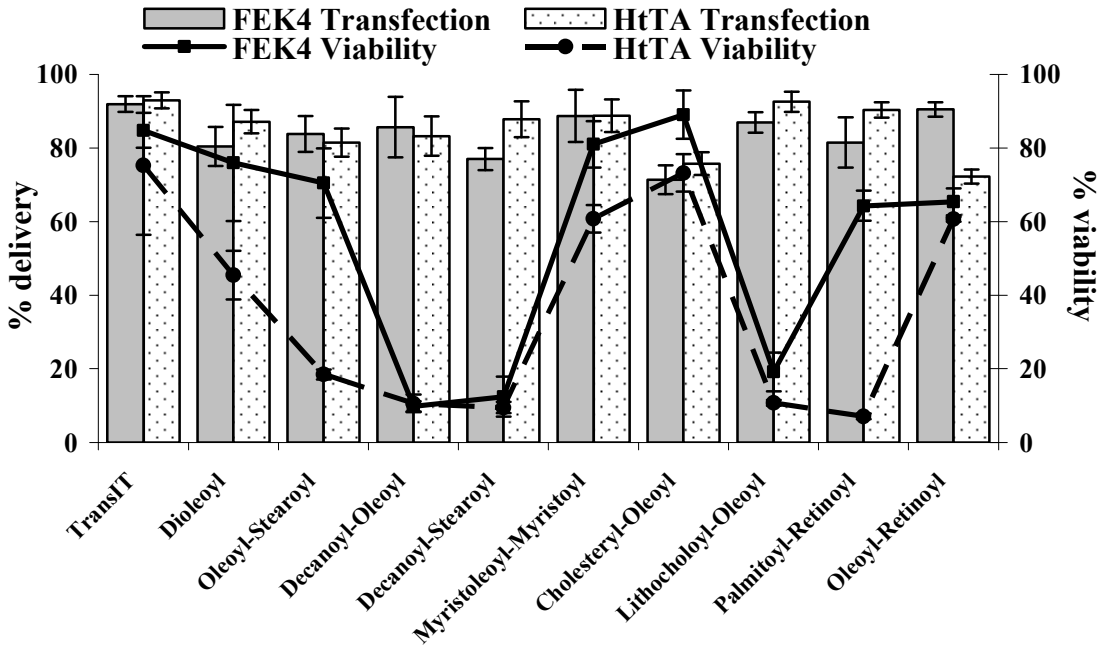

Fig. 4.21. Lipofection and cytotoxicity effects of siRNA (12.5 pmol) complexed with TransIT- TKO (4 µl), Dioleolyl (N^4,N^9-dioleoyl spermine) (8.0 µg), Oleoyl-Stearoyl (N^4-oleoyl,N^9-stearoyl spermine) (20.0 µg), Decanoyl-Oleoyl (N^4-decanoyl,N^9-oleoyl spermine) (10.0 µg), Decanoyl-Stearoyl (N^4-decanoyl,N^9-stearoyl spermine) (30.0 µg), Myristoleoyl-Myristoyl (N^4-Myristoleoyl,N^9-myristoyl spermine) (20.0 µg), Cholesteryl-Oleoyl (N^4-cholesteryl,N^9-oleoyl spermine) (8.0 µg), Lithocholoyl-Oleoyl (N^4-lithocholoyl,N^9-oleoyl spermine) (8.0 µg), Palmitoyl-Retinoyl (N^4-palmitoyl,N^9-retinoyl spermine) (4.0 µg) and Oleoyl-Retinoyl (N^4-oleoyl,N^9-retinoyl spermine) (6.0 µg) on the primary skin cell line FEK4 and the HeLa derived cancer cell line HtTA.

The siFection results (Fig. 4.21, histograms) indicate that the transfection ability of the tested unsymmetrical lipospermines are comparable with the results obtained with a market leader TransIT, a commercially available reagent (91% FEK4 and 93% HtTA). The highest transfection of primary skin cell line FEK4 cells was found with N^4-oleoyl,N^9-retinoyl spermine (91%), then N^4-myristoleoyl,N^9-myristoyl spermine (89%), N^4-lithocholoyl,N^9-oleoyl spermine (87%), N^4-decanoyl,N^9-oleoyl spermine (86%), N^4-oleoyl,N^9-stearoyl spermine (84%), N^4-palmitoyl,N^9-retinoyl spermine (82%), N^4-decanoyl,N^9-stearoyl spermine (77%) and the lowest was N^4-cholesteryl,N^9-oleoyl spermine (72%). The siRNA delivery results into cancer HtTA cells (Fig. 4.21) follows the pattern from the highest with N^4-lithocholoyl,-N^9-oleoyl spermine (93%) to the lowest N^4-oleoyl,N^9-retinoyl spermine (72%).

The cell viability (MTT assay) results (Fig. 4.21, lines) indicate that there is not a large difference in the viability between the commercially available TransIT-TKO, which shows viability for FEK4 cells of 84% and for HtTA cells of 75%, and N^4-myristoleoyl,N^9-myristoyl spermine and N^4-cholesteryl,N^9-oleoyl spermine then N^4-oleoyl,N^9-stearoyl spermine, N^4-oleoyl,N^9-retinoyl spermine and N^4-palmitoyl,N^9-retinoyl spermine, while N^4-decanoyl,N^9-stearoyl spermine, N^4-decanoyl,N^9-oleoyl spermine and N^4-lithocholoyl,N^9-oleoyl spermine lipospermines are more toxic to both cell lines.

We have investigated the biological effects of using novel lipospermines with two unsymmetric lipid moieties which differ in length, degree of saturation or nature of the fatty chain on the formulation, condensation and cellular delivery of siRNA. The results from RNA condensation (Fig. 4.16), investigated using the fluorescence quenching assay, revealed that most of our synthetic lipospermines were able to condense RNA to less than 10% fluorescence at N/P charge ratio 4.5; however, N^4-oleoyl,N^9-stearoyl spermine was able to quench the fluorescence by 80% at the same N/P charge ratio 6 (Fig. 4.16). The particle size of the final RNA formulation is also an important factor in improving delivery (187,188). Results for siRNA showed particle size around 155 nm (Table 4.4), e.g., N^4-oleoyl,N^9-stearoyl spermine and N^4-myristoleoyl,N^9-myristoyl spermine showed an siRNA lipoplex particle size of 170 nm (mean value ± S.D, n = 9). These lipoplexes are in the range 130-170 nm, and they transfected target cell lines efficiently.

Incorporating two unsymmetrical chains or other lipid moieties, our siRNA delivery results (Fig. 4.21) show that of our synthesized unsymmetric lipospermines N^4-oleoyl,N^9-stearoyl spermine typically 84% FEK4 and 81% HtTA, N^4-myristoleoyl,N^9-myristoyl spermine typically 89% FEK4 and 89% HtTA, N^4-cholesteryl,N^9-oleoyl spermine typically 71% FEK4 and 76% HtTA, N^4-palmitoyl,N^9-retinoyl spermine typically 82% FEK4 and 91% HtTA and N^4-oleoyl,N^9-retinoyl spermine typically 91% FEK4 and 72% HtTA are efficient delivery vectors that work in primary cell lines and in the presence of serum. They demonstrate efficiencies comparable to the results obtained with TransIT typically 91% FEK4 and 93% HtTA, along with cell viability at least as high as TransIT (>80%). These novel unsymmetric lipopolyamines are remarkably non-toxic and capable of delivering siRNA to hard-to-transfect primary cell lines in the presence of serum and with efficiency equalling a market leader, TransIT-TKO.

It is now generally agreed that the length and type of the aliphatic chains (the hydrophobic domain) incorporated into cationic lipids significantly affect their pDNA transfection efficiency, but this factor is not really understood yet for siRNA delivery. This series of vectors have differing hydrophobic domains. A shorter chain length may facilitate intermembrane mixing, an important factor in endosomal escape which will deliver the siRNA directly into the cytosol, experimental evidence for this is that the di-C14 vector N^4-myristoleoyl,N^9-myristoyl spermine was one of the best in this series.

As lipopolyamines possess substantial buffering capacity near physiological pH, they are efficient transfection agents without the addition of cell targeting or membrane-disruption agents. This observation led us to test nitrogen-containing heterocyclic-substituted lipospermines for their siRNA delivery potential because the increase in the pK_a of the protonatable amino nitrogen atom may make a significant difference, as above with the polyamines acting as an effective proton sponge (38). Our idea is that its efficiency relies on extensive lysosome buffering which protects siRNA from RNase nuclease degradation. The protonation reservoir of a molecule around neutral pH has not previously been studied in siRNA delivery. This relationship may be the basis for the design of new synthetic vectors.

4.6. HETEROCYCLIC N^4,N^9-DIACYL SPERMINES: NON-VIRAL LIPOPOLYAMINE VECTORS FOR EFFICIENT siRNA DELIVERY

There are three series of *N*-heterocycles (imidazole, pyridine and quinoline) investigated in this section, as: 4-imidazolylmethyl, 2-pyridinylmethyl, and 2-quinolinylmethyl derivatives. They are all N^4,N^9-diacyl spermines, acylated with myristoyl (C14), palmitoyl (C16), stearoyl (saturated C18) and oleoyl (mono-cis-unsaturated C18). They will each carry only two positive charges at physiological pH (7.4) as the aliphatic amines are much more basic than the heterocyclic amines, whose typical pK_as are: imidazole 7.0, pyridine 5.2, and quinoline 4.9 (198).

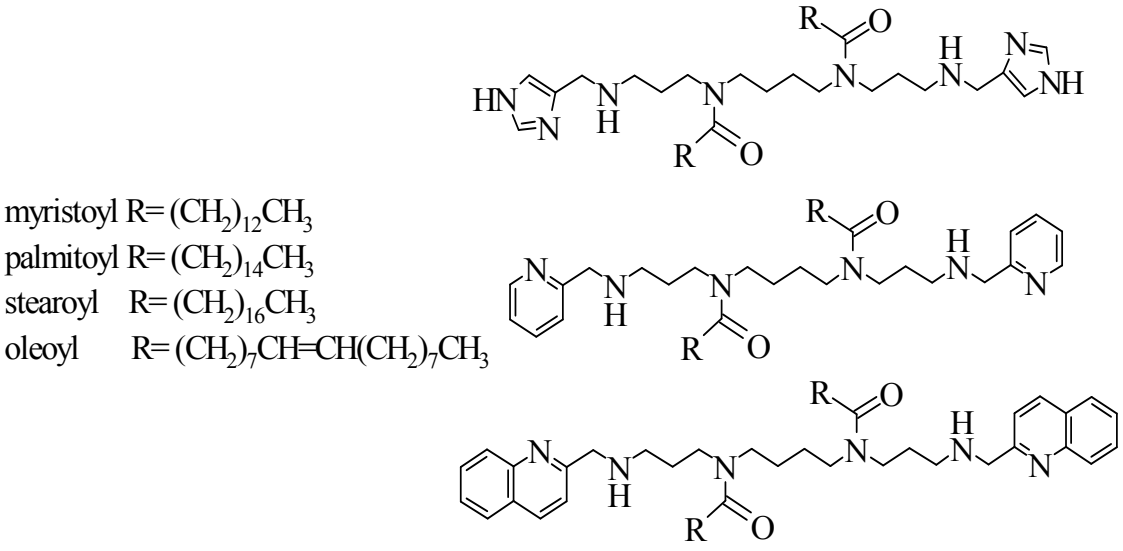

Fig. 4.22. Heterocyclic derivatives of lipospermines.

4.6.1. Zeta-Potential Measurements

The ζ-potential characterization measurements were carried out on the lipoplexes at their optimum concentration for transfection (see: Table 4.5). The surface charge, as determined by ζ-potential measurements on the lipoplexes at their optimum concentration of transfection, show three typical values are positive and ranged from +7.55 mV (Di-2-pyridinylmethyl N^4,N^9-dioleoyl spermine) to +11.76 mV (di-4-imidazolylmethyl N^4,N^9-dipalmitoyl spermine); the measured ζ-potential for naked siRNA -0.3, and for the siRNA lipoplex with TransIT-TKO +2.6 mV.

Table 4.5. Zeta potential of siRNA lipoplexes

Lipospermine	siRNA-Lipoplex ζ-Potential (+) mV
Di-2-quinolinylmethyl N^4,N^9-dipalmitoyl spermine	9.63
Di-2-pyridinylmethyl N^4,N^9-dioleoyl spermine	7.55
Di-4-imidazolylmethyl N^4,N^9-dipalmitoyl spermine	11.76

4.6.2. siRNA Delivery and In Vitro Cytotoxicity

The transduction of fluorescein-tagged siRNA (RNAi Delivery Control, Mirus) into a primary skin cell line FEK4 and a cancer cell line (HeLa-derived HtTA) was investigated, the optimum concentrations for transfection (in a final volume of 0.5 ml) were experimentally determined by using ascending amounts of lipospermines, and high transfection efficiency is immediately seen from our FACS analyses in both cell lines (Fig. 4.23) with gating to measure mainly live cells.

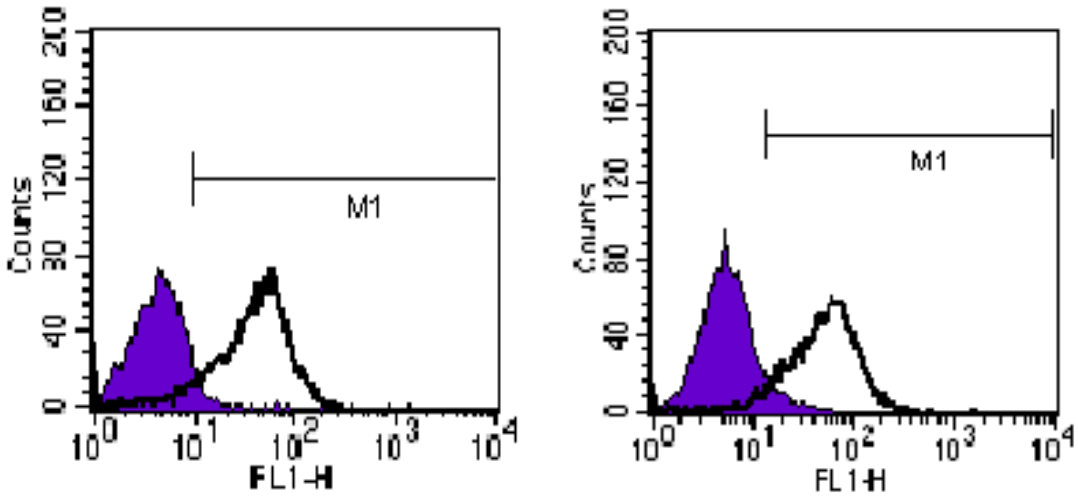

Fig. 4.23. Gated FACS analysis of FEK4 (left) and HtTA (right) after 48 h transfection of fluorescein-tagged siRNA complexed with Stear-Pyri: ■ untransduced cells, □ fluorescein-positive cells.

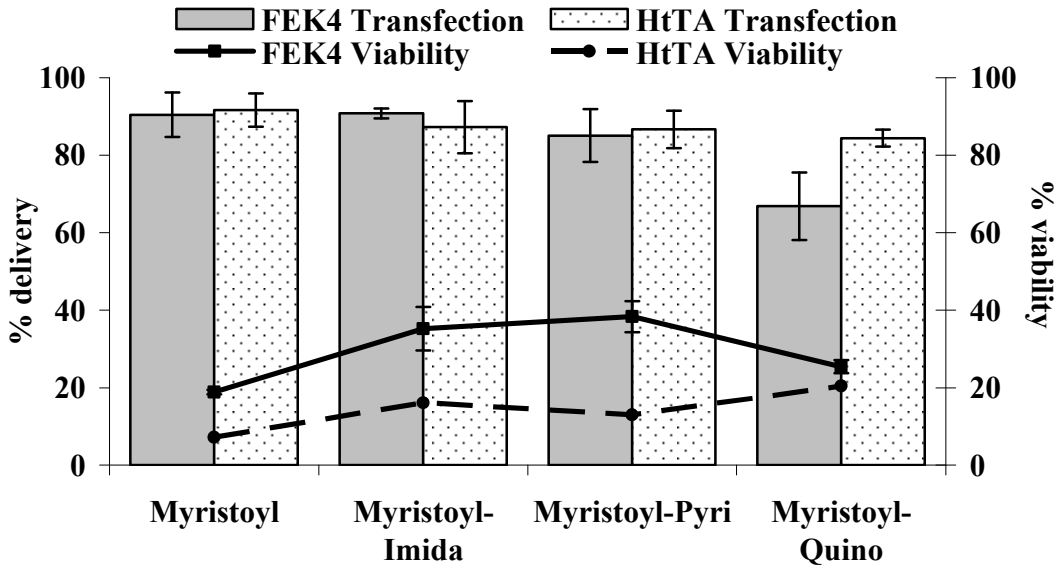

Fig. 4.24. Lipofection and cytotoxicity effects of siRNA (12.5 pmol) complexed with (left) Myristoyl (12.0 µg), Myristoyl-Imida (8.0 µg), Myristoyl-Pyri (6.0 µg) and Myristoyl-Quino (8.0 µg) on the primary skin cell line FEK4 and the HeLa derived cancer cell line HtTA.

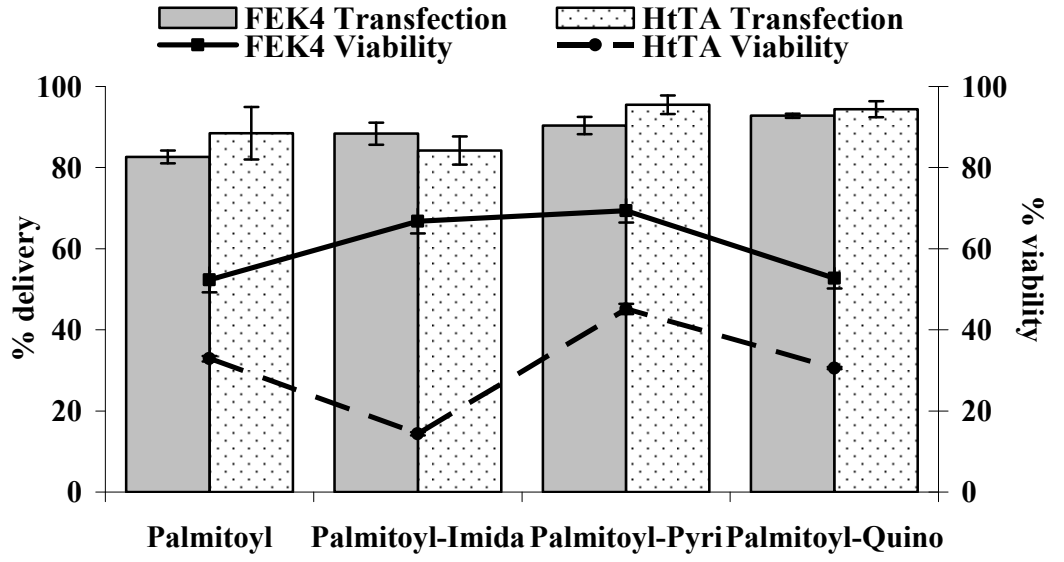

Fig. 4.25. Lipofection and cytotoxicity effects of siRNA (12.5 pmol) complexed with Palmitoyl (12.0 µg), Palmitoyl-Imida (6.0 µg), Palmitoyl-Pyri (6.0 µg) and Palmitoyl-Quino (4.0 µg) on the primary skin cell line FEK4 and the HeLa derived cancer cell line HtTA.

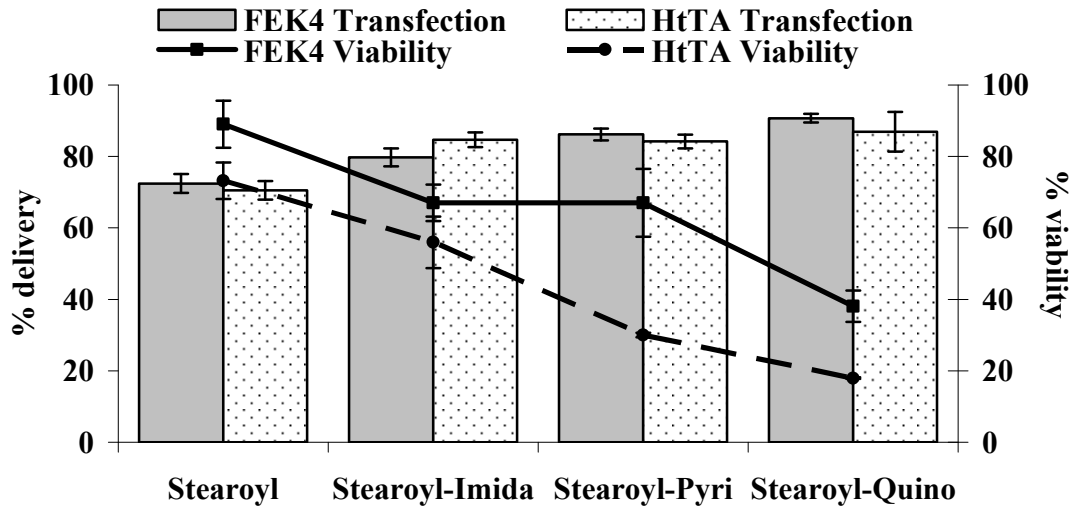

Fig. 4.26. Lipofection and cytotoxicity effects of siRNA (12.5 pmol) complexed with (left) Stearoyl (8.0 µg), Stearoyl-Imida (4.0 µg), Stearoyl-Pyri (4.0 µg) and Stearoyl-Quino (4.0 µg) on the primary skin cell line FEK4 and the HeLa derived cancer cell line HtTA.

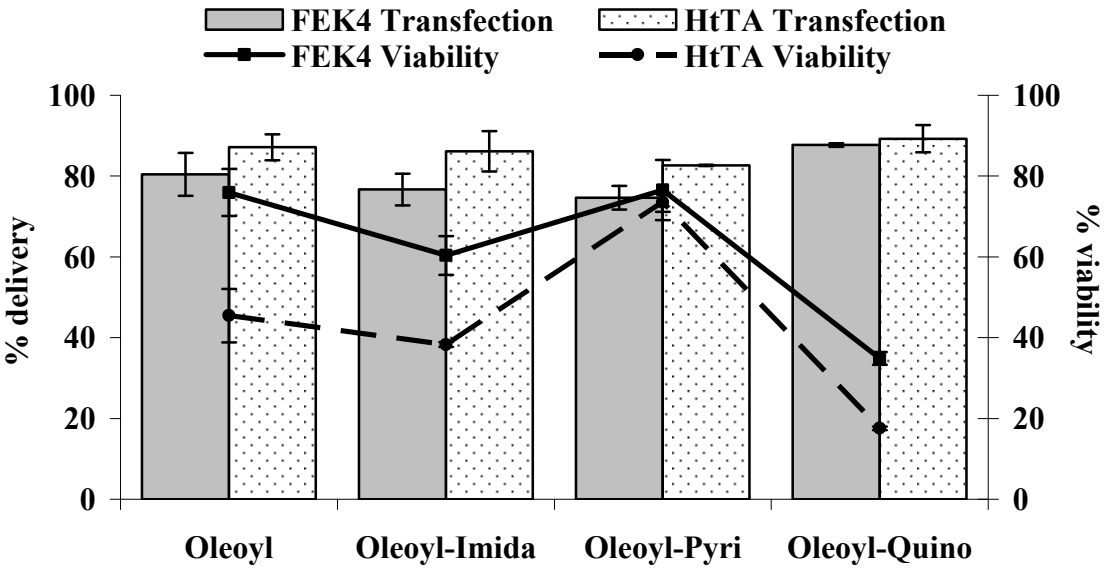

Fig. 4.27. Lipofection and cytotoxicity effects of siRNA (12.5 pmol) complexed with Oleoyl (8.0 µg), Oleoyl-Imida (6.0 µg), Oleoyl-Pyri (4.0 µg) and Oleoyl-Quino (4.0 µg) on the primary skin cell line FEK4 and the HeLa derived cancer cell line HtTA.

The siRNA transfection efficiency results (carried out in triplicate on 3 separate experiments, n = 9, histograms in Figs. 4.24-4.27) show the optimum concentrations (in 0.5 ml) for transfection were found to be di-4-imidazolylmethyl N^4,N^9-dimyristoyl spermine (8.0 μg), di-2-pyridinylmethyl N^4,N^9-dimyristoyl spermine (6.0 μg), di-2-quinolinylmethyl N^4,N^9-dimyristoyl spermine (8.0 μg), di-4-imidazolylmethyl N^4,N^9-dipalmitoyl spermine (6.0 μg), di-2-pyridinylmethyl N^4,N^9-dipalmitoyl spermine (6.0 μg), di-2-quinolinylmethyl N^4,N^9-dipalmitoyl spermine (4.0 μg), di-4-imidazolylmethyl N^4,N^9-distearoyl spermine (4.0 μg), di-2-pyridinylmethyl N^4,N^9-distearoyl spermine (4.0 μg), di-2-quinolinylmethyl N^4,N^9-distearoyl spermine (4.0 μg), di-4-imidazolylmethyl N^4,N^9-dioleoyl spermine (6.0 μg), di-2-pyridinylmethyl N^4,N^9-dioleoyl spermine (4.0 μg) and di-2-quinolinylmethyl N^4,N^9-dioleoyl spermine (4.0 μg).

The results (Figs. 4.24 and 4.25) indicate that for N^4,N^9-dimyristoyl spermine and N^4,N^9-dipalmitoyl spermine (all three heterocyclic) derivatives there is no improvement neither in the transfection ability nor in the cell viability over the results obtained with N^4,N^9-dimyristoyl spermine and N^4,N^9-dipalmitoyl spermine (at their optimum delivery ratio) on both cell lines, but there was a significant decrease in the amount of transfecting agent required to achieve these comparably efficient transfection levels. The results for N^4,N^9-distearoyl spermine and N^4,N^9-dioleoyl spermine heterocyclic derivatives (Figs. 4.26 and 4.27) show that all the tested lipospermines are equally good in transfection efficiency, but the N^4,N^9-distearoyl spermine derivative becomes more toxic from imidazole to quinoline through pyridine while in the N^4,N^9-dioleoyl spermine derivative series, the pyridine one is as low as N^4,N^9-dioleoyl spermine in cytotoxicity, then imidazole, and finally comes the quinoline derivative. So we can conclude from the above results of siRNA transfection efficiency and cytotoxicity that di-2-pyridinylmethyl N^4,N^9-dioleoyl spermine is the best of all these heterocyclic derivatives which show high siRNA transfection efficiency typically 75% and 83% transfection ability and 77% and 74% cell viability for FEK4 and HtTA cells respectively and it can be compared with N^4,N^9-dioleoyl spermine, but there was a significant decrease in the amount of transfecting agent required to achieve this comparably efficient transfection, a decrease for di-2-pyridinylmethyl N^4,N^9-dioleoyl spermine to only half of that required for N^4,N^9-dioleoyl spermine.

The heterocyclic substituted lipospermines show higher transfection efficiency over lipospermines as they show the same result at lower concentrations than the lipospermine analogues even as low as half of the concentration. Their high siRNA delivery potential is because of the increase on the pK_a of the vector due to increasing the number of nitrogen atoms in the lipospermines that can be protonated in the endosome as the pH drops to 5.5, i.e., their pK_as are around 5-7. Indeed, it makes the polymeric network an effective proton sponge at virtually any physiological pH (38). This extensive lysosome buffering effect protects both DNA and siRNA from nuclease degradation, and consequently lysosomal swelling and rupture provide an escape mechanism for the particles, based on the hypothesis that a causal relationship exists between the protonation reservoir of a molecule below neutral pH and its transfection efficiency. Endosome buffering may protect DNA and siRNA from lysosomal nucleases, but it may also perturb either the trafficking of endosomes or their osmolarity. For instance, massive vesicular ATPase-driven proton accumulation followed by passive chloride influx into endosomes buffered with lipospermine should cause osmotic swelling and subsequent endosome disruption. Furthermore, because the monomeric unit has such low molecular mass, the whole molecule will behave as an extensive proton sponge (38).

Even all the tested heterocyclic lipopolyspermines show high transfection efficiency at lower concentrations, and we found that di-2-pyridinylmethyl N^4,N^9-dioleoyl spermine is an efficient siRNA delivery agent that is non toxic with a required concentration only half that of N^4,N^9-dioleoyl spermine. This is a new vector for efficient siRNA delivery.

CHAPTER 5

Conclusions

CONCLUSIONS

The ultimate goal of designing synthetic poly-nucleic acid-delivery vehicles is to build multimolecular nucleic acid/vector assemblies that are non-toxic and yet efficient enough to be used in therapy. In this way, practical non-viral gene delivery can be achieved in a clinical setting. Whilst there was an assumption in the early siRNA-delivery literature that it will follow pDNA delivery, or at least that gene delivery will be an indicator or guide to siRNA delivery efficiency, it is clear from these studies that this is incorrect. Furthermore, as there is a large charge difference between pDNA and siRNA, different concentrations of lipopolyamine vectors (N/P ratio) are going to be required, so overall cell viability cannot be assumed in moving from pDNA to siRNA delivery.

From this thesis it can be concluded that our new vectors can potentially be used to formulate and efficiently deliver DNA and siRNA as the drug. In formulation terms, DNA is a medicinal substance that is difficult to formulate. This is because of the nature of both its size that is usually in Mega-Daltons, and the many thousands of negative charges (typically 10,000) on the phosphate backbone of the polynucleotide. The use of an efficient carrier (delivery vehicle) responsible for the complex process of successful DNA delivery to the nucleus is a determinant factor for the successful application of gene therapy. DNA is condensed naturally by basic proteins, histones with their many arginine and lysine amino acids each carrying a positive charge, and this is aided by positively charged polyamines spermine and spermidine. So, polycationic polyamines were utilized in the design of our gene carriers.

Delivery vehicles for DNA formulation are either viral or non-viral vectors relying on (poly) cationic compounds. Non-viral formulation has to overcome cellular barriers (cell membrane entry, endosomal escape, nuclear entry, decomplexation, then transcription and translation) to achieve a successful delivery of the prodrug DNA. To overcome these barriers, investigations were carried out to improve the delivery of DNA through several approaches including: the use of novel carriers, the delivery and internalisation to selected cell lines in the presence of serum, incorporating cationic moieties to improve endosomal escape e.g., utilising the proton sponge effect, or incorporating different fusogenic lipids. In these studies, the condensation of DNA and the formation of nanoparticles was monitored using EthBr fluorescence quenching and gel electrophoresis assays. In addition, EthBr was used to determine the binding affinity of the condensing agents for DNA. The binding of cationic

molecules with DNA is not entirely responsible for the release of EthBr, but alteration of the molecular flexibility of DNA through cationic compaction facilitated the release of bound EthBr. The number and/or the distribution of the positive charges on the molecule could have a significant effect on the affinity of the vector for DNA that leads to the efficient displacement of EthBr. Condensation of DNA into nanoparticles is a way to decrease the volume of the delivered gene in order to facilitate cellular membrane entry by endocytosis and subsequent trafficking to the nucleus. The characterization of particle size by laser light scattering revealed that the lipoplex particle sizes range from 90-250 nm.

Transfection efficiency and cell viability (toxicity) experiments were carried out using pEGFP as a reporter gene, either complexed with DNA condensing agents, or free (naked) DNA as a negative control. DNA yields and purity were determined spectroscopically (OD_{260}/OD_{280} = 1.80–1.90) and by agarose gel (1 %) analysis. FEK4 cells are human primary fibroblasts derived from newborn foreskin explants were used as model for human primary cells. HeLa derived and transformed cell line (HtTA) was used as a model for an immortal cancer cell line. The cytotoxicity (cell viability) of these compounds was studied in both primary skin and immortalised cancer cell lines using an MTT assay. The formed lipoplexes (nanoparticles) were characterized by both average particle size (n = 9) and ζ-potential measurements.

Zeta potential is an important parameter to predict the stability as well as the ability of the positively charged particles to interact with cell membranes. ζ-Potential results revealed that the surface charge was positive. In addition, gel electrophoresis results revealed that all spermine conjugates were able to condense pEGFP DNA and completely inhibit the migration of the circular plasmid DNA from lipoplexes in the agarose gel at their respective charge ratio of transfection.

The transfection efficiencies of the synthesized lipopolyamines were studied in primary skin cells (FEK4) and in an immortalized (HeLa derived HtTA) cancer cell line using pEGFP as the reporter macromolecule with its fluorescent imidazolidinone moiety analysed by FACS. The results revealed high transfection efficiencies with many novel lipospermines (Table 5.1). These highly efficient transfecting agents were selected based on a combination of pDNA transfection efficiency for both cell lines (typically about 60%) and from the cytotoxicity of these compounds in both cell lines, using the MTT assay, selecting lipospermines that showed average viability for both cell lines of more than 40% (Table 5.2).

Table 5.1. Transfection efficiency (mean ± S.D.) of pEGFP complexes with the studied lipo-polyamines on the primary skin cell line FEK4 and the HeLa derived cancer cell line HtTA.

Lipospermine	Charge ratio	% FEK4 Transfection	% HtTA Transfection	Average ± (6) %
N^4,N^9-Dioleoyl spermine	2.5	85.3±(1.4)	78.0±(1.7)	82
N^4,N^9-Diarachidonoyl spermine	8	82.1±(6.4)	81.8±(4.8)	82
N^4-Palmitoyl,N^9-retinoyl spermine	4	80.0±(4.0)	80.7±(3.6)	80
Di-4-imidazolylmethyl N^4,N^9-dioleoyl spermine	6	76.3±(10.1)	82.6±(5.1)	80
N^4,N^9-Dinervonoyl spermine	4	79.9±(1.6)	61.6±(1.4)	71
N^4-Oleoyl,N^9-stearoyl spermine	8	72.7±(4.7)	67.0±(1.6)	70
N^4,N^9-Dierucoyl spermine	4	69.5±(12.2)	65.5±(5.7)	68
N^1,N^{12}-Dioleoyl spermine	3	68.6±(2.3)	64.6±(2.4)	67
N^4,N^9-Dieicosenoyl spermine	10	67.1±(7.0)	62.4±(2.4)	65
N^4-Cholesteryl,N^9-oleoyl spermine	12	58.6±(9.7)	56.9±(8.7)	58
N^4-Myristoleoyl,N^9-myristoyl spermine	20	52.2±(2.2)	62.7±(7.7)	58
N^4-Decanoyl,N^9-oleoyl spermine	8	62.5±(5.3)	44.8±(8.6)	54

Table 5.2. Viability (mean ± S.D.) of the primary skin cell line FEK4 and the HeLa derived cancer cell line HtTA transfected by pEGFP complexes with the studied lipopolyamines.

Lipospermine	Charge ratio	% FEK4 Viability	% HtTA Viability	Average ± (6) %
Di-4-imidazolylmethyl N^4,N^9-dioleoyl spermine	6	92.8(3.9)	59.4±(2.1)	76
N^4,N^9-Dioleoyl spermine	2.5	82.9±(11.3)	65.4±(7.5)	74
N^4-Myristoleoyl,N^9-myristoyl spermine	20	70.9±(6.7)	72.6±(6.8)	72
N^4-Decanoyl,N^9-oleoyl spermine	8	58.6±(5.1)	74.7±(9.5)	67
N^4-Oleoyl,N^9,stearoyl spermine	8	61.0±(3.3)	70.4±(5.6)	66
N^1,N^{12}-Dioleoyl spermine	3	68.8±(8.3)	59.2±(7.1)	64
N^4,N^9-Dinervonoyl spermine	4	76.5±(8.3)	48.7±(6.6)	63
N^4,N^9-Dieicosenoyl spermine	10	58.5±(4.7)	49.4±(5.1)	54
N^4-Cholesteryl,N^9-oleoyl spermine	12	89.1±(3.7)	19.2±(3.2)	54
N^4-Palmitoyl,N^9-retinoyl spermine	4	63.9±(2.9)	37.0±(2.1)	50
N^4,N^9-Dierucoyl spermine	4	62.6±(10.8)	24.9±(3.4)	44
N^4,N^9-Diarachidonoyl spermine	8	74.4±(7.9)	10.1±(1.6)	42

The transfection of pEGFP (analysed by gated FACS) showed a higher transfection efficiency of N^4,N^9-dioleoyl spermine (at N/P charge ratio of 2.5) than that obtained using commercially available liposomal Lipofectin® formulation in FEK4 primary skin fibroblast and HtTA cell lines. On the other hand, there is no significant difference in the transfection activity between non-liposomal N^4,N^9-

dioleoyl spermine and the commercially available standard liposomal formulation Lipofectamine™ and non-liposomal cationic lipid Transfectam®.

Cell viability results for N^4,N^9-dioleoyl spermine showed a significant improvement in cell viability over the other commercial formulations. N^4,N^9-Dioleoyl spermine shows promising transfection results in tissue cultured cancer and skin fibroblast primary cell lines. Therefore, we investigated the effects on DNA formulation with variation in the position, length, degree of unsaturation and the symmetry of the two fatty chains of the synthetic lipospermines or even attaching nitrogen-containing heterocycles: imidazole, pyridine and quinoline to four selected N^4,N^9-diacyl spermines (i.e., myristoyl, palmitoyl, stearoyl, and oleoyl).

From the combination of the results obtained with our novel lipopolyamines, transfection efficiencies typically about 60% (Table 5.1), and cell viabilities more than 40% (Table 5.2), we have experimental evidence for eleven new effective transfecting agents which are able to deliver the gene payload to cultured cells with good viability. Some of them e.g., N^4,N^9-diarachidonoyl spermine, N^4-palmitoyl,N^9-retinoyl spermine and di-4-imidazolylmethyl N^4,N^9-dioleoyl spermine are as good as N^4,N^9-dioleoyl spermine in the transfection efficiency, but not much better than it. While di-4-imidazolylmethyl N^4,N^9-dioleoyl spermine and N^4-myristoleoyl,N^9-myristoyl spermine are equally as active as N^4,N^9-dioleoyl spermine in their cell viability (cytotoxicity) effects on those cultured cells.

So after these detailed studies on saturated and mono-unsaturated aliphatic chains, poly-unsaturated chains (from arachidonoic and retinoic acids), steroids and mixtures of these lipids conjugated to spermine, making a series of symmetrical and unsymmetrical, saturated or unsaturated novel N^4,N^9- and N^1,N^{12}-lipopolyamines for pEGFP DNA formulation and delivery to the primary skin cell line FEK4 and the HeLa derived cancer cell line HtTA, and even including the heterocyclic derivative di-4-imidazolylmethyl N^4,N^9-dioleoyl spermine which shows the same level of transfection efficiency and viability, we can conclude that N^4,N^9-dioleoyl spermine is the best transfecting agent from all tested novel lipospermines. N^4,N^9-Dioleoyl spermine displays the lowest N/P ratio, highest transfection efficiency and the lowest cytotoxicity on both tested cell lines compared to all the tested lipospermines in this study.

Further studies and characterizations were then carried out to examine if we can apply these results in an SAR study of siRNA delivery.

Table 5.3. Delivery efficiency (mean ± S.D.) of 12.5 pmol siRNA complexes with the studied lipopolyamines on the primary skin cell line FEK4 and the HeLa derived cancer cell line HtTA.

Lipospermine	μg	% FEK4 Delivery	% HtTA Delivery	Average ± (4) %
Di-2-pyridinylmethyl N^4,N^9-dipalmitoyl spermine	6	90.4±(2.1)	95.5±(2.3)	93
N^4-Myristoleoyl,N^9-myristoyl spermine	20	88.7±(7.1)	88.7±(4.5)	89
N^4,N^9-Dierucoyl spermine	6	88.6±(7.2)	84.9±(4.4)	87
N^4,N^9-Dioleoyl spermine	4	80.4±(5.3)	87.2±(3.2)	84
N^4-Oleoyl,N^9-stearoyl spermine	20	83.8±(4.9)	81.4±(3.8)	83
Di-4-imidazolylmethyl N^4,N^9-distearoyl spermine	4	79.7±(2.5)	84.7±(2.0)	82
Di-4-imidazolylmethyl N^4,N^9-dioleoyl spermine	6	76.7±(3.9)	86.1±(5.0)	81
N^4-Oleoyl,N^9-retinoyl spermine	6	90.5±(2.0)	72.2±(1.9)	81
N^1,N^{12}-Dioleoyl spermine	12	76.6±(4.2)	85.3±(3.1)	81
N^1,N^{12}-Dimyristoleoyl spermine	12	81.3±(4.0)	77.8±(6.2)	80
Di-2-pyridinylmethyl N^4,N^9-dioleoyl spermine	4	74.7±(2.9)	82.7±(2.2)	79
N^4,N^9-Dieicosenoyl spermine	4	77.9±(6.3)	73.7±(4.1)	76
N^4-Cholesteryl,N^9-oleoyl spermine	8	71.3±(3.9)	75.7±(3.1)	74
N^4,N^9-Distearoyl spermine	8	72.4±(2.6)	70.5±(2.6)	72
N^4,N^9-Dinervonoyl spermine	6	62.8±(2.1)	67.7±(3.0)	65

Table 5.4. Viability (mean ± S.D.) of the primary skin cell line FEK4 and the HeLa derived cancer cell line HtTA transfected by siRNA complexes with the studied lipopolyamines.

Lipospermine	μg	% FEK4 Viability	% HtTA Viability	Average ± (3) %
N^4,N^9-Dinervonoyl spermine	6	98.2±(1.7)	77.1±(6.7)	88
N^4,N^9-Distearoyl spermine	8	89.1±(6.6)	73.2±(5.1)	81
N^4,N^9-Dierucoyl spermine	6	81.6±(7.1)	75.5±(3.2)	79
N^4,N^9-Dieicosenoyl spermine	4	85.9±4.4)	68.8±(8.7)	77
Di-2-pyridinylmethyl N^4,N^9-dioleoyl spermine	4	76.6±(7.4)	73.6±(2.4)	75
N^4-Myristoleoyl,N^9-myristoyl spermine	20	81.0±(6.3)	60.8±(3.8)	71
N^4-Oleoyl,N^9-retinoyl spermine	6	65.4±(3.6)	60.7±(1.7)	63
Di-4-imidazolylmethyl N^4,N^9-distearoyl spermine	4	67.0±(5.1)	56±(7.2)	62
N^4,N^9-Dioleoyl spermine	4	75.9±(5.8)	45.5±(6.6)	61
Di-2-pyridinylmethyl N^4,N^9-dipalmitoyl spermine	6	69.4±(2.9)	45.1±(1.3)	58
N^1,N^{12}-Dioleoyl spermine	12	65.3±(10.2)	46.6±(9.9)	56
N^1,N^{12}-Dimyristoleoyl spermine	12	56.7±(5.3)	48.7±(1.5)	53
Di-4-imidazolylmethyl N^4,N^9-dioleoyl spermine	6	60.4±(4.8)	38.3±(0.6)	49
N^4-Cholesteryl,N^9-oleoyl spermine	8	66.6±(3.0)	26±(0.6)	47
N^4-Oleoyl,N^9-stearoyl spermine	20	70.5±(9.4)	18.4±(1.4)	45

Using fluorescein-labelled siRNA (Label IT® RNAi Delivery Control, a 21-mer from Mirus) as a reporter, FEK4 primary skin cells and transformed HtTA cells

were examined in siFection efficiency and cytotoxicity (cell viability) experiments. The cytotoxicity of these compounds was studied using the MTT assay. The formed siRNA lipoplexes were monitored with the RiboGreen intercalation assay and characterized by both average particle size (n = 9) by laser light scattering, which revealed that the particle sizes range from 90-170 nm, and ζ-potential measurements (typically +3 to +19 mV). Gated FACS analysis of the delivery of Label IT® RNAi Delivery Control, which has the same length, charge, and configuration as a standard siRNA, showed a higher siRNA transfection efficiency with many of our novel lipospermines compared to the commercially available market leader Trans-IT™.

From the combination of the siRNA delivery (Table 5.3) and cell viability (Table 5.4) results obtained with our novel lipopolyamines, we have obtained experimental evidence for fifteen new effective transfecting agents which are able to deliver siRNA to cultured cells with good viability. Many (twelve) of these non-viral vectors have transfection efficiency more than 75% e.g., di-2-pyridinylmethyl N^4,N^9-dipalmitoyl spermine, N^4-myristoleoyl,N^9-myristoyl spermine, N^4,N^9-dierucoyl spermine, N^4,N^9-dioleoyl spermine, N^4-oleoyl,N^9-stearoyl spermine, di-4-imidazolylmethyl N^4,N^9-distearoyl spermine, di-4-imidazolylmethyl N^4,N^9-dioleoyl spermine, N^4-oleoyl,N^9-retinoyl spermine, N^1,N^{12}-dioleoyl spermine, N^1,N^{12}-dimyristoleoyl spermine, di-2-pyridinylmethyl N^4,N^9-dioleoyl spermine and N^4,N^9-dieicosenoyl spermine. While N^4,N^9-dinervonoyl spermine, N^4,N^9-distearoyl spermine, N^4,N^9-dierucoyl spermine, N^4,N^9-dieicosenoyl spermine and di-2-pyridinylmethyl N^4,N^9-dioleoyl spermine have more than 75% cell viability (cytotoxicity) effect on the cultured cells, so lipospermines N^4,N^9-dierucoyl spermine, N^4,N^9-dieicosenoyl spermine and di-2-pyridinylmethyl N^4,N^9-dioleoyl spermine are at the top of the best transfecting agents from the all tested novel lipospermines, as they display the highest transfection efficiency and the lowest cytotoxicity on both the tested cell lines.

While nine lipopolyamine conjugates occur in both series (Tables 5.1-5.4), there is no obvious correlation or SAR linking gene and siRNA delivery. What can be readily concluded from this study is that these selected small, non-polymeric and non-liposomal lipopolyamine molecules show efficient transfection and siFection of primary cell lines with pDNA and siRNA with good cell viability even in the presence of serum nucleases.

REFERENCES

1. H. Eliyahu, Y. Barenholz, and A. J. Domb. Polymers for DNA delivery. *Molecules* **10**:34-64 (2005).

2. P. L. Felgner, T. R. Gadek, M. Holm, R. Roman, H. W. Chan, M. Wenz, J. P. Northrop, G. M. Ringold, and M. Danielsen. Lipofection - A highly efficient, lipid-mediated DNA-transfection procedure. *Proc. Natl. Acad. Sci. U. S. A.* **84**:7413-7417 (1987).

3. H. Farhood, N. Serbina, and L. Huang. The role of dioleoyl phosphatidylethanolamine in cationic liposome-mediated gene-transfer. *Biochim. Biophys. Acta, Biomembr.* **1235**:289-295 (1995).

4. W. C. Tseng and L. Huang. Liposome-based gene therapy. *Pharm. Sci. Technol. Today* **1**:206-213 (1998).

5. J. P. Behr. Gene-transfer with synthetic cationic amphiphiles - prospects for gene-therapy. *Bioconjug. Chem.* **5**:382-389 (1994).

6. C. Chittimalla, L. Zammut-Italiano, G. Zuber, and J. P. Behr. Monomolecular DNA nanoparticles for intravenous delivery of genes. *J. Am. Chem. Soc.* **127**:11436-11441 (2005).

7. H. Eliyahu, A. Makovitzki, T. Azzam, A. Zlotkin, A. Joseph, D. Gazit, Y. Barenholz, and A. J. Domb. Novel dextran-spermine conjugates as transfecting agents: comparing water-soluble and micellar polymers. *Gene Ther.* **12**:494-503 (2005).

8. P. L. Kan, A. I. Gray, L. Tetley, C. A. Converse, A. G. Schatzlein, and I. F. Uchegbu. Tumour gene expression from C12 spermine amphiphile gene delivery systems. *J. Drug Target.* **13**:345-357 (2005).

9. B. Martin, M. Sainlos, A. Aissaoui, N. Oudrhiri, M. Hauchecorne, J. P. Vigneron, J. M. Lehn, and P. Lehn. The design of cationic lipids for gene delivery. *Curr. Pharm. Des.* **11**:375-394 (2005).

10. I. Yudovin-Farber, C. Yanay, T. Azzam, M. Linial, and A. J. Domb. Quaternary ammonium polysaccharides for gene delivery. *Bioconjug. Chem.* **16**:1196-1203 (2005).

11. V. A. Bloomfield. DNA condensation by multivalent cations. *Biopolymers* **44**:269-282 (1997).

12. I. S. Blagbrough, A. J. Geall, and A. P. Neal. Polyamines and novel polyamine conjugates interact with DNA in ways that can be exploited in non-viral gene therapy. *Biochem. Soc. Trans.* **31**:397-406 (2003).

13. T. V. Chirila, P. E. Rakoczy, K. L. Garrett, X. Lou, and I. J. Constable. The use of synthetic polymers for delivery of therapeutic antisense oligodeoxynucleotides. *Biomaterials* **23**:321-342 (2002).

14. G. A. Pietersz, C. K. Tang, and V. Apostolopoulos. Structure and design of polycationic carriers for gene delivery. *Mini-Rev. Med. Chem.* **6**:1285-1298 (2006).

15. J. S. Remy, C. Sirlin, P. Vierling, and J. P. Behr. Gene-transfer with a series of lipophilic DNA-binding molecules. *Bioconjug. Chem.* **5**:647-654 (1994).

16. S. A. L. Audouy, L. F. M. H. De Leij, D. Hoekstra, and G. Molema. In vivo characteristics of cationic liposomes as delivery vectors for gene therapy. *Pharm. Res.* **19**:1599-1605 (2002).

17. R. I. Mahato, A. Rolland, and E. Tomlinson. Cationic lipid-based gene delivery systems: Pharmaceutical perspectives. *Pharm. Res.* **14**:853-859 (1997).

18. M. Lee and S. W. Kim. Polyethylene glycol-conjugated copolymers for plasmid DNA delivery. *Pharm. Res.* **22**:1-10 (2005).

19. R. W. Wilson and V. A. Bloomfield. Counter-ion-Induced condensation of deoxyribonucleic-acid - light-scattering study. *Biochemistry.* **18**:2192-2196 (1979).

20. F. LabatMoleur, A. M. Steffan, C. Brisson, H. Perron, O. Feugeas, P. Furstenberger, F. Oberling, E. Brambilla, and J. P. Behr. An electron microscopy study into the mechanism of gene transfer with lipopolyamines. *Gene Ther.* **3**:1010-1017 (1996).

21. M. Langner. The intracellular fate of non-viral DNA carriers. *Cell. Mol. Biol. Lett.* **5**:295-313 (2000).

22. T. Blessing, J. S. Remy, and J. P. Behr. Template oligomerization of DNA-Bound cations produces calibrated nanometric particles. *J. Am. Chem. Soc.* **120**:8519-8520 (1998).

23. A. J. Geall, R. J. Taylor, M. E. Earll, M. A. W. Eaton, and I. S. Blagbrough. Synthesis of cholesteryl polyamine carbamates: pK(a) studies and condensation of calf thymus DNA. *Bioconjug. Chem.* **11**:314-326 (2000).

24. G. Zuber, E. Dauty, M. Nothisen, P. Belguise, and J. P. Behr. Towards synthetic viruses. *Adv. Drug Deliv. Rev.* **52**:245-253 (2001).

25. M. Ruponen, S. Yla-Herttuala, and A. Urtti. Interactions of polymeric and liposomal gene delivery systems with extracellular glycosaminoglycans: physicochemical and transfection studies. *Biochim. Biophys. Acta* **1415**:331-341 (1999).

26. S. I. Michael and D. T. Curiel. Strategies to achieve targeted gene delivery via the receptor-mediated endocytosis pathway. *Gene Ther.* **1**:223-232 (1994).

27. J. S. Remy, A. Kichler, V. Mordvinov, F. Schuber, and J. P. Behr. Targeted gene-transfer into hepatoma-cells with lipopolyamine- condensed DNA particles presenting galactose ligands - A stage toward artificial viruses. *Proc. Natl. Acad. Sci. U. S. A.* **92**:1744-1748 (1995).

28. J. C. Perales, G. A. Grossmann, M. Molas, G. Liu, T. Ferkol, J. Harpst, H. Oda, and R. W. Hanson. Biochemical and functional characterization of DNA complexes capable of targeting genes to hepatocytes via the asialoglycoprotein receptor. *J. Biol. Chem.* **272**:7398-7407 (1997).

29. C. M. Ward. Folate-targeted non-viral DNA vectors for cancer gene therapy. *Curr. Opin. Mol. Ther.* **2**:182-187 (2000).

30. L. Xu, P. Frederik, K. F. Pirollo, W. H. Tang, A. Rait, L. M. Xiang, W. Q. Huang, I. Cruz, Y. Z. Yin, and E. H. Chang. Self-assembly of a virus-mimicking nanostructure system for efficient tumor-targeted gene delivery. *Hum. Gene Ther.* **13**:469-481 (2002).

31. I. Roy, S. Mitra, A. Maitra, and S. Mozumdar. Calcium phosphate nanoparticles as novel non-viral vectors for targeted gene delivery. *Int. J. Pharm.* **250**:25-33 (2003).

32. Y. W. Cho, J. D. Kim, and K. Park. Pollycation gene delivery systems: escape from endosomes to cytosol. *J. Pharm. Pharmacol.* **55**:721-734 (2003).

33. T. Merdan, J. Kopecek, and T. Kissel. Prospects for cationic polymers in gene and oligonucleotide therapy against cancer. *Adv. Drug Deliv. Rev.* **54**:715-758 (2002).

34. C. M. Wiethoff and C. R. Middaugh. Barriers to nonviral gene delivery. *J. Pharm. Sci.* **92**:203-217 (2003).

35. I. S. Zuhorn and D. Hoekstra. On the mechanism of cationic amphiphile-mediated transfection. To fuse or not to fuse: Is that the question? *J. Membr. Biol.* **189**:167-179 (2002).

36. Y. H. Xu and F. C. Szoka. Mechanism of DNA release from cationic liposome/DNA complexes used in cell transfection. *Biochemistry (Mosc).* **35**:5616-5623 (1996).

37. Z. Y. Zhang and B. D. Smith. High-generation polycationic dendrimers are unusually effective at disrupting anionic vesicles: membrane bending model. *Bioconjug. Chem.* **11**:805-814 (2000).

38. O. Boussif, F. Lezoualch, M. A. Zanta, M. D. Mergny, D. Scherman, B. Demeneix, and J. P. Behr. A versatile vector for gene and oligonucleotide transfer into cells in culture and in-vivo - polyethylenimine. *Proc. Natl. Acad. Sci. U. S. A.* **92**:7297-7301 (1995).

39. T. B. Wyman, F. Nicol, O. Zelphati, P. V. Scaria, C. Plank, and F. C. Szoka, Jr. Design, synthesis, and characterization of a cationic peptide that binds to nucleic acids and permeabilizes bilayers. *Biochemistry.* **36**:3008-3017 (1997).

40. E. Wagner. Application of membrane-active peptides for nonviral gene delivery. *Adv. Drug Deliv. Rev.* **38**:279-289 (1999).

41. C. Pichon, C. Goncalves, and P. Midoux. Histidine-rich peptides and polymers for nucleic acids delivery. *Adv. Drug Deliv. Rev.* **53**:75-94 (2001).

42. G. L. Lukacs, P. Haggie, O. Seksek, D. Lechardeur, N. Freedman, and A. S. Verkman. Size-dependent DNA mobility in cytoplasm and nucleus. *J. Biol. Chem.* **275**:1625-1629 (2000).

43. H. Kamiya, H. Tsuchiya, J. Yamazaki, and H. Harashima. Intracellular trafficking and transgene expression of viral and non-viral gene vectors. *Adv. Drug Deliv. Rev.* **52**:153-164 (2001).

44. W. T. Godbey, K. K. Wu, and A. G. Mikos. Tracking the intracellular path of poly(ethylenimine)/DNA complexes for gene delivery. *Proc. Natl. Acad. Sci. U. S. A.* **96**:5177-5181 (1999).

45. W. T. Godbey, K. K. Ku, G. J. Hirasaki, and A. G. Mikos. Improved packing of poly(ethylenimine)/DNA complexes increases transfection efficiency. *Gene Ther.* **6**:1380-1388 (1999).

46. L. Ringenbach, A. Bohbot, P. Tiberghien, F. Oberling, and O. Feugeas. Polyethylenimine-mediated transfection of human monocytes with the IFN-gamma gene: an approach for cancer adoptive immunotherapy. *Gene Ther.* **5**:1508-1516 (1998).

47. W. T. Godbey, M. A. Barry, P. Saggau, K. K. Wu, and A. G. Mikos. Poly(ethylenimine)-mediated transfection: A new paradigm for gene delivery. *J. Biomed. Mater. Res.* **51**:321-328 (2000).

48. J. X. Tang and P. A. Janmey. The polyelectrolyte nature of F-actin and the mechanism of actin bundle formation. *J. Biol. Chem.* **271**:8556-8563 (1996).

49. K. J. Ryan and S. R. Wente. The nuclear pore complex: A protein machine bridging the nucleus and cytoplasm. *Curr. Opin. Cell Biol.* **12**:361-371 (2000).

50. M. A. Zanta, P. Belguise-Valladier, and J. P. Behr. Gene delivery: A single nuclear localization signal peptide is sufficient to carry DNA to the cell nucleus. *Proc. Natl. Acad. Sci. U. S. A.* **96**:91-96 (1999).

51. W. C. Tseng and L. Huang. Liposome-based gene therapy. *Pharm. Sci. Technol. Today* **1**:206-213 (1998).

52. S. Mehier-Humbert and R. H. Guy. Physical methods for gene transfer: Improving the kinetics of gene delivery into cells. *Adv. Drug Deliv. Rev.* **57**:733-753 (2005).

53. Y. D. Tan, F. Liu, Z. Y. Li, S. Li, and L. Huang. Sequential injection of cationic liposome and plasmid DNA effectively transfects the lung with minimal inflammatory toxicity. *Mol. Ther.* **3**:673-682 (2001).

54. T. Y. Shih and J. Bonner. Template properties of DNA-polypeptide complexes. *J. Mol. Biol.* **50**:333-340 (1970).

55. J. Haensler and F. C. Szoka. Polyamidoamine cascade polymers mediate efficient transfection of cells in culture. *Bioconjug. Chem.* **4**:372-379 (1993).

56. Y. Shoji and H. Nakashima. Current status of delivery systems to improve target efficacy of oligonucleotides. *Curr. Pharm. Des.* **10**:785-796 (2004).

57. A. V. Kabanov, S. V. Vinogradov, Y. G. Suzdaltseva, and V. Y. Alakhov. Water-soluble block polycations as carriers for oligonucleotide delivery. *Bioconjug. Chem.* **6**:639-643 (1995).

58. S. V. Vinogradov, T. K. Bronich, and A. V. Kabanov. Self-assembly of polyamine-poly(ethylene glycol) copolymers with phosphorothioate oligonucleotides. *Bioconjug. Chem.* **9**:805-812 (1998).

59. A. V. Kabanov. Taking polycation gene delivery systems from in vitro to in vivo. *Pharm. Sci. Technol. Today* **2**:365-372 (1999).

60. S. Pirotton, C. Muller, N. Pantoustier, F. Botteman, B. Collinet, C. Grandfils, G. Dandrifosse, P. Degee, P. Dubois, and M. Raes. Enhancement of transfection efficiency through rapid and noncovalent post-PEGylation of poly(dimethylaminoethyl methacrylate)/DNA complexes. *Pharm. Res.* **21**:1471-1479 (2004).

61. S. A. Cryan, R. Donohue, B. J. Ravo, R. Darcy, and C. M. O'Driscoll. Cationic cyclodextrin amphiphiles as gene delivery vectors. *J. Drug. Del. Sci. Technol.* **14**:57-62 (2004).

62. A. T. Stopeck, E. M. Hersh, J. L. Brailey, P. R. Clark, J. Norman, and S. E. Parker. Transfection of primary tumor cells and tumor cell lines with plasmid DNA/lipid complexes. *Cancer Gene Ther.* **5**:119-126 (1998).

63. J. A. Roth and R. J. Cristiano. Gene therapy for cancer: What have we done and where are we going? *J. Natl. Cancer Inst.* **89**:21-39 (1997).

64. E. W. F. W. Alton, M. Stern, R. Farley, A. Jaffe, S. L. Chadwick, J. Phillips, J. Davies, S. N. Smith, J. Browning, M. G. Davies, M. E. Hodson, S. R. Durham, D. Li, P. K. Jeffery, M. Scallan, R. Balfour, S. J. Eastman, S. H. Cheng, A. E. Smith, D. Meeker, and D. M. Geddes. Cationic lipid-mediated CFTR gene transfer to the lungs and nose of patients with cystic fibrosis: a double-blind placebo-controlled trial. *Lancet* **353**:947-954 (1999).

65. R. C. Boucher. Status of gene therapy for cystic fibrosis lung disease. *J. Clin. Invest.* **103**:441-445 (1999).

66. T. Niidome and L. Huang. Gene therapy progress and prospects: Nonviral vectors. *Gene Ther.* **9**:1647-1652 (2002).

67. P. Vierling, C. Santaella, and J. Greiner. Highly fluorinated amphiphiles as drug and gene carrier and delivery systems. *J. Fluorine Chem.* **107**:337-354 (2001).

68. J. W. Gordon, G. A. Scangos, D. J. Plotkin, J. A. Barbosa, and F. H. Ruddle. Genetic-transformation of mouse embryos by micro-Injection of purified DNA. *Proc. Natl. Acad. Sci. U. S. A.* **77**:7380-7384 (1980).

69. P. L. Felgner and G. M. Ringold. Cationic liposome-mediated transfection. *Nature* **337**:387-388 (1989).

70. C. Nicolau and C. Sene. Liposome-mediated DNA transfer in eukaryotic cells - dependence of the transfer efficiency upon the type of liposomes used and the host-cell cycle stage. *Biochim. Biophys. Acta* **721**:185-190 (1982).

71. C. Nicolau, A. Lepape, P. Soriano, F. Fargette, and M. F. Juhel. Invivo expression of rat insulin after intravenous administration of the liposome-entrapped gene for rat insulin-I. *Proc. Natl. Acad. Sci. U. S. A.* **80**:1068-1072 (1983).

72. J. P. Behr, B. Demeneix, J. P. Loeffler, and J. P. Mutul. Efficient gene-transfer into mammalian primary endocrine-cells with lipopolyamine-coated DNA. *Proc. Natl. Acad. Sci. U. S. A.* **86**:6982-6986 (1989).

73. X. Gao and L. Huang. A novel cationic liposome reagent for efficient transfection of mammalian-cells. *Biochem. Biophys. Res. Commun.* **179**:280-285 (1991).

74. M. Vidal and D. Hoekstra. In-Vitro fusion of reticulocyte endocytic vesicles with liposomes. *J. Biol. Chem.* **270**:17823-17829 (1995).

75. J. Smisterova, A. Wagenaar, M. C. A. Stuart, E. Polushkin, G. ten Brinke, R. Hulst, J. B. F. N. Engberts, and D. Hoekstra. Molecular shape of the cationic lipid controls the structure of cationic lipid/dioleylphosphatidylethanolamine-DNA complexes and the efficiency of gene delivery. *J. Biol. Chem.* **276**:47615-47622 (2001).

76. D. Niculescu-Duvaz, J. Heyes, and C. J. Springer. Structure-activity relationship in cationic lipid mediated gene transfection. *Curr. Med. Chem.* **10**:1233-1261 (2003).

77. L. H. Lindner, R. Brock, D. Arndt-Jovin, and H. Eibl. Structural variation of cationic lipids: Minimum requirement for improved oligonucleotide delivery into cells. *J. Control. Release* **110**:444-456 (2006).

78. D. Hoekstra, J. Rejman, L. Wasungu, F. Shi, and I. Zuhorn. Gene delivery by cationic lipids: in and out of an endosome. *Biochem. Soc. Trans.* **35**:68-71 (2007).

79. I. S. Zuhorn, J. B. F. N. Engberts, and D. Hoekstra. Gene delivery by cationic lipid vectors: overcoming cellular barriers. *Eur. Biophys. J. Biophys.* **36**:349-362 (2007).

80. N. J. Caplen, E. Kinrade, F. Sorgi, X. Gao, D. Gruenert, D. Geddes, C. Coutelle, L. Huang, E. W. F. W. Alton, and R. Williamson. In-vitro liposome-mediated DNA transfection of epithelial-cell lines using the cationic liposome Dc-Chol/Dope. *Gene Ther.* **2**:603-613 (1995).

81. X. Gao and L. Huang. Cationic liposome-mediated gene transfer. *Gene Ther.* **2**:710-722 (1995).

82. S. Hasegawa, N. Hirashima, and M. Nakanishi. Comparative study of transfection efficiency of cationic cholesterols mediated by liposomes-based gene delivery. *Bioorg. Med. Chem. Lett.* **12**:1299-1302 (2002).

83. N. Schmid and J. P. Behr. Location of spermine and other polyamines on DNA as revealed by photoaffinity cleavage with polyaminobenzenediazonium salts. *Biochemistry.* **30**:4357-4361 (1991).

84. D. Moradpour, J. I. Schauer, V. R. Zurawski, J. R. Wands, and R. H. Boutin. Efficient gene transfer into mammalian cells with cholesteryl-spermidine. *Biochem. Biophys. Res. Commun.* **221**:82-88 (1996).

85. F. Barthel, J. S. Remy, J. P. Loeffler, and J. P. Behr. Gene-transfer optimization with lipospermine-coated DNA. *DNA Cell Biol.* **12**:553-560 (1993).

86. J. P. Loeffler and J. P. Behr. Gene-transfer into primary and established mammalian-cell lines with lipopolyamine-coated DNA. *Methods Enzymol.* **217**:599-618 (1993).

87. Y. K. Ghosh, S. S. Visweswariah, and S. Bhattacharya. Nature of linkage between the cationic headgroup and cholesteryl skeleton controls gene transfection efficiency. *FEBS Lett.* **473**:341-344 (2000).

88. S. Spagnou, A. D. Miller, and M. Keller. Lipidic carriers of siRNA: Differences in the formulation, cellular uptake, and delivery with plasmid DNA. *Biochemistry.* **43**:13348-13356 (2004).

89. C. Cogoni and G. Macino. Post-transcriptional gene silencing across kingdoms. *Curr. Opin. Genet. Dev.* **10**:638-643 (2000).

90. A. Fire, S. Q. Xu, M. K. Montgomery, S. A. Kostas, S. E. Driver, and C. C. Mello. Potent and specific genetic interference by double-stranded RNA in Caenorhabditis elegans. *Nature* **391**:806-811 (1998).

91. M. T. McManus and P. A. Sharp. Gene silencing in mammals by small interfering RNAs. *Nat. Rev. Genet.* **3**:737-747 (2002).

92. G. J. Hannon. RNA interference. *Nature* **418**:244-251 (2002).

93. J. Heyes, L. Palmer, K. Bremner, and I. MacLachlan. Cationic lipid saturation influences intracellular delivery of encapsulated nucleic acids. *J. Control. Release* **107**:276-287 (2005).

94. C. X. Li, A. Parker, E. Menocal, S. L. Xiang, L. Borodyansky, and J. H. Fruehauf. Delivery of RNA interference. *Cell Cycle* **5**:2103-2109 (2006).

95. D. L. Lewis, J. E. Hagstrom, A. G. Loomis, J. A. Wolff, and H. Herweijer. Efficient delivery of siRNA for inhibition of gene expression in postnatal mice. *Nat. Genet.* **32**:107-108 (2002).

96. R. Moriguchi, K. Kogure, H. Akita, S. Futaki, M. Miyagishi, K. Taira, and H. Harashima. A multifunctional envelope-type nano device for novel gene delivery of siRNA plasmids. *Int. J. Pharm.* **301**:277-285 (2005).

97. C. L. Zhang, N. Tang, X. J. Liu, W. Liang, W. Xu, and V. P. Torchilin. siRNA-containing liposomes modified with polyarginine effectively silence the targeted gene. *J. Control. Release* **112**:229-239 (2006).

98. J. H. Zhou, J. Y. Wu, N. Hafdi, J. P. Behr, P. Erbacher, and L. Peng. PAMAM dendrimers for efficient siRNA delivery and potent gene silencing. *Chem. Commun.* 2362-2364 (2006).

99. A. Muratovska and M. R. Eccles. Conjugate for efficient delivery of short interfering RNA (siRNA) into mammalian cells. *FEBS Lett.* **558**:63-68 (2004).

100. S. M. Elbashir, J. Harborth, W. Lendeckel, A. Yalcin, K. Weber, and T. Tuschl. Duplexes of 21-nucleotide RNAs mediate RNA interference in cultured mammalian cells. *Nature* **411**:494-498 (2001).

101. M. Amarzguioui, T. Holen, E. Babaie, and H. Prydz. Tolerance for mutations and chemical modifications in a siRNA. *Nucleic Acids Res.* **31**:589-595 (2003).

102. M. Hamada, T. Ohtsuka, R. Kawaida, M. Koizumi, K. Morita, H. Furukawa, T. Imanishi, M. Miyagishi, and K. Taira. Effects on RNA interference in gene expression (RNAi) in cultured mammalian cells of mismatches and the introduction of chemical modifications at the 3 '-ends of siRNAs. *Antisense Nucleic Acid Drug Dev.* **12**:301-309 (2002).

103. Y. Ikeda and K. Taira. Ligand-targeted delivery of therapeutic siRNA. *Pharm. Res.* **23**:1631-1640 (2006).

104. S. M. Elbashir, W. Lendeckel, and T. Tuschl. RNA interference is mediated by 21-and 22-nucleotide RNAs. *Genes & Development* **15**:188-200 (2001).

105. J. Y. Yu, S. L. DeRuiter, and D. L. Turner. RNA interference by expression of short-interfering RNAs and hairpin RNAs in mammalian cells. *Proc. Natl. Acad. Sci. U. S. A.* **99**:6047-6052 (2002).

106. C. P. Paul, P. D. Good, I. Winer, and D. R. Engelke. Effective expression of small interfering RNA in human cells. *Nat. Biotechnol.* **20**:505-508 (2002).

107. R. M. Schiffelers, M. C. Woodle, and P. Scaria. Pharmaceutical prospects for RNA interference. *Pharm. Res.* **21**:1-7 (2004).

108. A. A. Chen, A. M. Derfus, S. R. Khetani, and S. N. Bhatia. Quantum dots to monitor RNAi delivery and improve gene silencing. *Nucleic Acids Res.* **33**: (2005).

109. B. Dalby, S. Cates, A. Harris, E. C. Ohki, M. L. Tilkins, P. J. Price, and V. C. Ciccarone. Advanced transfection with Lipofectamine 2000 reagent: primary neurons, siRNA, and high-throughput applications. *Methods* **33**:95-103 (2004).

110. L. D. Shea and T. L. Houchin. Modular design of non-viral vectors with bioactive components. *Trends Biotechnol.* **22**:429-431 (2004).

111. D. W. Bartlett and M. E. Davis. Insights into the kinetics of siRNA-mediated gene silencing from live-cell and live-animal bioluminescent imaging. *Nucleic Acids Res.* **34**:322-333 (2006).

112. S. T. Crooke. Potential roles of antisense technology in cancer chemotherapy. *Oncogene* **19**:6651-6659 (2000).

113. Y. L. Chiu and T. M. Rana. siRNA function in RNAi: A chemical modification analysis. *Rna-A Publication of the Rna Society* **9**:1034-1048 (2003).

114. Y. L. Liu and Y. C. Chiu. Novel approach to the chemical modification of poly(vinyl alcohol): Phosphorylation. *J. Polym. Sci. , Part A: Polym. Chem.* **41**:1107-1113 (2003).

115. M. A. Behlke. Progress towards in vivo use of siRNAs. *Mol. Ther.* **13**:644-670 (2006).

116. D. R. Sorensen, M. Leirdal, and M. Sioud. Gene silencing by systemic delivery of synthetic siRNAs in adult mice. *J. Mol. Biol.* **327**:761-766 (2003).

117. M. Sioud and D. R. Sorensen. Cationic liposome-mediated delivery of siRNAs in adult mice. *Biochem. Biophys. Res. Commun.* **312**:1220-1225 (2003).

118. A. Santel, M. Aleku, O. Keil, J. Endruschat, V. Esche, G. Fisch, S. Dames, K. Loffler, M. Fechtner, W. Arnold, K. Giese, A. Klippel, and J. Kaufmann. A novel siRNA-lipoplex technology for RNA interference in the mouse vascular endothelium. *Gene Ther* **13**:1222-1234 (2006).

119. L. De Laporte, J. C. Rea, and L. D. Shea. Design of modular non-viral gene therapy vectors. *Biomaterials* **27**:947-954 (2006).

120. F. Y. Xie, M. C. Woodle, and P. Y. Lu. Harnessing in vivo siRNA delivery for drug discovery and therapeutic development. *Drug Discovery Today* **11**:67-73 (2006).

121. R. Ardaillou. Gene therapy: present situation and prospects. *Rev. Med. Interne* **23**:679-682 (2002).

122. Y. Zeng and B. R. Cullen. RNA interference in human cells is restricted to the cytoplasm. *Rna-A Publication of the Rna Society* **8**:855-860 (2002).

123. D. V. Morrissey, J. A. Lockridge, L. Shaw, K. Blanchard, K. Jensen, W. Breen, K. Hartsough, L. Machemer, S. Radka, V. Jadhav, N. Vaish, S. Zinnen, C. Vargeese, K. Bowman, C. S. Shaffer, L. B. Jeffs, A. Judge, I. MacLachlan, and B. Polisky. Potent and persistent in vivo anti-HBV activity of chemically modified siRNAs. *Nat. Biotechnol.* **23**:1002-1007 (2005).

124. E. W. Song, P. C. Zhu, S. K. Lee, D. Chowdhury, S. Kussman, D. M. Dykxhoorn, Y. Feng, D. Palliser, D. B. Weiner, P. Shankar, W. A. Marasco, and J. Lieberman. Antibody mediated in vivo delivery of small interfering RNAs via cell-surface receptors. *Nat. Biotechnol.* **23**:709-717 (2005).

125. R. M. Schiffelers, A. Ansari, J. Xu, Q. Zhou, Q. Q. Tang, G. Storm, G. Molema, P. Y. Lu, P. V. Scaria, and M. C. Woodle. Cancer siRNA therapy by tumor selective delivery with ligand-targeted sterically stabilized nanoparticle. *Nucleic Acids Res.* **32**:e149 (2004).

126. A. P. McCaffrey, L. Meuse, T. T. T. Pham, D. S. Conklin, G. J. Hannon, and M. A. Kay. Gene expression - RNA interference in adult mice. *Nature* **418**:38-39 (2002).

127. E. W. Song, S. K. Lee, J. Wang, N. Ince, N. Ouyang, J. Min, J. S. Chen, P. Shankar, and J. Lieberman. RNA interference targeting Fas protects mice from fulminant hepatitis. *Nat. Med.* **9**:347-351 (2003).

128. P. K. Dubey, V. Mishra, S. Jain, S. Mahor, and S. P. Vyas. Liposomes modified with cyclic RGD peptide for tumor targeting. *J. Drug Target.* **12**:257-264 (2004).

129. W. D. Zhang, H. Yang, X. Y. Kong, S. Mohapatra, H. San Juan-Vergara, G. Hellermann, S. Behera, R. Singam, R. F. Lockey, and S. S. Mohapatra. Inhibition of respiratory syncytial virus infection with intranasal siRNA nanoparticles targeting the viral NS1 gene. *Nat. Med.* **11**:56-62 (2005).

130. V. Bitko, A. Musiyenko, O. Shulyayeva, and S. Barik. Inhibition of respiratory viruses by nasally administered siRNA. *Nat. Med.* **11**:50-55 (2005).

131. E. Fattal and A. Bochot. Ocular delivery of nucleic acids: antisense oligonucleotides, aptamers and siRNA. *Adv. Drug Deliv. Rev.* **58**:1203-1223 (2006).

132. K. Ui-Tei, Y. Naito, F. Takahashi, T. Haraguchi, H. Ohki-Hamazaki, A. Juni, R. Ueda, and K. Saigo. Guidelines for the selection of highly effective siRNA sequences for mammalian and chick RNA interference. *Nucleic Acids Res.* **32**:936-948 (2004).

133. A. W. Tong, Y. A. Zhang, and J. Nemunaitis. Small interfering RNA for experimental cancer therapy. *Curr. Opin. Mol. Ther.* **7**:114-124 (2005).

134. S. L. Uprichard. The therapeutic potential of RNA interference. *FEBS Lett.* **579**:5996-6007 (2005).

135. J. Sambrook and D. W. Russell. *Molecular Cloning: a laboratory manual*, Cold Spring Harbor Laboratory Press, New York, 2001.

136. K. L. Manchester. Value of A260/A280 ratios for measurement of purity of nucleic acids. *Biotechniques* **19**:208-210 (1995).

137. K. L. Manchester. Use of UV methods for measurement of protein and nucleic acid concentrations. *Biotechniques* **20**:968-970 (1996).

138. A. J. Geall and I. S. Blagbrough. Rapid and sensitive ethidium bromide fluorescence quenching assay of polyamine conjugate-DNA interactions for the analysis of lipoplex formation in gene therapy. *J. Pharm. Biomed. Anal.* **22**:849-859 (2000).

139. P. L. Felgner, Y. Barenholz, J. P. Behr, S. H. Cheng, P. Cullis, L. Huang, J. A. Jessee, L. Seymour, F. Szoka, A. R. Thierry, E. Wagner, and G. Wu. Nomenclature for synthetic gene delivery systems. *Hum. Gene Ther.* **8**:511-512 (1997).

140. A. R. Morgan, J. S. Lee, D. E. Pulleyblank, N. L. Murray, and D. H. Evans. Ethidium fluorescence assays. Part 1. Physicochemical studies. *Nucleic Acids Res.* **7**:547-569 (1979).

141. B. F. Cain, B. C. Baguley, and W. A. Denny. Potential antitumor agents. 28. deoxyribonucleic acid polyintercalating agents. *J. Med. Chem.* **21**:658-668 (1978).

142. R. M. Tyrrell and M. Pidoux. Quantitative differences in host cell reactivation of ultraviolet-damaged virus in human skin fibroblasts and epidermal keratinocytes cultured from the same foreskin biopsy. *Cancer Res.* **46**:2665-2669 (1986).

143. G. F. Vile and R. M. Tyrrell. Oxidative stress resulting from ultraviolet-A irradiation of human skin fibroblasts leads to a heme oxygenase-dependent increase in ferritin. *J. Biol. Chem.* **268**:14678-14681 (1993).

144. J. L. Zhong, A. Yiakouvaki, P. Holley, R. M. Tyrrell, and C. Pourzand. Susceptibility of skin cells to UVA-induced necrotic cell death reflects the intracellular level of labile iron. *J. Invest. Dermatol.* **123**:771-780 (2004).

145. M. Gossen and H. Bujard. Tight control of gene-expression in mammalian-cells by tetracycline-responsive promoters. *Proc. Natl. Acad. Sci. U. S. A.* **89**:5547-5551 (1992).

146. E. Kvam, V. Hejmadi, S. Ryter, C. Pourzand, and R. M. Tyrrell. Heme oxygenase activity causes transient hypersensitivity to oxidative ultraviolet A radiation that depends on release of iron from heme. *Free Radic. Biol. Med.* **28**:1191-1196 (2000).

147. L. A. Herzenberg, D. Parks, B. Sahaf, O. Perez, M. Roederer, and L. A. Herzenberg. The history and future of the fluorescence activated cell sorter and flow cytometry: A view from Stanford. *Clin. Chem.* **48**:1819-1827 (2002).

148. T. Mosmann. Rapid colorimetric assay for cellular growth and survival - application to proliferation and cyto-toxicity assays. *J. Immunol. Methods* **65**:55-63 (1983).

149. D. Fischer, T. Bieber, Y. X. Li, H. P. Elsasser, and T. Kissel. A novel non-viral vector for DNA delivery based on low molecular weight, branched polyethylenimine: Effect of molecular weight on transfection efficiency and cytotoxicity. *Pharm. Res.* **16**:1273-1279 (1999).

150. K. Fabio, J. Gaucheron, C. Di Giorgio, and P. Vierling. Novel galactosylated polyamine bolaamphiphiles for gene delivery. *Bioconjug. Chem.* **14**:358-367 (2003).

151. S. A. Cryan and C. M. O'Driscoll. Mechanistic studies on nonviral gene delivery to the intestine using in vitro differentiated cell culture models and an in vivo rat intestinal loop. *Pharm. Res.* **20**:569-575 (2003).

152. E. Wagner. Strategies to improve DNA polyplexes for in vivo gene transfer: Will "artificial viruses" be the answer? *Pharm. Res.* **21**:8-14 (2004).

153. M. Thomas, Q. Ge, J. J. Lu, J. Z. Chen, and A. M. Klibanov. Cross-linked small polyethylenimines: While still nontoxic, deliver DNA efficiently to mammalian cells in vitro and in vivo. *Pharm. Res.* **22**:373-380 (2005).

154. E. Dauty, J. S. Remy, T. Blessing, and J. P. Behr. Dimerizable cationic detergents with a low cmc condense plasmid DNA into nanometric particles and transfect cells in culture. *J. Am. Chem. Soc.* **123**:9227-9234 (2001).

155. S. C. De Smedt, J. Demeester, and W. E. Hennink. Cationic polymer based gene delivery systems. *Pharm. Res.* **17**:113-126 (2000).

156. P. L. Felgner, C. N. Sridhar, C. J. Wheeler, and J. Felgner. Enhanced gene delivery and mechanism studies with a novel series of cationic lipid formulations. *J. Cell. Biochem.* 206 (1993).

157. A. Roosjen, J. Smisterova, C. Driessen, J. T. Anders, A. Wagenaar, D. Hoekstra, R. Hulst, and J. B. F. N. Engberts. Synthesis and characteristics of biodegradable pyridinium amphiphiles used for in vitro DNA delivery. *Eur. J. Org. Chem.* 1271-1277 (2002).

158. B. Buchberger, E. Fernholz, H. v.d.Eltz, and M. Hinzepeter. DOSPER liposomal transfection reagent: a reagent with unique transfection properties. *Biochem. Inform.* **98**:27-29 (1996).

159. A. D. Miller. Cationic liposomes for gene therapy. *Angewandte Chemie-International Edition* **37**:1769-1785 (1998).

160. S. A. Cryan, M. Devocelle, P. J. Moran, A. J. Hickey, and J. G. Kelly. Increased intracellular targeting to airway cells using octaarginine-coated liposomes: In vitro assessment of their suitability for inhalation. *Mol. Pharm.* **3**:104-112 (2006).

161. A. J. Geall, M. A. W. Eaton, T. Baker, C. Catterall, and I. S. Blagbrough. The regiochemical distribution of positive charges along cholesterol polyamine carbamates plays significant roles in modulating DNA binding affinity and lipofection. *FEBS Lett.* **459**:337-342 (1999).

162. I. S. Blagbrough, D. Al-Hadithi, and A. J. Geall. Cheno-, urso- and deoxycholic acid spermine conjugates: Relative binding affinities for calf thymus DNA. *Tetrahedron* **56**:3439-3447 (2000).

163. A. J. Geall, D. Al-Hadithi, and I. S. Blagbrough. Efficient calf thymus DNA condensation upon binding with novel bile acid polyamine Amides. *Bioconjug. Chem.* **13**:481-490 (2002).

164. A. J. Geall and I. S. Blagbrough. Homologation of polyamines in the rapid synthesis of lipospermine conjugates and related lipoplexes. *Tetrahedron* **56**:2449-2460 (2000).

165. O. Rosella, A. Sinclair, and P. R. Gibson. Polyunsaturated fatty acids reduce non-receptor-mediated transcellular permeation of protein across a model of intestinal epithelium in vitro. *J. Gastroenterol. Hepatol.* **15**:626-631 (2000).

166. Z. Siprashvili, F. A. Scholl, S. F. Oliver, A. Adams, C. H. Contag, P. A. Wender, and P. A. Khavari. Gene transfer via reversible plasmid condensation with cysteine-flanked, internally spaced arginine-rich peptides. *Hum. Gene Ther.* **14**:1225-1233 (2003).

167. J. Rothbard, P. Robbins, S. Sheu, S. Oliver, J. Goodnough, P. Wender, and P. Khavari. Molecular transporters facilitate topical protein transduction into the skin. *J. Invest. Dermatol.* **117**:955 (2001).

168. J. B. Rothbard, T. C. Jessop, R. S. Lewis, B. A. Murray, and P. A. Wender. Role of membrane potential and hydrogen bonding in the mechanism of translocation of guanidinium-rich peptides into cells. *J. Am. Chem. Soc.* **126**:9506-9507 (2004).

169. B. Razani and M. P. Lisanti. Caveolins and caveolae: Molecular and functional relationships. *Exp. Cell Res.* **271**:36-44 (2001).

170. O. A. A. Ahmed, N. Adjimatera, C. Pourzand, and I. S. Blagbrough. N^4,N^9-Dioleoyl spermine is a novel nonviral lipopolyamine vector for plasmid DNA formulation. *Pharm. Res.* **22**:972-980 (2005).

171. O. A. A. Ahmed, C. Pourzand, and I. S. Blagbrough. Varying the unsaturation in N^4,N^9-dioctadecanoyl spermines: Nonviral lipopolyamine vectors for more efficient plasmid DNA formulation. *Pharm. Res.* **23**:31-40 (2006).

172. S. Simoes, C. Fonseca, H. Faneca, N. Duzgunes, and M. C. P. de Lima. Protein-associated lipoplexes: novel strategies to enhance gene delivery mediated by lipid-based particles. *STP Pharma Sci.* **12**:339-344 (2002).

173. V. A. Bloomfield. Condensation of DNA by multivalent cations - considerations on mechanism. *Biopolymers* **31**:1471-1481 (1991).

174. B. Lepecq and C. Paoletti. A fluorescent complex between ethidium bromide and nucleic acids. Physical-chemical characterization. *J Mol Biol* **27**:87-106 (1967).

175. C. G. Reinhardt and T. R. Krugh. Comparative study of ethidium bromide complexes with dinucleotides and DNA: Direct evidence for intercalation and nucleicv acid sequence Preferences. *Biochemistry.* **17**:4845-4854 (1978).

176. A. J. Geall and I. S. Blagbrough. Rapid and sensitive ethidium bromide fluorescence quenching assay of polyamine conjugate-DNA interactions for the analysis of lipoplex formation in gene therapy. *J. Pharm. Biomed. Anal.* **22**:849-859 (2000).

177. J. Olmsted and D. R. Kearns. Mechanism of ethidium-bromide fluorescence enhancement on binding to nucleic-acids. *Biochemistry.* **16**:3647-3654 (1977).

178. V. Vijayanathan, T. Thomas, A. Shirahata, and T. J. Thomas. DNA condensation by polyamines: A laser light scattering study of structural effects. *Biochemistry.* **40**:13644-13651 (2001).

179. V. Vijayanathan, T. Thomas, and T. J. Thomas. DNA nanoparticles and development of DNA delivery vehicles for gene therapy. *Biochemistry.* **41**:14085-14094 (2002).

180. L. C. Gosule and J. A. Schellman. Compact form of DNA induced by spermidine. *Nature* **259**:333-335 (1976).

181. L. C. Gosule and J. A. Schellman. DNA condensation with polyamines I. Spectroscopic studies. *J. Mol. Biol.* **121**:311-326 (1978).

182. R. M. Tyrrell and M. Pidoux. Quantitative differences in host cell reactivation of ultraviolet-damaged virus in human skin fibroblasts and epidermal keratinocytes cultured from the same foreskin biopsy. *Cancer Res.* **46**:2665-2669 (1986).

183. K. Romoren, A. Aaberge, G. Smistad, B. J. Thu, and O. Evensen. Long-term stability of chitosan-based polyplexes. *Pharm. Res.* **21**:2340-2346 (2004).

184. D. D. Dunlap, A. Maggi, M. R. Soria, and L. Monaco. Nanoscopic structure of DNA condensed for gene delivery. *Nucleic Acids Res.* **25**:3095-3101 (1997).

185. B. Sternberg, F. L. Sorgi, and L. Huang. New structures in complex formation between DNA and cationic liposomes visualized by freeze-fracture lectron-microscopy. *FEBS Lett.* **356**:361-366 (1994).

186. L. Ciani, S. Ristori, L. Calamai, and G. Martini. DOTAP/DOPE and DC-Chol/DOPE lipoplexes for gene delivery: zeta potential measurements and electron spin resonance spectra. *Biochim. Biophys. Acta-Biomembr.* **1664**:70-79 (2004).

187. C. F. Hung, T. L. Hwang, C. C. Chang, and J. Y. Fang. Physicochemical characterization and gene transfection efficiency of lipid,emulsions with various co-emulsifiers. *Int. J. Pharm.* **289**:197-208 (2005).

188. D. G. Anderson, A. Akinc, N. Hossain, and R. Langer. Structure/property studies of polymeric gene delivery using a library of poly(beta-amino esters). *Mol. Ther.* **11**:426-434 (2005).

189. X. Gao and L. Huang. Potentiation of cationic liposome-mediated gene delivery by polycations. *Biochemistry.* **35**:1027-1036 (1996).

190. J. Panyam and V. Labhasetwar. Biodegradable nanoparticles for drug and gene delivery to cells and tissue. *Adv. Drug Deliv. Rev.* **55**:329-347 (2003).

191. F. Lamarche, M. Mevel, T. Montier, L. Burel-Deschamps, P. Giamarchi, R. Tripier, P. Delepine, T. Le Gall, D. Cartier, P. Lehn, P. A. Jaffrees, and J. C. Clement. Lipophosphoramidates as lipidic part of lipospermines for gene delivery. *Bioconjug. Chem.* **18**:1575-1582 (2007).

192. A. S. Snygg, M. Hung, and S. K. C. Elmroth. The polyamines spermidine and spermine retard the platination rate of single-stranded DNA oligomers and plasmid. *J. Inorg. Biochem.* **101**:1153-1164 (2007).

193. Y. Takeda, K. Samejima, K. Nagano, M. Watanabe, H. Sugeta, and Y. Kyogoku. Determination of protonation sites in thermospermine and in some other polyamines by ^{15}N and ^{13}C nuclear magnetic-resonance spectroscopy. *Eur. J. Biochem.* **130**:383-389 (1983).

194. C. Frassineti, S. Ghelli, P. Gans, A. Sabatini, M. S. Moruzzi, and A. Vacca. Nuclear-Magnetic-Resonance as a tool for determining protonation constants of natural polyprotic bases in solution. *Anal. Biochem.* **231**:374-382 (1995).

195. M. M. Kimberly and J. H. Goldstein. Determination of pka values and total proton distribution pattern of spermidine by C13 nuclear magnetic resonance titrations. *Anal. Chem.* **53**:789-793 (1981).

196. E. Rowatt and R. J. P. Williams. The effect of multivalent ions on the inactivation of bacteriophage-phi-x174 by lipopolysaccharide from Escherichia coli C. *Biochem. J.* **231**:765-768 (1985).

197. J. F. Coetzee and Padmanabhan G.R. Properties of bases in acetonitrile as solvent. IV. Proton acceptor power and homoconjugation of mono- and diamines. *J. Am. Chem. Soc.* **87**:5005-5010 (1965).

198. A. Albert and E. P. Serjeant. In *The Determination of Ionization Constants*, Chapman and Hall Ltd., London pp 91-95 (1971).

199. J. H. Larson, P. C. Frost, and G. A. Lamberti. Variable toxicity of ionic liquid-forming chemicals to Lemna minor and the influence of dissolved organic matter. *Environ. Toxicol. Chem.* **27**:676-681 (2008).

200. C. W. Cho, T. P. T. Pham, Y. C. Jeon, K. Vijayaraghavan, W. S. Choe, and Y. S. Yun. Toxicity of imidazolium salt with anion bromide to a phytoplankton Selenastrum capricornutum: Effect of alkyl-chain length. *Chemosphere* **69**:1003-1007 (2007).

201. K. M. Docherty and C. F. Kulpa. Toxicity and antimicrobial activity of imidazolium and pyridinium ionic liquids. *Green Chemistry* **7**:185-189 (2005).

202. J. Ranke, K. Molter, F. Stock, U. Bottin-Weber, J. Poczobutt, J. Hoffmann, B. Ondruschka, J. Filser, and B. Jastorff. Biological effects of imidazolium ionic liquids with varying chain lengths in acute Vibrio fischeri and WST-1 cell viability assays. *Ecotoxicol. Environ. Saf.* **58**:396-404 (2004).

203. Y. Yang, X. L. Ye, X. G. Li, J. Zhen, B. S. Zhang, and L. J. Yuan. Synthesis and antimicrobial activity of 8-alkylberberine derivatives with a long aliphatic chain. *Planta Med.* **73**:602-604 (2007).

204. C. McGregor, C. Perrin, M. Monck, P. Camilleri, and A. J. Kirby. Rational approaches to the design of cationic gemini surfactants for gene delivery. *J. Am. Chem. Soc.* **123**:6215-6220 (2001).

205. G. Byk, C. Dubertret, V. Escriou, M. Frederic, G. Jaslin, R. Rangara, B. Pitard, J. Crouzet, P. Wils, B. Schwartz, and D. Scherman. Synthesis, activity, and structure-activity relationship studies of novel cationic lipids for DNA transfer. *J. Med. Chem.* **41**:224-235 (1998).

206. J. H. Felgner, R. Kumar, C. N. Sridhar, C. J. Wheeler, Y. J. Tsai, R. Border, P. Ramsey, M. Martin, and P. L. Felgner. Enhanced gene delivery and mechanism studies with a novel series of cationic lipid formulations. *J. Biol. Chem.* **269**:2550-2561 (1994).

207. J. K. Wang, X. Guo, Y. H. Xu, L. Barron, and F. C. Szoka. Synthesis and characterization of long chain alkyl acyl carnitine esters. Potentially biodegradable cationic lipids for use in gene delivery. *J. Med. Chem.* **41**:2207-2215 (1998).

208. J. A. Heyes, D. Niculescu-Duvaz, R. G. Cooper, and C. J. Springer. Synthesis of novel cationic lipids: Effect of structural modification on the efficiency of gene transfer. *J. Med. Chem.* **45**:99-114 (2002).

209. S. A. Cryan, A. Holohan, R. Donohue, R. Darcy, and C. M. O'Driscoll. Cell transfection with polycationic cyclodextrin vectors. *Eur. J. Pharm. Sci.* **21**:625-633 (2004).

210. J. Sen and A. Chaudhuri. Design, syntheses, and Transfection biology of novel non-cholesterol-based guanidinylated cationic lipids. *J. Med. Chem.* **48**:812-820 (2005).

211. H. S. Yoo, J. E. Lee, H. Chung, I. C. Kwon, and S. Y. Jeong. Self-assembled nanoparticles containing hydrophobically modified glycol chitosan for gene delivery. *J. Control. Release* **103**:235-243 (2005).

212. M. Ruponen, P. Honkakoski, M. Tammi, and A. Urtti. Cell-surface glycosaminoglycans inhibit cation-mediated gene transfer. *J. Gene Med.* **6**:405-414 (2004).

213. C. M. Wiethoff, J. G. Koe, G. S. Koe, and C. R. Middaugh. Compositional effects of cationic lipid/DNA delivery systems on transgene expression in cell culture. *J. Pharm. Sci.* **93**:108-123 (2004).

214. A. Kichler, A. J. Mason, and B. Bechinger. Cationic amphipathic histidine-rich peptides for gene delivery. *Biochim. Biophys. Acta, Biomembr.* **1758**:301-307 (2006).

215. G. T. Hess, W. H. Humphries, N. C. Fay, and C. K. Payne. Cellular binding, motion, and internalization of synthetic gene delivery polymers. *Biochim. Biophys. Acta* **1773**:1583-1588 (2007).

216. F. D. Nascimento, M. A. F. Hayashi, A. Kerkis, V. Oliveira, E. B. Oliveira, G. Radis-Baptista, H. B. Nader, T. Yamane, I. L. dos Santos Tersariol, and I. Kerkis. Crotamine mediates gene delivery into cells through the binding to heparan sulfate proteoglycans. *J. Biol. Chem.* **282**:21349-21360 (2007).

217. E. G. Saravolac, O. Ludkovski, R. Skirrow, M. Ossanlou, Y. P. Zhang, C. Giesbrecht, J. Thompson, S. Thomas, H. Stark, P. R. Cullis, and P. Scherrer. Encapsulation of plasmid DNA in stabilized plasmid-lipid particles composed of different cationic lipid concentration for optimal transfection activity. *J. Drug Target.* **7**:423-437 (2000).

218. Y. P. Zhang, L. Sekirov, E. G. Saravolac, J. J. Wheeler, P. Tardi, K. Clow, E. Leng, R. Sun, P. R. Cullis, and P. Scherrer. Stabilized plasmid-lipid particles for regional gene therapy: formulation and transfection properties. *Gene Ther.* **6**:1438-1447 (1999).

219. K. W. C. Mok, A. M. I. Lam, and P. R. Cullis. Stabilized plasmid-lipid particles: factors influencing plasmid entrapment and transfection properties. *Biochim. Biophys. Acta, Biomembr.* **1419**:137-150 (1999).

220. D. J. Taxman, L. R. Livingstone, J. H. Zhang, B. J. Conti, H. A. Iocca, K. L. Williams, J. D. Lich, J. P. Y. Ting, and W. Reed. Criteria for effective design, construction, and gene knockdown by shRNA vectors. *BMC Biotech.* **6**: (2006).

221. M. A. Matzke and J. A. Birchler. RNAi-mediated pathways in the nucleus. *Nat. Rev. Genet.* **6**:24-35 (2005).

222. I. S. Blagbrough, E. Moya, and S. Taylor. Polyamines and polyamine amides from wasps and spiders. *Biochem. Soc. Trans.* **22**:888-893 (1994).

223. I. S. Blagbrough, A. J. Geall, and S. A. David. Lipopolyamines incorporating the tetraamine spermine, bound to an alkyl chain, sequester bacterial lipopolysaccharide. *Bioorg. Med. Chem. Lett.* **10**:1959-1962 (2000).

224. J. G. Delcros, S. Tomasi, S. Carrington, B. Martin, J. Renault, I. S. Blagbrough, and P. Uriac. Effect of spermine conjugation on the cytotoxicity and cellular transport of acridine. *J. Med. Chem.* **45**:5098-5111 (2002).

225. N. Adjimatera, T. Kral, M. Hof, and I. S. Blagbrough. Lipopolyamine-mediated single nanoparticle formation of calf thymus DNA analyzed by fluorescence correlation spectroscopy. *Pharm. Res.* **23**:1564-1573 (2006).

226. D. McLaggan, N. Adjimatera, K. Sepcic, M. Jaspars, D. J. MacEwan, I. S. Blagbrough, and R. H. Scott. Pore forming polyalkylpyridinium salts from marine sponges versus synthetic lipofection systems: distinct tools for intracellular delivery of cDNA and siRNA. *BMC Biotech.* **6**: (2006).

227. R.G.Crystal. Transfer of genes to humans :Early lessons and hurdles to success. *Science* **270**:404-410 (1995).

228. P. Kreiss, B. Cameron, R. Rangara, P. Mailhe, O. guerre-Charriol, M. Airiau, D. Scherman, J. Crouzet, and B. Pitard. Plasmid DNA size does not affect the physicochemical properties of lipoplexes but modulates gene transfer efficiency. *Nucleic Acids Res.* **27**:3792-3798 (1999).

229. G. de Jong, A. Telenius, S. Vanderbyl, A. Meitz, and J. Drayer. Efficient in-vitro transfer of a 60-Mb mammalian artificial chromosome into murine and hamster cells using cationic lipids and dendrimers. *Chromosome Res.* **9**:475-485 (2001).

230. S. W. Dow, L. G. Fradkin, D. H. Liggitt, A. P. Willson, T. D. Heath, and T. A. Potter. Lipid-DNA complexes induce potent activation of innate immune responses and antitumor activity when administered intravenously. *J. Immunol.* **163**:1552-1561 (1999).

231. M. Whitmore, S. Li, and L. Huang. LPD lipopolyplex initiates a potent cytokine response and inhibits tumor growth. *Gene Ther.* **6**:1867-1875 (1999).

232. F. E. Ruiz, J. P. Clancy, M. A. Perricone, Z. Bebok, J. S. Hong, S. H. Cheng, D. P. Meeker, K. R. Young, R. A. Schoumacher, M. R. Weatherly, L. Wing, J. E. Morris, L. Sindel, M. Rosenberg, F. W. van Ginkel, J. R. Mcghee, D. Kelly, R. K. Lyrene, and E. J. Sorscher. A clinical inflammatory syndrome attributable to aerosolized lipid-DNA administration in cystic fibrosis. *Hum. Gene Ther.* **12**:751-761 (2001).

233. M. M. Whitmore, S. Li, L. Falo, and L. Huang. Systemic administration of LPD prepared with CpG oligonucleotides inhibits the growth of established pulmonary metastases by stimulating innate and acquired antitumor immune responses. *Cancer Immunol. Immunother.* **50**:503-514 (2001).

234. D. Bumcrot, M. Manoharan, V. Koteliansky, and D. W. Y. Sah. RNAi therapeutics: a potential new class of pharmaceutical drugs. *Nature Chemical Biology* **2**:711-719 (2006).

235. A. L. C. Cardoso, S. Simoes, L. P. de Almeida, J. Pelisek, C. Culmsee, E. Wagner, and M. C. P. de Lima. SiRNA delivery by a transferrin-associated lipid-based vector: a non-viral strategy to mediate gene silencing. *J. Gene Med.* **9**:170-183 (2007).

236. R. M. Schiffelers, A. Ansari, J. Xu, Q. Zhou, Q. Q. Tang, G. Storm, G. Molema, P. Y. Lu, P. V. Scaria, and M. C. Woodle. Cancer siRNA therapy by tumor selective delivery with ligand-targeted sterically stabilized nanoparticle. *Nucleic Acids Res.* **32**:e149 (2004).

237. T. Tagami, J. M. Barichello, H. Kikuchi, T. Ishida, and H. Kiwada. The gene-silencing effect of siRNA in cationic lipoplexes is enhanced by incorporating pDNA in the complex. *Int. J. Pharm.* **333**:62-69 (2007).

APPENDIX

Publications and Presentations Arising from this Work

Publications

1. H. M. Ghonaim, S. Li, and I. S. Blagbrough. Very long chain N^4,N^9-diacyl spermines: Non-viral lipopolyamine vectors for efficient plasmid DNA and siRNA delivery. *Pharm. Res.* **26**: In Press (2009).

2. M. K. Soltan, H. M. Ghonaim, M. El Sadek, M. Abou Kull, L. Abd El-aziz, and I. S. Blagbrough. Design and synthesis of N^4,N^9-disubstituted spermines for non-viral siRNA delivery - structure-activity relationship studies of sifection efficiency versus toxicity. *Pharm. Res.* **26**: In Press (2009).

3. H. M. Ghonaim, O. A. A. Ahmed, C. Pourzand, and I. S. Blagbrough. Varying the chain length in N^4,N^9-diacyl spermines: non-viral lipopolyamine vectors for efficient plasmid DNA formulation. *Mol. Pharm.* **6**: In Press (2009).

Presentations

1. **Design of Lipospermine Non-Viral Gene Delivery Vectors for Self-Assembly DNA Nanoparticle Formulations (POSTER)**
   5th World Meeting on Pharmaceutics, Biopharmaceutics and Pharmaceutical Technology, Geneva, Switzerland, March 27th-30th, (PBP 2006).

2. **Design of Lipospermine Non-Viral Gene Delivery Vectors for Self-Assembly DNA Nanoparticle Formulations (POSTER)**
   British Pharmaceutical Conference, Royal Pharmaceutical Society of Great Britain, Manchester, U.K., September 4th -6th (BPC 2006).

3. **Efficient Novel Gene and siRNA Delivery by Designed Lipopolyamine Formulations (ORAL)**
   Roche Symposium for Leading Scientists of the Next Decade, Basel, Switzerland, March 14th -16th (2007).

4. **Effect of Chain Length Modulation in Symmetrical Lipopolyamines on Nanoparticle Formulations for Gene Delivery (ORAL)**
   Pharmaceutical Sciences World Congress, Amsterdam, The Netherlands, April 22nd -25th (PSWC 2007).

5. **Efficient Novel Unsymmetrical Lipopolyamine Formulations for Gene Delivery (POSTER)**
   Pharmaceutical Sciences World Congress, Amsterdam, The Netherlands, April 22nd -25th (PSWC 2007).

6. **Formulation and Delivery of Fluorescent siRNA by Lipospermine Nanoparticle Complex Formation (POSTER)**
   Pharmaceutical Sciences World Congress, Amsterdam, The Netherlands, April 22nd -25th (PSWC 2007).

7. **Chain Length Modulation in Symmetrical Lipopolyamines and the effect on Nanoparticle Formulations for Gene Delivery (POSTER)**
   British Pharmaceutical Conference, Royal Pharmaceutical Society of Great Britain, Manchester, U.K., September 10^{th}-12^{th} (BPC 2007).

8. **Efficient Novel Unsymmetrical Lipopolyamine Formulations for Gene Delivery (POSTER)**
   British Pharmaceutical Conference, Royal Pharmaceutical Society of Great Britain, Manchester, U.K., September 10^{th} -12^{th} (BPC 2007).

9. **Formulation and Delivery of Fluorescent siRNA by Lipospermine Nanoparticle Complex Formation (POSTER)**
   British Pharmaceutical Conference, Royal Pharmaceutical Society of Great Britain, Manchester, U.K., September 10^{th} -12^{th} (BPC 2007).

10. **Self-Assembly Non-Liposomal Lipospermine Nanoparticle Formulations For Efficient Non-Toxic siRNA Delivery (ORAL)**
    6^{th} World Meeting on Pharmaceutics, Biopharmaceutics and Pharmaceutical Technology, Barcelona, Spain, April 7^{th} -10^{th} (PBP 2008).

11. **Self-Assembled Complex Formulations of Lipid-Aminoglycoside Conjugates: Nanoparticles for Efficient Gene and siRNA Delivery (POSTER)**
    6^{th} World Meeting on Pharmaceutics, Biopharmaceutics and Pharmaceutical Technology, Barcelona, Spain, April 7^{th} -10^{th} (PBP 2008).